AL/EQ-TR-1996-0030

UNITED STATES AIR FORCE ARMSTRONG LABORATORY

Subsurface Transport of Hydrocarbon Fuel Additives and a Dense Chlorinated Solvent

O. Guven
J. H. Dane
W. E. Hill
C. Hofstee
R. C. Walker
R. Mamballikalathi

AUBURN UNIVERSITY
Departments of Agronomy and Soils, Chemistry, and Civil Engineering
Auburn, Alabama 36849

December 1996

Environics Directorate
Environmental Risk Assessment Division
139 Barnes Drive, Suite 2
Tyndall Air Force Base FL 32403-5323

NOTICES

This report was prepared as an account of work sponsored by an agency of the United States Government. Neither the United States Government nor any agency thereof, nor any employees, nor any of their contractors, subcontractors, or their employees, make any warranty, expressed or implied, or assume any legal liability or responsibility for the accuracy, completeness, or usefulness of any privately owned rights. Reference herein to any specific commercial products, process, or service by trade name, trademark, manufacturer, or otherwise, does not necessarily constitute or imply its endorsement, recommendation, or favoring by the United States Government or any agency, contractor, or subcontractor thereof. The views and opinions of the authors expressed herein do not necessarily state or reflect those of the United States Government or any agency, contractor, or subcontractor thereof.

When Government drawings, specifications, or other data are used for any purpose other than in connection with a definitely Government-related procurement, the United States Government incurs no responsibility or any obligation whatsoever. The fact that the Government may have formulated or in any way supplied the said drawings, specifications, or other data, is not to be regarded by implication, or otherwise in any manner construed, as licensing the holder or any other person or corporation; or as conveying any rights or permission to manufacture, use, or sell any patented invention that may in any way be related thereto.

This technical report has been reviewed by the Public Affairs Office (PA) and is releasable to the National Technical Information Service, where it will be available to the general public, including foreign nationals.

This report has been reviewed and is approved for publication.

FOR THE COMMANDER:

MICHAEL A. GEER, Capt, USAF
Project Manager

MARK H. VANBENTHEM, Maj, USAF
Chief, Risk Assessment Technology Division

REPORT DOCUMENTATION PAGE

Form Approved
OMB No. 0704-0188

1. AGENCY USE ONLY (Leave Blank)

2. REPORT DATE
21 October 1996

3. REPORT TYPE AND DATES COVERED
Final Report 1 July 1993 - 30 September 1995

4. TITLE AND SUBTITLE
Subsurface Transport of Hydrocarbon Fuel Additives and a Dense Chlorinated Solvent

5. FUNDING NUMBERS
F08635-93-00071

6. AUTHOR(S)
O. Güven, J.H. Dane, W.E. Hill, C. Hofstee, R.C. Walker, and R. Mamballikalathil

7. PERFORMING ORGANIZATION NAME(S) AND ADDRESSES(ES)
Auburn University
Departments of Agronomy and Soils, Chemistry, and Civil Engineering
Auburn University, AL 36849

8. PERFORMING ORGANIZATION REPORT NUMBER
N/A

9. SPONSORING/MONITORING AGENCY NAME(S) AND ADDRESS(ES)
AL/EQ
139 Barnes Drive, Suite 2
Tyndall Air Force Base, Florida 32403-5323

10. SPONSORING/MONITORING AGENCY REPORT NUMBER
AL/EQ-TR-1996-0030

11. SUPPLEMENTARY NOTES
Contracting Officer's Technical Rep.: Lt Michael Geer, Phone: 904 283 6205

12A. DISTRIBUTION/AVAILABILITY STATEMENT
Unlimited

12b. DISTRIBUTION CODE

13. ABSTRACT (Maximum 200 words)

This report provides a description of the work done at Auburn University for the research project "Subsurface Transport of Hydrocarbon Fuel additives and a Chlorinated Solvent", supported by Armstrong Laboratory, Headquarters Air Force Civil Engineering Support Agency, Environics Directorate, under contract F08635-93-C-0071. The project is focused on the subsurface environmental behavior of quadricyclane, which is a light nonaqueous phase liquid (LNAPL) cyclic hydrocarbon fuel additive, and on the behavior of tetrachloroethylene (or, perchloroethylene), which is a dense nonaqueous phase liquid (DNAPL) chlorinated hydrocarbon solvent.

14. SUBJECT TERMS
Subsurface chemistry; Contaminant transport

15. NUMBER OF PAGES
185

16. PRICE CODE

17. SECURITY CLASSIFICATION OF REPORT	18. SECURITY CLASSIFICATION OF THIS PAGE	19. SECURITY CLASSIFICATION OF ABSTRACT	20. LIMITATION OF ABSTRACT
UNCLASSIFIED	UNCLASSIFIED	UNCLASSIFIED	UL

NSN 7540-01-280-5500

Standard Form 298 (Rev. 2-89)
Prescribed by ANSI Std. Z39-18
298-102

(The reverse of this page is blank.)

PREFACE

This report was prepared by Auburn University, 202 Samford Hall, Auburn University, Alabama 36849, for the Armstrong Laboratory, Headquarters Air Force Civil Engineering Support Agency, Environics Directorate (AL/EQ), 139 Barnes Drive, Suite 2, Tyndall Air Force Base, Florida, 32403-5323, under contract F08635-93-C-0071.

This report describes the work done at Auburn University for the research project "Subsurface Transport of Hydrocarbon Fuel Additives and a Chlorinated Solvent." The project is focused on the subsurface environmental behavior of quadricyclane, which is a light nonaqueous-phase liquid (LNAPL) cyclic hydrocarbon fuel additive, and on the behavior of tetrachloroethylene (or, perchloroethylene), which is a dense nonaqueous-phase liquid (DNAPL) chlorinated hydrocarbon solvent.

The authors wish to thank Dr. B.F. Hajek, who assisted with the selection, collection, and characterization of the field soil samples, Mr. B.C. Missildine who assisted with the design and construction of some of the experimental equipment and with the performance of some of the experiments, Ms. J. Szechi who performed the chemical analyses, Mr. Guirong Qin who assisted with the performance of some of the experiments, and Ms. S. Beech and Ms. S.L. Davis who typed the report.

This project started on July 1, 1993 and ended on September 30, 1995. The AL/EQ project officers were Capt Thomas P. DeVenoge and Lt Michael Geer. Dr. Thomas B. Stauffer provided technical guidance through various stages of the work.

(The reverse of this page is blank.)

EXECUTIVE SUMMARY

A. OBJECTIVE

The objective of this research was to study the subsurface transport of quadricyclane and tetrachloroethylene. The research project was entitled "Subsurface Transport of Hydrocarbon Fuel Additives and a Chlorinated Solvent," and supported by the Armstrong Laboratory, Headquarters Air Force Civil Engineering Support Agency, Environics Division, under contract F08635-93-C0071. The project began on July 1, 1993 and ended on September 30, 1995.

B. BACKGROUND

This project is focused on the subsurface environmental behavior of quadricyclane, which is a light non-aqueous-phase liquid (LNAPL) cyclic hydrocarbon, and on the behavior of tetrachloroethylene, or, as it is also called, perchloroethylene (PCE), which is a dense non-aqueous-phase liquid (DNAPL) chlorinated hydrocarbon solvent. Quadricyclane is being tested by the United States Air Force for possible use as a high performance aviation fuel additive. This potential future application stressed the need to study the subsurface behavior of quadricyclane, in the event of a spill. This project includes a series of laboratory experiments in batch reactors, soil columns and a flow container to improve the present understanding of quadricyclane chemistry and transport behavior in various subsurface media. Regarding the subsurface transport behavior of PCE, the project includes a number of detailed laboratory experiments in flow columns and flow containers, utilizing a unique dual-energy gamma radiation system to measure water and PCE saturations, to provide detailed quantitative data sets on the multiphase transport of PCE in homogeneous and heterogenous porous media.

C. SCOPE

This report is organized into several sections, each devoted to a particular task or a major component of a task. For convenience, the literature references for each section are listed at the end of the particular section. Section II presents the laboratory chemical analyses, reaction rates, and batch studies of quadricyclane and its reaction products. Section III describes the one-dimensional (1-D) leaching experiments with quadricyclane and its reaction products. Section IV describes a set of two-dimensional spill and cleanup experiments with quadricyclane in a laboratory flow container. Section V presents a series of 1-D static-equilibrium experiments with PCE in laboratory columns, while Section VI describes a set of transient flow experiments with water, PCE and air in nominally 1-D, homogeneous and heterogeneous porous media. Section VII describes a set of clean up experiments on the surfactant enhanced removal of entrapped PCE from 1-D columns of homogeneous and heterogeneous porous media. Section VIII presents a set of 2-D spill and cleanup experiments with PCE in a laboratory flow container, while Section IX describes a set of very detailed quantitative multiphase flow experiments with PCE in a larger flow container utilizing the dual-energy gamma radiation system. Finally, the report is concluded with Section X.

D. CONCLUSIONS

Specific conclusions of this research related to each major task of the project are presented in the corresponding sections of the report. The experiments with quadricyclane, presented in Sections II, II and IV, have provided new, detailed information on the subsurface behavior of this compound, while the experiments with PCE, presented in Sections V, VI, VII, VIII and IX, have resulted in unique data sets providing detailed quantitative information on the behavior of this chemical.

(The reverse of this page is blank.)

TABLE OF CONTENTS

LIST OF FIGURES

Figure Page

Figure Page

Figure Page

Figure Page

LIST OF TABLES

TABLE PAGE

SECTION I
INTRODUCTION

A. OBJECTIVE

The objective of this research was to study the subsurface transport of quadricyclane and tetrachloroethylene. The research project was entitled "Subsurface Transport of Hydrocarbon Fuel Additives and a Dense Chlorinated Solvent," and supported by the Armstrong Laboratory, Headquarters Air Force Civil Engineering Support Agency, Environics Division, under contract F08635-93-C-0071. The project began on July 1, 1993 and ended on September 30, 1995.

B. BACKGROUND

The project is focused on the subsurface environmental behavior of quadricyclane, which is a light non-aqueous phase liquid (LNAPL) cyclic hydrocarbon fuel additive, and on the behavior of tetrachloroethylene, or, as it is also called, perchloroethylene (PCE), which is a dense nonaqueous phase liquid (DNAPL) chlorinated hydrocarbon solvent. Quadricyclane has been investigated as an energy storage medium in solar cells, and is now being tested by the United States Air Force for possible use as a high performance aviation fuel additive. The latter potential future application stressed the need to study into the subsurface behavior of quadricyclane, in the event of a spill. This project includes a series of laboratory experiments in batch reactors, soil columns and a flow container to improve the present understanding of quadricyclane chemistry and transport behavior in various subsurface media. Regarding the subsurface transport behavior of PCE, the project includes a number of detailed laboratory experiments in flow columns and flow containers, utilizing a unique dual-energy gamma radiation system to measure water and PCE saturations, to provide detailed quantitative data sets on the multiphase transport of PCE in homogeneous and heterogenous porous media.

C. SCOPE

This report is organized into several sections, each devoted to a particular task or a major component of a task. For convenience, the literature references for each section are listed at the end of the particular section. Section II presents the laboratory chemical analyses, reaction rates, and batch studies of quadricyclane and its reaction products. Section III describes the one-dimensional (1-D) leaching experiments with quadricyclane and its reaction products. Section IV describes a set of two-dimensional spill and cleanup experiments with quadricyclane in a laboratory flow container. Section V presents a series of 1-D static-equilibrium experiments with PCE in laboratory columns, while Section VI describes a set of transient flow experiments with water, PCE and air in nominally 1-D, homogeneous and heterogeneous porous media. Section VII describes a set of cleanup experiments on the surfactant enhanced removal of entrapped PCE from 1-D columns of homogeneous and heterogeneous porous media. Section VIII presents a set of 2-D spill and cleanup experiments with PCE in a laboratory flow container, while Section IX describes a set of very detailed quantitative multiphase flow experiments with PCE in a larger flow container utilizing the dual-energy gamma radiation system. Finally, the report is concluded with Section X.

SECTION II
CHEMICAL ANALYSES, REACTION RATES, AND BATCH STUDIES OF QUADRICYCLANE AND ITS REACTION PRODUCTS

A. INTRODUCTION

Quadricyclane (quadricyclo(2.2.1.$0^{2,6}$.$0^{3,5}$)heptane) is a clear liquid with a relatively high boiling point (108°C) and a specific gravity of 0.982 (Aldrich, 1992), which is made by photoirradiation of norbornadiene. The highly strained structure of the quadricyclane molecule is reflected in a high formation enthalpy with reported values of 253.3 (Hall et al., 1973) to 325 kJ/mol (Kabakoff et al., 1975). The compound has been investigated as an energy storage medium in solar cells, and is now being tested by the United States Air Force for possible use as a high-performance aviation fuel additive. The latter potential future application stressed the need for a study into the subsurface behavior of quadricyclane in the event of a spill.

The high formation enthalpy of quadricyclane makes it very reactive. A wide variety of chemical transformations have been reported, but studies into the aqueous behavior of quadricyclane to date have been restricted to the observation that it is stable in neutral to alkaline solutions (Maruyama et al, 1985).

Quadricyclane is an organic liquid, which is slightly less dense than water and immiscible. Its behavior in porous media will therefore probably resemble that of other light non-aqueous-phase liquids (LNAPLs). Study of LNAPL transport in porous media following a release at the surface has been conducted in various laboratory experiments (e.g., Lenhard et al., 1988) and after accidental occurrences at contaminated sites. Additionally, a lot of effort has been put in the development of numerical computer codes to predict the fate of LNAPL in the subsurface (e.g., Abriola and Pinder, 1985). The highly strained nature of quadricyclane will probably cause it to undergo chemical reactions when exposed to a natural soil environment and these reactions may be soil type dependent. This makes prediction of the fate of quadricyclane and other highly strained hydrocarbons in the subsurface very complicated.

The work reported here includes the measurements of some previously unknown or uncertain properties of quadricyclane such as aqueous solubility and density. The test soils used in the batch experiments had pH values between 4.6 and 6.4, and we therefore investigated the chemical reactions of quadricyclane in water in that pH range. Overall rate constants were measured for pure water, pure isopropanol, and a 50/50 wt% mixture of water and isopropanol and reaction products identified. A probable reaction mechanism is presented. Batch experiments were conducted to investigate the chemical stability of quadricyclane in four natural test soils.

B. SOLUBILITY OF QUADRICYCLANE IN WATER

1. Materials and Methods

Dodecane, norbornadiene, 5-norbornen-2-ol, norcamphor, norborneol and quadricyclane were obtained from Aldrich Chemical Company and used without further purification. Quadricyclane and norbornadiene purity was determined by gas chromatography prior to each experiment.

a. Gas Chromatographic Analyses

Analyses were carried out on a Shimadzu GC14 gas chromatograph equipped with a flame ionization detector (FID), an AOC-17 autoinjector, and a CR501 computing integrator/data processor. The

FID was coupled to a Restek RTX-1 capillary column (30 m, 0.25 mm ID). To a weighed amount of the aqueous solution (typically 0.4-0.8 gram), 0.4-1.0 gram of a standard solution (881.8 ppm of decane in isopropanol) was added as an internal standard. Multiple injections were made over the range of 0.2 to 1.0 μL. Injections were made at 40°C. After holding for 4 minutes, the temperature was raised at a rate of 25°C/min to 250°C and held at that temperature for 10 minutes. The areas of the components of the solutions were plotted against the area of the decane standard for each injection and the data fitted to a linear plot with correlation coefficients of greater than 0.99 (e.g., Figure 1).

b. Mass Spectral Analyses

Mass spectral analyses were carried out on a VG 7070 EHF mass spectrometer equipped with a Varian 3700 gas chromatograph and a data station. One micro liter aqueous injections were made at 40°C. After holding for 4 minutes, the temperature was raised at a rate of 25°C/min to 200°C and held at that temperature for 10 minutes. Ionization was carried out in the electron impact mode.

2. Experimental Determination of the Solubility of Quadricyclane and Norbornadiene

Early attempts at determining the solubility of quadricyclane in water revealed that quadricyclane has a great propensity to form micro emulsions in water. This is probably because it has a high density compared to other hydrocarbons (0.982 g/cm^3), very near that of water itself. The reported density (0.919 gm/cm^3) in the interim report (Güven et al., 1995) was obtained from Aldrich Chemical Co. (1992) and determined by us to be incorrect. Aldrich has subsequently confirmed our results and corrected their catalog. Several approaches were carried out to insure that microemulsions were not present.

a. Centrifugation

One cm^3 of quadricyclane and 10 cm^3 of water were shaken mechanically for 15 minutes and then allowed to sit undisturbed for 1 hour. The top layer (excess quadricyclane) was removed by a pipette and the aqueous layer was transferred to a test tube, centrifuged for 15 minutes, and then injected into the gas chromatograph. The average quadricyclane concentration from three runs was 342 ppm.

b. Settling

One cm^3 of quadricyclane was added to 5 cm^3 of deionized water in a vial fitted with a cap and shaken by hand for 0.5 hour. The cloudy emulsion was allowed to sit undisturbed for two days. A 1 cm^3 syringe with an 0.1 cm^3 of air was inserted to the bottom of the vial. The air was injected very slowly to minimize the disturbance and 1 cm^3 of the water layer was slowly withdrawn. The syringe needle was washed twice with deionized water and wiped dry. About 0.4 cm^3 of the sample was expelled. The aqueous layer was then analyzed by gas chromatography as described above. The result was 364 ppm solubility of quadricyclane. In a variation of this procedure, a 5 cm^3 syringe was charged with 4 cm^3 of deionized water and 0.5 cm^3 of quadricyclane. The syringe was inverted and the air was expelled. A removable septum was then placed over the end of the syringe and the apparatus was vigorously shaken for 2 minutes and allowed to sit undisturbed for 0.5 hour. To a weighed sample vial equipped with a syringe cap, decane-isopropanol standard was added and the aqueous quadricyclane solution was added displacing the air. Injections were made from this vial. The result was a solubility of 324 ppm for quadricyclane (Figure 1). Norbornadiene solubility was also determined, using the settling method, and a value of 260 ppm was obtained.

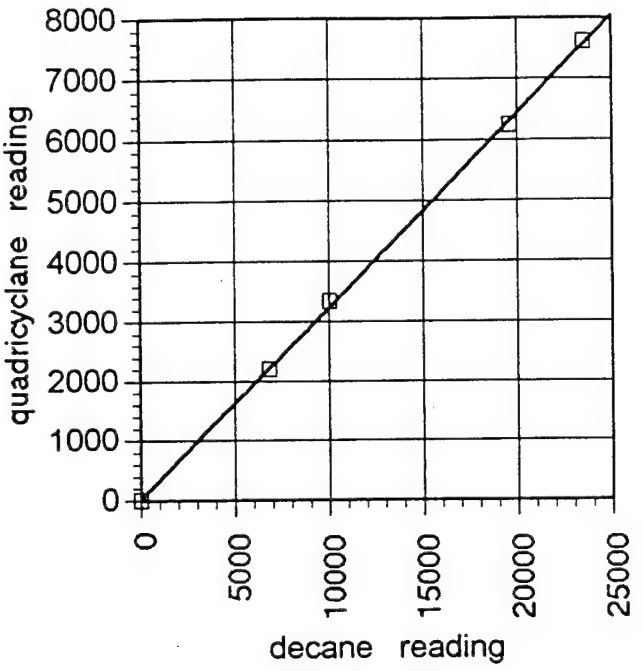

Figure 1. Example of a Linear Plot Used to Determine the Quadricyclane Concentration in a Sample Obtained by the Settling Method.

c. Filtration With 0.45 and 0.1 μm Microfilters

Aqueous solutions of quadricyclane obtained from (b) were filtered through 0.45 and 0.1 μm microfilters before gas chromatographic analysis. The results from these experiments were very close to those obtained in (b).

d. Column Elution

A glass column (350 mm long and 15 mm ID), equipped with a syringe needle as an outlet, was charged with 120 mm of dry sea sand. Quadricyclane, 0.6 cm^3, was dripped onto the top of the sand taking care to spread it as evenly as possible. An additional 25 mm of sea sand was then added to the top of the column. The column was then left to stabilize for 1/2 hour. Elution was then carried out with deionized water and samples were collected every 15 minutes. These samples were run immediately or kept on ice until tested. The results are reported in Figure 2. The maximum solubility was determined to be ~380 ppm.

e. Etzweiler Method (Etzweiler et al, 1995)

This method involves the generation of a saturated aqueous solution by migration of organic substrates across a dialysis membrane, from an emulsified mixture where the organic is in quite high concentrations compared to pure water. The concentrations of the organics were measured by gas chromatography.

To test the method, an apparatus was built using Spectra/por membrane tubing with a molecular weight cut-off of 12,000-14,000 Daltons. The solubility of benzene was determined to be 1788 ppm, which compares favorably to the accepted value of 1790 ppm.

Both quadricyclane and norbornadiene were measured by this technique. The results are shown in Figure 3. A value of 410 ppm was found for norbornadiene and a value of 245 ppm was found for quadricyclane.

3. Results and Discussion

Because quadricyclane tends to form microemulsions, wide variations in the solubility were detected. In coarse sand with a relatively high flow rate, for example, quadricyclane forms microemulsions which are swept off the free NAPL phase by the water flowing through the column, leading to an artificially high value for the solubility. These microemulsions can be seen under high magnification using an intense light source, but cannot be filtered out using the smallest available microfilters which merely allow the emulsions to pass through, or break up the emulsion, allowing it to reform after the supersaturated solution passes through. The method of Etzweiler et al (see method e above and Figure 3) is designed to counter these problems, and we believe the values obtained from this determination are the best available. Thus, the solubility of quadricyclane in water is 245 ppm, and norbornadiene is 410 ppm.

C. REACTION OF QUADRICYCLANE AND WATER

1. Product Identification

During the solubility measurements of quadricyclane, it was noted that the concentration of quadricyclane in water diminished with time. Thus, an aqueous solution containing 107 ppm of

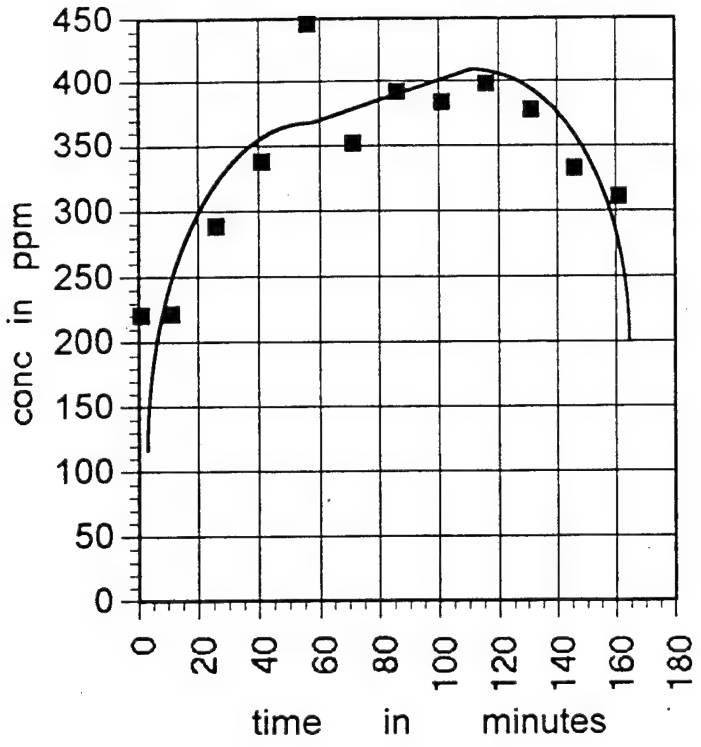

Figure 2. Quadricyclane Concentration as a Function of Time Obtained by Elution From a Column of Sea Sand.

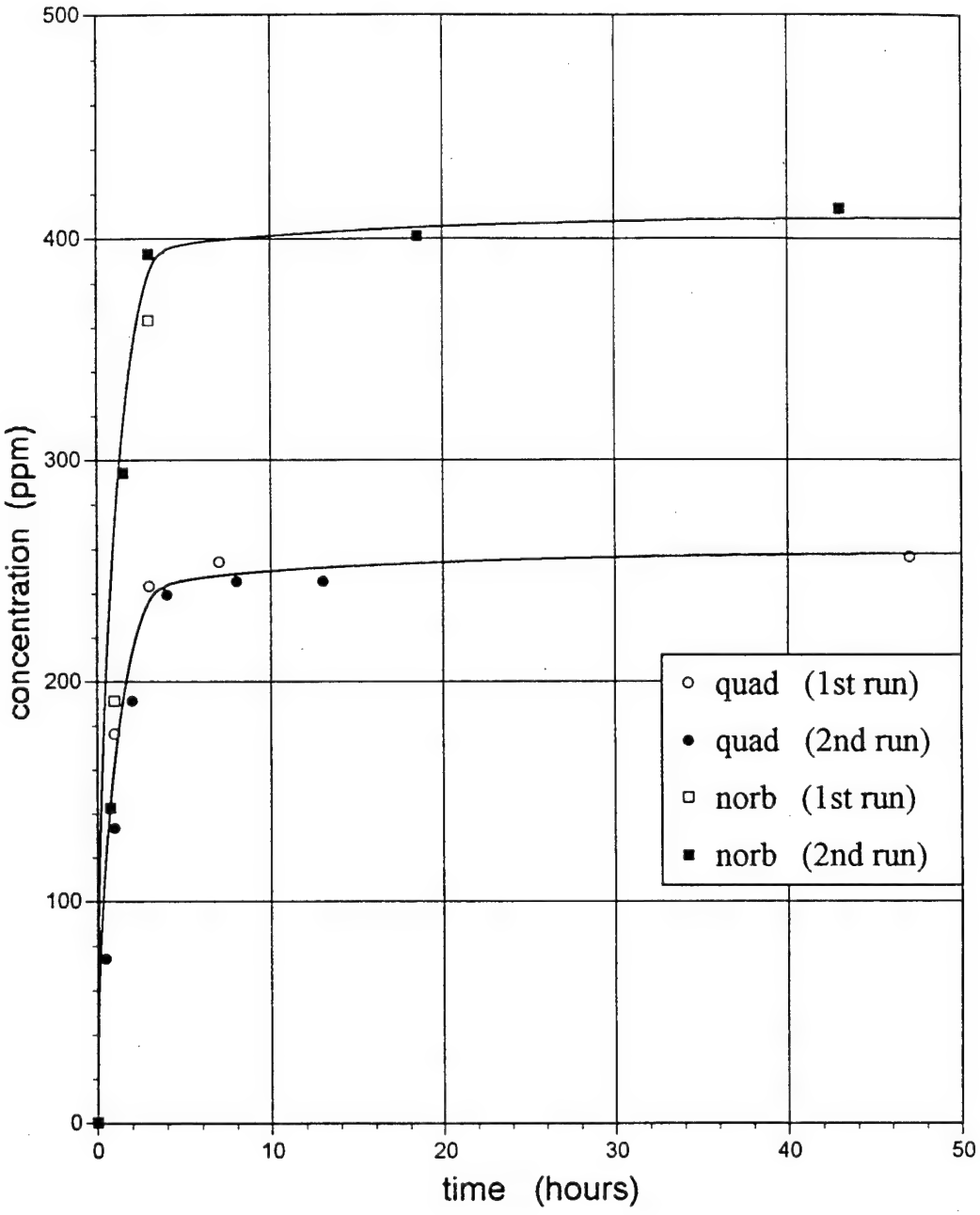

Figure 3. Solubility of Quadricyclane and Norbornadiene in Water, According to the Method of Etzweiler et al. (1995).

quadricyclane showed a decrease to 25 ppm in 24 hours and no quadricyclane could be detected after 4 days. This disappearance was coupled with the appearance of two new peaks in the gas chromatogram with retention times of 6.41 and 6.79 min. Mass spectral analysis of the products is given in Table 1 along with the mass spectra of quadricyclane and norbornadiene. Assignments were made and the fragmentation pattern of quadricyclane is given in Figure 4 and that of 5-norbornen-2-ol in Figure 5. A comparison of the fragmentation pattern of 5-norbornen-2-ol with that of the product observed at 6.41 min in the gas chromatogram of the products (Product A in Table 2) leaves little doubt as to its identity. Furthermore, although 5-norbornen-2-ol exists in endo and exo isomers, only the exo isomer is formed (Table 2). A far more complicated fragmentation pattern is observed for Product B and this product has been identified as nortricyclyl alcohol.

In order to generate quantities of products of quadricyclane and water that would be great enough for identification, a reactor was set up containing deionized water with a quadricyclane layer on top of the water. After 9 days gas chromatographic analysis showed that the water layer had 42 ppm of quadricyclane, 215 ppm of the product with a retention time of 6.41 minutes and 3,815 ppm of the 6.79 minutes retention time product. A second apparatus containing D_2O and quadricyclane gave quite similar results with the products showing some deuterium incorporation into the parent ion. Mass spectral data are given in Tables 1, 2 and 3.

2. Kinetic Analysis of the Acid-Catalyzed Reaction of Quadricyclane with Water, 50/50 Water /Isopropanol and Isopropanol.

Kinetic data were collected by taking quadricyclane (ca 200 ppm) in deionized water and adding HBF_4 as the H^+ source. Due to the low solubility of quadricyclane in water and its tendency to form emulsions, kinetic data was collected in a 50/50% by weight solution of water and isopropanol and in pure isopropanol for comparison.

Samples in water were prepared by vigorously shaking a mixture of 0.5 cm^3 of quadricyclane and 5.0 cm^3 of deionized water, centrifuging for 5 minutes, and carefully extracting ca 1.5 cm^3 of the lower layer. This extract was placed in a vial, weighed, and an aqueous solution of a known concentration of HBF_4 was weighed in. Samples in 50/50 water/isopropanol were prepared by taking an isopropanol solution of quadricyclane and decane and combining with an aqueous solution of HBF_4. The H^+ concentration was varied by adding deionized water to make the aqueous portion 50% by weight. Samples in isopropanol were prepared by weighing an isopropanol solution containing a known concentration of HBF_4 into an isopropanol solution containing a known concentration of quadricyclane and decane.

The temperature was maintained at 25°C and samples were withdrawn and analyzed by gas chromatography using a Shimadzu GC14 gas chromatograph equipped with a flame ionization detector (FID), an AOC-17 auto-injector, and a CR501 computing integrator/data processor. The FID was coupled to a Restek RTX-1 capillary column (30 m, 0.25 mm ID). Injections were made at 40°C, held at that temperature for 4 min, and then raised at a rate of 25°C/min to 250°C. The auto injector was used to repeat the injections at regular intervals.

Plots of ln $[quadricyclane]_0/[quadricyclane]_t$ vs. time at different H^+ concentrations in aqueous solution are given in Figure 6. Figures 7 and 8 contain similar plots for the 50/50 water/isopropanol solvent system and pure isopropanol respectively. Plots of the pseudo-first-order rate constants vs. the H^+ concentrations for each solvent system are given in Figures 9, 10 and 11, respectively.

TABLE 1. MASS SPECTRAL DATA OF WATER SOLUTIONS OF QUADRICYCLANE.[1]

m/z	Relative Intensity[2]				Assignment
	Quad.	Norb.	Product A	Product B	
39	24.1	14.0	17.7	51.4	$C_3H_3^+$
40				12.2	$C_3H_4^+$
41				38.2	$C_3H_5^+$
43				17.6	$C_3H_7^+$
51				14.4	$C_4H_3^+$
53				31.0	$C_4H_5^+$
54				25.1	$C_4H_6^+$
55				49.6	$C_4H_7^+$
65	36.8	14.0	15.6	18.1	$C_5H_5^+$
66	36.5	32.6	100.0	100.0	$C_5H_6^+$
67			20.4	78.3	$C_5H_7^+$
68				18.1	$C_5H_8^+$
69				22.2	$C_5H_9^+$
77				35.6	$C_6H_5^+$
78				17.8	$C_6H_6^+$
79			13.7	88.0	$C_6H_7^+$
80				11.9	$C_6H_8^+$
81				52.8	$C_6H_9^+$
82				18.9	$C_6H_{10}^+$
91	100.0	100.0		48.9	$C_7H_7^+$
92	42.0	47.9		29.3	$C_7H_8^+$
95				48.0	$C_6H_7O^+$
109				18.1	$C_7H_9O^+$
110			19.8	48.9	$C_7H_{10}O^+$

1. Quadricyclane and water aged for more than 2 weeks.
2. Intensities less than 10% were ignored.

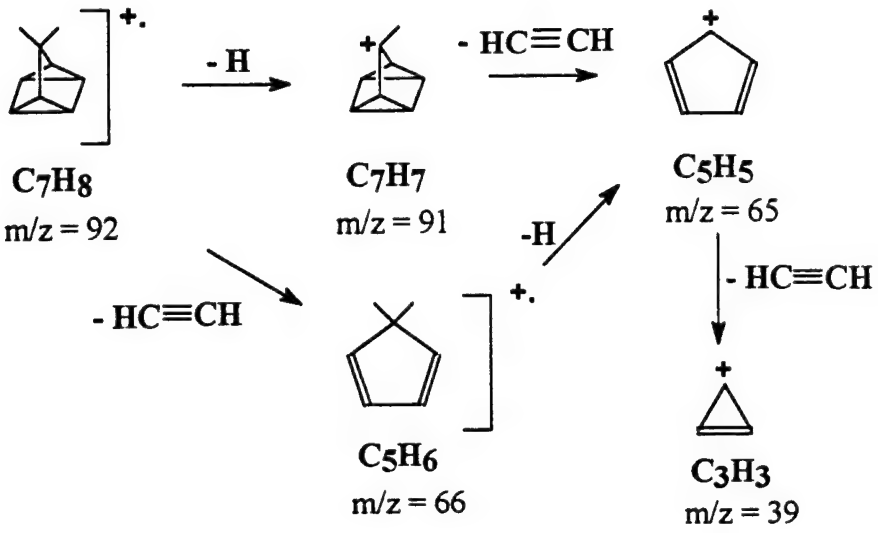

Figure 4. Mass Fragmentation Pattern for Quadricyclane.

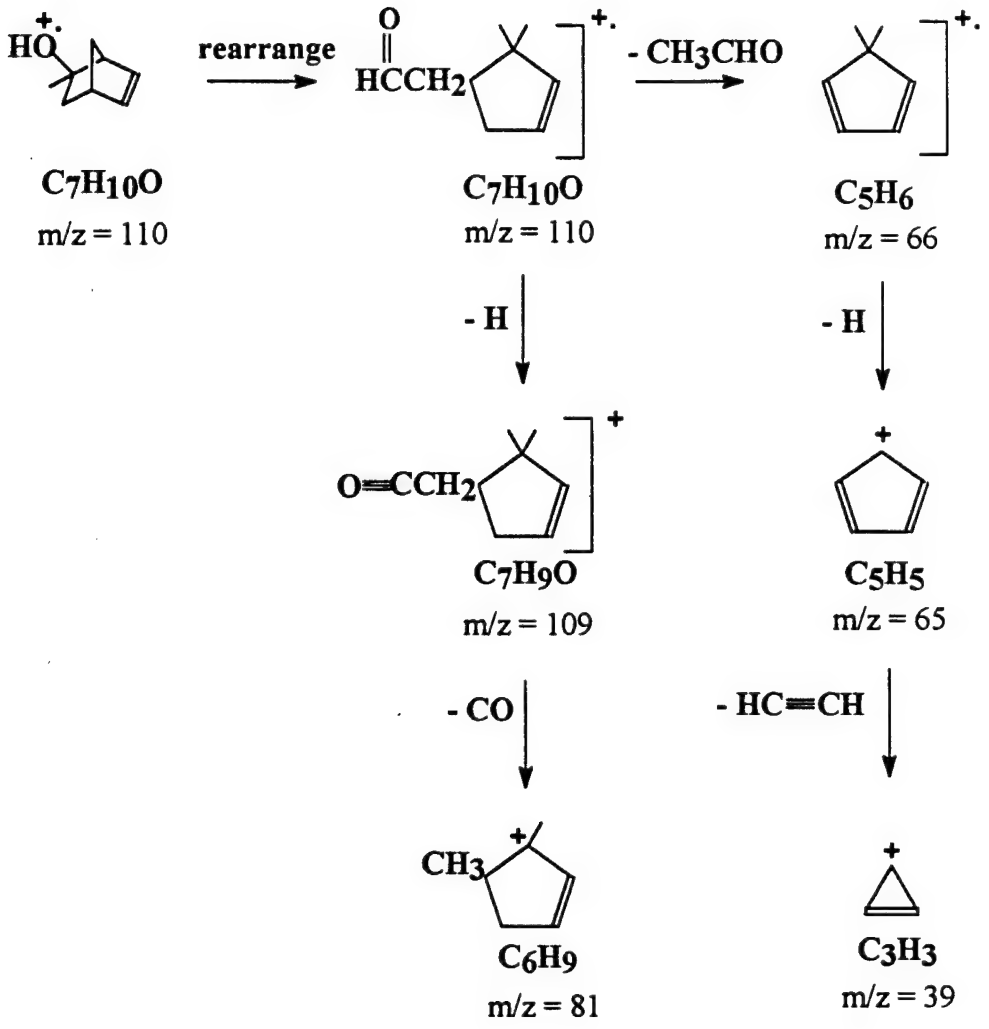

Figure 5. Mass Fragmentation Pattern for 5-Norbornen-2-ol.

TABLE 2. MASS SPECTRAL DATA FOR THE *endo* AND *exo* FORMS OF 5-NORBORNEN-2-OL, NORTRICYCLYL ALCOHOL AND PRODUCTS OF QUADRICYCLANE AND WATER.[1]

m/z	Relative Intensity[2]					Assignment
	5-Norbornen-2-ol		Product A	Product B	Nortricyclyl alcohol	
	exo	endo				
39	15.5	47.0	17.7	51.4	48.2	C_3H_3
40		22.8		12.2		C_3H_4
41		19.2		38.2	37.1	C_3H_5
43				17.6	12.4	C_3H_7
51		11.9		14.4	22.3	C_4H_3
53		13.1		31.0	34.2	C_4H_5
54				25.1	26.0	C_4H_6
55				49.6	51.2	C_4H_7
65	12.0	32.5	15.6	18.1	30.1	C_5H_5
66	100.0	100.0	100.0	100.0	95.0	C_5H_6
67	18.9	49.1	20.4	78.3	82.2	C_5H_7
68				18.1	24.2	C_5H_8
69				22.2	19.1	C_5H_9
77		17.2		35.6	53.2	C_6H_5
78				17.8	16.7	C_6H_6
79	12.4	24.5	13.7	88.0	100.0	C_6H_7
80				11.9		C_6H_8
81		12.4		52.8	73.3	C_6H_9
82				18.9	19.5	C_6H_{10}
91		10.0		48.9	66.2	C_7H_7
92				29.3	24.8	C_7H_8
95				48.0	50.0	C_6H_7O
109				18.1		C_7H_9O
110	17.7	41.0	19.8	48.9	27.3	$C_7H_{10}O$

1. Quadricyclane and water aged for more than 2 weeks.
2. Intensities less than 10% were ignored.

TABLE 3. MASS SPECTRAL DATA FOR THE *endo* AND *exo* FORMS OF 5-NORBORNEN-2-OL, NORCAMPHOR, NORBORNEOL, AND PRODUCTS OF QUADRICYCLANE AND WATER.[1]

m/z	Relative Intensity[2]					Assignment	
	5-Norbornen-2-ol		Product A	Product B	Nor-	nor-	
	exo/endo	endo/exo			camphor	borneol	
39	15.5	47.0	17.7	51.4	41.0	30.1	C_3H_3
40		22.8		12.2			C_3H_4
41		19.2		38.2	36.1	40.0	C_3H_5
43				17.6		10.4	C_3H_7
51		11.9		14.4			C_4H_3
53		13.1		31.0	16.3	17.0	C_4H_5
54				25.1	37.1		C_4H_6
55				49.6	11.0	23.1	C_4H_7
56						12.9	C_4H_8
57						34.0	C_4H_9
65		2.0	32.5	15.6	18.1		C_5H_5
66	100.0	100.0	100.0	100.0	89.8	76.8	C_5H_6
67	18.9	49.1	20.4	78.3	100.0	89.5	C_5H_7
68				18.1	18.3	81.8	C_5H_8
69				22.2			C_5H_9
70						15.9	C_5H_{10}
77		17.2		35.6			C_6H_5
78				17.8			C_6H_6
79	12.4	24.5	13.7	88.0	91.9		$C_6H_7^+$
80			11.9				$C_6H_8^+$
81	12.4		52.8	20.6	14.7		$C_6H_9^+$
82			18.9				$C_6H_{10}^+$
83					19.1		$C_6H_7^+$
91		10.0		48.9			$C_7H_7^+$
92				29.3			$C_7H_8^+$
94					100.0		$C_7H_{10}^+$
95				48.0			$C_6H_7O^+$
109				18.1			$C_7H_9O^+$
110	17.7	41.0	19.8	48.9	47.4		$C_7H_{10}O^+$

1. Quadricyclane and water aged for more than 2 weeks.
2. Intensities less than 10% were ignored.

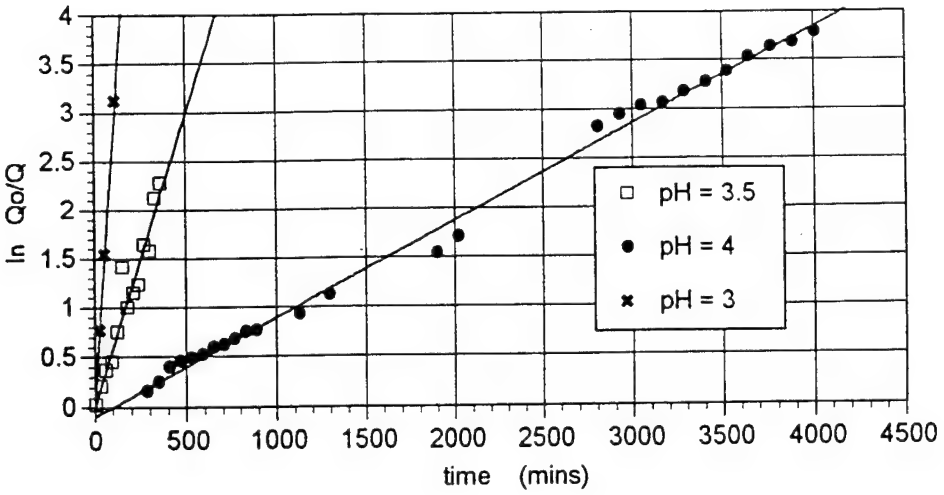

Figure 6. Kinetic Plots of the Disappearance of Quadricyclane with Time in Aqueous Solution at Different pH Values. T = 25°C.

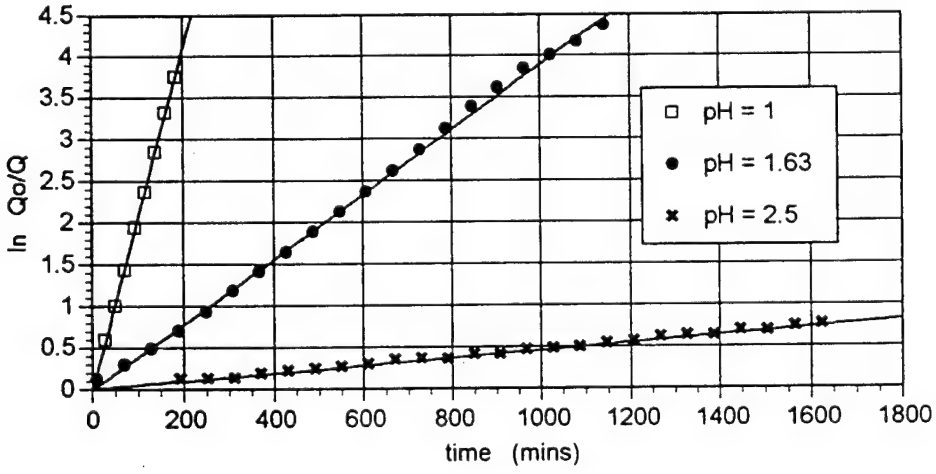

Figure 7. Kinetic Plots for the Disappearance of Quadricyclane with Time in 50/50 Weight% Water/ Isopropanol at Different pH Values. T = 25°C.

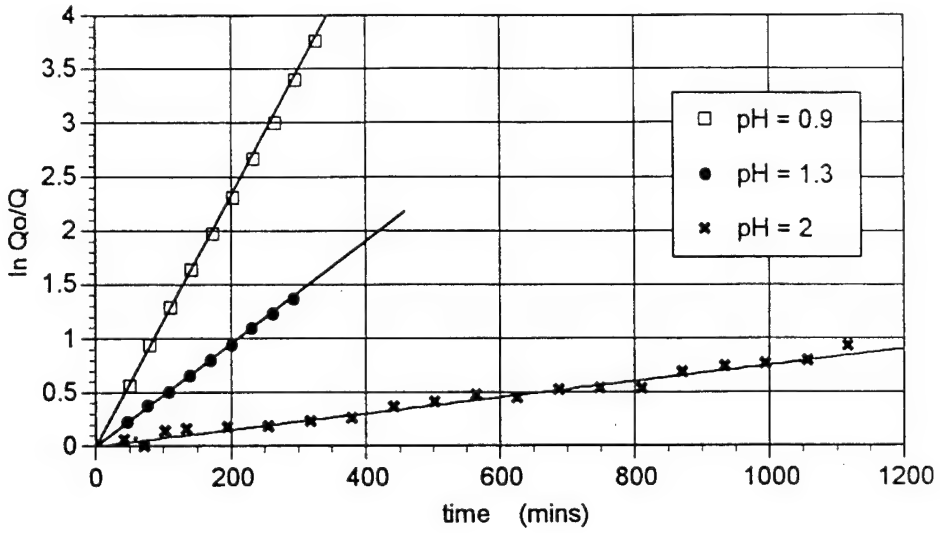

Figure 8. Kinetic Plots of the Disappearance of Quadricyclane With Time in Isopropanol at Different pH Values. T = 25°C.

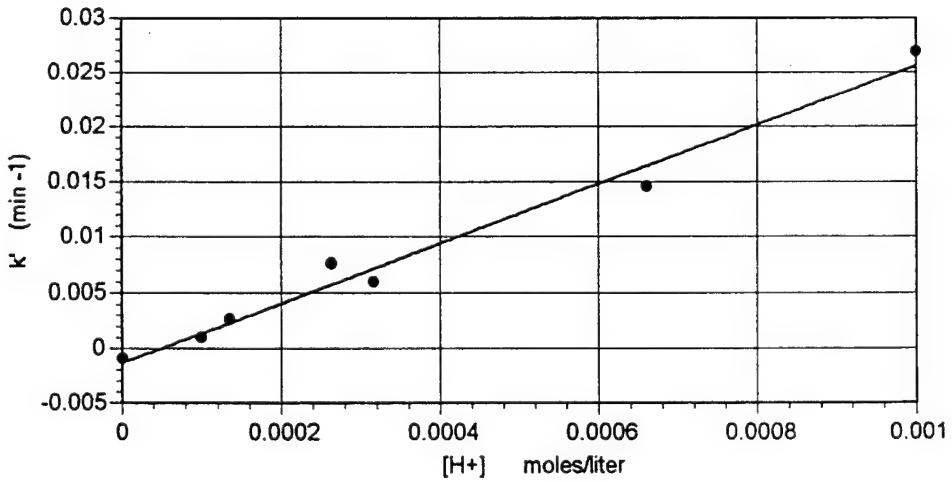

Figure 9. Variation in Pseudo-First-Order Rate Constants with H^+ Concentrations in Water. T = 25°C.

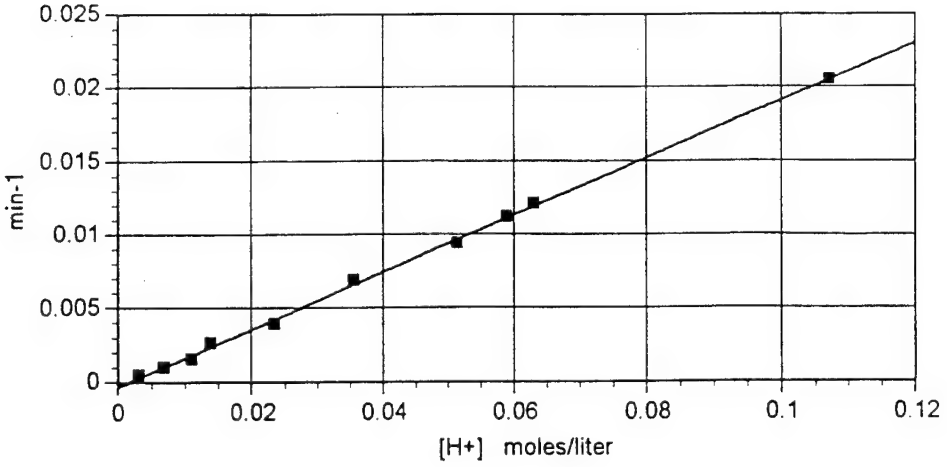

Figure 10. Variation in Pseudo-First-Order Rate Constants With H^+ Concentration in 50/50 Weight% Water/Isopropanol. T = 25°C.

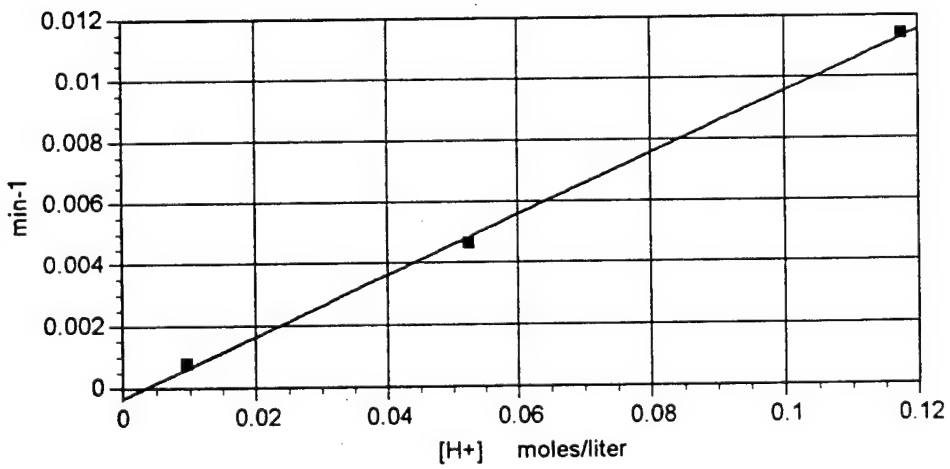

Figure 11. Variation in Pseudo-First-Order Rate Constants With H^+ Concentration in Isopropanol. T = 25°C.

3. Discussion

The disappearance of quadricyclane follows pseudo-first-order kinetics and has been analyzed using the kinetic model:

$$Q + H^+ \xrightarrow{k_1} QH^+$$

$$QH^+ + H_2O \xrightarrow{k_2} Q{\cdot}H_2O + H^+$$

$$QH^+ + H_2O \xrightarrow{k_3} Q^*{\cdot}H_2O + H^+$$

where $Q{\cdot}H_2O$ represents nortricyclyl alcohol and $Q^*{\cdot}H_2O$ represents 5-norbornen-2-ol.

Thus,

$$d[Q]/dt = k'_1 [Q]$$

where $k'_1 = k_1[H^+]$. Integration of this equation gives

$$\text{rate} = -d[Q]/dt = k_1 [Q] [H^+]$$

and since H^+ is regenerated (catalytic), the equation can be simplified to:

$$\ln [Q]_t = -k'_1 t + \ln [Q]_0$$

and

$$\ln ([Q]_o/[Q]_t) = k'_1 t$$

Table 4 gives the values for k'_1 and k_1 in isopropanol, 50/50 (by weight) water/isopropanol, and water at 25°C. As can be seen, the reactivity in water is much faster than in isopropanol or 50/50 water/isopropanol. In fact the value of k' for the reaction of quadricyclane in water at pH 5.0 and 25°C (calculated from the data given in Table 4) is 2.6×10^{-4} /min and the half life is 1.85 days. The k' value for 50/50 water/isopropanol at pH 5.0 is 1.95×10^{-6}/min and the half life is 0.68 years. In isopropanol, k' is 9.9×10^{-7}/min and the half life is 1.33 years. These results mirror those previously observed for the reactions of norbornadiene with acetic acid in various solvents (Cristol, Morrill and Sanchez, 1966a, b) and to those reported for the reaction of quadricyclane with acetic acid (Tabushi, Yamamura and Togashi, 1976).

The mechanistic scheme shown above is indistinguishable with our data from the following scheme:

$$Q + H^+ \underset{k_{-1}}{\overset{k_1}{<====>}} QH^+$$

$$QH^+ + H_2O \xrightarrow{k_2} Q{\cdot}H_2O + H^+$$

$$QH^+ + H_2O \xrightarrow{k_3} Q^*{\cdot}H_2O + H^+$$

TABLE 4. RATE OF QUADRICYCLANE DISAPPEARANCE AS A FUNCTION OF pH FOR THE SOLVENT SYSTEMS OF ISOPROPANOL, 50/50% BY WEIGHT WATER/ISOPROPANOL, AND WATER.

Solvent	pH	k'_1, min^{-1}	$t_{1/2}$, min	k_1, min^{-1}
isopropanol	0.93	1.14×10^{-2}	60.8	
	1.28	4.64×10^{-3}	149.4	
	2.02	7.58×10^{-4}	914.2	9.90×10^{-2}
50/50	0.97	2.05×10^{-2}	33.8	
	1.20	1.21×10^{-2}	57.7	
	1.23	1.12×10^{-2}	61.9	
	1.29	9.41×10^{-3}	73.6	
	1.45	6.87×10^{-3}	100.9	
	1.63	3.90×10^{-3}	177.7	
	1.86	2.61×10^{-3}	265.5	
	1.96	1.52×10^{-3}	455.9	
	2.17	9.64×10^{-4}	718.9	
	2.51	4.71×10^{-4}	1471.3	1.95×10^{-1}
water	3.00	2.68×10^{-2}	25.9	
	3.18	1.45×10^{-2}	47.8	
	3.50	6.00×10^{-3}	115.5	
	3.58	7.55×10^{-3}	91.8	
	3.87	2.58×10^{-3}	268.6	
	4.00	9.45×10^{-4}	733.3	
	5.96	9.67×10^{-4}	716.6	$2.60 \times 10^{+1}$

k' obtained by plotting ln $\{[\text{quadricyclane}]_o/[\text{quadricyclane}]_t\}$ vs. t in minutes; k obtained by plotting k' vs. $[H^+]$. Temperature is 25°C for all runs.

Table 5 gives the product distribution observed in the three solvent systems studied. As the solvent polarity decreases from water to 50/50 water/isopropanol to pure isopropanol, the olefinic product (Product A) is favored over the nortricyclyl product (Product B). Furthermore, examination of the product distribution in the 50/50 solvent system reveals that the formation of the alcohols (products A + B) occurs preferentially to the formation of the ethers (products C + D) by a ratio of 3.3 in keeping with the higher nucleophilicity of water compared to isopropanol.

TABLE 5. MOLAR RATIOS OF THE PRODUCT DISTRIBUTIONS IN THE VARIOUS SOLVENT SYSTEMS UTILIZED.

Solvent	B/A	D/C	B/D	A/C	A+B/C+D
H_2O	15.4	---	---	---	---
isopropanol	---	2.4	---	---	---
50/50	3.8	3.8	3.3	3.3	3.3

A= *exo*-5-norbornen-2-ol; B= nortricyclyl alcohol; C= exo-5-norbornen-2-isopropoxide; D= norticyclyl isopropoxide

A possible scheme for the reaction of quadricyclane in water is shown in Figure 12. This reaction scheme involves electrophilic attack by H^+ on one of the carbons in a three-membered ring to give a carbonium ion which adds H_2O and regenerates H^+.

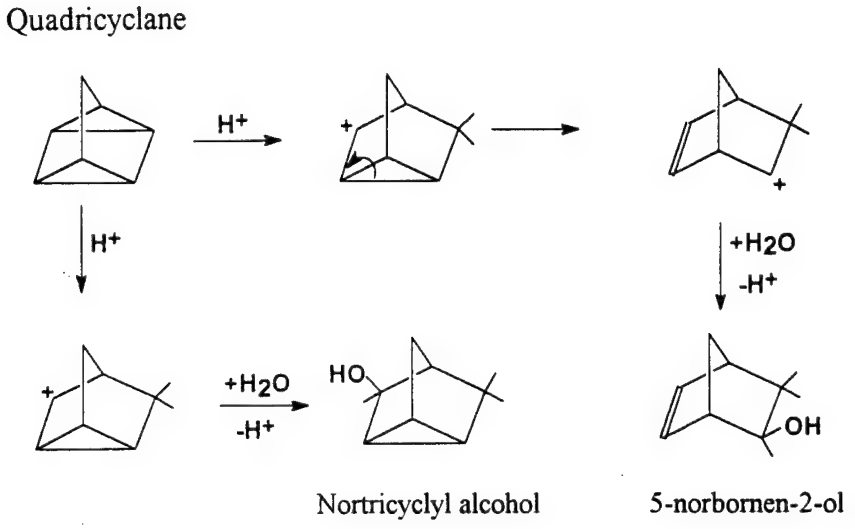

Figure 12. Reaction Scheme for the Reaction of Quadricyclane With Water.

D. BATCH EXPERIMENTS IN SOILS

1. Materials and Methods

For the batch experiments, two topsoils with a high pH and two with a low pH were collected. Within each of these two categories, one soil was collected which naturally occurs with a low organic matter content and one with a high organic matter content. All the soils selected have similar but rather small clay fractions. Soil classification, pH and organic matter content are given in Table 6.

TABLE 6. CLASSIFICATION, ACRONYMS ASSIGNED, pH VALUES AND % ORGANIC MATTER CONTENT FOR THE FOUR TEST SOILS.

Soil acronym*	Family Description	pH	% organic matter
ALOLPL	Typic Kanhaplaquults	5.12	1.0
ALOHPL	Plintic Kandiudults	4.60	6.0
TNOLPH	Cumilic Hapdudolls	5.93	2.2
TNOHPH	Typic Eutrochepts	6.35	2.8

* The first part of the acronyms (AL or TN) indicate the origin (i.e., Alabama or Tennessee) of the soil: OL and OH indicate a low and high organic matter content, respectively, and PL and PH refer to the low and high pH soil, respectively.

Twelve grams of the ALOLPL soil and 10 grams of each of the other three test soils (Güven et al., 1995) was placed in a vial and 2 mL of deionized water and 3 mL of quadricyclane was added. Most of the liquids infiltrated into the soil samples. Twelve grams (instead of 10 grams) of the ALOLPL soil were used because the porosity of this soil appeared to be somewhat lower. Subsequently, the vials were gently rotated for various periods of time in a jar mill. The samples were then removed from the vials and placed in 250 mL centrifuge bottles. 75 mL of dodecane (Aldrich Chemical Company) and 30 mL of a saturated NaCl solution was added. Dodecane was chosen as the solvent because of its favorable retention time on the GC, its low specific gravity of 0.749 (Aldrich Chemical Company, 1992), and its low volatilization, which made unsupervised shaking possible. The saturated NaCl solution was used because of its relatively high density, which reduces the amount of emulsions in the aqueous phase. Furthermore, the high ionic strength lowers the solubility of hydrocarbons. Preliminary experiments also indicated that quadricyclane is chemically stable in a NaCl solution, at least for short periods of time. The centrifuge bottles were shaken for about 12 hours with a mechanical shaker. Subsequently, the bottles were centrifuged to separate the soil, aqueous extractant and the dodecane extractant. The two liquids were then decanted from the centrifuge bottle into a separation funnel and the two immiscible liquids were separated. A 0.45 μm syringe filter was used to remove suspended soil particles. The extraction with dodecane and NaCl solution was conducted twice.

Dodecane extracts were weighed and the amount of quadricylcane in the extract determined by taking 0.4 to 0.5 gram of the extract, adding 0.275 gram of standard (decane @ 4,981 ppm in dodecane) to the first extract or 0.05 gram of standard to the second extract, and injecting into the gas chromatograph. Details of the equipment and measuring procedures used are given in Section II.B.1.

The pH swing, which was described in Güven et al. (1995), was found to be cumbersome and inefficient. Instead, we determined partitioning coefficients which were used to calculate the concentration of chemical species in the NaCl solution from their concentration in the dodecane extractant. It was assumed that chemical equilibrium had been reached after 12 hours of intensive shaking. The partitioning coefficients for *exo* 5-norbornen-2-ol and nortricyclyl alcohol, the reaction products found in acidic soils, were measured for two different solvent ratios and are shown in Table 7.

TABLE 7. PARTITIONING COEFFICIENTS* FOR 5-NORBORNEN-2-OL AND NORTRICYCLYL ALCOHOL IN A MIXTURE OF SATURATED SALT WATER AND DODECANE.

	saturated salt water/dodecane	
	5.0 mL/5.0 mL	3.0 mL/7.5 mL
exo 5-norbornen-2-ol	0.069	0.129
nortricyclyl alcohol	0.119	0.227

* partitioning coefficients are expressed as the concentration in salt water / concentration in dodecane.

The performance of the extraction procedure was measured by comparing the total mass of the extracted quadricyclane and its reaction products with the mass of the quadricyclane which was initially added to the soil samples. The effect of the extraction procedure on the final analytical results was determined by extracting soil samples immediately after the water and the quadricyclane had been added. The extraction efficiencies of the two reaction products of quadricyclane were determined by repeating the batch experiments with 5 mL of an aqueous solution containing the reaction products of quadricyclane. These samples were extracted after 2 weeks. Additionally, loss of mass due to leakage from the vials was investigated by measuring the weight loss as a function of time of a closed vial containing deionized water. Water was chosen because its boiling point is fairly close to that of quadricyclane.

2. Results and Discussion

Figures 13 - 16 show the results of the batch experiments with quadricyclane. The data of the immediate extraction (time=0 days) indicate that the extraction procedure did not affect the reactions of quadricyclane. No reaction products were detected in any soil sample and the ratio between the extracted quadricyclane and norbornadiene was close to that of the added mixture for all four soils. Significant transformation of quadricyclane into 5-norbornen-2-ol and nortricyclyl-alcohol was observed in the ALOLPL and especially in the ALOHPL as the time of exposure increased. The batch experiment with the ALOHPL was aborted after 6 months, because the concentration of the two reaction products became very high. On the other hand, in the more alkaline TNOHPH and TNOLPH soils, quadricyclane appeared to be chemically stable (Figures 15 and 16, respectively). Even after nine months, only traces of 5-norbornen-2-ol and nortricyclyl alcohol were detected. The rate of cycloaddition reactions clearly depends on the natural pH of the soil type. The amount of norbornadiene seems to increase only slightly with time for all four test soils. This indicates that the isomerization of quadricyclane into norbornadiene is either very slow or nonexistent. Table 8 shows the recovery efficiencies for 5-norbornen-2-ol and nortricyclyl-alcohol. The values for 5-norbornen-2-ol range from 56.6 % for the ALOHPL to 68.8 for the TNOLPH sample. The lower recovery

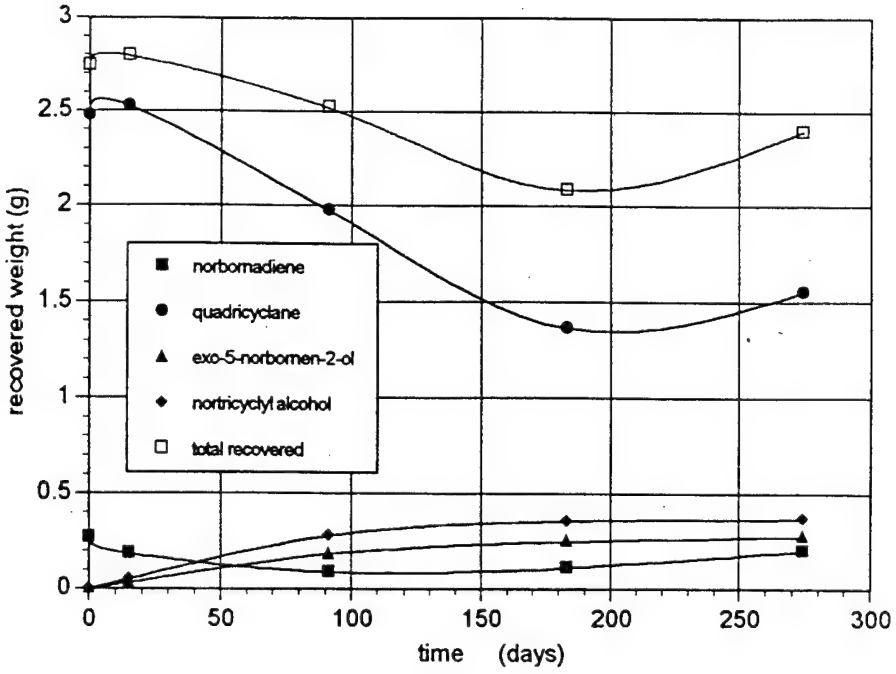

Figure 13. Results of the ALOHPL Batch Experiments.

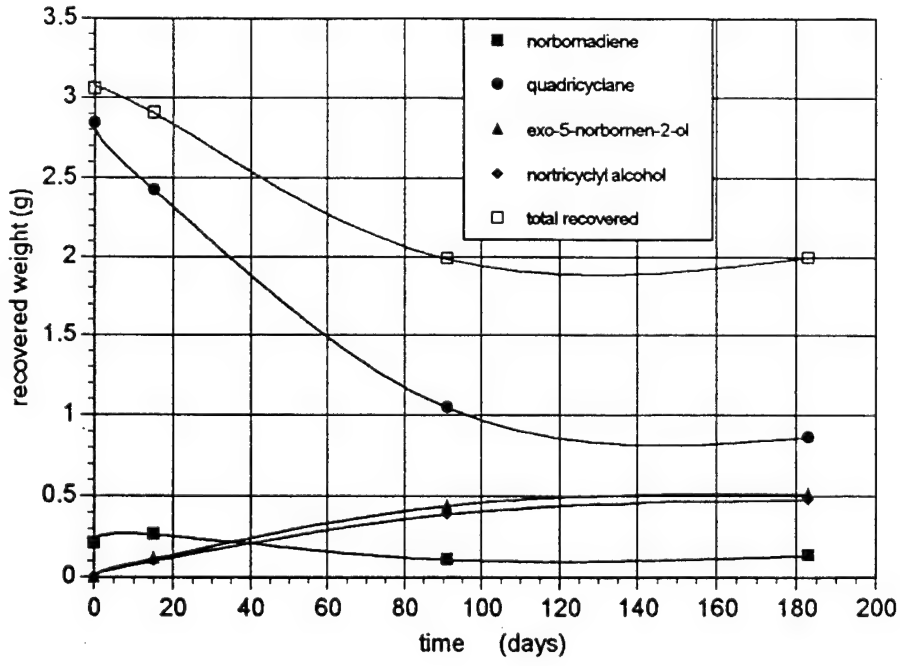

Figure 14. Results of the ALOLPL Batch Experiments.

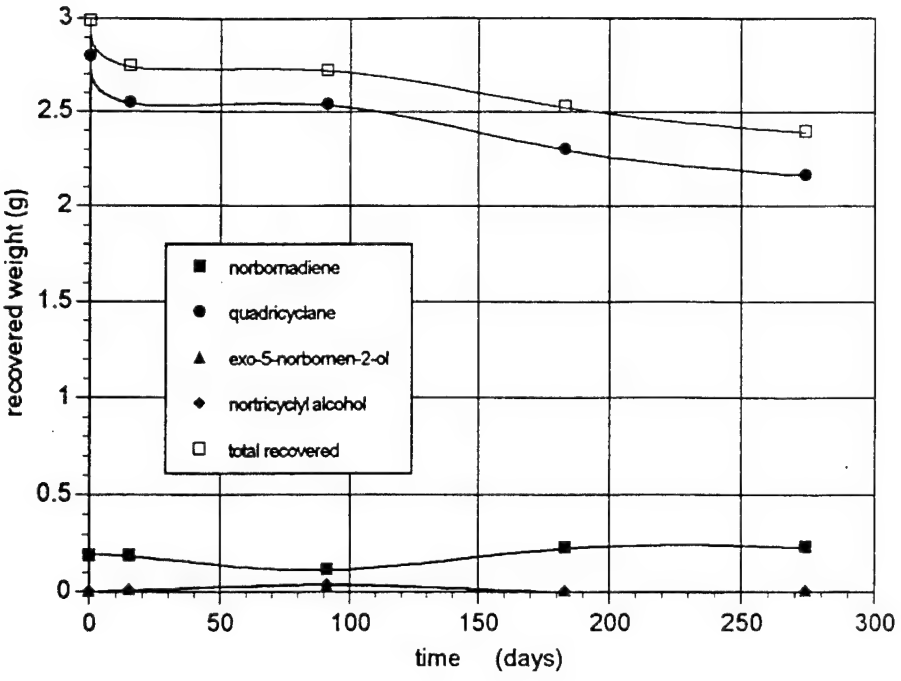

Figure 15. Results of the TNOHPH Batch Experiments.

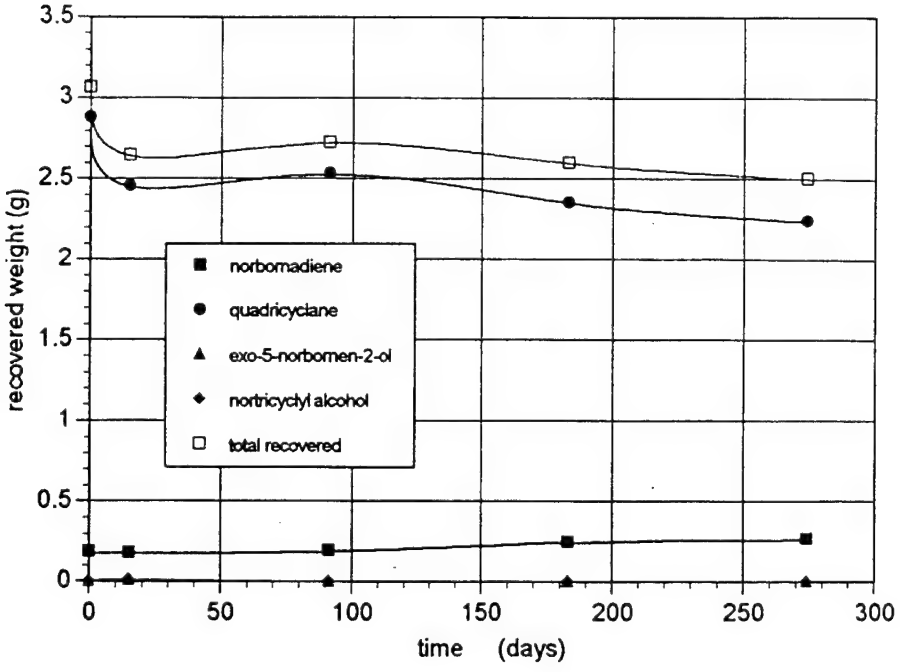

Figure 16. Results of the TNOLPH Batch Experiments.

for the ALOHPL sample can probably be attributed to the higher organic matter content of this soil type. The extraction procedure was more efficient in recovering the nortricyclyl alcohol with values of 71.4 % for the ALOHPL and 84.7 % for the TNOLPH. The overall recovery efficiencies for the two reaction products of quadricyclane are low compared to those of both quadricyclane and norbornadiene.

Figure 17 shows the results of the weight loss of the sealed vials containing deionized water over time. As quadricyclane is the most volatile component present in the soil mixtures being rolled, this is the most likely reason for the small weight loss observed in the high pH soils over long periods of time. The lower recovery rates of the reaction products are accounted for by the higher losses in the more acidic soils.

3. Conclusions

In a homogeneous acidic aqueous environment, dissolved quadricyclane has a short half-life and reacts rapidly to form two reaction products, identified as exo-5-norbornen-2-ol and nortricyclyl alcohol. The breakdown rates of quadricyclane in the four natural soils were observed to be much slower than those found for dissolved quadricyclane. Quadricyclane was found to be chemically stable in soils at pH 6.0 and higher and unstable in more acidic soils. The observed differences in pH dependence between the quadricyclane dissolved in water and exposed to a natural soil environment indicate that in soils, the acid-catalyzed reaction (in which alcohols are produced) takes place at the interface between the quadricyclane and the aqueous phase. The H^+ concentration at that interface can be expected to be much lower than that of the ambient water phase. This would explain the "amplified" pH dependence of quadricyclane in soils compared to quadricyclane dissolved in water. Surprisingly, the composition of the soil solution, soil particles and organic matter did not seem to induce any additional reactions of quadricyclane or its reaction products.

The breakdown of quadricyclane in natural soils is slow, compared to the time scales associated with the migration of NAPLs in the vadose zone of porous media. This means after a spill, quadricyclane can be expected to migrate as a LNAPL. In low pH soils the NAPL will then gradually react to form compounds which are soluble in water. Most of the migration in the second stage after a spill in these soils will therefore take place as organic solutes in the aqueous phase. In soils with near neutral pH, however, the contaminants can be expected to possess little or no mobility after the initial migration as a NAPL.

Due to its density being very close to that of water, quadricyclane has a propensity to form long-lived micro emulsions. This could play a role in the aqueous migration of quadricyclane, especially in areas with significant groundwater flow.

As predicted, chemical reactions play an important role in predicting the fate of quadricyclane when exposed to a subsurface environment. The rate of reactions are strongly soil dependent. This will highly complicate any efforts to simulate the environmental behavior of quadricyclane and probably of other highly strained hydrocarbons.

TABLE 8. MEASURED RECOVERY EFFICIENCIES OF THE EXTRACTION OF THREE TEST SOILS FOR 5- NORBORNEN-2-OL AND NORTRICYCLYL-ALCOHOL AFTER 14 DAYS.

Soil acronym	5-norbornen-2-ol	nortricyclyl-alcohol
	recovery efficiency (%)	
ALOLPL	56.6	71.4
ALOHPL	65.5	82.2
TNOLPH	68.8	84.7

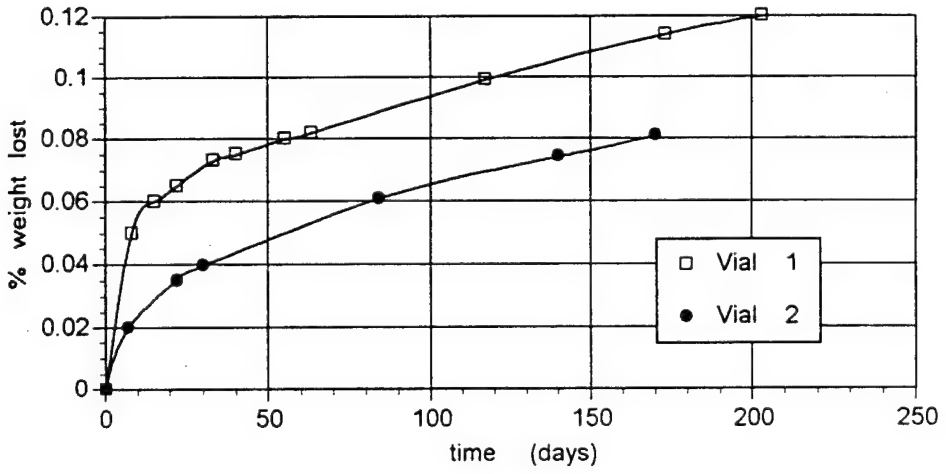

Figure 17. Weight Loss from the Water-Filled Sealed Vials Over Time.

REFERENCES FOR SECTION II

Abriola, L.M. and Pinder, G.F., "A Multiphase Approach to the Modelling of Porous Media Contamination by Organic Compounds, 2. Numerical Simulation." Water Resour. Res., 21, 19-26, 1985.

Aldrich Chemical Company, Catalog Handbook Of Fine Chemicals 1992/1993. Aldrich Chemical Company, Inc, Milwaukee, WI, 1992.

Cristol, S.J., Morrill T.C., and Sanchez, R.A., "Bridged Polycyclic Compounds. XL. The Catalyzed Addition of Acetic Acid to Norbornadiene." J. Org. Chem., 31, 2726-2732, 1966a.

Cristol, S.J., Morrill T.C., and Sanchez, R.A., "Bridged Polycyclic Compounds. XLI. The Uncatalyzed Addition of Acetic Acid to Norbornadiene." J. Org. Chem., 31, 2733-2737, 1966b.

Etzweiler, F., Senn, E.,and Schmidt, H.W.H.," Method for Measuring Aqueous Solubilities of Organic Compounds." Anal. Chem., 67, No. 3, 655-658, 1995.

Güven, O., Dane, J.H., Hill, W.E., Hofstee, C., and Mamballikalathil, R., Subsurface Transport of Hydrocarbon Fuel Additives and a Dense Chlorinated Solvent, Interim Report, AL/EQ-TR-1994-0039, Armstrong Laboratory, Tyndall Air Force Base, Florida, January 1995.

Hall, H.K., Jr., Smith, C.D., and Baldt, J.H.,"Enthalpies of Formation of Nortricyclene, Norbornene, Norbornadiene and Quadricyclane." JACS, 95, 3197-3201, 1973.

Kabakoff, D.S., Bunzli, J.C.G., Oth, J.F.M., Hammond, W.B., and Berson, J.A.," Enthalpy and Kinetics of Isomerization of Quadricyclane to Norbornadiene. Strain Energy of Quadricyclane." JACS, 97, 1510-1512, 1975.

Lenhard, R.J., Dane, J.H., Parker, J.C., and Kaluarachchi, J.J., "Measurement And Simulation Of One-Dimensional Transient Three-Phase Flow For Monotonic Liquid Drainage." Water Resour. Res., 24, 853-863, 1988.

Maruyama, K., Tamiaki, H., and Kawabata, S., "Development of a Solar Energy Storage Process. Photoisomerization of a Norbornadiene Derivative to a Quadricyclane Derivative in An Aqueous Alkaline Environment." J. Org. Chem., 50, 4742-4749, 1985.

Tabushi, I., Yamamura, K., and Togashi, A., "Mechanism and Stereochemistry in Addition of Acetic Acid to Quadricyclane." J. Org. Chem., 41, 2169-2172, 1976.

SECTION III

1-D LEACHING EXPERIMENTS WITH QUADRICYCLANE AND ITS REACTION PRODUCTS

A. INTRODUCTION

The aqueous migration of dissolved hydrocarbons is affected by the physical and chemical properties of both the organic compounds and the porous medium. This section describes 1-D column leaching experiments, which were conducted to investigate the transport of dissolved quadricyclane and its reaction products *exo*-5-norbornen-2-ol and nortricyclyl alcohol in a sand and four selected natural soils. The main objective was to obtain the retardation factors for the respective organic compounds and the longitudinal dispersivity values of the porous media from measured breakthrough curves of the dissolved organic compounds and tritiated water.

B. THEORY

Under the assumptions of a constant volumetric water content (-) and a mean pore water velocity v (m/s), the one-dimensional advection-dispersion-sorption equation can be written as:

$$R \frac{\partial C}{\partial t} = D \frac{\partial^2 C}{\partial x^2} - v \frac{\partial C}{\partial x} \qquad (1)$$

where R is the dimensionless retardation factor, C is the concentration (moles/m^3 of solution), t is time (s), and x is the spatial coordinate (m) (Domenico and Schwartz, 1990). The longitudinal hydrodynamic dispersion coefficient (D, m^2/s) can be written as:

$$D = D_d + D_m = D_d + \alpha_l * v, \qquad (2)$$

where D_d and D_m are the coefficients of effective molecular diffusion and mechanical dispersion (m^2/s), respectively, and α_l is the longitudinal dispersivity (m).

C. QUADRICYCLANE

1. Materials and Methods

A 30 cm long glass column (I.D. 5 cm) with Teflon® end caps was packed as homogeneously as possible with one of the previously collected natural test soils (Güven et al., 1995), viz., TNOLPH (low organic matter; high pH; Table 6). This soil was selected for the first leaching experiment because the low organic matter content would minimize adsorption and the relatively high pH would minimize the chemical reactions. The mass of the soil packed into the column was measured to estimate the porosity. Because the soil pH affects the chemical reaction rate of quadricyclane, the common practice of first flushing the column with CO_2, to attain complete saturation when water is introduced, was avoided. Instead, the column was saturated under vacuum with degassed water. After full saturation had been achieved, the column was flushed with several pore volumes of a base solution, whose pH and ionic strength had been adjusted to match the natural composition of the soil water, while trace amounts of thymol and mercuric chloride were added to inhibit microbial activity. A volumetric infusion pump (Imed 980C) was used to inject the base solution into the column at a flow rate of 3.4 mL/hour. After several pore volumes had been flushed through the column,

a pulse of about 1.5 pore volumes of base solution, to which a known quantity of dissolved quadricyclane and 0.5μCi Tritium had been added, was applied. The effluent of the columns was sampled every 10 minutes and the collected samples divided into two parts: 1.5 mL was analyzed for tritium using a Tricarb 1900 TR liquid scintillation counter (Packard Instruments), while the remaining solution was analyzed for hydrocarbons using a Shimadzu gas chromatograph (Section II).

The CXTFIT 2.0 program (Toride et al., 1995), which, through optimization of the D and R values, minimizes the difference between measured effluent concentration values and those obtained by the solution to Equation 1, was used to analyze the effluent data.

2. Results

The leaching experiment was conducted over 3 months. During that period we did not detect any measurable amounts of quadricyclane or its reaction products in the effluent. Occasionally, however, we observed small peaks, with retention times close to those of exo-5-norbornen-2-ol and nortricyclyl alcohol. After three months the column was sliced into 10 pieces three cm in height. These slices were then used for the extraction of any organic compounds which were possibly present using the method described in Section II. No quadricyclane, norbornadiene, nortricyclyl alcohol, or exo-5-norbornen-2-ol was detected anywhere in the column. We hypothesized that the quadricyclane initially sorbed to the TNOLPH soil and subsequently slowly formed the two reaction products. We speculate that these reaction products are less hydrophobic than quadricyclane (Section II); consequently, they have lower retardation factors. Since the pH of the TNOLPH soil was rather high, reaction of quadricyclane into the reaction products can, indeed, be expected to be fairly slow. This would explain the lack of measurable concentrations of the two reaction products in the effluent solutions.

3. Conclusions

For the selected soil, which has a relatively high pH (Table 6), we did not detect quadricyclane in the effluent and only occasionally had indications of very small concentrations of its reaction products. Kinetic studies, described in Section II, showed that dissolved quadricyclane undergoes rapid reactions in acidic aqueous environments. This indicates that the aqueous migration of quadricyclane under such conditions should not be a significant problem. Based on these two conclusions, we decided to switch our attention to the aqueous movement of the two identified reaction products of quadricyclane: nortricyclyl alcohol and *exo*-5-norbornen-2-ol.

D. NORTRICYCLYL ALCOHOL AND *exo*-5-NORBORNEN-2-OL

1. Materials and Methods

The leaching experiments with the two reaction products were conducted as described under C.1 with the exception of the flow rates, which were adjusted to obtain a mean pore water velocity of 0.75 m/day. One column was packed with clean FS 2.8 sand, while the other column was packed with the ALOLPL soil (low organic matter; low pH, Table 2). The pH and ionic strength of the leaching solutions were again adjusted to those of the natural soil. For the sand the ionic strength was also set to 0.0005 N, and the pH was adjusted to neutral.

2. Results

Figures 18 and 19 show the breakthrough curves for nortricyclyl alcohol, *exo*-5-norbornen-2-ol and tritiated water from the columns filled with the clean sand and the ALOLPL natural soil. The curves show extreme scatter for the concentration of the two reaction products. After further investigation, this scatter was attributed to a so far unexplained problem with the analytical procedure. Figure 20 shows the results of an experiment in which quadricyclane, norbornadiene, exo 5-norbornen-2-ol and nortricyclyl alcohol in a natural soil were extracted in dodecane, and then analyzed using the four point measurement with the GC (see Section 2, II.A.1. for details of the method). The confidence level of a linear regression line through the data points was greater than 0.9999, implying good reproducibility for the measurements. When quadricyclane and norbornadiene were analyzed as part of an aqueous/isopropanol mixed solvent system (Figure 21a), the confidence level was reduced to 0.9990. Using the same procedure for exo-5-norbornen-2-ol and nortricyclyl alcohol in the isopropanol/water mix, however, the scatter in the data is much greater, as shown in Figure 21b. The confidence level dropped to an unacceptable level of 0.89, and no accurate and reproducible measurements could be made.

3. Conclusions

We were unable to measure the concentrations of *exo*-5-norbornen-2-ol and nortricyclyl alcohol in the effluent solution with the existing analytical procedure. The reason for this poor result is not obvious, but is clearly related to the solvents used. The decision was therefore made to abort the experiments until a more successful analytical procedure can be developed. Initial experiments to examine the feasibility of monitoring the *exo*-5-norbornen-2-ol and the nortricyclyl alcohol using High Performance Liquid Chromatography are outside the scope of this report, and have not been reported here. Good separation has been obtained, but it has not yet been determined if the method is sufficiently sensitive to detect the low levels found in the column experiments.

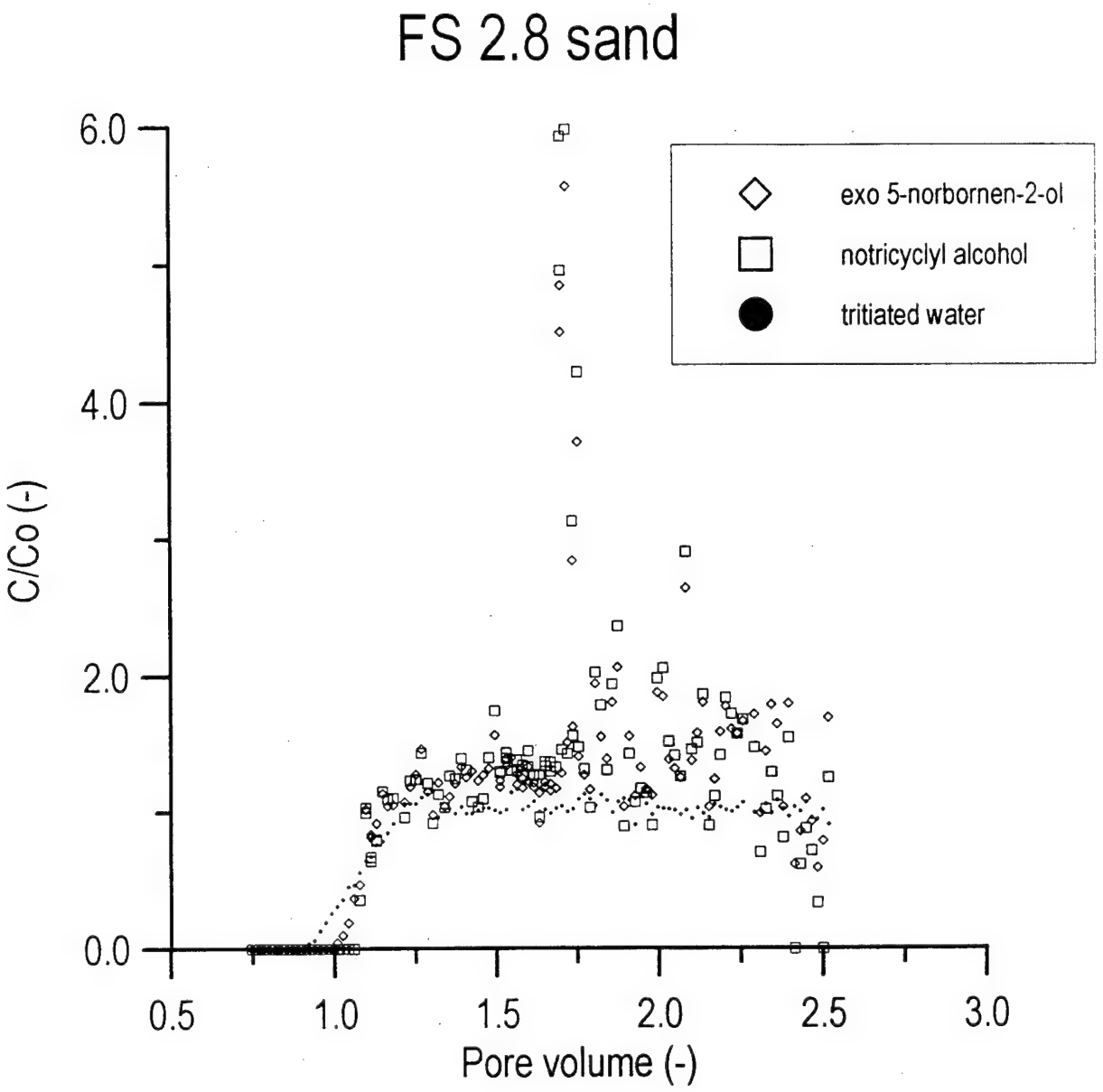

Figure 18. Measured Breakthrough Curves of *exo*-5-norbornen-2-ol, Nortricyclyl Alcohol, and Tritiated Water from a Column Filled with FS 2.8 Sand.

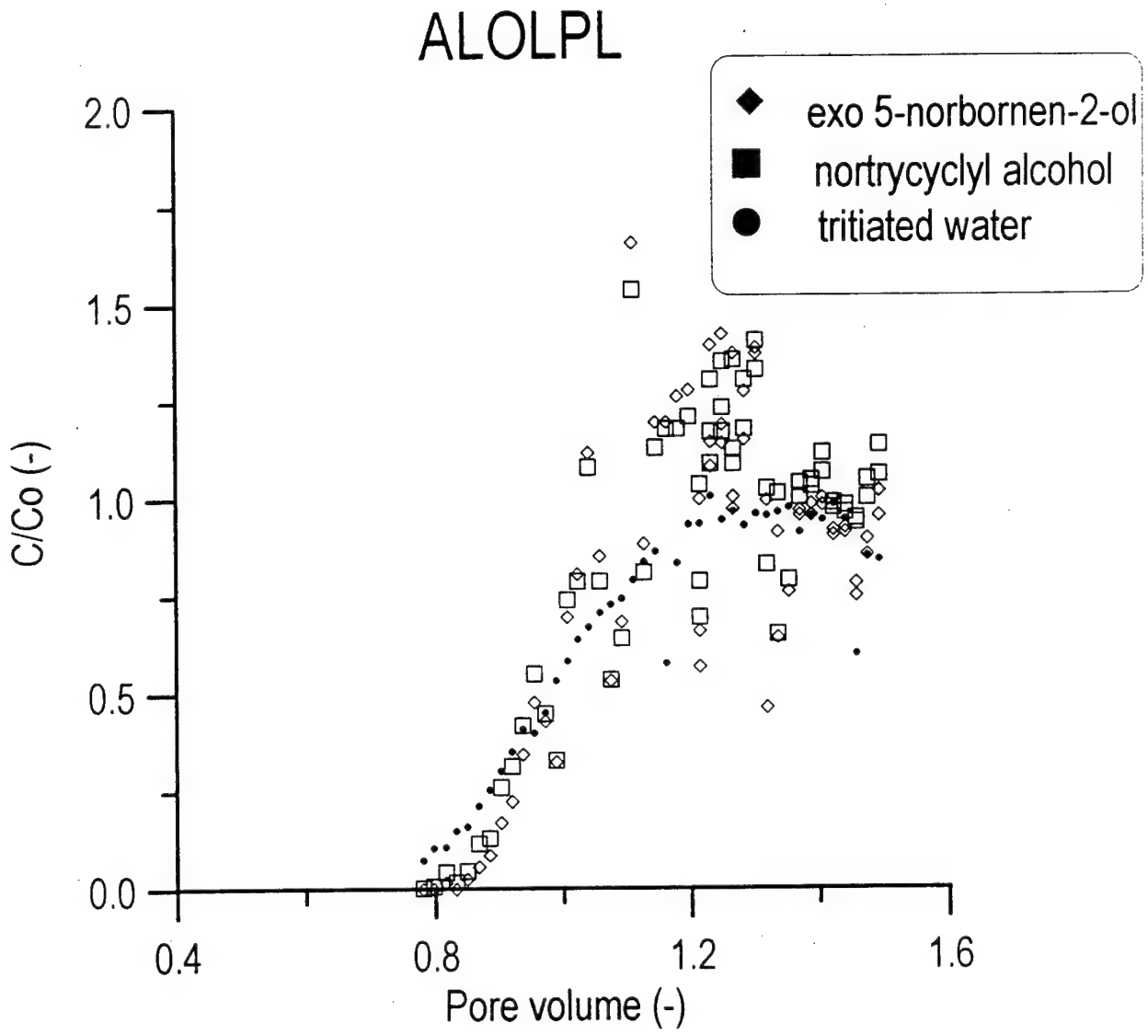

Figure 19. Measured Breakthrough Curves of *exo*-5-norbornen-2-ol, Nortricyclyl Alcohol, and Tritiated Water from a Column Filled with the ALOLPL Soil.

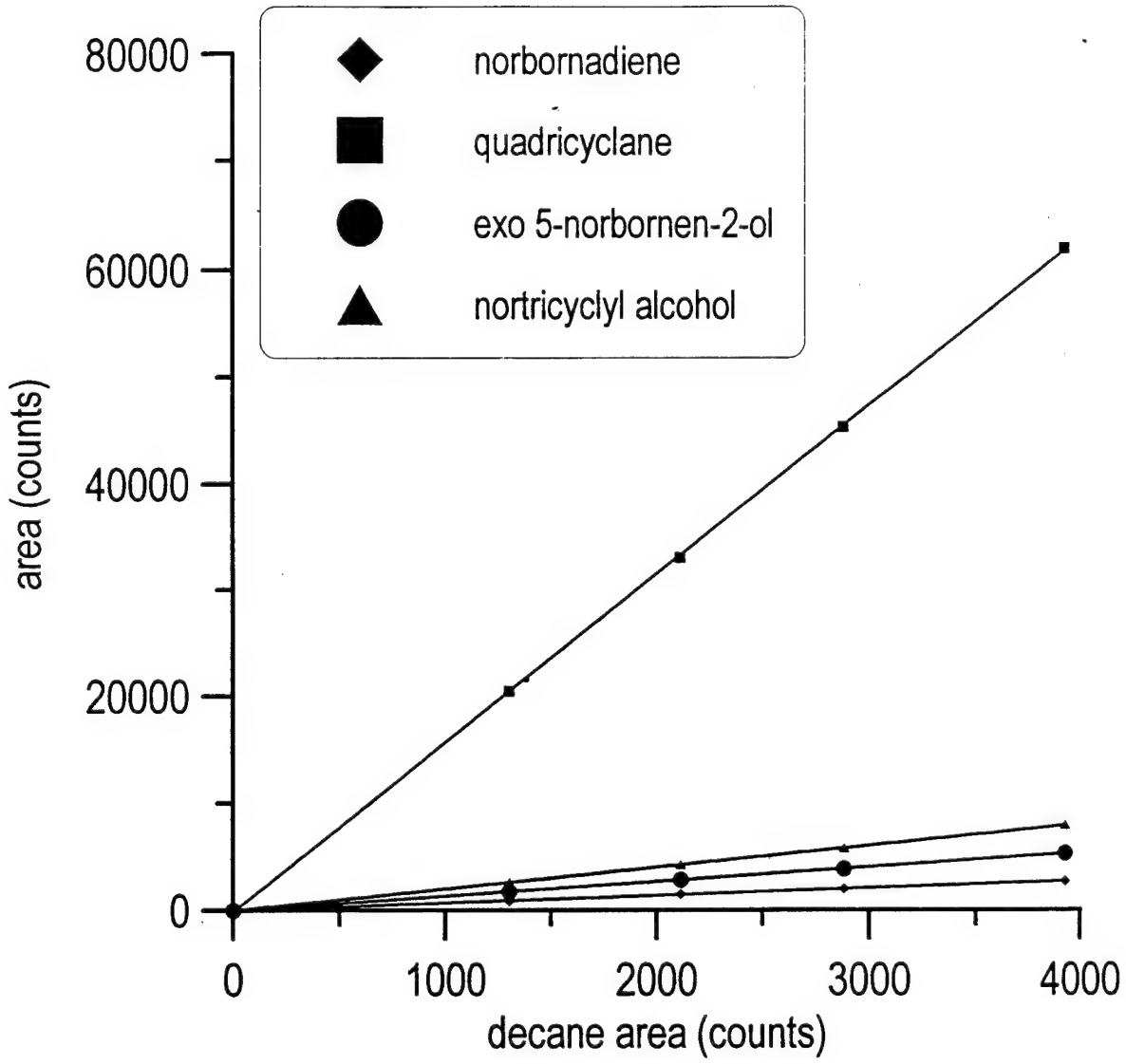

Figure 20. Typical Results of GC Analysis of Compounds Norbornadiene, Quadricyclane, 5-norbornen-2-ol, and Nortricyclyl Alcohol in a Mixed Dodecane/Decane Solvent.

(a)

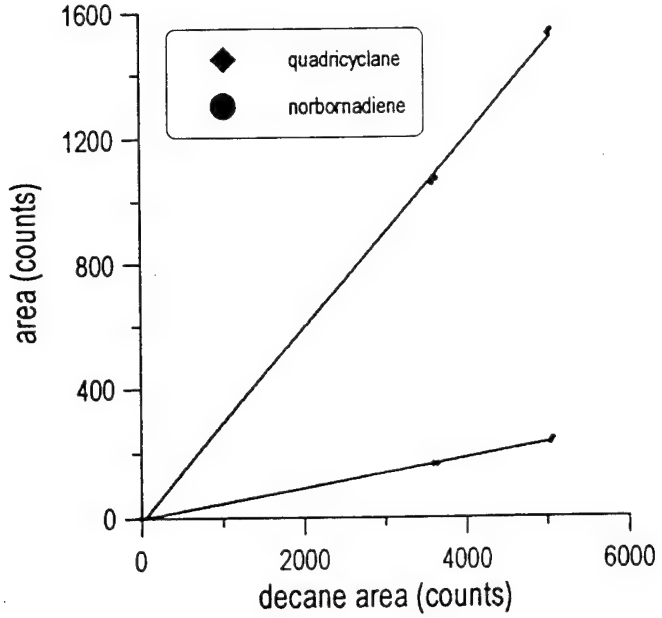

(b)

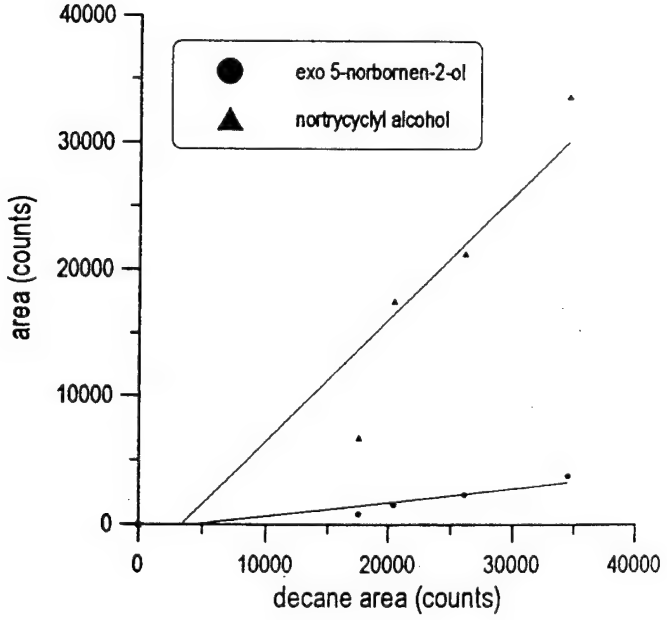

Figure 21. Result of GC Analysis of Norbornadiene/Quadricyclane (a), and 5-Norbornen-2-ol/ Nortricyclyl Alcohol (b), Respectively.

REFERENCES FOR SECTION III

Güven, O., Dane, J.H., Hill, W.E., Hofstee, C., and Mamballikalathil, R., Subsurface Transport of Hydrocarbon Fuel Additives and a Dense Chlorinated Solvent, Interim Report, AL/EQ-TR-1994-0039, Armstrong Laboratory, Tyndall Air Force Base, Florida, January 1995.

Domenico, P.A., and Schwartz, F.W., Physical and Chemical Hydrogeology. John Wiley & Sons, New York, N.Y., 824 pp, 1990.

Toride, N., Leij, F.J., and Van Genuchten, M. Th., The CXTFIT Code for Estimating Transport Parameters from Laboratory or Field Tracer Experiments, Version 2.0., Research Report Nr 137. US Salinity Laboratory, Riverside, California, 1995.

SECTION IV
TWO-DIMENSIONAL EXPERIMENTS WITH QUADRICYCLANE IN FLOW CONTAINER FC1

A. INTRODUCTION

This section describes a set of nominally two-dimensional laboratory experiments simulating spills of quadricyclane in a flow container packed with various homogeneous and heterogeneous porous media. A good understanding of the subsurface behavior of quadricyclane is important because of the potential that exists for the contamination of a large portion of an aquifer in the event of a spill (Mercer and Cohen, 1990). Therefore, the purpose of the experiments described in this section was to provide information on the transport and subsequent dissolution of quadricyclane in porous media, by means of flow visualization photographs and quantitative chemical analyses of fluid samples. The experiments also included an investigation of the cleanup of quadricylane spills with a nonionic surfactant solution. While a number of similar studies have been performed previously (see, e.g., Mercer and Cohen, 1990) with other non-aqueous-phase liquids (NAPLs), this is the first time that such quantitative information is documented on the subsurface behavior of quadricylane.

B. MATERIALS AND METHODS

1. Flow Container

The flow container used to carry out the experiments described in this section is designated as flow container FC1. Figures 22, 23, and 24 show the details of the flow container. The flow container consists of two end inlet and outlet constant-head chambers and a middle porous medium chamber. The dimensions of the porous medium chamber are 80 cm long, 40 cm high and 10 cm wide. The flow container was constructed of Teflon®, glass and stainless steel materials which do not react with the chemicals used during the experiments. The front side of the porous medium chamber was made of glass to allow visualization and to be able to take photographs during the experiments. The back side was constructed of a Teflon® plate and provided with holes to allow insertion of a set of injection and extraction ports. A photograph of the back of the flow container is shown in Figure 25. The Teflon® parts were etched and put together using a Chemgrip® Bonding Kit (AIN Plastics, Norfolk, VA). The pieces were also screwed together for greater strength. The joints were then sealed using a solvent resistant Silicon RTV sealant (DOW Corning, Midland, MI) to prevent any leaks. This sealant is resistant to PCE and most other organic solvents.

The inlet and outlet head chambers and the porous medium chamber are separated by filters. The filters are made of perforated Teflon sheets with 1/16 inch holes drilled at 1/8 inch spacing and a stainless steel wire cloth (70x70 mesh, purchased from McMaster Carr Co., Atlanta, GA) in between (see Figure 26). The filters prevent the porous medium grains from getting into the end head chambers. The inlet and outlet head chambers are provided with piezometric tubes in order to observe the levels (head) of water in them. The bottom of the flow container is provided with five drain valves (as shown in Figure 23) which can be used to drain the water or NAPL from the flow container.

2. Ambient Water Supply

The inlet and outlet head chambers were connected to constant head tanks which could be raised or lowered using laboratory jacks. The horizontal ambient water flow could be established through the porous medium by adjusting the levels of the head tanks. The water used during these experiments was deionized

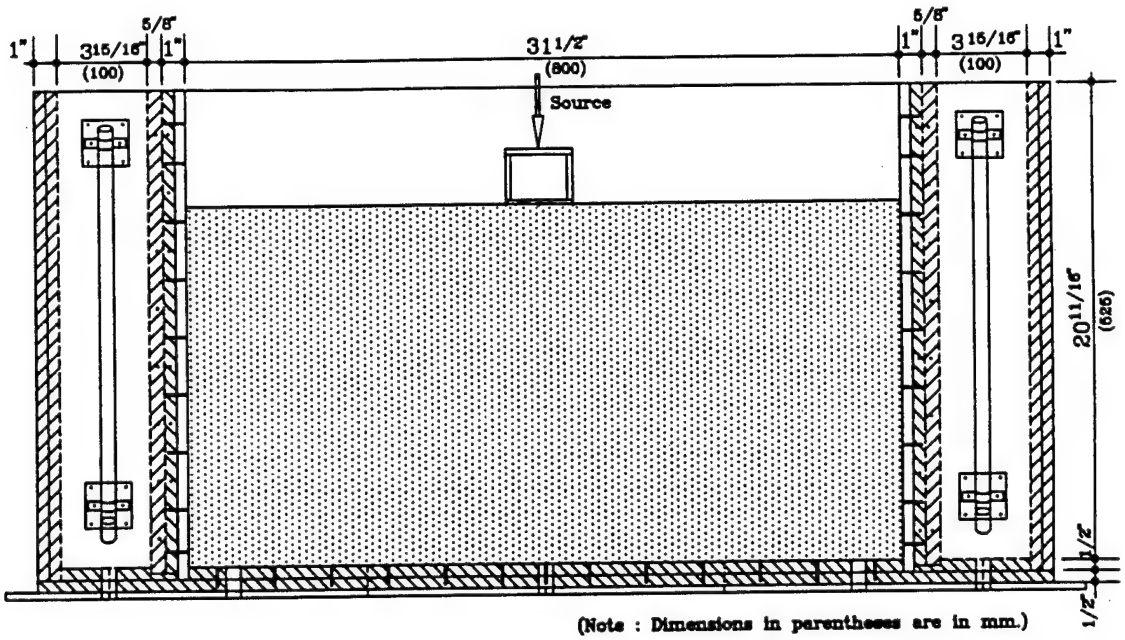

Figure 22. Front Elevation View of the Flow Container.

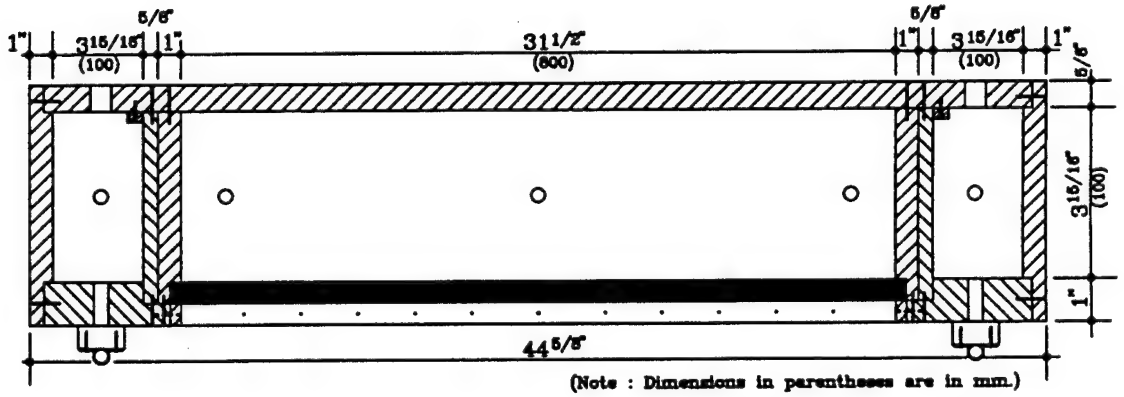

Figure 23. Plan View of the Flow Container.

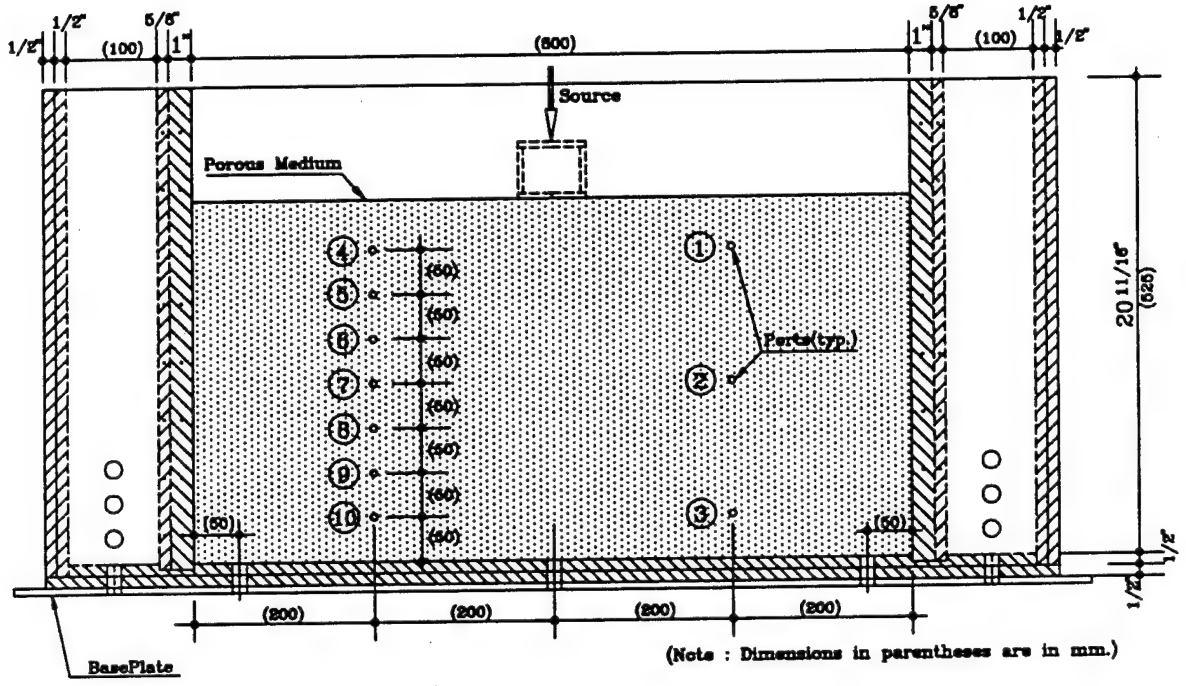

Figure 24. Back Elevation View of the Flow Container Showing the Port Hole Locations.

Figure 25 Photograph of the Back of the Flow Container

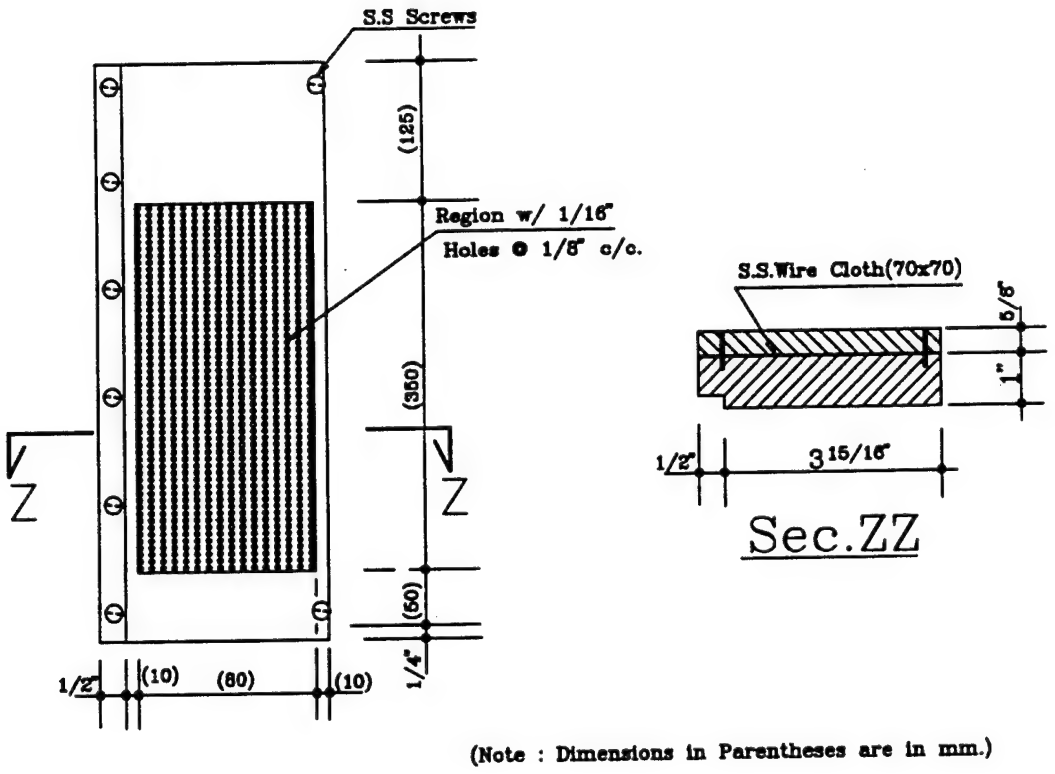

Figure 26. Details of the Porous Medium End Filters.

water low in ionic, organic, and particulate contamination obtained with a Millipore Milli-RO system which deionizes the water and a Millipore Milli-Q system which removes the organic and particulate contaminants (both purchased from Millipore Corp., Bedford, MA).

3. Injection and Extraction System

The porous medium chamber is provided with ten injection and extraction ports through which liquids can be pumped in and out. Each port is made of a stainless steel tube 1/4 inch in diameter with 3/64-inch diameter holes drilled around it at uniform spacing and staggered so as to cause the liquid injected or extracted to flow uniformly in all directions. A photograph of an injection and extraction port is shown in Figure 27. The ports were wrapped with stainless steel wire cloth to prevent clogging of the holes and also to cause the flow in or out of the ports to be more uniform. The locations of the ports are shown in Figure 24. The ports were inserted into the flow container through the back wall (see Figure 25) and extended over the full width of the flow container. The tips of the ports were sealed and rested on the inside of the front glass wall. The tips of the ports are visible in the flow visualization photographs presented later in this section. Peristaltic pumps and viton tubing (Cole-Parmer Instrument Co., Niles, IL) were used to inject and extract the liquids through the ports.

4. Contaminant Source

A line source was designed and built (as shown in Figure 28) for the introduction of the NAPL into the porous medium. The line source had a slit of approximately 0.2 cm width and length equal to the width of the porous medium. The contaminant was introduced through viton tubing into a T-shaped glass tube, the ends of which were sealed and which had small holes on its sides. The contaminant dripped through the holes onto a wire cloth and flowed out through the slit at the bottom of the glass box. This system provided a fairly uniform loading rate of the contaminant across the width of the porous medium.

5. Porous Media Properties and Packing

The porous media used were Flintshot FS 4.0 Ottawa (coarse) sand and Flintshot FS 2.8 Ottawa (medium) sand. The sands were purchased from F&S Abrasive, Birmingham, AL. The particle size distributions for the Flintshot FS 4.0 and 2.8 sands are presented in Table 9. The median grain size (d_{50}) for Flintshot FS 4.0 and FS 2.8 sand is 0.60 mm and 0.50 mm respectively.

The packing of the test sands in the flow container to obtain nominally homogeneous media was done in a systematic manner following the procedure of Hayworth (1993) and Mamballikalathil (1995). The

TABLE 9. PARTICLE SIZE DISTRIBUTION OF POROUS MEDIA.*

	Particle Size Class (mm)				
	<0.106	0.106 to 0.25	0.25 to 0.50	0.50 to 1.0	1.0 to 2.0
Coarse sand (FS 4.0)	trace	0.2	38.4	61.4	0.0
Medium sand (FS 2.8)	0.6	7.2	53.6	38.6	0.0

*References: Dane et al.,1994; Hayworth,1993; Oostrom,1991

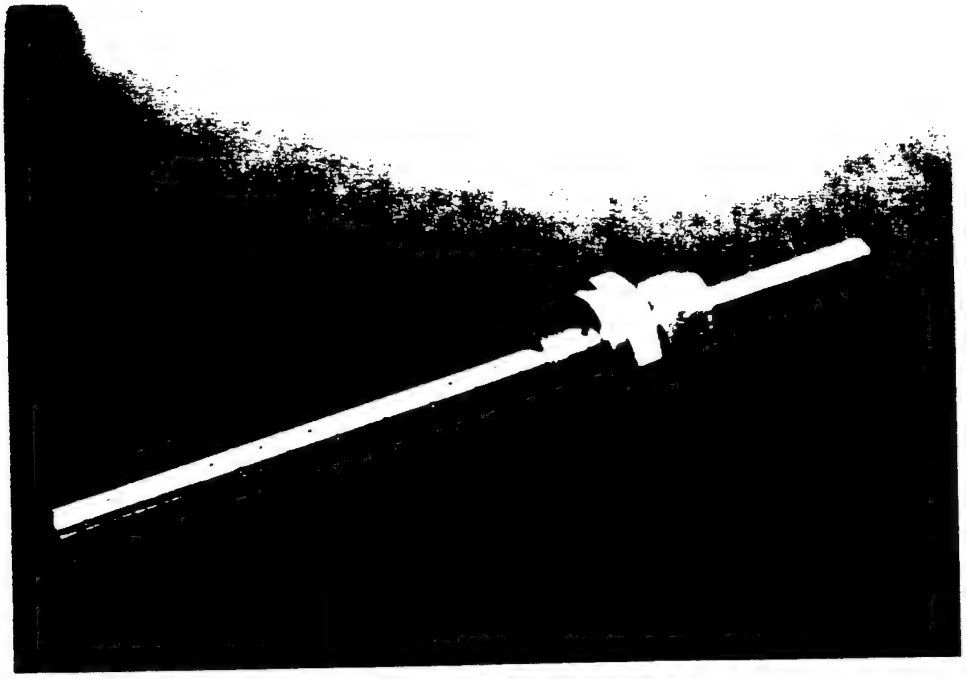

Figure 27 Photograph of a Typical Injection and Extraction Port

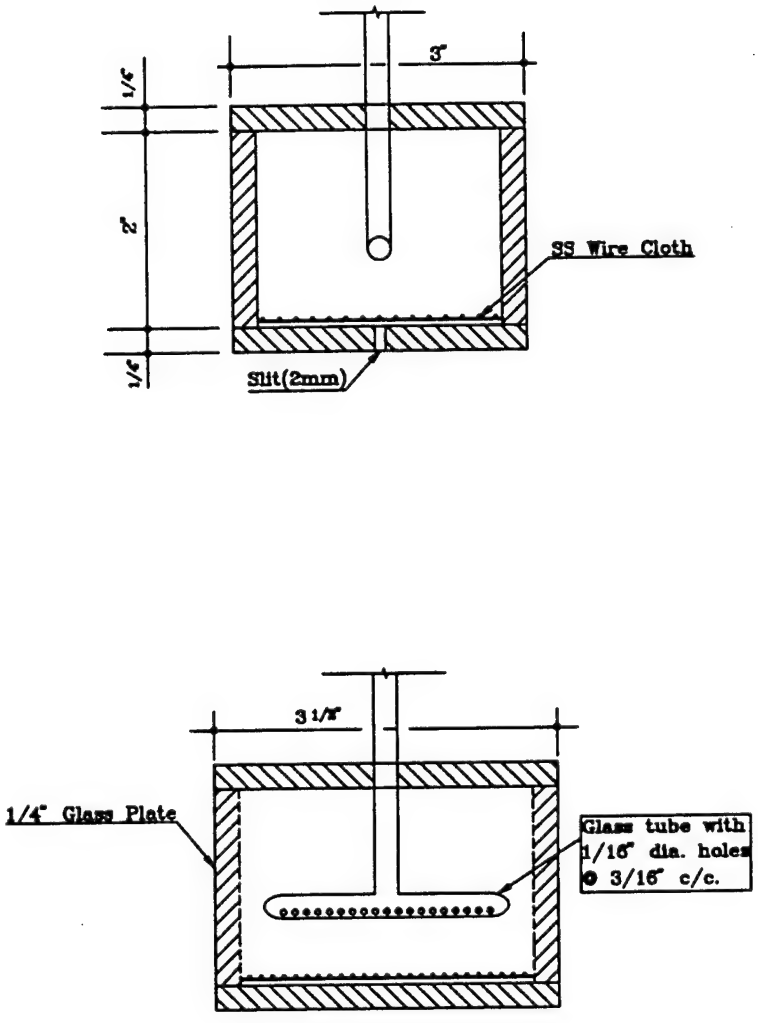

Figure 28. Front View (Top) and Side View (Bottom) of the Contaminant Line Source Showing the Details.

technique involved putting in the sand (porous medium) in 1-cm layers and mixing each layer systematically with the previous layer. This procedure was continued until the porous medium reached a height of about 40 cm.

6. Experimental Methods

Four experiments were conducted with quadricyclane in flow container FC1, in which quadricyclane was first emplaced, then flushed with water, and finally flushed with a surfactant solution. Table 10 lists the important experimental parameters for each experiment. In three experiments, the container was packed homogeneously with Flintshot FS 4.0 or 2.8 sand. In one experiment, the test medium was heterogeneous and consisted of layers of FS 4.0 and 2.8 sands. The layers were formed by first packing FC1 with 5 cm of coarse (FS 4.0) sand. Next, 5 cm of fine material (FS 2.8) was packed in the box on top of the coarse sand. This procedure was repeated until a total of 40 cm of FC1 was filled with sand. Prior to each experiment, the medium was first saturated gradually by raising the water table to the top of the medium. The water table was then lowered to approximately halfway to the top of the medium and a quadricyclane spill was simulated. Quadricyclane (purchased from Aldrich Chemical Company) was dyed red using Oil Red EBN. In the first experiment, designated as 1QAF, a continuous source spill was simulated in which 30 mL of quadricyclane was introduced continuously through the source. In the subsequent experiments, discontinuous source spills were simulated. In Experiments 3QAF and 4QAF, the discontinuous spills consisted of one 10 mL dose of quadricyclane added every 10 minutes over a twenty minute period for a total of a 30 mL. In experiment 2QAF, an additional 5 mL was spilled after 30 ml, for a total spill of 35 mL. The quadricyclane allowed to redistribute for approximately 24 hours, upon which the water table was slowly raised to the top of the porous medium.

TABLE 10. EXPERIMENTAL PARAMETERS USED IN EACH EXPERIMENT.

Experiment	Type of Medium	Total Horizontal Flow Rate(*) (mL/min)	Heterogeneous/ Homogeneous	Volume of Quadricyclane Spilled (mL)
1QAF	Flintshot FS 4.0	-----	Homogeneous	30
2QAF	Flintshot FS 4.0	79.47	Homogeneous	35
3QAF	Flintshot FS 2.8	25.47	Homogeneous	30
4QAF	Flintshot FS 2.8 and 4.0	74.53	Heterogeneous 5 cm Layers of FS 2.8 and 4.0	30

(*) Average value for the water flushing segment.

After the water table was brought to the top of the porous medium following the emplacement segment of each experiment, a horizontal flow was started in the flow container to flush the spilled quadricyclane with water and to study the dissolution which took place. The flow was from left to right relative to the front (glass) wall of the container, as depicted in Figure 29. The flow field was established by imposing a head difference of 2 cm between the end chambers and by simultaneously allowing a continuous outflow of water through the seven extraction ports shown in Figure 29. The rates of outflow from the downstream (right) end chamber and from the extraction ports were monitored throughout this segment of each experiment. In the first two experiments (1QAF and 2QAF), the outflows from the ports were controlled by means of adjustable clamps attached to the outflow tubing. In the last two experiments (3QAF and 4QAF), the extraction port outflows were controlled by means of Masterflex pumps with cartridge pump heads, to provide a more steady and even distribution of the outflows. Effluent samples were taken from the extraction port outflows during the water flushing segment of each experiment. The extraction port closest to the center of the spilled contaminant source (Extraction Port 2, Figure 29) was sampled regularly. The other six ports were sampled at three different times during the course of an experiment for producing a concentration snap shot over the vertical section of the seven extraction ports. This segment of each experiment was conducted over a 12-hour period.

The last segment of each experiment consisted of injecting a surfactant solution dyed with fluorescein into an injection port and extracting fluid from an extraction port, while an ambient stream of water, flowing from left to right, was simultaneously maintained in the flow container by imposing a head difference of 2 cm between the end chambers. The general flow pattern in the flow container during the surfactant flushing segment of the experiments is depicted in Figure 30. The surfactant solution used in the experiments was a mixture of deionized water and Tween 80 (a commercially produced surfactant) with a surfactant concentration of 4.0% by volume. The apparent solubility of quadricyclane in this surfactant solution was determined to be 140,900 mg/kg by means of batch experiments. The surfactant solution was injected through the top injection port (numbered 1 in Figures 29 and 30) at a constant flow rate by means of a peristaltic pump, while another pump was used to extract fluid at the same flow rate from the top extraction port (Extraction Port 1 in Figures 29 and 30). Samples of the effluent from the extraction port were collected until quadricyclane concentrations fell below the detection limit of the gas chromatograph (GC).

C. RESULTS AND DISCUSSION

Experiments 1QAF and 2QAF:

The first two experiments, 1QAF and 2QAF, were useful in testing the operation of the experimental setup and in establishing the experimental procedures. They also allowed an evaluation of the effects of the spill type on the infiltration and spatial distribution of the spilled quadricyclane. As may be seen from Figures 31 and 32 which show photographs taken during the emplacement segments of experiments 1QAF and 2QAF, the extent of the lateral spreading in the unsaturated zone was larger for the discontinuous spill of experiment 2QAF (Figure 32) compared with that of the continuous spill of experiment 1QAF (Figure 31). In experiment 1QAF, it was observed that the quadricyclane infiltrated the medium as a relatively narrow finger. It appeared that, due to the continuous manner of the spill, the pressure at the tip of the finger always exceeded the necessary displacement pressure as the finger traveled downward to the top of the capillary fringe and the lateral spreading was minimized. However, in experiment 2QAF, it was observed that the spilled quadricyclane, which was introduced in discontinuous increments, initially infiltrated downward as a finger following each spill increment but discontinued its downward movement as the pressure at the tip of the finger dropped below the displacement pressure due to the discontinuation of the supply. The finger then

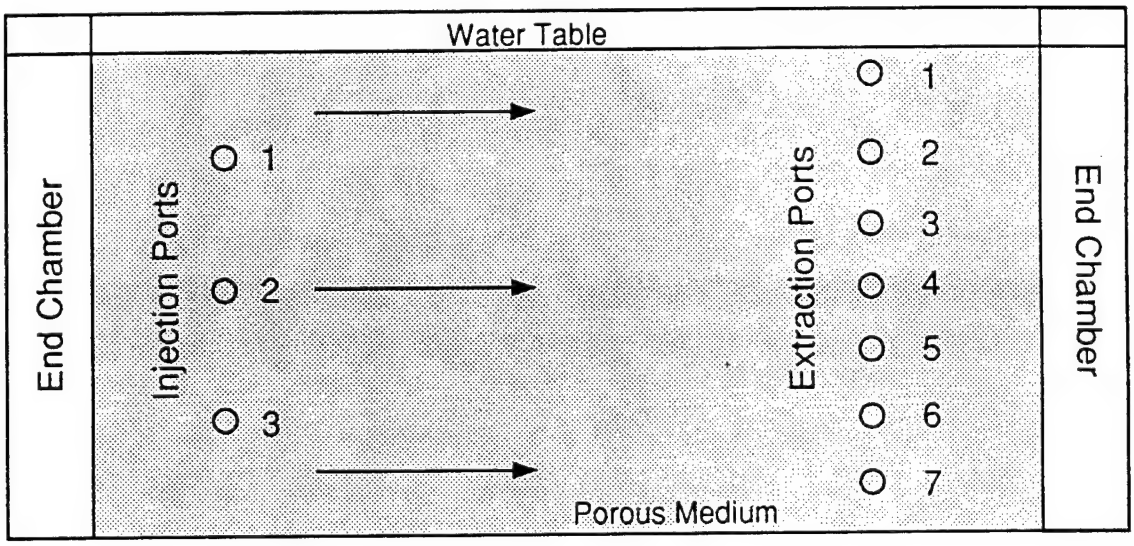

Figure 29. Sketch Showing the Flow Pattern During the Water Flushing Segment of the Experiments With Quadricyclane in Flow Container FC1.

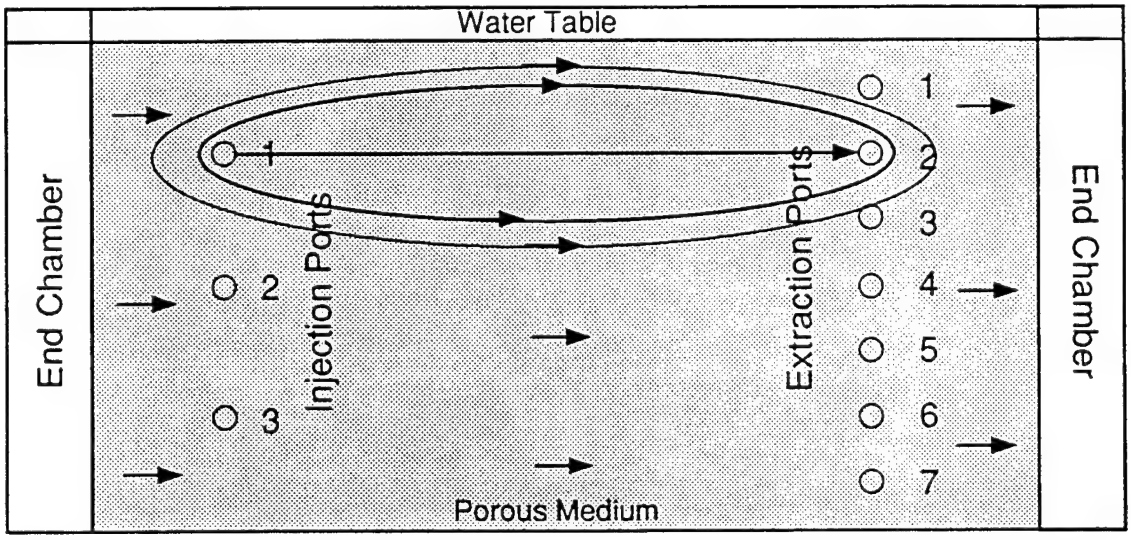

Figure 30. Sketch Showing the Flow Pattern During the Surfactant Flushing Segment of the Experiments With Quadricyclane in Flow Container FC1.

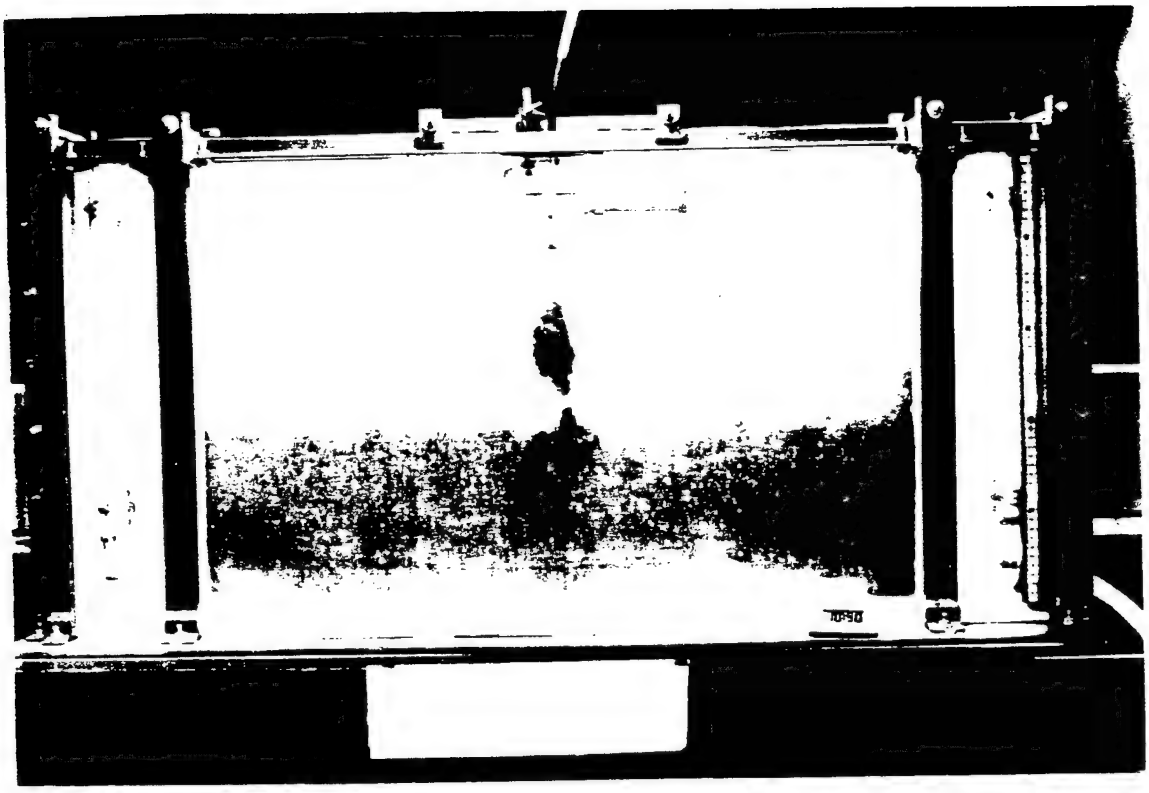

Figure 31 Quadricyclane Distribution 3.5 Hours after the Injection of the Continuous Spill Experiment (QAF)

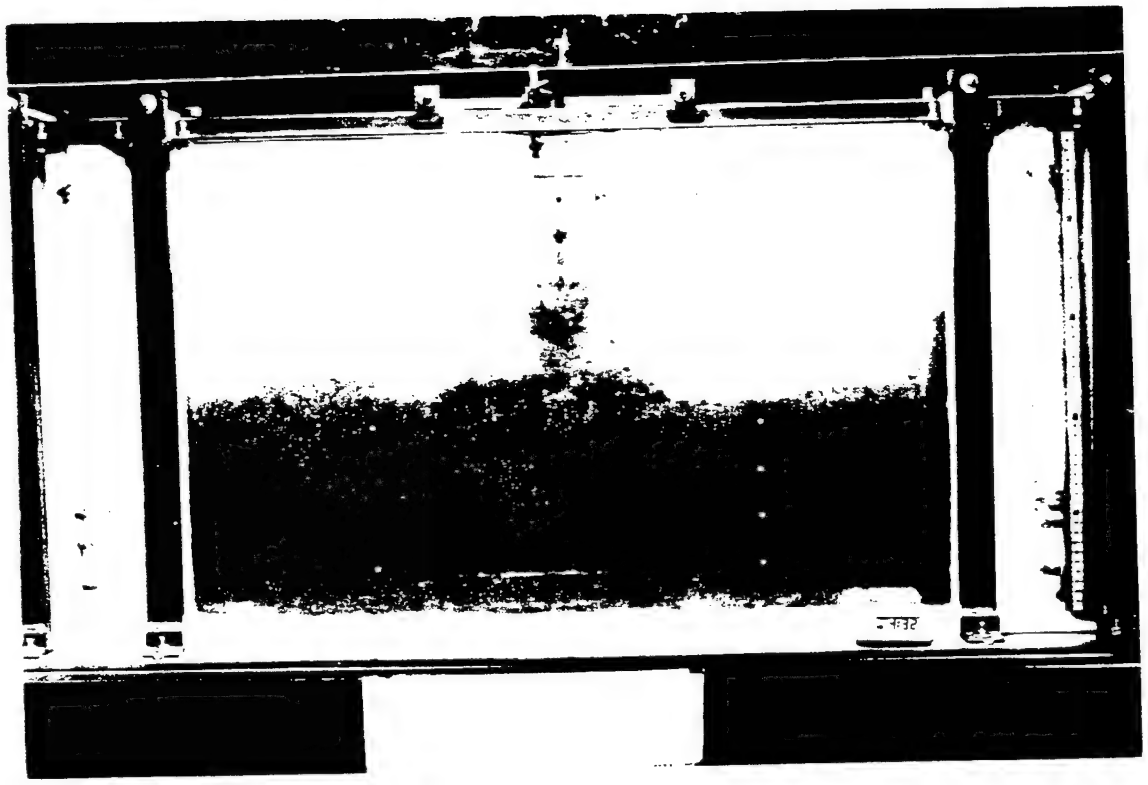

Figure 3. Quadricyclane Distribution 12 Hours after the First Injection of the Discontinuous Spill Experiment 2QAF1

tended to flatten and spread out laterally. The discontinuous spill of experiment 2QAF seemed to result in a somewhat more balanced spatial distribution of the spilled quadricyclane compared with the continuous spill of experiment 1QAF. In view of this, discontinuous spills were utilized in the subsequent experiments.

As experiment 1QAF was intended primarily as a preliminary experiment several different flow conditions were tested during the water flushing and surfactant flushing segments of this experiment. Although the results were useful for making decisions about the subsequent experiment, they are not included here because of their exploratory and preliminary nature. While experiment 2QAF also was partially exploratory in nature, data obtained during the water flushing and the surfactant flushing segments of this experiment are presented below.

Figure 33 is a plot of quadricyclane concentration (mg/kg) of the effluent from Extraction Port 2 and flow rate (mL/min) as a function of time during the water flushing segment of experiment 2QAF. The quadricyclane concentration is seen to fluctuate about an average of 250 mg/kg, which is close to but below the apparent aqueous solubility limit of quadricyclane (see Section II). The total horizontal flow rate (defined as the sum of all the outflows from the seven extraction ports and the effluent outflow from the downstream end chamber) also showed some fluctuation during the experiment. These two sets of data are plotted together to determine a relationship, if any, between the quadricyclane concentration and the flow rate.

Figure 34 is a plot of quadricyclane concentration as a function of time where samples were taken from all seven extraction ports during the water flushing segment of experiment 2QAF. Samples taken from Extraction Ports 1-3 showed that the quadricyclane concentration varied little with elevation and time. The lower four extraction ports had no trace of quadricyclane, therefore, the concentrations were set to zero and were not plotted on this graph. It can be inferred that the concentrations at ports 1-3 are consistent with the spatial distribution of the spilled quadricyclane seen in Figure 32. As shown in Figure 32, the upper three extraction ports were within the vertical extent of the quadricyclane spill while the lower four ports were below. Figure 34 shows that Ports 1-3 all had elevated quadricyclane concentrations, while Ports 4-7 produced no quadricyclane.

Figure 35 is a photograph taken near the end of the water flushing segment of experiment 2QAF. Notice how the residual near the surface has shifted in the direction of horizontal flow. This indicates that multiphase movement has occurred and could possibly be partly due to microemulsion formation and transport.

During the surfactant flushing segment of experiment 2QAF, the injection and extraction flow rates of the surfactant solution were each set at 30 mL/min. Figure 36 shows a picture taken near the termination of the surfactant flushing segment. It is seen that the surfactant solution was effective at removing the entrapped quadricyclane from the sand. Figure 37 shows a plot of the quadricyclane concentration in the extracted fluid as a function of time. Also shown in the plot is the variation of the flow rate of the effluent from the outlet end chamber as a function of time. From Figure 37, it may be seen that the concentrations undergo a sharp increase and then decrease and asymptotically approach zero. The sharp increase is due to the surfactant front passing through the region of quadricyclane residual. At this point there are a large number of blobs, so the interfacial area for dissolution is large, therefore, the concentrations are the largest. As the experiment progressed the number and size of the blobs decreased which reduced the interfacial area for mass transfer, thereby decreasing the concentrations. As a result of the surfactant flushing, the portion of the medium under the influence of the surfactant solution was remediated efficiently.

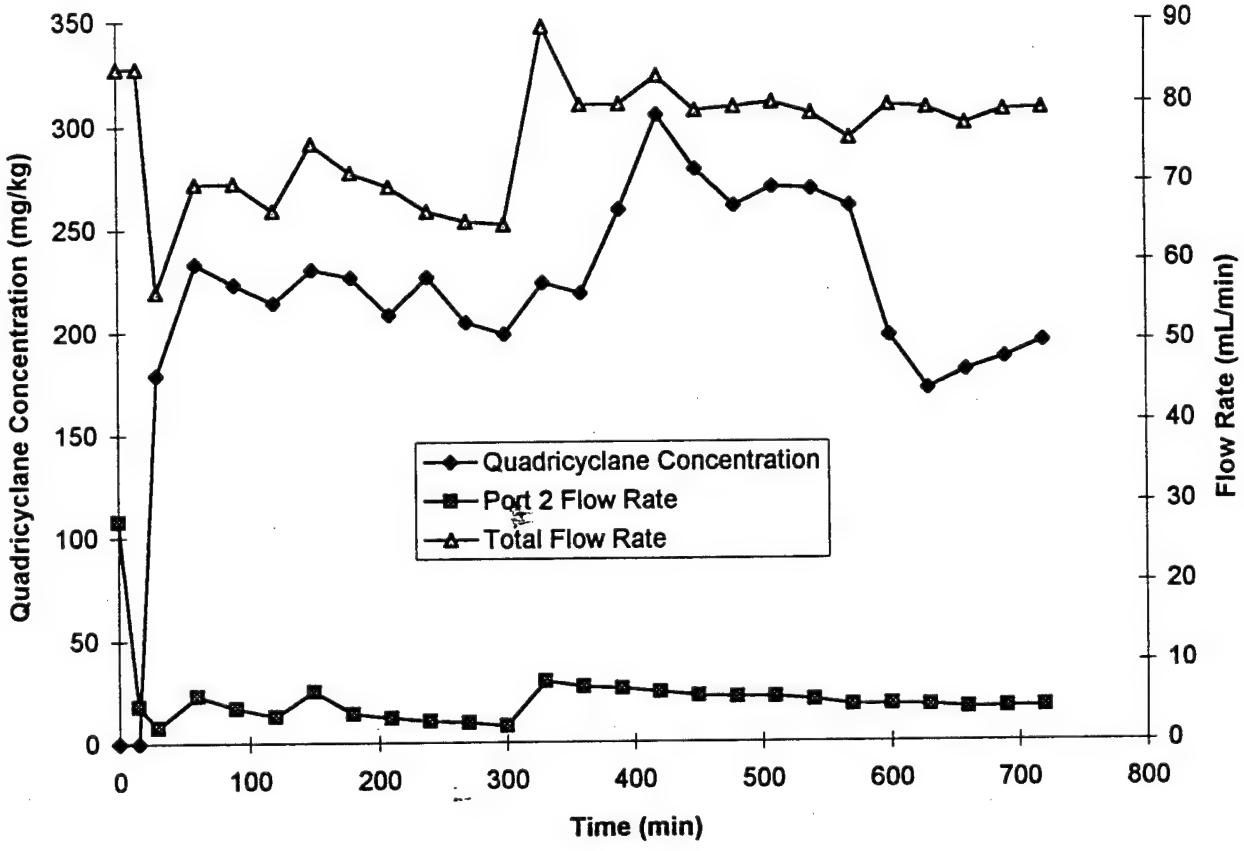

Figure 33. Quadricyclane Concentration and Flow Rate as Functions of Time for Experiment 2QAF. Samples Were Taken From Extraction Port 2 as the Quadricyclane Was Flushed with Water.

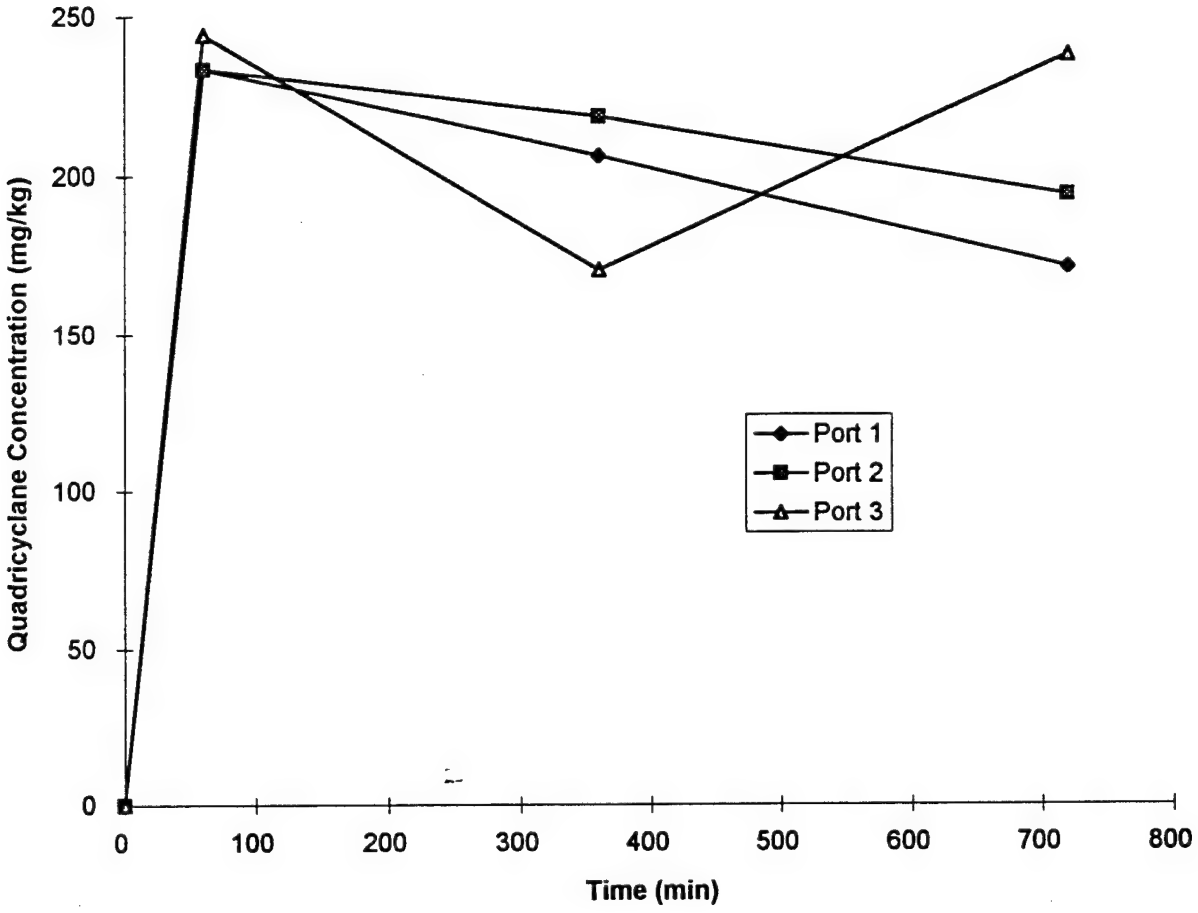

Figure 34. Quadricyclane Concentration as a Function of Time for the Water Flushing Segment of Experiment 2QAF. Samples Were Taken from Extraction Ports 1-7 as the Quadricyclane Was Flushed with Water. Samples Taken from Extraction Ports 4-7 Did Not Contain Any Quadricyclane.

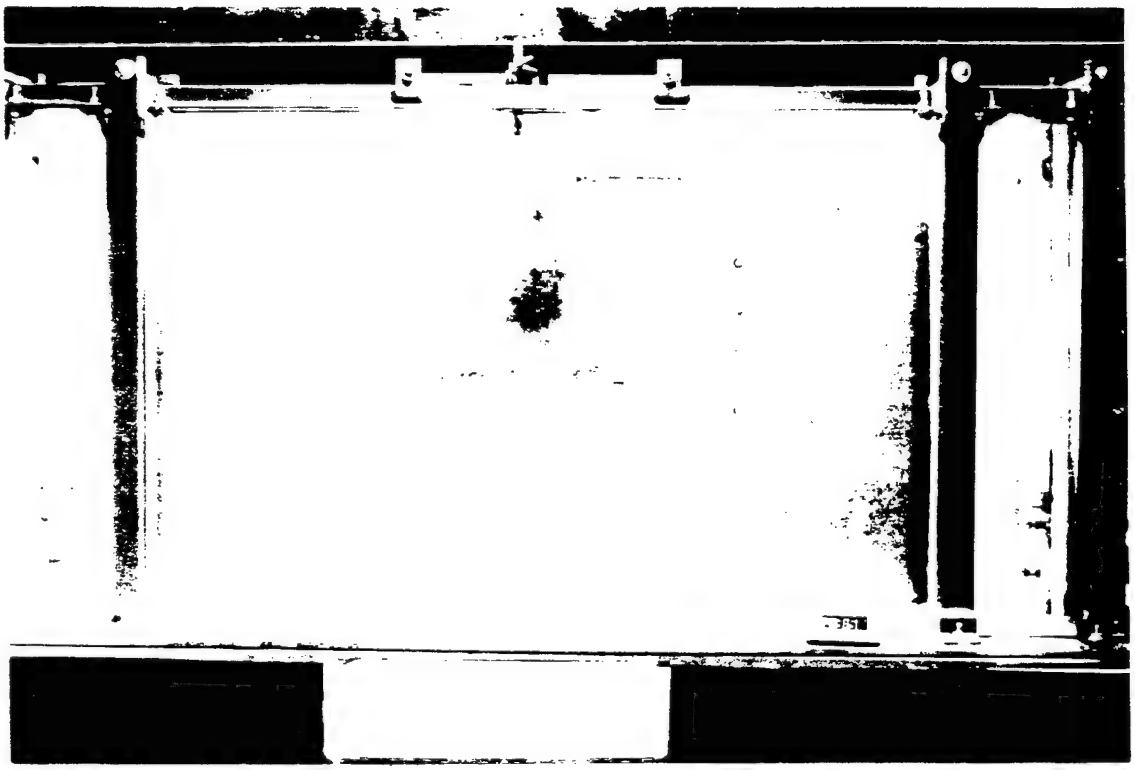

Figure 35 Quadricyclane Distribution Near the Termination of the Water Flushing Segment of Experiment 2QAF

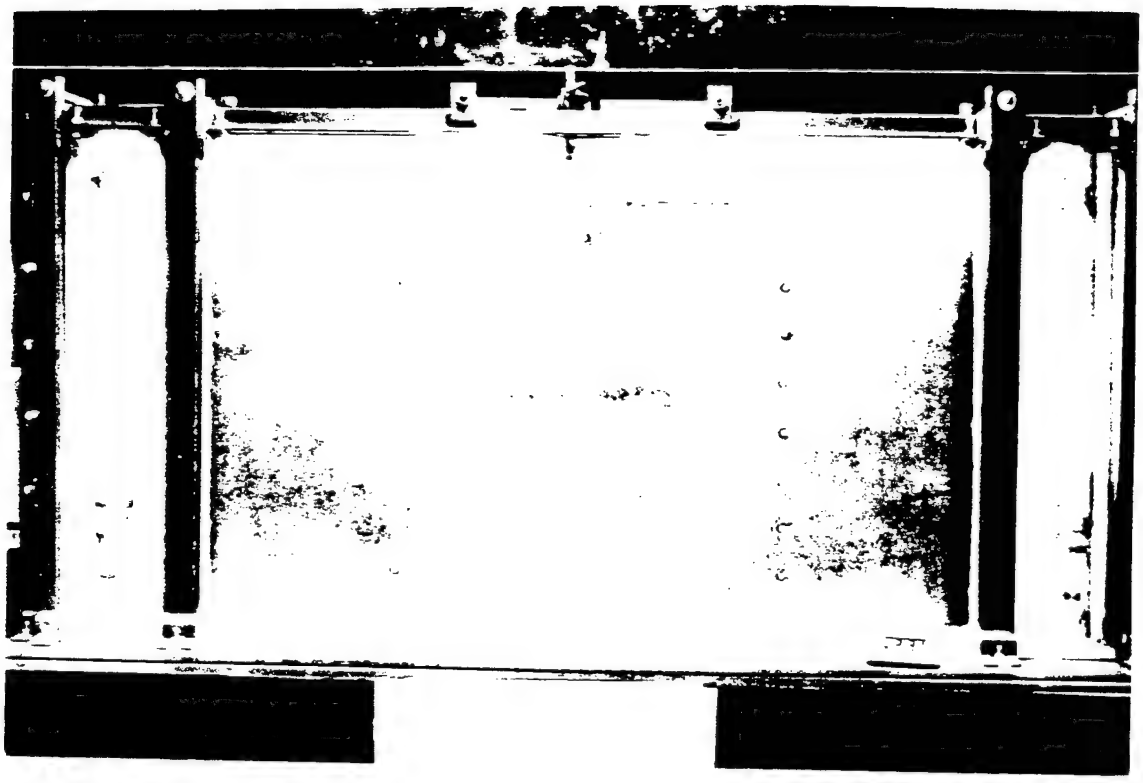

Figure 36 Quadricyclane Distribution Near the Termination of the Surfactant Flushing Segment of Experiment 2QAF

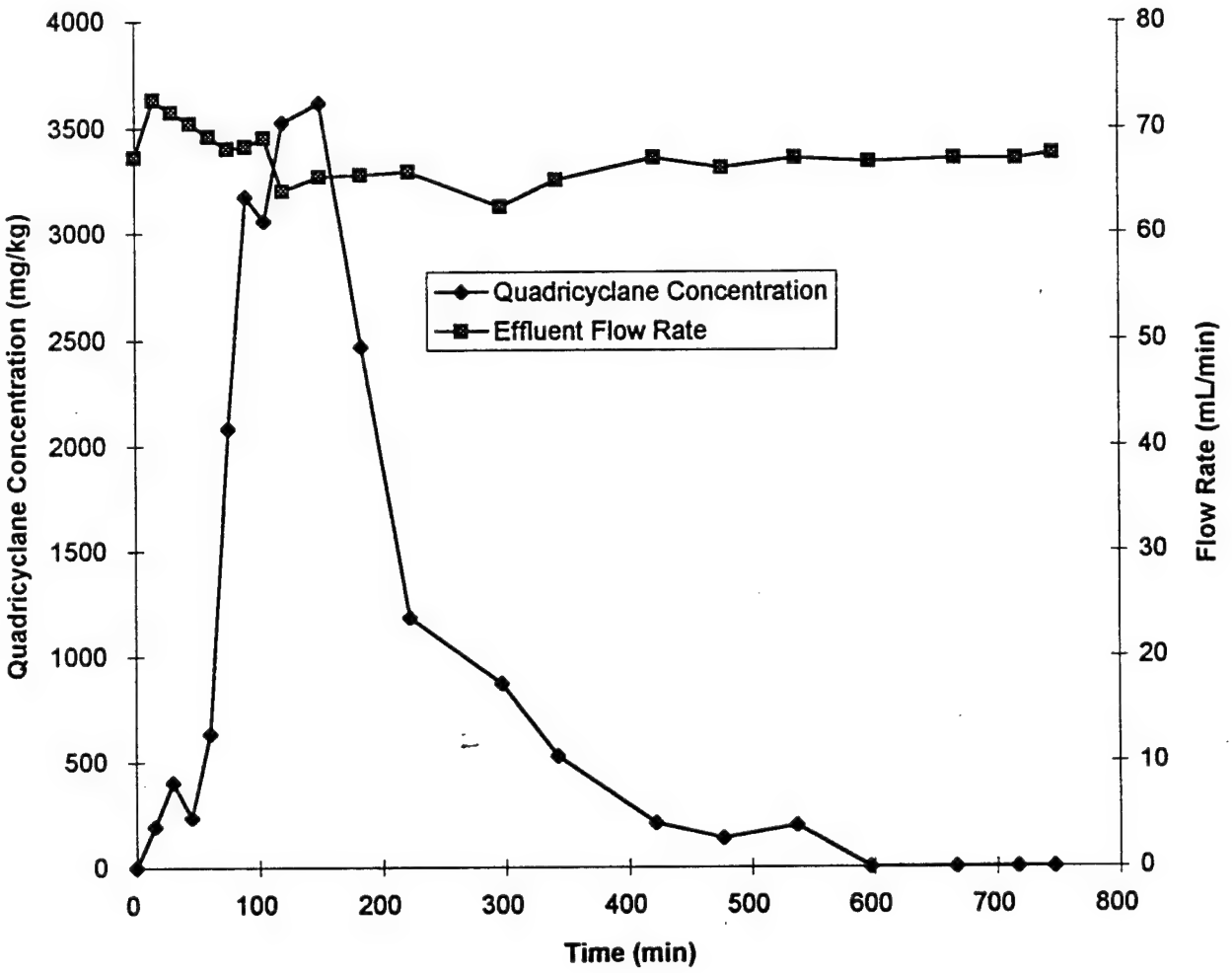

Figure 37. Quadricyclane Concentration and Flow Rate as Functions of Time for the Surfactant Flushing Segment of Experiment 2QAF.

Experiment 3QAF:

In this experiment, Flintshot FS 2.8 was used as the porous medium replacing the Flintshot FS 4.0 used in 2QAF. The first segment of this experiment involved emplacing the quadricyclane and studying its movement. Figure 38 is a photograph taken after the quadricyclane was assumed to be at static equilibrium (approximately one day after the start of the experiment). Notice that the quadricyclane has spread laterally a significant distance. The extent of the plume has been outlined by a red marker. Compared with Figure 32 the shape and size of the plume are different. The larger lateral spreading may have been caused by smaller pore sizes and, therefore, larger water saturations above the capillary fringe than in the case of FS 4.0.

The second segment of this experiment involved raising the water table and flushing the trapped quadricyclane with a horizontal flow while collecting samples from the extraction ports. The extraction port outflow pumping rates were set at 2 mL/min each throughout this segment of the experiment. As was the case in experiment 2QAF, samples were collected frequently from Extraction Port 2. Figure 39 is a plot of quadricyclane concentration and total flow rate as a function of time as the trapped quadricyclane was flushed by horizontal flow. This figure shows that the quadricyclane concentrations for Port 2 are approximately equal to 205 mg/kg during most of this segment, which is below the apparent aqueous solubility limit of quadricyclane. Finally Figure 40 is a plot of quadricyclane concentration for Extraction Ports 1, 2, 3 and 4 as a function of time during the water flushing segment. The overall behavior seen in this figure is similar to the behavior observed previously in experiment 2QAF (Figure 34).

During the surfactant flushing segment of this experiment, the injection and extraction flow rates of the surfactant solution were each set at 20 mL/min. Figure 41 shows a plot of the quadricyclane concentration in the extracted fluid as a function of time. Also shown in the plot is the flow rate of the effluent from the outlet end chamber as a function of time. The quadricyclane concentrations remain low until the surfactant front passes through the zone of entrapped residual. At this time the concentrations increase dramatically to 5500 mg/kg. Comparing Figure 41 to Figure 32 reveals that higher concentrations were obtained in this experiment (3QAF) than in the previous experiment (2QAF), the difference in the peaks being about 2000 mg/kg, although the curves are similar with respect to shape. The difference may be attributed in part to the lower flow rate and the smaller pore size used in this experiment as compared with 2QAF. The lower flow rate would allow for larger contact times between the surfactant solution and the quadricyclane. Also, the contact area would be increased as a result of the smaller pore size, and this would lead to more mass transfer, therefore larger concentrations in the aqueous phase. It is seen from Figure 41 that quadricyclane concentrations in the extracted fluid were reduced to very low levels by the end of the surfactant flushing segment, as was the case in the previous experiment (2QAF). This, along with additional visual evidence, presented in Figure 42, where a photograph taken at the end of the surfactant flushing segment is shown, indicates that the surfactant solution was effective at removing the spilled quadricyclane from the porous medium.

Experiment 4QAF:

All procedures described in the materials and methods section were followed except that during the surfactant flushing segment the injection and extraction flow rates were doubled from 20 mL/min to 40 mL/min near the end of the surfactant flushing segment to check the effect of a larger surfactant solution flow rate on the cleanup of the trapped quadricyclane.

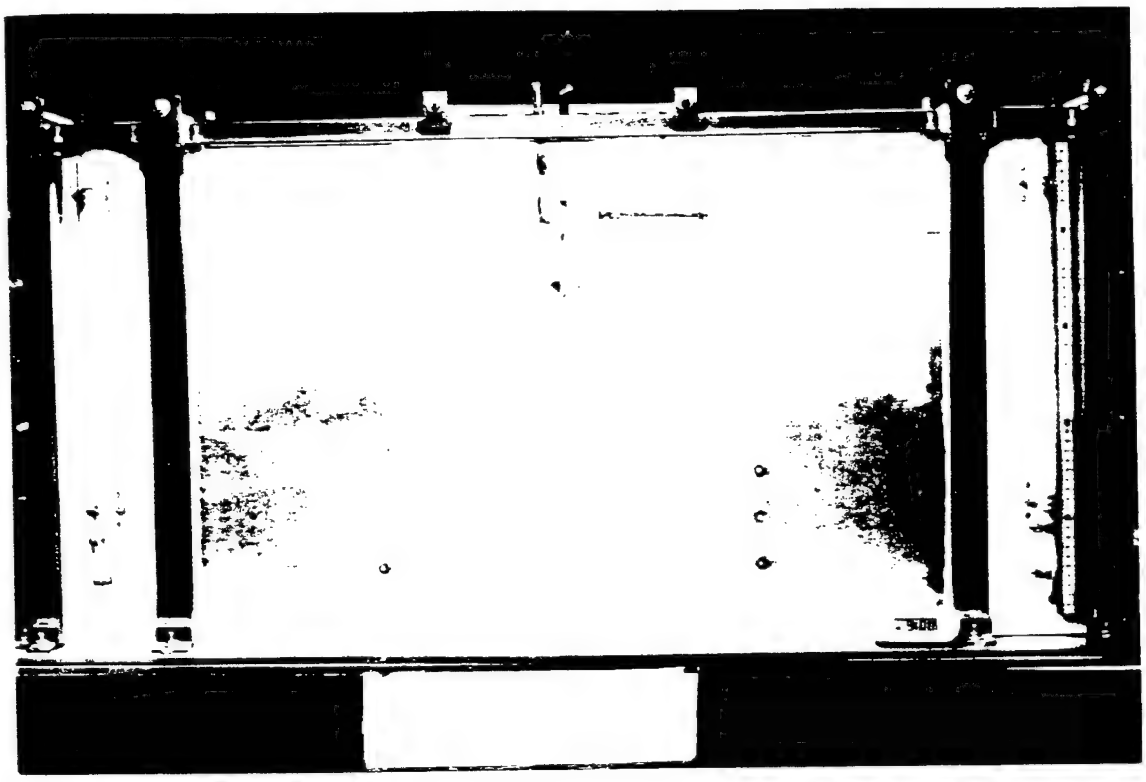

Figure 38 Photograph of the Final Quadricyclane Distribution after the Emplacement Segment of Experiment 3QAF

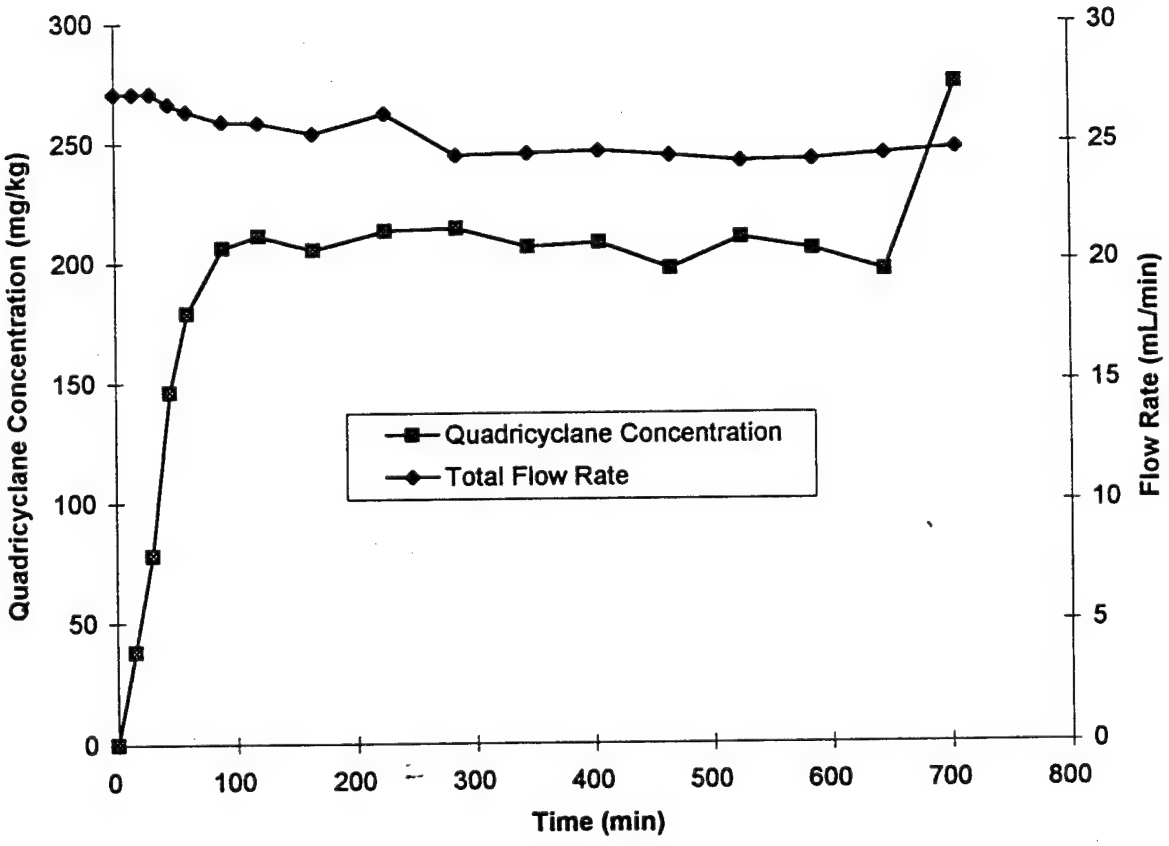

Figure 39. Quadricyclane Concentration and Flow Rate as Functions Time for the Water Flushing Segment of Experiment 3QAF. Samples Were Taken From Extraction Port 2.

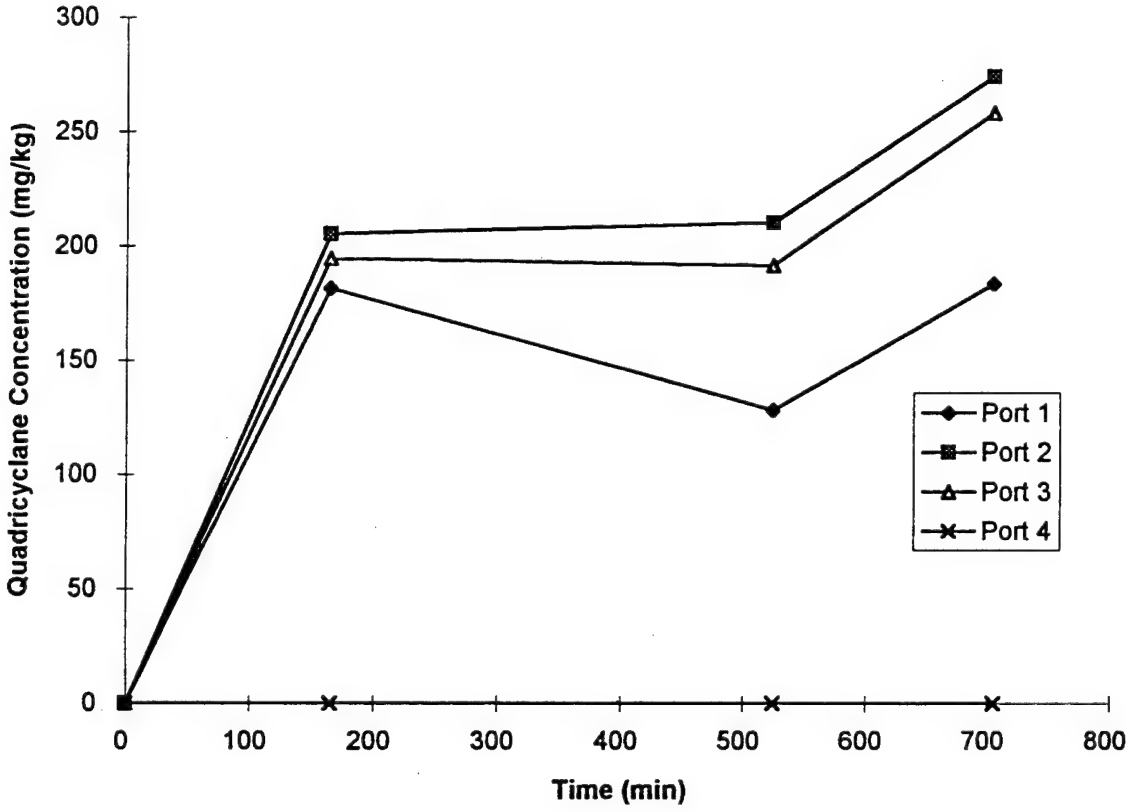

Figure 40. Quadricyclane Concentration as a Function of Time for the Water Flushing Segment of Experiment 3QAF. Samples Were Taken from Extraction Ports 1-4.

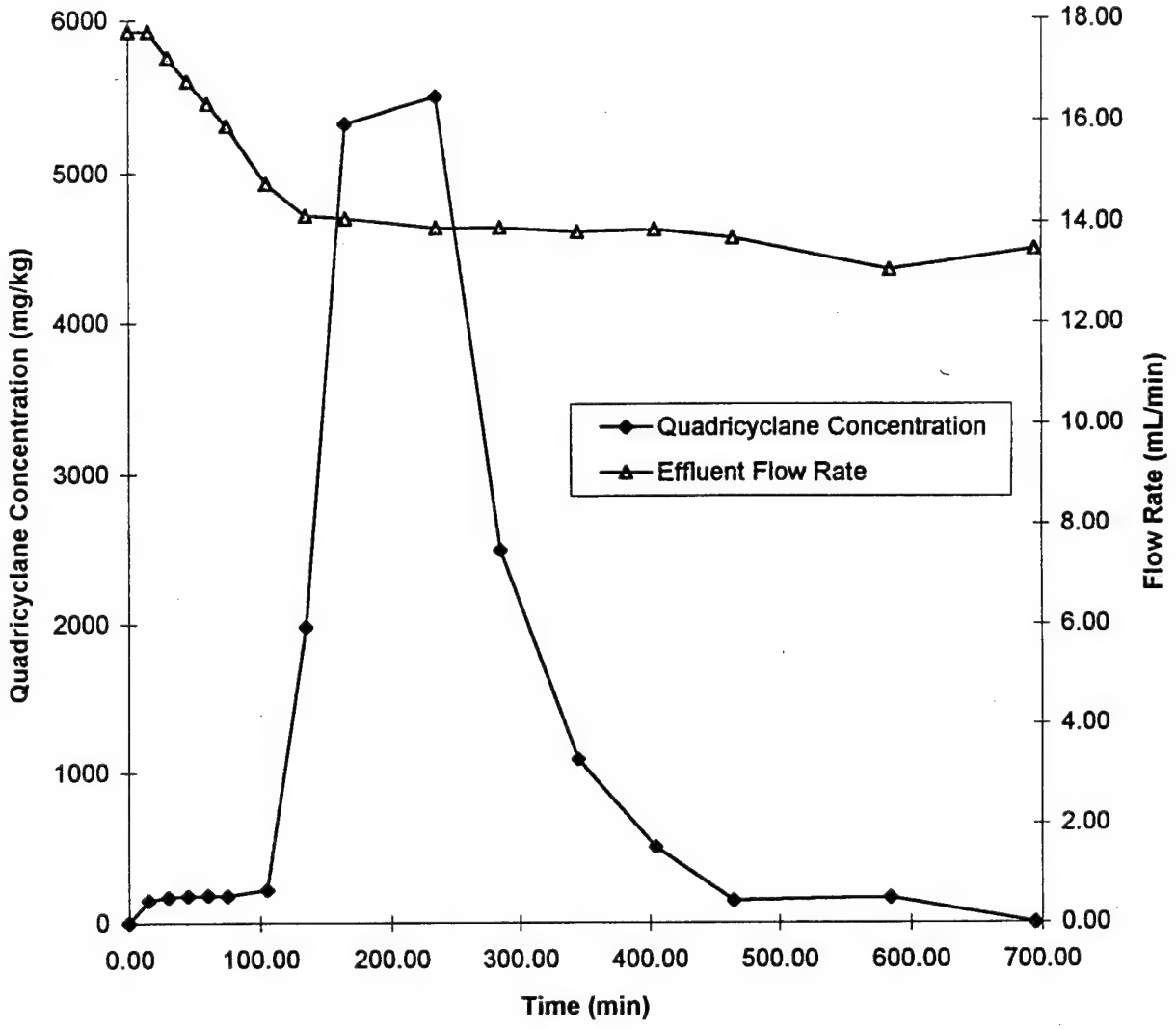

Figure 41. Quadricyclane Concentration and Flow Rate as Functions of Time for the Surfactant Flushing Segment of Experiment 3QAF.

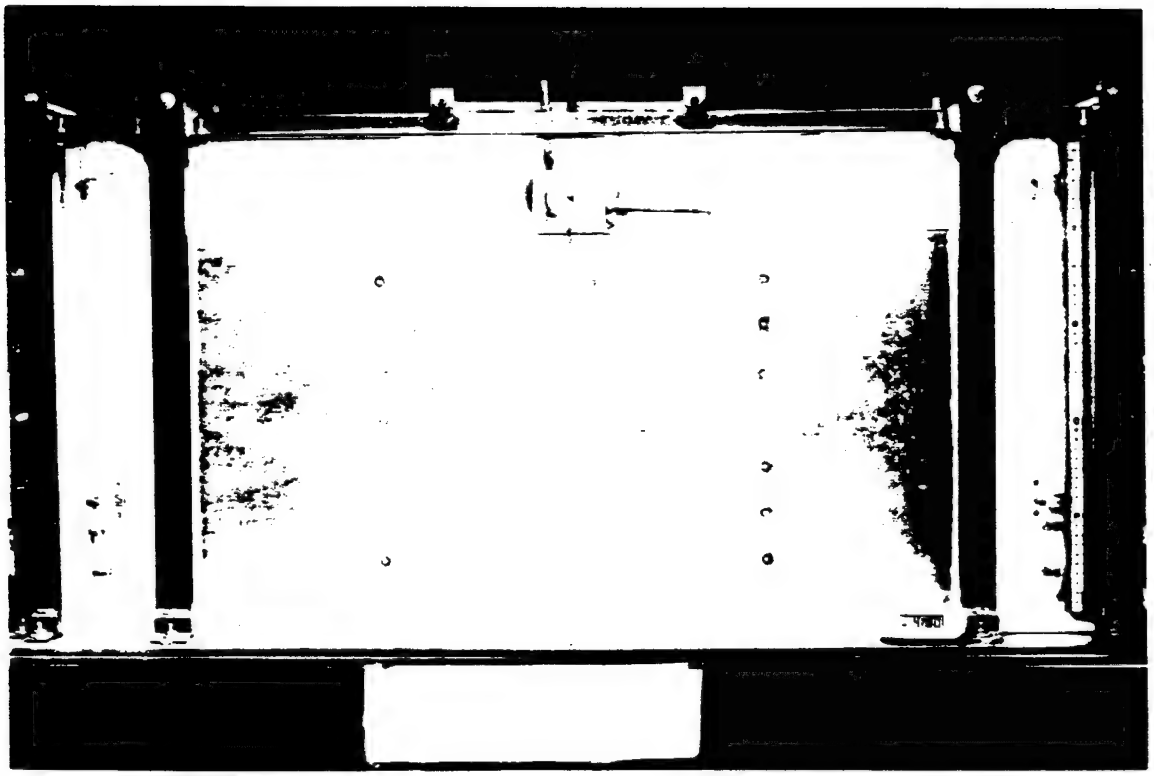

Figure 42 Photograph of the Quadricyclane Distribution upon Termination of the Surfactant Flushing Segment for Experiment 3QAF

Results from the first two segments of this experiment are shown in Figures 43 through 47. Figure 43 is a photograph of the quadricyclane distribution at the end of the emplacement segment. As shown, the quadricyclane passed directly through the coarse layer and the fine layer directly beneath the coarse layer. This was not unexpected since in both homogeneous cases the quadricyclane penetrated the surface and traveled directly to the top of the capillary fringe (Figures 32 and 38). Figure 43 also shows the effect of higher water contents and nonhomogeneity within each layer. The second interface between fine and coarse layers approximately 10 cm from the top of the medium had significantly higher water contents than the two layers above it, therefore, when the quadricyclane contacted the water it began to spread laterally. Quadricyclane could not displace the water in this layer because the displacement pressure for water is high; therefore, it began to spread laterally. Heterogeneities incurred during packing probably forced some of the finer particles into the coarse material which would increase the entry pressure and decrease the hydraulic conductivities. Because of this, longer times were needed for the fingers to penetrate into the coarse layer.

During the water flushing segment the extraction port flow rates were each set at 2.5 mL/min. Figure 44 shows a plot of quadricyclane concentration at Extraction Port 2 as a function of time. After about 60 minutes, the concentrations fluctuate about a mean of 257 mg/kg. As compared to Figure 39, Figure 44 is similar except for the scatter in some of the data points. Figure 45 is a plot of quadricyclane concentration as a function of time with the samples taken from Extraction Ports 1-3. In this case Extraction Ports 4-7 did not produce any quadricyclane. This figure is similar to the previous experiments where a snap shot of the concentration was taken. Again, comparing the photograph taken at the beginning of the water flushing segment (Figure 46) to the one taken at the end of the segment (Figure 47) reveals that some movement has occurred from left to right. This movement is probably due to the viscous forces acting on the quadricyclane blobs trapped in the largest pores.

During the surfactant flushing segment of this experiment, the injection and extraction flow rates of the surfactant solution were each set at 20 mL/min at the beginning of the segment. These flow rates were later increased to 40 mL/min at 420 minutes after the beginning of this segment. Figure 48 shows a plot of quadricyclane concentration in the extracted fluid as a function of time. A comparison with the results of experiment 3QAF shown in Figure 41 indicates that the plots are similar, although the concentrations are slightly lower in Figure 48. Lower concentrations and a slightly wider curve in experiment 4QAF is most likely due to the heterogeneity of the medium. As was the case in the previous experiments, it was observed that the surfactant solution was effective in removing the entrapped quadricyclane from the porous medium. In this segment, the flow rate of the extraction and injection ports was elevated from 20 to 40 mL/min at 420 minutes to observe the effect of increased surfactant solution flow rate on the concentration. As seen in Figure 48, there is a change in the slope of the quadricyclane breakthrough curve at times greater than 420 minutes. Detailed numerical calculations with advanced computer codes of multiphase flow, interphase mass transfer and solute transport would be very useful in providing explanations of this observation as well as other observations made throughout these physical model experiments. Comparisons of the experimental and the numerical model results would also constitute a good test of the numerical models used. Such numerical calculations, however, are not within the scope of this study.

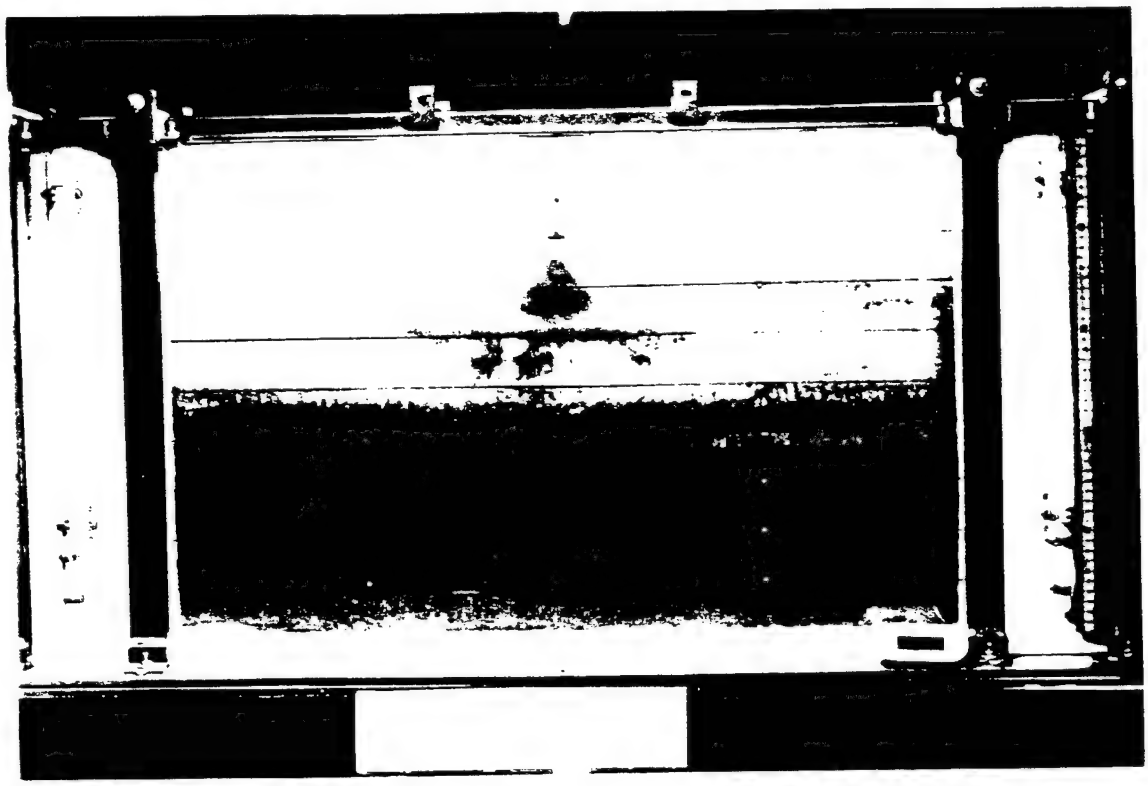

Figure 43 Photograph of the Final Quadricyclane Distribution after the Emplacement Segment of Experiment 4QAF

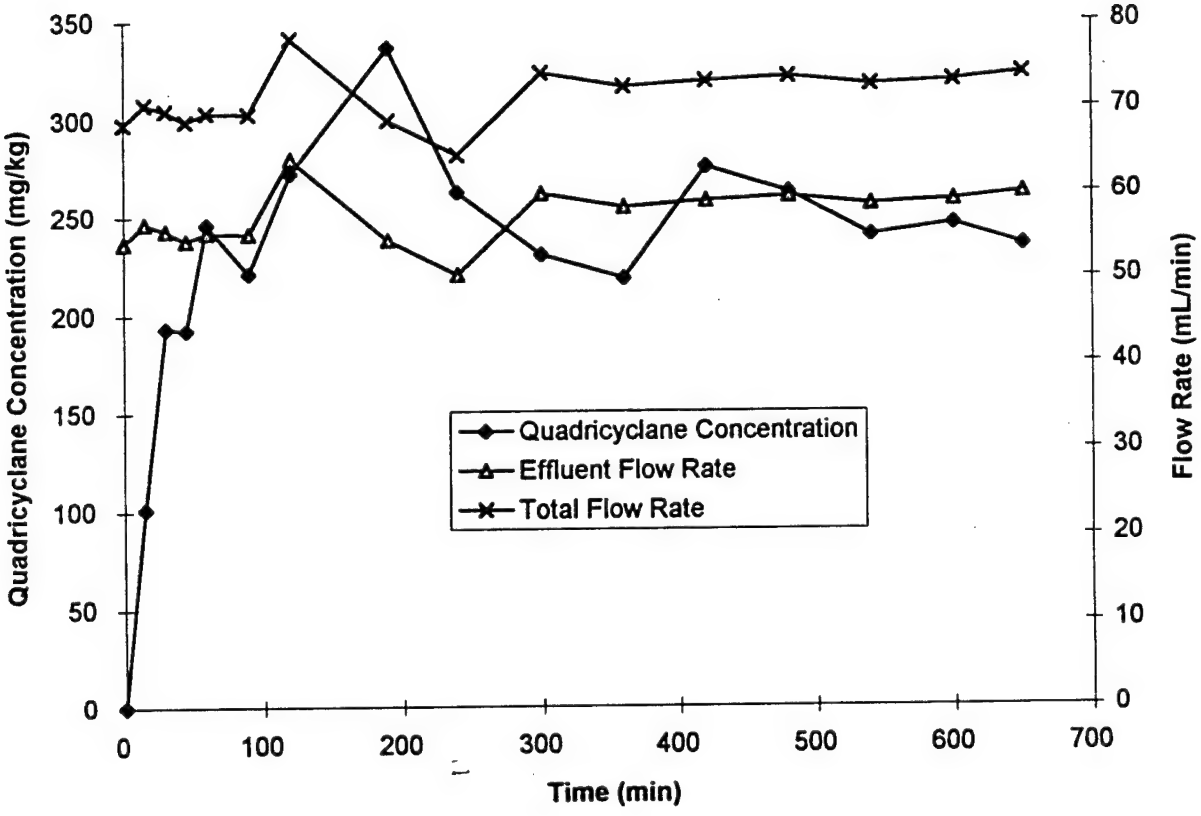

Figure 44. Quadricyclane Concentration and Flow Rates as Functions of Time for the Water Flushing Segment of Experiment 4QAF. Samples Were Taken from Extraction Port 2.

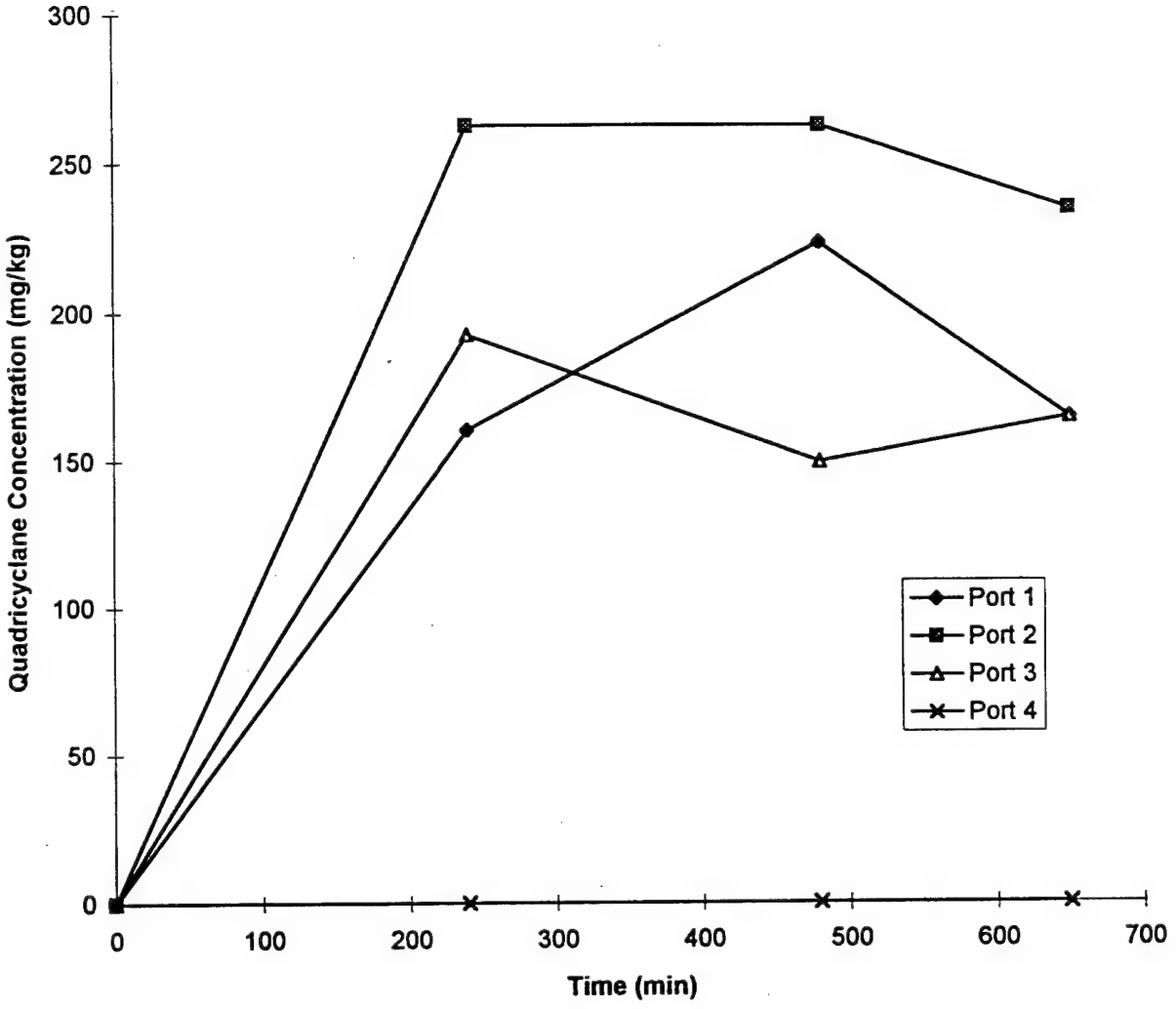

Figure 45. Quadricyclane Concentration as a Function of Time for the Water Flushing Segment of Experiment 4QAF. Data Are Plotted for Ports 1-4. Samples Taken from Extraction Ports 5-7 Contained No Quadricyclane.

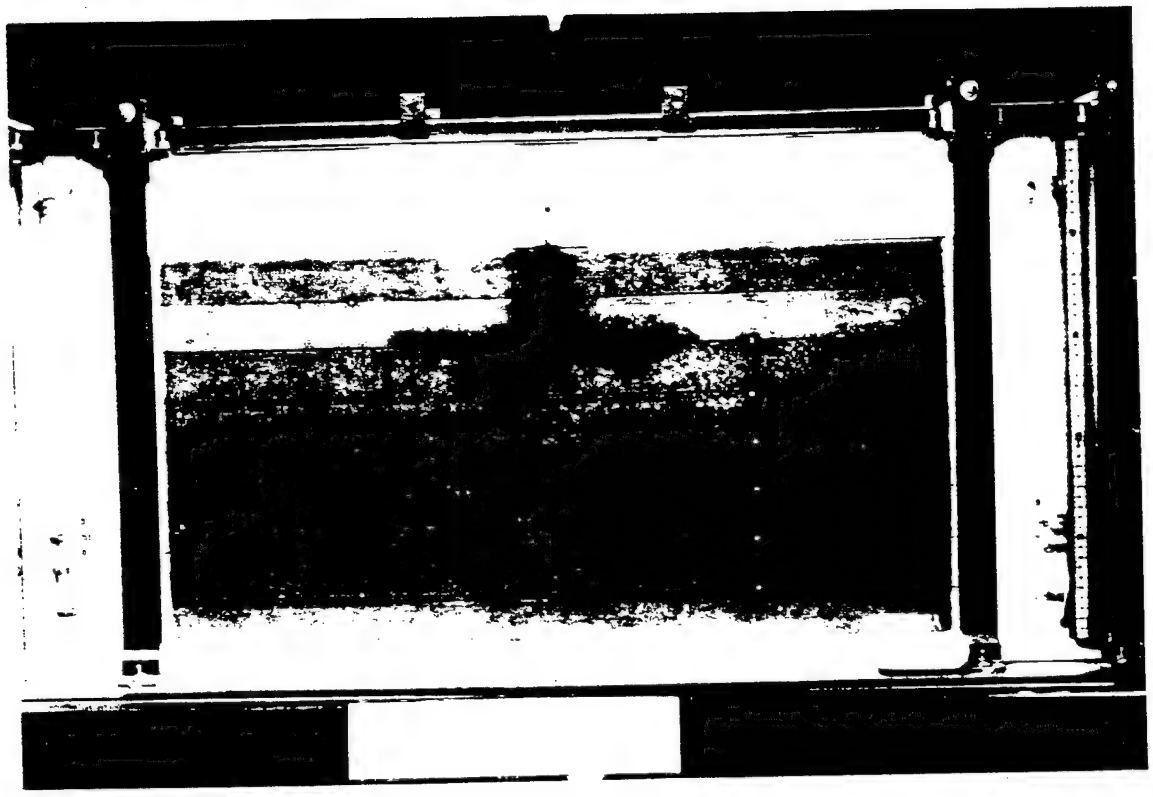

Figure 46 Photograph Taken at the Termination of the Entrapment Segment Prior to the Start of the Water Flushing Segment for Experiment 4QAF

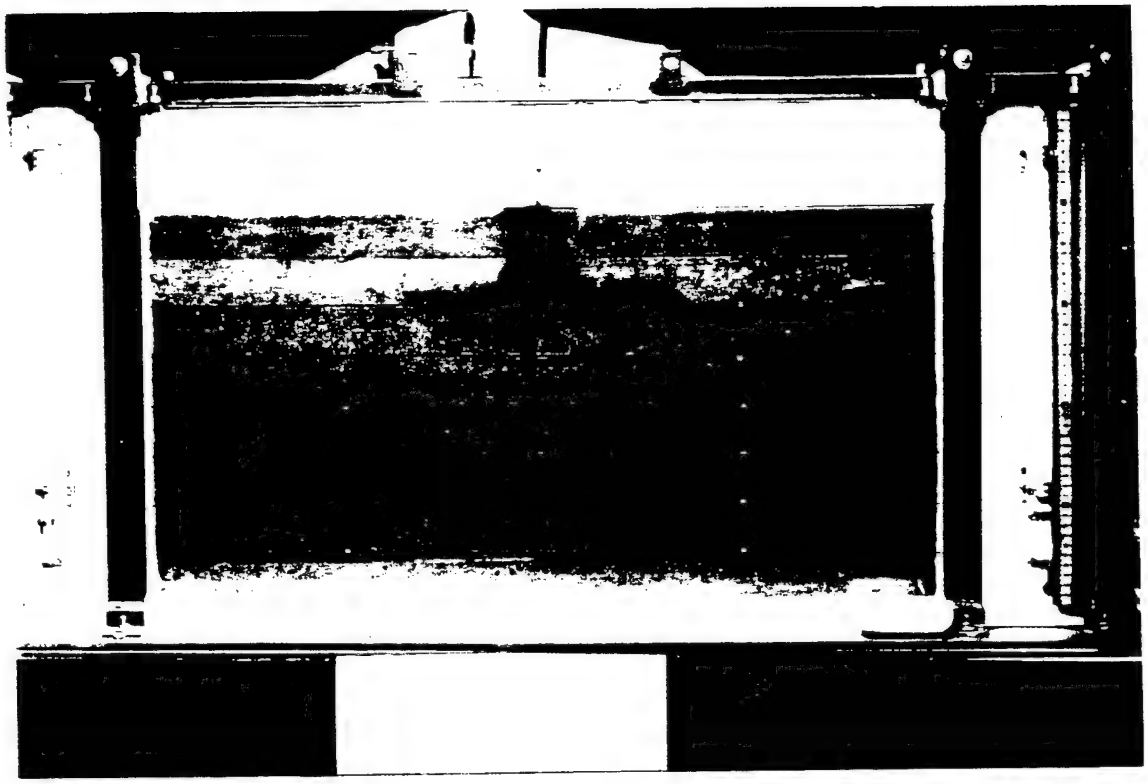

Figure 47 Photograph Taken at the Termination of the Water Flushing Segment Prior to the Start of the Surfactant Flushing Segment of Experiment 4QAF

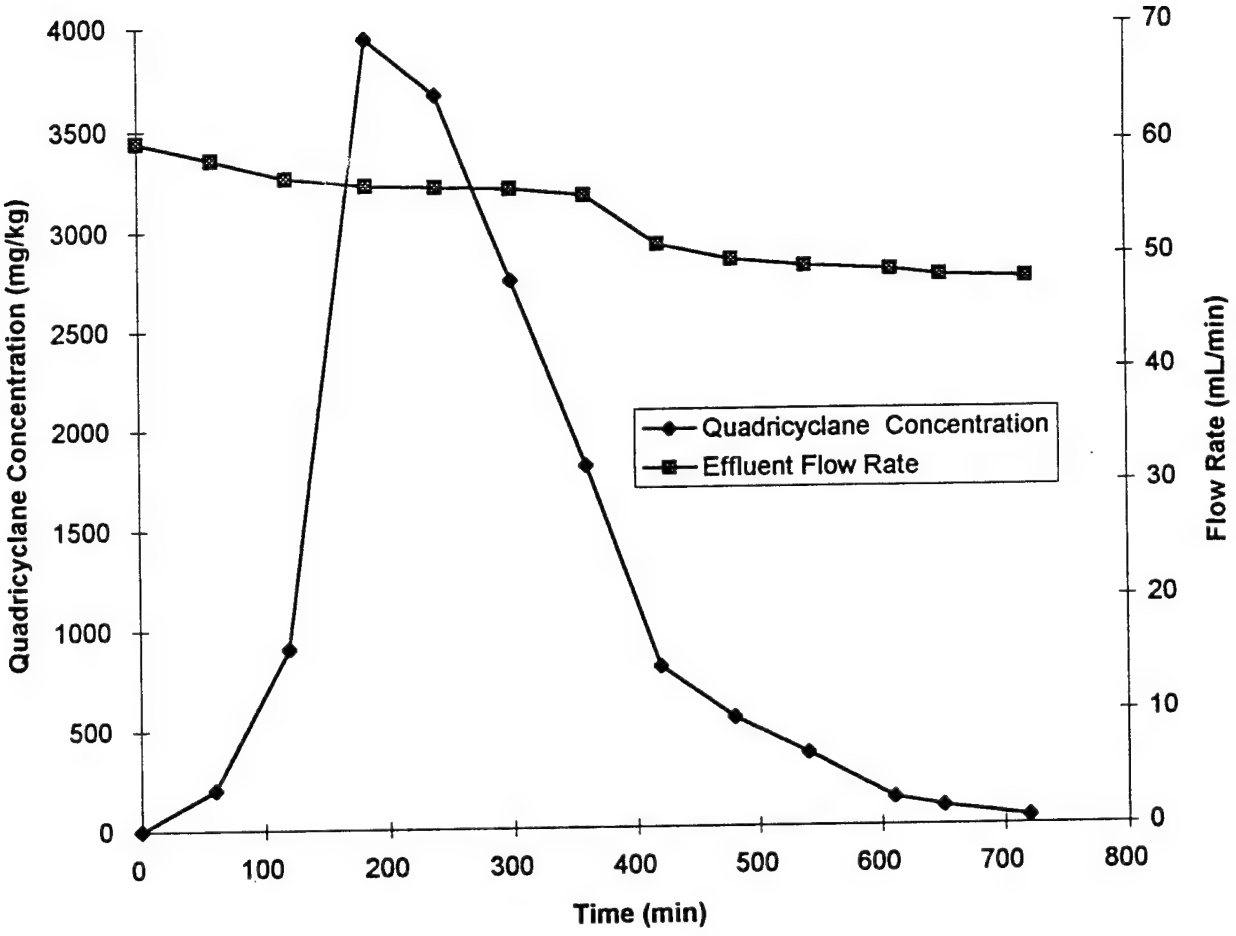

Figure 48. Quadricyclane Concentration as a Function of Time for the Surfactant Flushing Segment of Experiment DAF. All Samples Were Taken from Extraction Port 1. The Flow Rate Was Doubled from 20 mL/min to 40 mL/min at Time Equal to 420 Minutes.

D. CONCLUSIONS

The results of physical model experiments presented in this section have documented that, if a spill occurs, quadricyclane would behave as a light non-aqueous-phase liquid (LNAPL), as expected, in a porous medium. The experiments have provided quantitative information on the dissolution of quadricyclane in a water stream as well on the cleanup of the spilled quadricyclane with a surfactant solution. The surfactant solution was effective in removing the entrapped quadricyclane from sand media. The experimental data are expected to be useful in the future in testing advanced computer models of multiphase flow, interphase mass transfer and solute transport.

REFERENCES FOR SECTION IV

Dane, J.H., O. Güven, and B.C. Missildine, "Flow Visualization Studies of Dense Aqueous Phase Leachate Plumes in Coarse and Fine Sand." Department of Agronomy and Soils Special Report, Alabama Agricultural Experiment Station, Auburn University, 1994.

Hayworth, J.S., "A Physical and Numerical Model Study of Three-Dimensional Behavior of Dense Aqueous Phase Plumes in Porous Media." Ph.D. Dissertation, Department of Civil Engineering, Auburn University, 1993.

Mamballikalathil, R., "A Laboratory Study of the Subsurface Transport of Tetrachloroethylene and its Surfactant Enhanced Cleanup." M.S. Thesis, Department of Civil Engineering, Auburn University, 1995.

Mercer, J.W. and R.M. Cohen, "A Review of Immiscible Fluids in the Subsurface: Properties, Models, Characterization and Remediation." Journal of Contaminant Hydrology, 6, 107-163, 1990.

Oostrom, M., "Behavior of Dense Leachate Plumes in Unconfined Aquifer Models." Ph.D. Dissertation, Department of Agronomy and Soils, Auburn University, 1991.

SECTION V
ONE-DIMENSIONAL STATIC-EQUILIBRIUM EXPERIMENTS WITH TETRACHLOROETHYLENE (PCE)

A. INTRODUCTION

An essential component in understanding and simulating the migration of NAPLs in the vadose zone is the accurate determination of hydraulic properties of the three fluids (water-NAPL-air) involved. Most contemporary experimental procedures to determine constitutive relationships, however, pertain to two-phase porous medium systems. Investigators usually apply these two-phase relationships (i.e., NAPL-air, water-NAPL) to estimate fluid behavior in a three-phase system. One constitutive relationship, often used in computer codes, is the relationship between the capillary pressure (P_c) and saturation (S) or volumetric fluid content (θ).

This section describes follow-up experiments of earlier research, described in Güven et al. (1995). Capillary pressure head (h_c)- volumetric fluid content relations were determined for two different cases. First, we determined the $h_c(\theta)$ relation for PCE and air in F75 Ottawa sand. Second, an experiment was performed determining the $h_c(\theta)$ relations in a water-PCE-air system. A major objective was to compare the results of the first and second experiment to validate the so-called Leverett assumption for three-phase fluid retention curves.

B. THEORETICAL

The capillary pressure head, h_c (m), is defined as the difference between the pressure head of the nonwetting fluid, h_{nw} (m), and the wetting fluid, h_w (m). In a PCE-air system, PCE is the wetting fluid. Since the resistance to air flow in a PCE-air system can be assumed to be negligible, the pressure head of air, $h_a=h_{nw}$ = 0 m throughout the continuous gaseous phase. The equation for the capillary pressure head across the PCE-air interface, h_{cpa} (m), therefore reads:

$$h_{cpa} = h_a - h_p = \frac{-P_p}{\rho_{h_2o} \cdot g} \tag{3}$$

(P_p = PCE pressure ($N.m^{-2}$); ρ_{h2o} = density of water ($kg.m^{-3}$); g = gravitational field strength ($N.kg^{-1}$); h_p= pressure head of PCE (m)). The capillary pressure head, h_{cwp} (m) for a water-PCE system is expressed as:

$$h_{cwp} = h_p - h_w = \frac{P_p - P_w}{\rho_{h_2o} \cdot g} \tag{4}$$

(P_w = pressure of water ($N.m^{-2}$); h_w = pressure head of water (m)).

A classical way to obtain three-phase fluid retention curves from two-phase fluid measurements is based on a concept put forward by Leverett (1941), which states that in a water wet porous medium the total liquid content in a water-NAPL-air system is a function of the capillary pressure head between the continuous NAPL and air only, i.e.,

$$\theta_w + \theta_{PCE} = f_1 (h_{cpa}), \tag{5}$$

where

$$\theta_w = f_2 (h_{cwp}) \tag{6}$$

These functional relationships result from the assumption that in a three-phase fluid system, the intermediate wetting fluid, PCE, will spread over the water-air interface, eliminating the interface between the continuous water and gaseous phase (Figure 49). Indirect evidence for this conceptional model was provided by three-phase fluid conductivity measurements conducted by Leverett et al. (1941) and Corey (1956). Lenhard and Parker (1988) were the first to use pressure cell measurements to verify the Leverett assumption for a water-oil-air system. Excellent agreement was found between the total liquid saturation in a three-fluid phase water-oil-air system and a two-fluid phase oil-air system as a function of the oil-air capillary pressure head values. Furthermore, water saturation was found to be a function of the capillary pressure at the water-oil interface of either the water-oil or the water-oil-air system. The experiments were restricted to monotonic drainage paths of the total liquid content. Lenhard (1992) measured and modelled hysteretic behavior in a three-phase fluid system.

Wilson et al. (1990) used etched glass micromodels to investigate the pore-scale behavior of NAPLs. They made a distinction between so-called spreading and nonspreading NAPLs. A NAPL's tendency to spread on a water-air interface can be measured by the "spreading coefficient" after Adamson (1982): NAPL's tendency to spread on a water-air interface can be measured by the "spreading coefficient" after Adamson (1982):

$$\sum = \sigma_{wa} - (\sigma_{wn}\cos\alpha_1 + \sigma_{na}\cos\alpha_2), \tag{7}$$

where $\sum$ is the spreading coefficient ($N.m^{-1}$), σ_{wn}, σ_{wa}, σ_{na} ($N.m^{-1}$) are the interfacial tensions at the interfaces between water-NAPL, water-air and NAPL-air, respectively, and α_1 and α_2 are the contact angles between the water-NAPL and NAPL-air, respectively (Figure 50). Liquids with a positive spreading coefficient, like certain oils, will form a continuous film on top of a water-air interface. Other common organic pollutants, such as PCE and carbon tetrachloride, however, have a relatively greater internal cohesion, which is

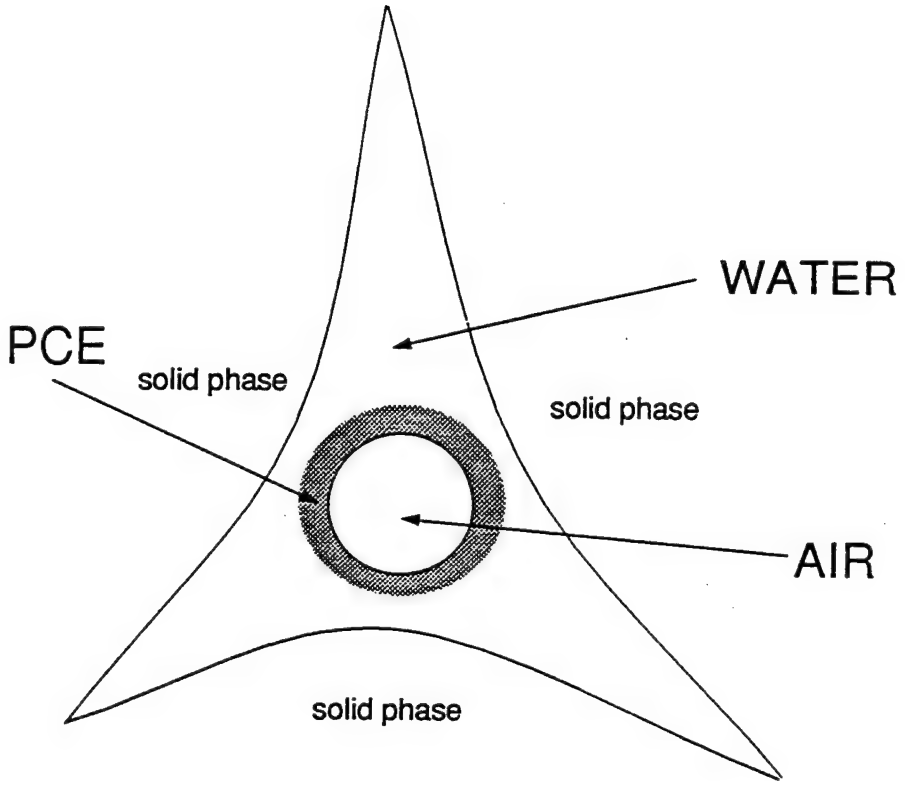

Figure 49. Diagram of the Distribution of Water, NAPL, and Air in a Three-Fluid Phase System (After Leverett, 1941).

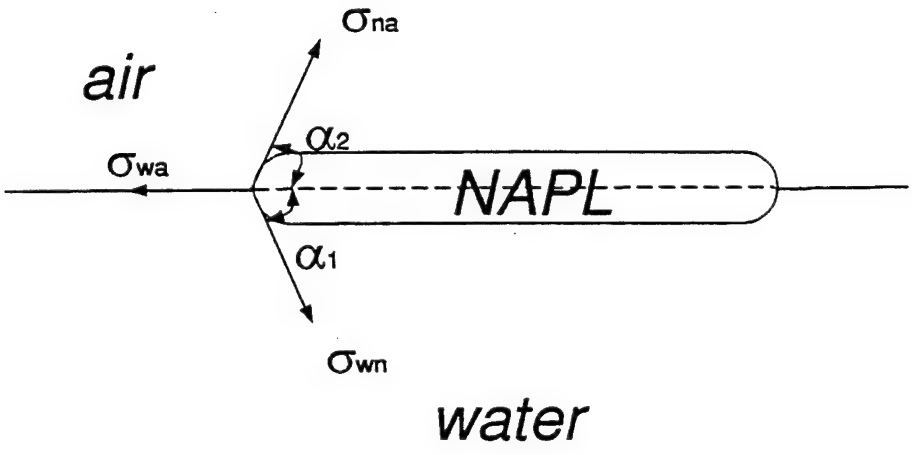

Figure 50. Diagram of Forces Present at the Interface of a Drop of Organic Liquid in Contact with a Water-Air Interface.

reflected in a negative spreading coefficient (Wilson, 1992). At equilibrium with a flat water-air interface, a non-spreading liquid will form a mono-molecular film, while any excess will coalesce into discontinuous lenses (Adamson, 1982). We speculate that a similar behavior occur in porous media.

The microscopic experiments by Wilson et al. (1990) show that, within the vadose zone, spreading liquids tend to form continuous layers, which fully coat water-air interfaces. This indicates that the Leverett assumption is applicable to spreading liquids. PCE (a nonspreading liquid), however, formed "golf-ball"-like parcels, and left large portions of the water-air interface uncovered. This indicates that the Leverett assumption is not applicable to nonspreading liquids.

C. MATERIALS AND METHODS

Two 1-meter long glass columns (I.D. = 8.0 cm) with Teflon® end caps were packed as uniformly as possible with clean oven-dry F75 Ottawa sand (US Silica, Ottawa, Illinois), following the procedure of Dane et al. (1992). The height of the sand was about 1 meter. One of the columns was first saturated with deionized water and then slowly drained, while the other column remained dry. The outlet at the bottom of each column was then connected to a reservoir of PCE (Tetrachloroethylene or Tetrachloroethene 99%, Aldrich Chemical Company Inc., Milwaukee, Wisconsin), indicated as an overflow in Figure 51. Upon introducing PCE into the columns as described below, one column constituted a three-phase water-PCE-air and one was a two-phase PCE-air system.

For the fluid displacement experiments, the initially dry and the initially water-drained columns were subjected to the following steps:

1. PCE was imbibed from the bottom of the column by slowly raising the reservoir until the PCE was ponded on top of the sand. The water, which was displaced from the porous medium in one of the columns, forming a layer on top of the ponded PCE, was removed with a syringe.

2. Air was allowed to enter the column by stepwise lowering the reservoir. When, during each step, the change in PCE content became negligible at all measurement locations, water and PCE saturations (drainage data) were determined using a dual-energy gamma radiation system (Oostrom and Dane, 1990; Dane et al., 1992).

3. Air was displaced by stepwise raising the reservoir until PCE was ponded on top of the sand in both columns. Again, each time static equilibrium was reached after a change in liquid levels, water and PCE saturations (imbibition data) were measured with a dual-energy gamma radiation system.

After each change in elevation, the system was allowed to come to static equilibrium. To assure that no flow occurred, flow rates were occasionally checked with a buret, installed between the port at the bottom of the column and the PCE reservoir. Normally, the PCE level in the buret was maintained at the same level as in the reservoir, but by temporarily closing a stopcock valve located between the buret and the reservoir small fluxes could be detected because of the small cross sectional area of the buret.

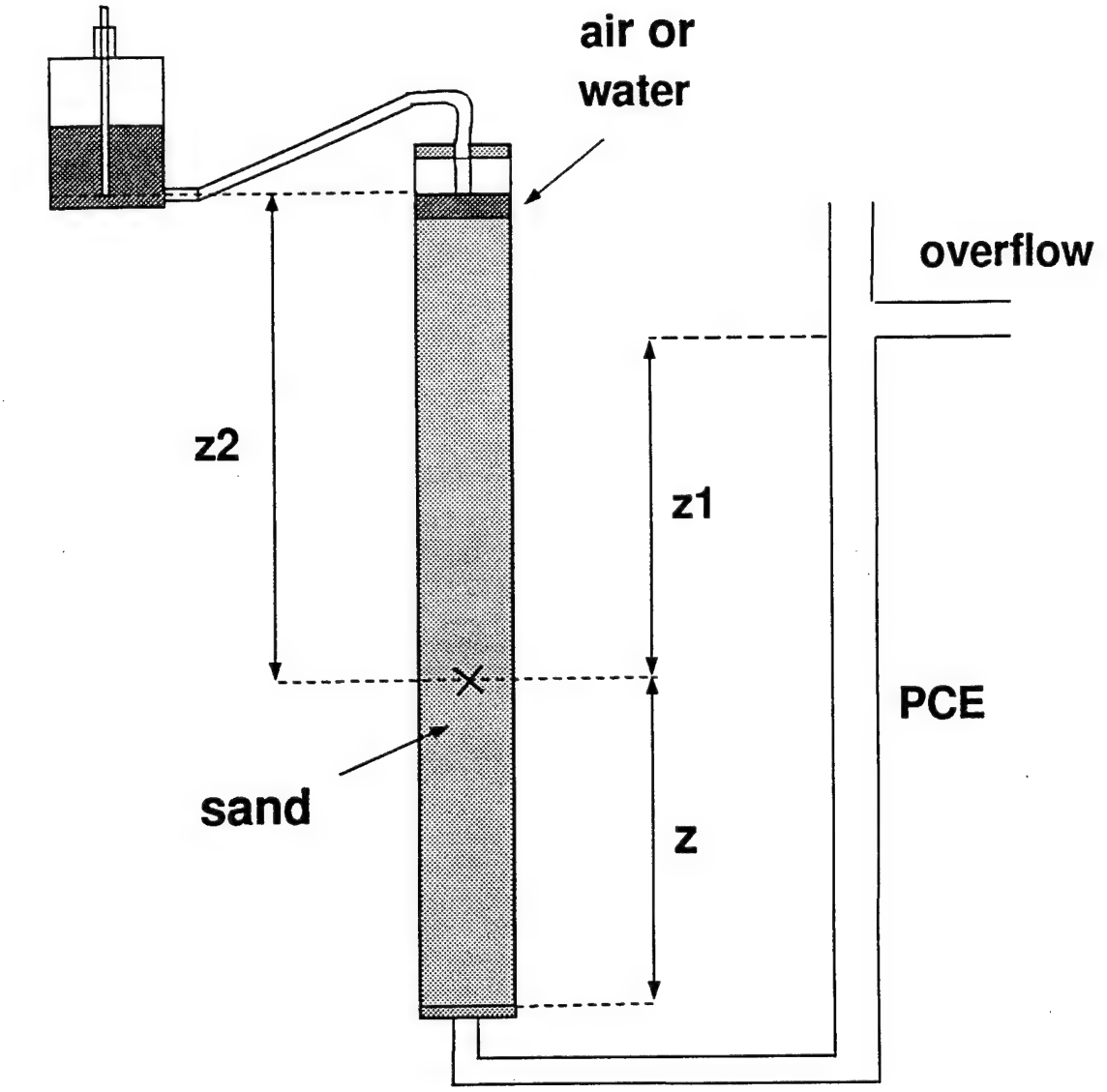

Figure 51. Simplified Schematic of the Experimental Setup.

The pressure head in the static PCE phase was calculated from

$$h_p = \gamma_p * z_1 \tag{8}$$

where z_1 (m) is the difference in elevation between the PCE overflow and the location of measurement (Figure 51) and is to be taken negative for overflow levels below the point of measurement; γ_p is the specific gravity (-) of PCE. The capillary pressure head across the PCE-air interface was then calculated using Equation (3).

Calculations of capillary pressure head values, as described above, are only valid if the fluids are continuous. The nonwetting fluid in a two-phase fluid system, however, is known to become discontinuous at low values for the capillary pressure head. Since the pressure head of a discontinuous fluid cannot be determined, we calculated capillary pressure head values in a two-phase fluid system as if both fluids were continuous for all saturations. Similarly, for a three-phase fluid system, we calculated capillary pressure head values as if the intermediate wetting fluid (PCE) was continuous for all saturations. Furthermore, we assumed the validity of the Leverett assumption.

The h_c-θ data for the two-phase fluid systems were fitted with the closed form van Genuchten expression (1979):

$$S_e = \frac{\theta - \theta_r}{\theta_s - \theta_r} = [1 + (\alpha * h_c)^n]^{-m} \tag{9}$$

where α (m^{-1}), m and n are curve fitting parameters (m=1-1/n), θ_s and θ_r are the saturated and residual volumetric fluid contents of the wetting fluid, respectively, and S_e is the effective saturation (-).

D. RESULTS

Values for the bulk density, porosity and initial fluid contents are given in Tables 11 and 12 for the columns with PCE-air, and water-PCE-air, respectively. The data indicate that both columns were packed reasonably uniformly and had comparable bulk density values. About 16 % of the pore space in the PCE "saturated" column (Table 11) was initially occupied by entrapped air. The initial amount of entrapped air in the water-PCE "saturated" system (Table 12) was about 23 %.

The PCE-air displacement curves for the column initially saturated with PCE only were determined for location 1 through 8. The results of the Van Genuchten curve fitting procedure are shown in Table 13. The fitted average air-entry capillary pressure head ($1/\alpha$) is 18 cm of water and the average irreducible PCE content is about 0.028. The measured data and fitted retention curves for the PCE-air system at location 1 are shown in Figure 52. The plot shows that the volumetric PCE content drops from its maximum to its minimum value in about 20 cm of capillary pressure head difference. The data also show significant hysteresis in the h_c-θ relationship.

Leverett's assumption states that the total liquid content in a water-PCE-air system is a function of the capillary pressure between the PCE and air only. Figures 53 and 54, respectively, show the PCE drainage and imbibition data at location 1 in the water-PCE-air system. For comparison, the fitted two-phase retention Van Genuchten curves (Table 13) for the same location in the column with PCE and air only are included

TABLE 11. VALUES FOR THE BULK DENSITY OF F75 SAND (ρ_b), THE CORRESPONDING POROSITY (ϵ) BASED ON A PARTICLE DENSITY OF 2.65 g cm^{-3}, AND THE INITIAL AVERAGE VOLUMETRIC PCE CONTENT (θ_{pce}) DURING PCE SATURATED CONDITIONS IN WHICH PCE WAS DISPLACED BY AIR AND VICE VERSA.

Location	z* (cm)	ρ_b (g cm^{-3})	ϵ (-)	θ_{PCE} (-)
1	68.0	1.5884	0.401	0.351
2	67.0	1.5717	0.407	0.339
3	66.0	1.5706	0.407	0.338
4	65.0	1.5689	0.408	0.338
5	64.0	1.5635	0.410	0.351
6	63.0	1.5702	0.407	0.337
7	62.0	1.5716	0.407	0.340
8	61.0	1.5719	0.407	0.342

* z is the elevation of the measurement location relative to the bottom of the 1-m long column (Figure 51).

TABLE 12. VALUES FOR THE BULK DENSITY OF F75 SAND (ρ_b), THE CORRESPONDING POROSITY (ϵ) BASED ON A PARTICLE DENSITY OF 2.65 g cm^{-3}, AND THE INITIAL AVERAGE VOLUMETRIC PCE (θ_{pce}) AND WATER CONTENT (θ_{h2o}) FOR THE INITIALLY WATER WETTED COLUMN, IN WHICH PCE WAS DISPLACED BY AIR AND VICE VERSA.

Location	z* (cm)	ρ_b (g cm^{-3})	ϵ (-)	θ_{PCE} (-)	θ_{h2o} (-)
1	68.0	1.5827	0.403	0.259	0.058
2	67.0	1.5729	0.406	0.268	0.054
3	66.0	1.5856	0.402	0.265	0.040
4	65.0	1.5727	0.407	0.272	0.028
5	64.0	1.5712	0.407	0.271	0.043
6	63.0	1.5700	0.408	0.278	0.031
7	62.0	1.5827	0.403	0.275	0.039
8	61.0	1.5869	0.401	0.282	0.025

* z is the elevation of the measurement location relative to the bottom of the 1-m long column (Figure 51).

TABLE 13. PARAMETERS FOR THE VAN GENUCHTEN LIQUID RETENTION EQUATION FOR THE PCE DRAINAGE CURVE (VS AIR) FOLLOWED BY THE PCE IMBIBITION CURVE (VS AIR) IN A 1-m COLUMN FILLED WITH F75 SAND. THE DATA APPLY TO THE COLUMN WHICH WAS INITIALLY SATURATED WITH PCE ONLY.

Location	θ_r	θ_s	α (cm^{-1})	n
		(PCE drainage versus air)		
1	0.027	0.339	0.057	6.873
2	0.028	0.338	0.057	7.179
3	0.028	0.336	0.058	6.886
4	0.028	0.331	0.057	7.332
5	0.028	0.339	0.053	7.340
6	0.031	0.336	0.054	7.228
7	0.026	0.332	0.056	7.294
8	0.028	0.333	0.056	7.352
		(PCE wetting versus air)		
1	0.025	0.347	0.090	5.754
2	0.027	0.349	0.090	5.932
3	0.027	0.346	0.091	5.885
4	0.029	0.342	0.089	5.974
5	0.028	0.345	0.084	6.275
6	0.027	0.345	0.085	6.001
7	0.025	0.339	0.087	6.456
8	0.030	0.343	0.089	6.795

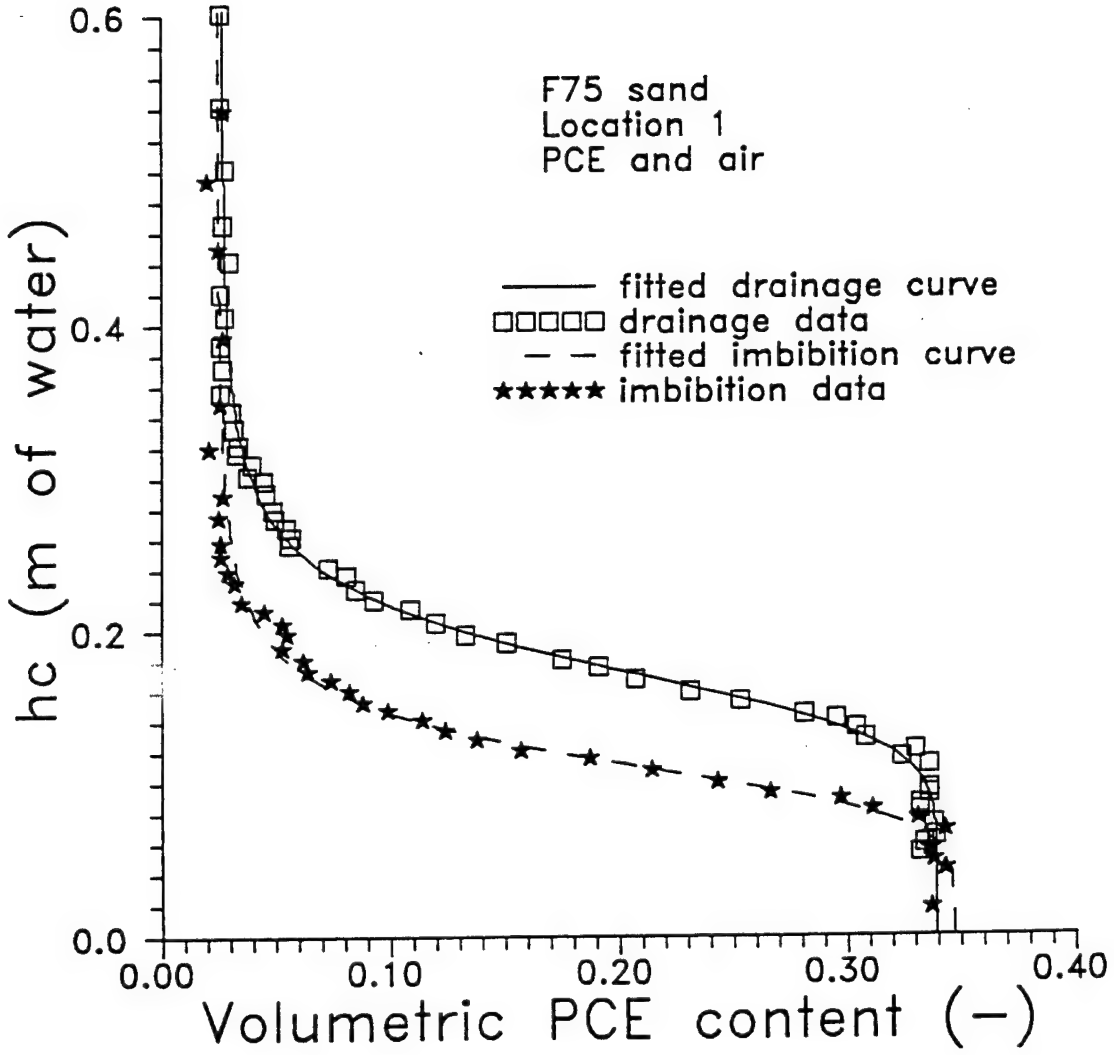

Figure 52. PCE Drainage Imbibition Curves Fitted by the Van Genuchten Equation and Measured Data at Locatic. for a F75 Sand Containing PCE and Air.

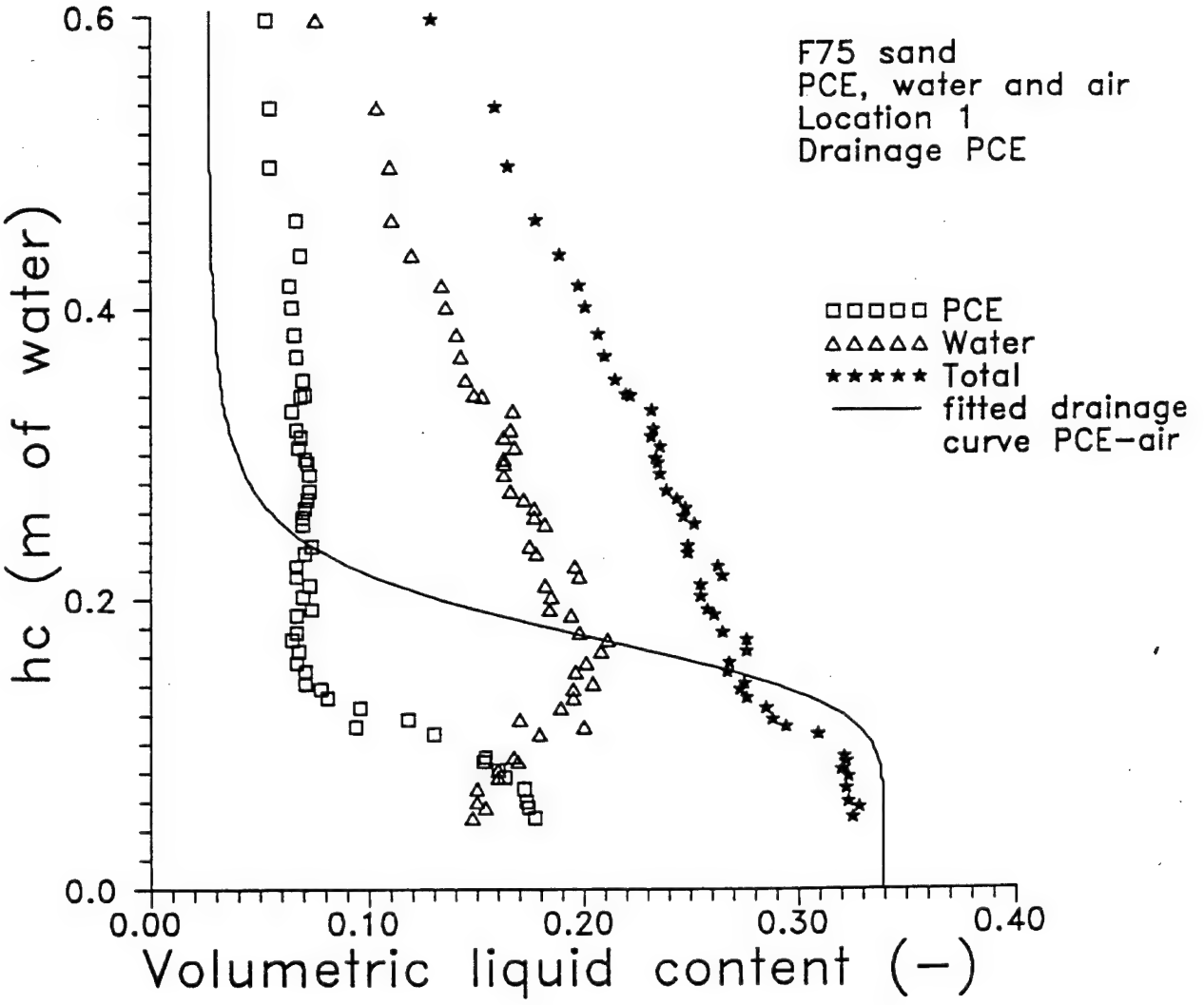

Figure 53. Comparison of Two-and Three-Phase Fluid Retention Curves (Drainage PCE).

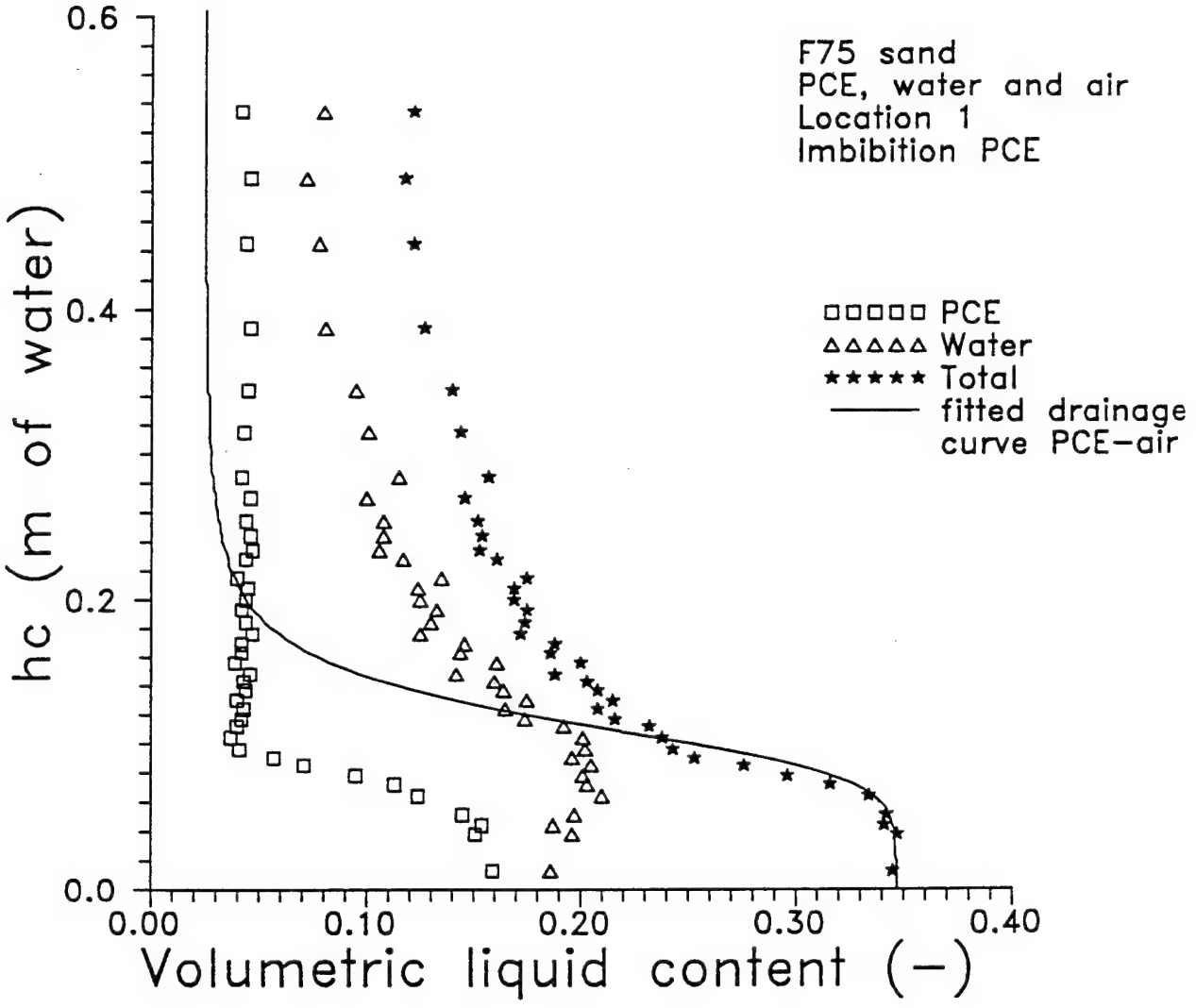

Figure 54. Comparison of Two-and Three-Phase Fluid Retention Curves (Imbibition PCE).

in the figures. The total liquid content (during drainage of PCE) in Figure 53 appears to be a function of the capillary pressure across the PCE-air interface (fitted curve) until the capillary pressure head becomes about 18 cm. Once the total liquid content started to deviate from the fitted PCE-air curve, the volumetric PCE content remained fairly constant while water was still being displaced. This indicates that the total liquid content at some point becomes a function of the capillary pressure across the water-air interface (possibly with a mono-molecular layer of PCE) rather than across the PCE-air interface. Our data would seem to corroborate the observation by Wilson et al. (1992) that water-PCE-air systems contain water-air interfaces. It should be noted that we did not measure the water pressure. Some minor displacement of PCE was measured, when a relatively large amount of water had been displaced by air. PCE previously entrapped by the aqueous phase may have regained some mobility due to the receding aqueous phase. Figure 54 shows the total liquid content during imbibition of PCE into the column. Again, the volumetric PCE content was fairly constant, until h_c had decreased to about 11 cm, when the PCE content increased rapidly, and the volumetric total liquid content again matched the fitted two-phase fluid retention curve closely. The results at the other seven locations were very similar to the data obtained at Location 1. Since the entire experiment was conducted over the course of several months, it is reasonable to assume that all phases were at chemical equilibrium with each other. The air entry pressure (during drainage of PCE) and the capillary pressure head values, at which all air became discontinuous during the monotonous imbibition path, were similar in the two and three-phase fluid systems. This indicates that the effect of dissolved water on the interfacial tension between PCE and air is not very significant.

E. DISCUSSION

Our experimental data indicate that the Leverett assumption can only be applied to a small portion of the water-PCE-air retention curves. In this subsection, we will outline a way of estimating water-NAPL-air retention curves from two-phase measurements if the NAPL is a nonspreading liquid.

For a drainage sequence, we have the following steps:

1) As long as the entire pore space is occupied with water and PCE, their saturations can be obtained from the two-phase water-PCE retention curves.
2) If the air entry pressure is exceeded, air will enter the porous medium and reduce the total volumetric liquid content. The PCE-air retention data can then be used to approximate the total volumetric liquid content as a function of the capillary pressure head across the PCE-air interface. The volumetric water content is a function of the capillary pressure head across the water-PCE interface.
3) When the volumetric PCE content has reached a certain minimum value, the total liquid content becomes a function of the capillary pressure across the water-air interface. The water- air interface is probably covered with a mono-molecular layer of PCE. Consequently, the surface tension associated with that interface is probably lower than that of a pure water-air interface. The minimum PCE value is the sum of the entrapped PCE and the amount of PCE existing as discontinuous lenses. This minimum PCE value may also depend somewhat on the volumetric water content. The existence of discontinuous PCE lenses makes the physical meaning of the so-called minimum PCE value different from that of either irreducible or residual saturation. The water saturation can be estimated by subtracting the minimum PCE content from the total liquid content (which is a function of the capillary pressure across the possibly contaminated water-air interface)

The above model requires one parameter (the minimum PCE content) in addition to the two-phase retention data involving water-air, PCE-air, and water-PCE. The physical interpretation of this new parameter is somewhat ambiguous, since it appears to include entrapped, as well as discontinuous PCE lenses. A similar approach can be applied to PCE imbibition in a three-phase system.

In order to further investigate the concepts presented above, it would be desirable to perform similar experiments in which the pressure in the water and the PCE are measured. This may be achieved by using hydrophilic tensiometers to measure the pressure in the water in conjunction with the existing experimental procedure to determine the PCE pressure using the hydrostatic equation.

REFERENCES FOR SECTION V

Adamson, A.W., Physical Chemistry of Surfaces, 4th edition. Wiley and Sons, New York: 629 pp, 1982.

Corey, A.T., "Three-Phase Relative Permeability." Petroleum Transactions AIME 207: 349-361, 1956.

Dane, J.H., Oostrom, M. and Missildine, B.C., "An Improved Method for the Determination of Capillary Pressure-Saturation Curves Involving TCE, Water and Air." Journal of Contaminant Hydrology 11: 69-81, 1992.

Güven, O, Dane, J.H., Hill, W.E., Hofstee, C., and Mamballikalathil, R., Subsurface Transport of Hydrocarbon Fuel Additives and a Dense Chlorinated Solvent. Interim Report, AL/EQ-TR-1994-0039, Armstrong Laboratory, Tyndall Air Force Base, Florida, January 1995.

Lenhard, R.J., "Measurements and Modelling of Three-Phase Saturation-Pressure Hysteresis." Journal of Contaminant Hydrology, 9, 243-269, 1992.

Lenhard, R.J., and Parker, J.C., "Experimental Validation of the Theory of Extending Two-Phase Saturation-Pressure Relations to Three-Fluid Phase Systems for Monotonic Drainage Paths." Water Resources Research, 24(3), 373-380, 1988.

Leverett, M. C. and Lewis, W. B., "Steady Flow of Gas-Oil-Water Mixtures Through Unconfined Sands." Petroleum Transactions AIME, 142: 107-116, 1941.

Leverett, M.C., "Capillary Behavior in Porous Solids." Petroleum Transactions AIME, 142: 152-169, 1941.

Oostrom, M and Dane, J.H., Calibration and Automation of a Dual-Energy Gamma System for Applications in Soil Science, Ala. Agric. Exp. Stn., Auburn University, Auburn, AL, Agron. Soils Dep. Ser. 145: 169pp, 1990.

Van Genuchten, M. Th., Calculating the Unsaturated Hydraulic Conductivity with a New Closed-Form Analytical Model, Research Report 78-WR-08. Department of Civil Engineering, Princeton University, 1979.

Wilson, J.L., "Pore-Scale Behavior of Spreading and Nonspreading Organic Liquids in the Vadose Zone." In: Weyer, K.U. (editor), Subsurface Contamination by Immicible Fluids, Balkema, Rotterdam, pp 107-114, 1992.

Wilson, J. L., Conrad, S.H., Mason, W.R., Peplinski, W. and Hagan, E., Laboratory Investigation of Residual Liquid Organics from Spills, Leaks, and the Disposal of Hazardous Wastes in Groundwater, EPA Report 600/6-90/004, 267 pp, 1990.

SECTION VI
TRANSIENT FLOW EXPERIMENTS WITH WATER, PCE, AND AIR IN NOMINALLY 1-D, HOMOGENEOUS AND HETEROGENEOUS POROUS MEDIA

A. INTRODUCTION

Multiphase fluid flow experiments are useful for formulating the basis on which numerical prediction codes are built and for validating existing computer simulation models.

This section deals with physically simulated PCE spills into and their redistribution in water-saturated and unsaturated, nominally 1-D, homogeneous and heterogeneous porous media. The effect of stratification of the porous medium on PCE behavior is investigated. Volumetric DNAPL and water content values, as well as bulk density values, were determined with a dual-energy gamma radiation system.

B. MATERIALS AND METHODS

Four experiments were conducted in 1.1-meter long glass columns (I.D. = 8.0 cm), which were packed either with layers of clean oven-dry Flintshot 2.8 and F-75 sand (US Silica, Ottawa, Illinois), or uniformly with Flintshot 2.8 Ottawa sand. The packing procedure is described in Dane et al. (1992). The coarser Flintshot 2.8 (F&S Abrasives, Birmingham, AL) contained over 50 % of its particles in the 0.250-0.500 mm range (Table 14). The F-75 sand had almost 79% of its particles in the 0.1-0.25 millimeter range (Table 14).

TABLE 14. PARTICLE SIZE DISTRIBUTION FOR COARSE (FS 2.8) AND FINE (F-75) SAND

	Particle size class (mm)				
	<0.106	0.106-0.25	0.25-0.5	0.5-1.0	1.0-2.0
Fine sand (pct)	5.3	78.9	5.7	0.10	0.0
Coarse sand (pct)	0.6	7.2	53.6	38.6	0.0

From top to bottom, the sublayers in the heterogeneous columns consisted of 30 cm of coarse, 30 cm of fine, and 40 cm of coarse sand, respectively. A schematic of the experimental setup is shown in Figure 55. The columns were repacked before each experiment with previously unused sand.

A Teflon® cap, attached to the bottom of each glass column, provided an outlet, which was connected to a water reservoir with overflow. During the saturated flow experiments, the water level in the reservoir maintained a constant zero pressure head in the water at the top of the sand column. The cumulative outflow volume of water from the overflow was measured gravimetrically for each experiment as a function of time. The cumulative drainage volume of PCE from the column was determined by a modified buret, which acted as a PCE trap (Figure 55). The top of the buret was connected to the outlet-overflow tubing. A Teflon cap attached to the top of each glass column contained a small ventilation hole to maintain atmospheric pressure at the liquid/air interface and an inlet to apply PCE during simulated spills.

Bulk density values of the porous medium, as used in each experiment, were measured at 34 prespecified locations (see Figure 55) with a dual-energy gamma radiation system. To minimize the formation of encaptured air during the imbibition of the water into the sand, especially near the interlayer planes, each column was first flushed with CO_2. After a column was wetted from the bottom, approximately four pore

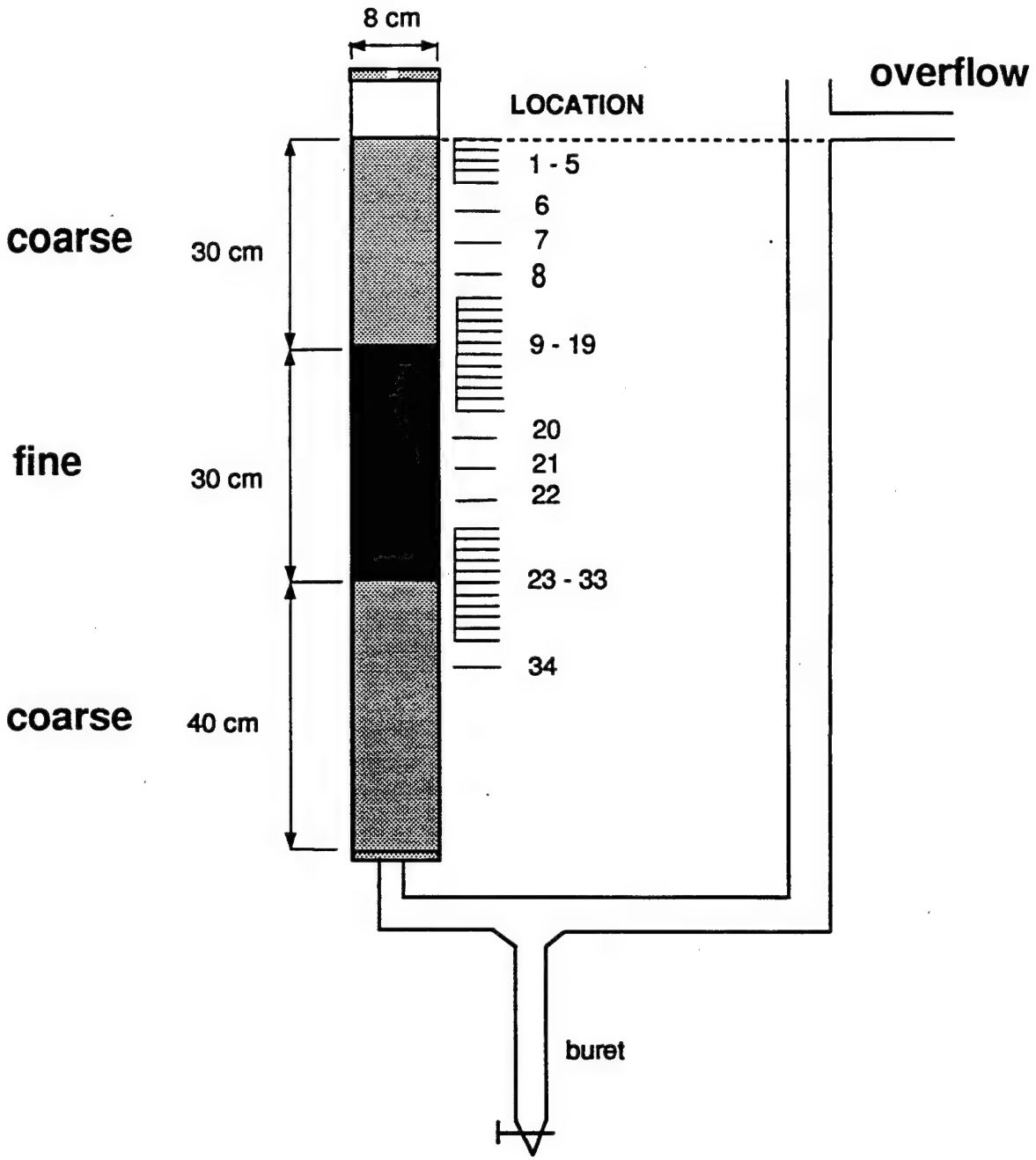

Figure 55. Simplified Schematic of the Experimental Setup.

volumes of water were flushed in the downward direction through the column to remove dissolved CO_2. All water used in the experiments had been deaired and contained traces of thymol and mercuric chloride to prevent bacterial growth. The PCE (Aldrich Chemical Company) used in the experiments was dyed with Oil Red (Aldrich Chemical Company) for visualization and photographic purposes.

In the first experiment PCE was introduced into a heterogeneous, water-saturated column with the overflow at the same height as the surface of the porous medium. Increments of 75 mL of PCE were added to the upper porous medium/air boundary. After each increment, the system was allowed to come to static equilibrium, before a next pulse of PCE was added. This routine was repeated until a significant amount of PCE was collected in the trap near the outlet of the column.

In the second experiment, the PCE spill consisted of a constant level of 6.3 cm of PCE on top of the heterogeneous, initially water-saturated sand. The constant PCE level was maintained by two mariot bottles connected by a valve to allow switching back and forth between the two bottles to avoid interruption of the PCE supply to the column. The level in the bottles was monitored regularly. A calibration curve was established so that the change of PCE level in the mariot bottles could be converted into infiltration volumes of PCE into the column. The outflow of water and PCE from the column was measured as previously described.

A third experiment was conducted to investigate the infiltration of PCE into an initially unsaturated stratified medium. After the column was first fully saturated with water, the overflow was lowered gradually until the water table in the column was 9.5 cm above the bottom of the sand column. The column was then allowed to come to static equilibrium. The gamma system was used to measure the soil water profile (initial condition for a PCE spill) along the 34 measurement locations. The spill consisted of 150 mL of PCE which was poured as quickly as possible on top of the sand.

For comparison with the second experiment, a fourth experiment was conducted with a column filled as homogeneously as possible with Flintshot 2.8 sand. This time, two mariot burets were used, which, while maintaining a constant level of 6.3 cm of PCE at the surface of the sand, improved the accuracy of the PCE inflow measurements. The gamma system was used only to measure bulk density and initial water content values during this experiment.

During and after each spill, the redistribution of the liquids within each column was measured with the dual-energy gamma radiation system. For this purpose, two different measurement schemes were used. Immediately after PCE had started to infiltrate, the change in liquid distribution with time was monitored at three different locations by continuous measurements with the gamma system. After static equilibrium or steady state conditions had been established, PCE and water content profiles were determined by measurements at all 34 locations.

C. RESULTS

Tables 15-18 show the bulk density, porosity and initial water content values at each measurement location for experiments 1 through 4, respectively. The data indicate that the pore space, during the first, second, and fourth experiment, was almost entirely occupied with water. The initial conditions in the third experiment consisted of a static water distribution in a stratified soil profile with a water table.

During the first experiment, the surface supplied PCE did not infiltrate the saturated sand until a 4.3 cm layer of PCE had formed. This corresponds to 3 increments of 75 mL each. The reason for this observed

TABLE 15. VALUES FOR THE BULK DENSITY (ρ_b), THE CORRESPONDING POROSITY (ϵ) BASED ON A PARTICLE DENSITY OF 2.65 g cm^{-3}, AND THE AVERAGE VOLUMETRIC WATER CONTENT (θ_w) FOR EXPERIMENT #1.

location	z* (cm)	ρ_b (g cm^{-3})	ϵ (-)	θ_w (-)	
1	99.5	1.734	0.346	0.310	
2	98.5	1.706	0.356	0.328	
3	97.5	1.681	0.366	0.326	
4	96.5	1.681	0.366	0.342	
5	95.5	1.663	0.372	0.347	
6	90.5	1.648	0.378	0.353	
7	85.5	1.632	0.384	0.356	
8	80.5	1.607	0.394	0.352	coarse sand
9	75.5	1.624	0.387	0.358	
10	74.5	1.623	0.388	0.361	
11	73.5	1.615	0.391	0.354	
12	72.5	1.598	0.397	0.354	
13	71.5	1.623	0.388	0.355	
14	70.5	1.716	0.352	0.341	
15	69.5	1.670	0.370	0.336	
16	68.5	1.639	0.382	0.370	
17	67.5	1.601	0.396	0.379	
18	66.5	1.569	0.408	0.387	
19	65.5	1.572	0.407	0.392	
20	60.5	1.566	0.409	0.382	
21	55.5	1.561	0.411	0.395	
22	50.5	1.596	0.398	0.380	fine sand
23	45.5	1.559	0.412	0.398	
24	44.5	1.567	0.409	0.395	
25	43.5	1.557	0.412	0.385	
26	42.5	1.576	0.405	0.416	
27	41.5	1.596	0.398	0.380	
28	40.5	1.609	0.393	0.378	
29	39.5	1.691	0.362	0.343	
30	38.5	1.644	0.380	0.333	
31	37.5	1.633	0.384	0.365	
32	36.5	1.627	0.386	0.348	coarse sand
33	35.5	1.626	0.386	0.386	
34	30.5	1.623	0.388	0.353	

* z is the elevation of the measurement location relative to the bottom of the 1.1-meter long column (Figure 55)

TABLE 16. VALUES FOR THE BULK DENSITY (ρ_b), THE CORRESPONDING POROSITY (ϵ) BASED ON A PARTICLE DENSITY OF 2.65 g cm^{-3}, AND THE AVERAGE INITIAL VOLUMETRIC WATER CONTENT (θ_w) FOR EXPERIMENT # 2.

location	z* (cm)	ρ_b (g cm^{-3})	ϵ (-)	θ_w (-)	
1	99.5	1.718	0.352	0.318	
2	98.5	1.705	0.357	0.339	
3	97.5	1.692	0.362	0.334	
4	96.5	1.675	0.378	0.340	
5	95.5	1.690	0.362	0.347	
6	90.5	1.664	0.372	0.330	
7	85.5	1.633	0.384	0.366	
8	80.5	1.622	0.388	0.358	coarse sand
9	75.5	1.622	0.388	0.364	
10	74.5	1.616	0.390	0.358	
11	73.5	1.622	0.388	0.349	
12	72.5	1.629	0.385	0.347	
13	71.5	1.641	0.380	0.354	
14	70.5	1.698	0.359	0.324	
15	69.5	1.669	0.370	0.353	
16	68.5	1.644	0.380	0.357	
17	67.5	1.614	0.391	0.364	
18	66.5	1.602	0.395	0.379	
19	65.5	1.594	0.398	0.359	
20	60.5	1.583	0.403	0.382	
21	55.5	1.577	0.405	0.386	
22	50.5	1.567	0.409	0.393	fine sand
23	45.5	1.573	0.406	0.403	
24	44.5	1.572	0.417	0.370	
25	43.5	1.567	0.409	0.389	
26	42.5	1.581	0.403	0.386	
27	41.5	1.584	0.402	0.379	
28	40.5	1.627	0.386	0.365	
29	39.5	1.710	0.355	0.316	
30	38.5	1.676	0.368	0.338	
31	37.5	1.671	0.369	0.324	
32	36.5	1.665	0.372	0.332	coarse sand
33	35.5	1.668	0.371	0.342	
34	30.5	1.671	0.369	0.344	

* z is the elevation of the measurement location relative to the bottom of the 1.1-meter long column (Figure 55)

TABLE 17. VALUES FOR THE BULK DENSITY (ρ_b), THE CORRESPONDING POROSITY (ϵ) BASED ON A PARTICLE DENSITY OF 2.65 g cm^{-3}, AND THE AVERAGE INITIAL VOLUMETRIC WATER CONTENT (θ_w) FOR EXPERIMENT # 3.

location	z* (cm)	ρ_b (g cm^{-3})	ϵ (-)	θ_w (-)	
1	99.5	1.712	0.354	0.030	
2	98.5	1.681	0.366	0.056	
3	97.5	1.649	0.378	0.055	
4	96.5	1.638	0.382	0.044	
5	95.5	1.635	0.383	0.032	
6	90.5	1.612	0.392	0.046	
7	85.5	1.622	0.388	0.057	
8	80.5	1.602	0.395	0.034	coarse sand
9	75.5	1.597	0.400	0.052	
10	74.5	1.601	0.396	0.043	
11	73.5	1.590	0.400	0.039	
12	72.5	1.579	0.404	0.043	
13	71.5	1.590	0.400	0.047	
14	70.5	1.657	0.375	0.039	
15	69.5	1.677	0.367	0.266	
16	68.5	1.637	0.382	0.244	
17	67.5	1.596	0.398	0.221	
18	66.5	1.588	0.401	0.217	
19	65.5	1.584	0.402	0.231	
20	60.5	1.585	0.402	0.375	
21	55.5	1.578	0.405	0.398	
22	50.5	1.577	0.405	0.393	fine sand
23	45.5	1.567	0.409	0.375	
24	44.5	1.581	0.403	0.382	
25	43.5	1.606	0.394	0.386	
26	42.5	1.606	0.394	0.389	
27	41.5	1.609	0.393	0.358	
28	40.5	1.677	0.367	0.378	
29	39.5	1.677	0.367	0.342	
30	38.5	1.682	0.365	0.337	
31	37.5	1.637	0.382	0.358	
32	36.5	1.623	0.388	0.371	coarse sand
33	35.5	1.627	0.386	0.343	
34	30.5	1.616	0.390	0.353	

* z is the elevation of the measurement location relative to the bottom of the 1.1-meter long column (Figure 55)

TABLE 18. VALUES FOR THE BULK DENSITY (ρ_b), THE CORRESPONDING POROSITY (ϵ) BASED ON A PARTICLE DENSITY OF 2.65 g cm^{-3}, AND THE AVERAGE INITIAL VOLUMETRIC WATER CONTENT (θ_w) FOR EXPERIMENT #4.

location	z* (cm)	ρ_b (g cm^{-3})	ϵ (-)	θ_w (-)
1	99.5	1.728	0.348	0.313
2	98.5	1.700	0.358	0.324
3	97.5	1.691	0.362	0.322
4	96.5	1.674	0.368	0.331
5	95.5	1.648	0.378	0.351
6	90.5	1.611	0.392	0.338
7	85.5	1.616	0.390	0.364
8	80.5	1.587	0.401	0.371
9	75.5	1.590	0.400	0.383
10	74.5	1.587	0.401	0.358
11	73.5	1.575	0.406	0.393
12	72.5	1.592	0.399	0.375
13	71.5	1.604	0.395	0.360
14	70.5	1.598	0.397	0.376
15	69.5	1.593	0.399	0.359
16	68.5	1.594	0.398	0.378
17	67.5	1.585	0.402	0.357
18	66.5	1.586	0.402	0.364
19	65.5	1.604	0.395	0.359
20	60.5	1.579	0.404	0.374
21	55.5	1.586	0.402	0.366
22	50.5	1.589	0.400	0.386
23	45.5	1.583	0.403	0.365
24	44.5	1.587	0.401	0.362
25	43.5	1.591	0.400	0.364
26	42.5	1.597	0.397	0.360
27	41.5	1.586	0.402	0.364
28	40.5	1.588	0.400	0.364
29	39.5	1.587	0.401	0.370
30	38.5	1.600	0.396	0.367
31	37.5	1.600	0.396	0.356
32	36.5	1.600	0.396	0.363
33	35.5	1.593	0.399	0.366
34	30.5	1.621	0.388	0.344

* z is the elevation of the measurement location relative to the bottom of the 1.1-meter long column (Figure 55)

phenomenon is that the entry pressure in the water-PCE system must first be exceeded before PCE can displace water. The entry pressure (between 2.9 and 4.3 cm) corresponds with values reported earlier (Güven et al., 1995). Once the PCE had started to infiltrate it continued to do so until all PCE at the surface had been depleted. Figure 56 shows the volumetric water and PCE content distributions after static equilibrium had been established, which occurred after about 2 days. All the infiltrated PCE had accumulated in the top layer consisting of the coarser Ottawa 2.8 sand (Figure 56 and 57). PCE had infiltrated readily into the top layer because of its relatively high conductivity for PCE. After encountering the coarse/fine sand interface, the PCE spread laterally above the interface, because the fine layer, with a relatively low conductivity for PCE, greatly inhibited the flow of PCE delivered to it. No PCE had drained from the column during this first stage of the experiment. After static equilibrium conditions had been reached, additional increments of PCE were supplied to the top of the sand. During this second series of spills, a total of 300 mL (4 increments) of PCE had to be added before infiltration restarted. The 5.95 cm PCE layer was higher than the layer required during the first series of spills. This may have been caused by the high resistance to water flow through the area just above the coarse-fine sand interface, where PCE had accumulated. This high resistance to water flow may also have caused an increase in water pressure immediately after PCE had been added to the top of the sand, which would require a higher pressure in the PCE before the NAPL would enter the sand. Again, all PCE added to the top of the sand infiltrated into the porous medium, although at a much lower rate than for the first set of spills. No water was displaced upwards from the top of the porous medium during or after the PCE infiltration. This indicates that during the PCE infiltration, the water pressure at the top of the sand gradually had decreased to zero. Following the second set of spills, 268 mL of PCE drained from the bottom of the column. Volumetric PCE and water content distributions (Figure 58) were determined again for all 34 locations after both water and PCE had ceased to flow from the column. The results reveal that almost all of the remaining PCE (257 mL) had accumulated above the coarse/fine sand interface and that the residual PCE saturations in the two lower layers were low. It should be noted that it took about 12 days to reach static equilibrium after the second series of spills, compared to two days for the first one. This was attributed to the low conductivity for PCE in the fine layer.

The second experiment simulated a continuous PCE spill by maintaining a constant level of PCE on top of the column. Figure 59 shows the flow rates of PCE and water into and out of the column. Initially the PCE infiltration rate went up rapidly, which was attributed to the increasing length of the PCE fingers. The rapid increase was followed by a sharp decrease, which was most likely due to the arrival of the tip of the fingers at the top of the fine layer, which had a much lower conductivity than the overlying coarse layer. Visual inspection of the column corroborated that the arrival of the PCE at the coarse/fine sand interface coincided with the reduction in PCE infiltration rate. Figure 61 shows the displacement of water by PCE over time just above the interface at Location 12. The data obtained at Location 8 (Figure 60), higher in the column, shows a similar pattern, although the displacement generally started to develop later, and the PCE content did not increase as much. This indicates that the accumulation of PCE started from the interface. Figure 62 shows the pattern at Location 17, which is located beneath the first interface. The start of the water displacement by PCE at this location was yet later than at either Location 8 or 12. After the initial drop in infiltration rate, it increased again (Figure 58) until the fingers reached the bottom of the column, as observed by visual inspection, when it decreased again. This second reduction was probably caused by the discontinuity of the capillary pressure across the sand-outflow tube interface, which causes a high resistance to the flow of PCE (Leverett, 1941). Once the first PCE had been collected in the buret, both the infiltration and outflow rate of PCE increased again. For most of the experiment, the PCE infiltration rate was higher than its outflow rate, which indicates an increase in storage of PCE in the column. The concomitant increase in PCE conductivity explains the general increase in infiltration rate. After about 1100 minutes, the infiltration rate of PCE became equal to its outflow rate. Since the outflow of water had also stopped, we assumed steady-state PCE flow in a porous medium with the water at static equilibrium. Corresponding

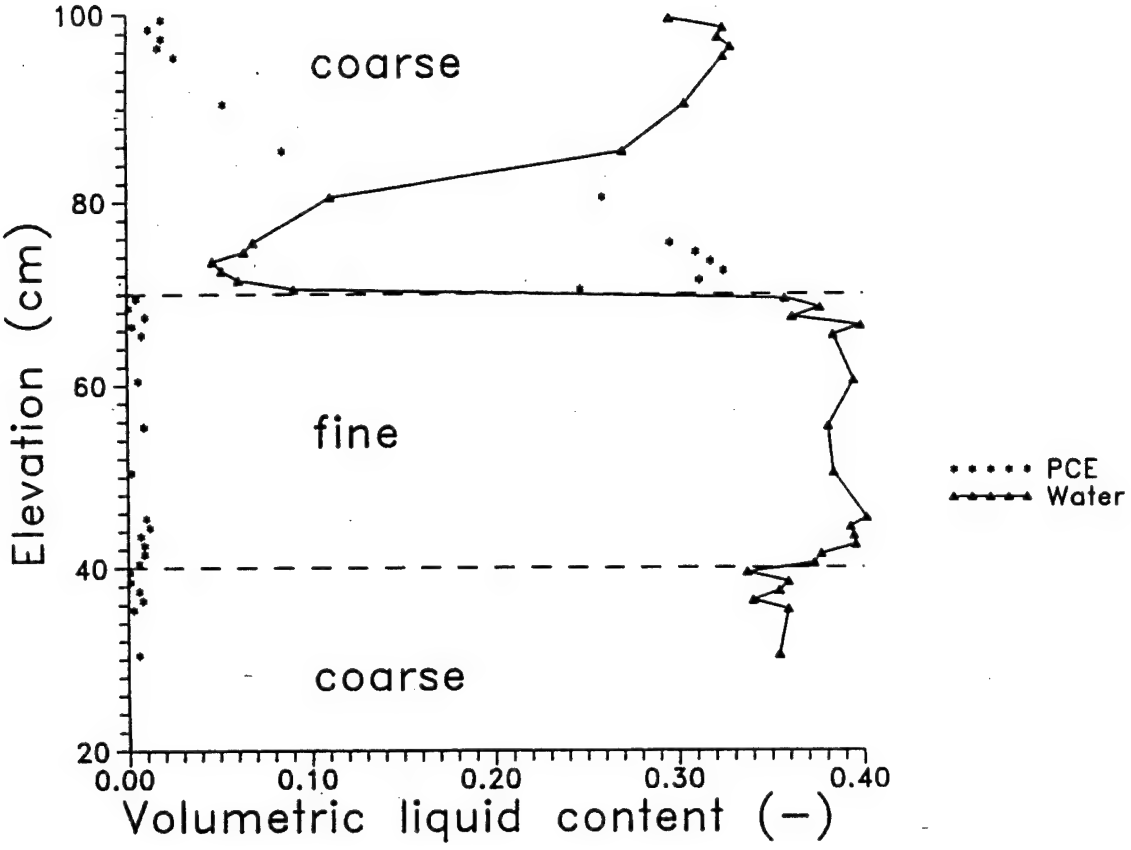

Figure 56. Profiles of Volumetric Water and PCE Content at Static Equilibrium after the First Series of Spills.

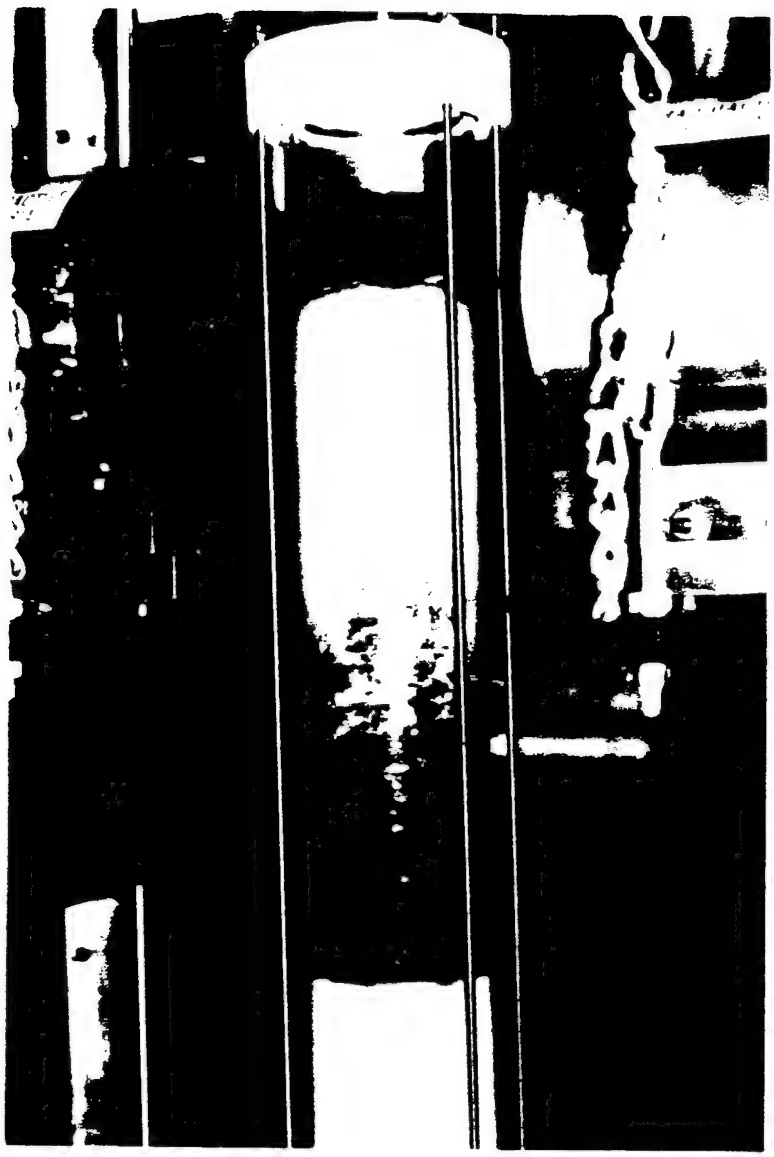

Figure 57 Experiment 1. Accumulation of PCE on Top of the Coarse Fine Sand Interface After the First Series of Spills

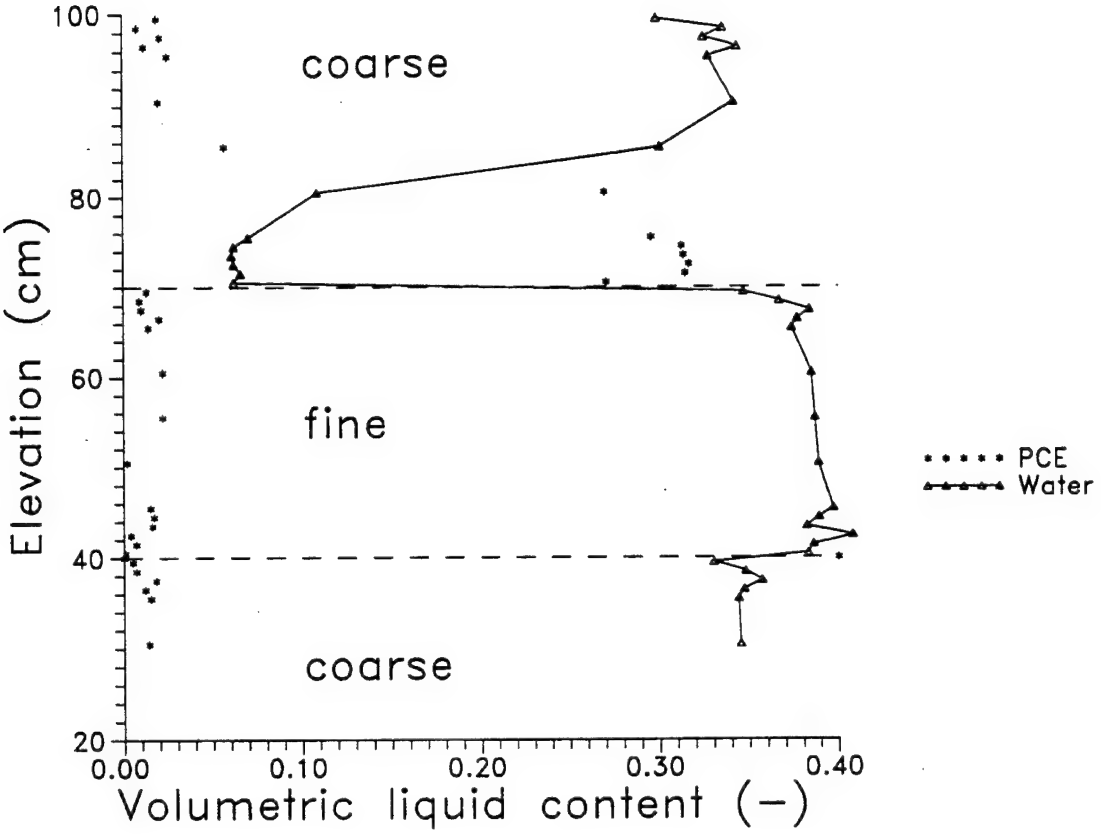

Figure 58. Profiles of Volumetric Water and PCE Content at Static Equilibrium After the Second Series of Spills.

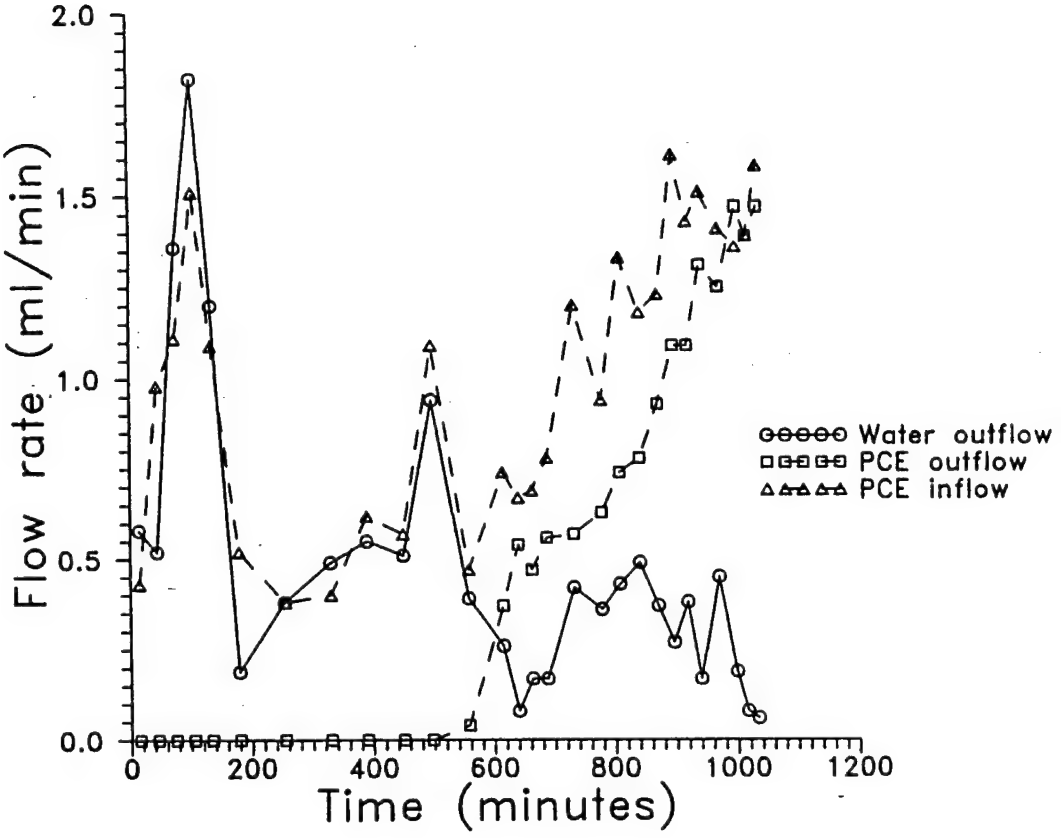

Figure 59. In- and Outflow Rates of Water and PCE Versus Time During Experiment #2.

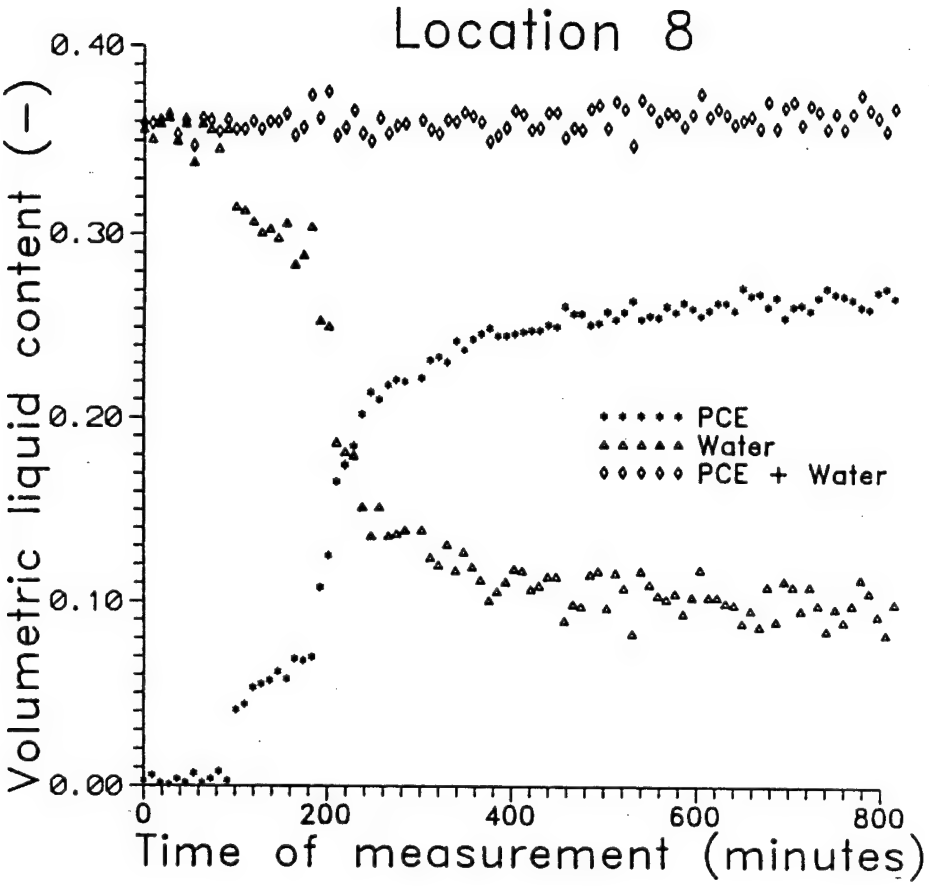

Figure 60. Displacement of Water by PCE at Location 8.

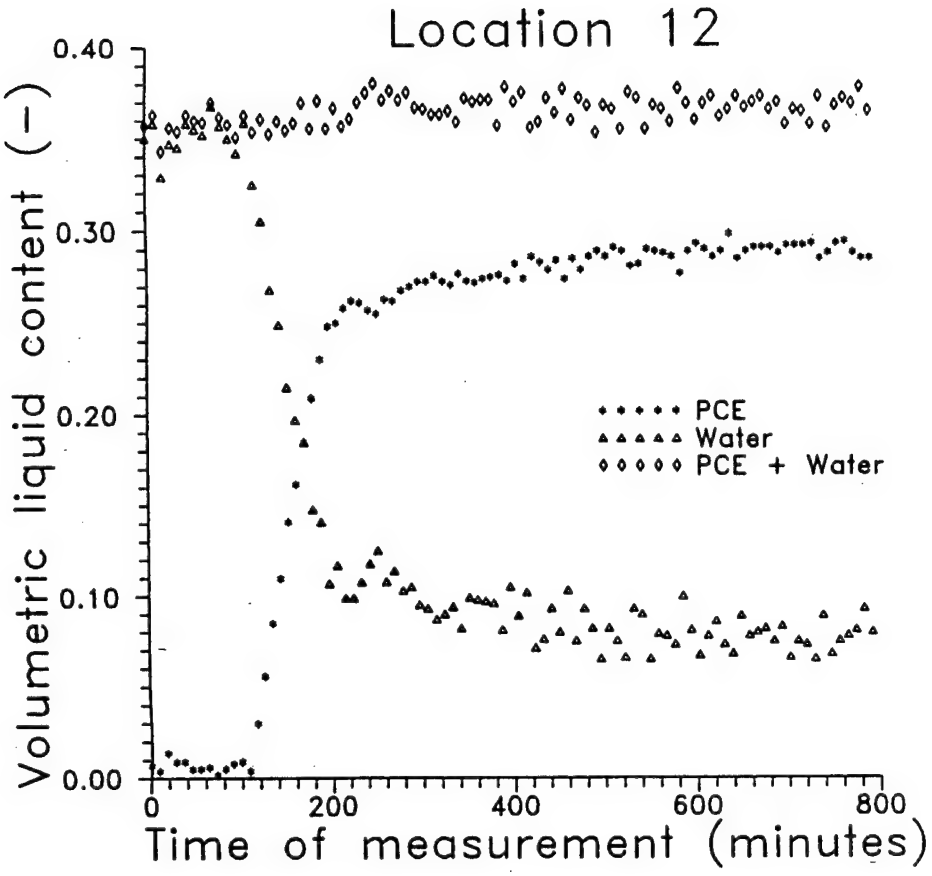

Figure 61. Displacement of Water by PCE at Location 12.

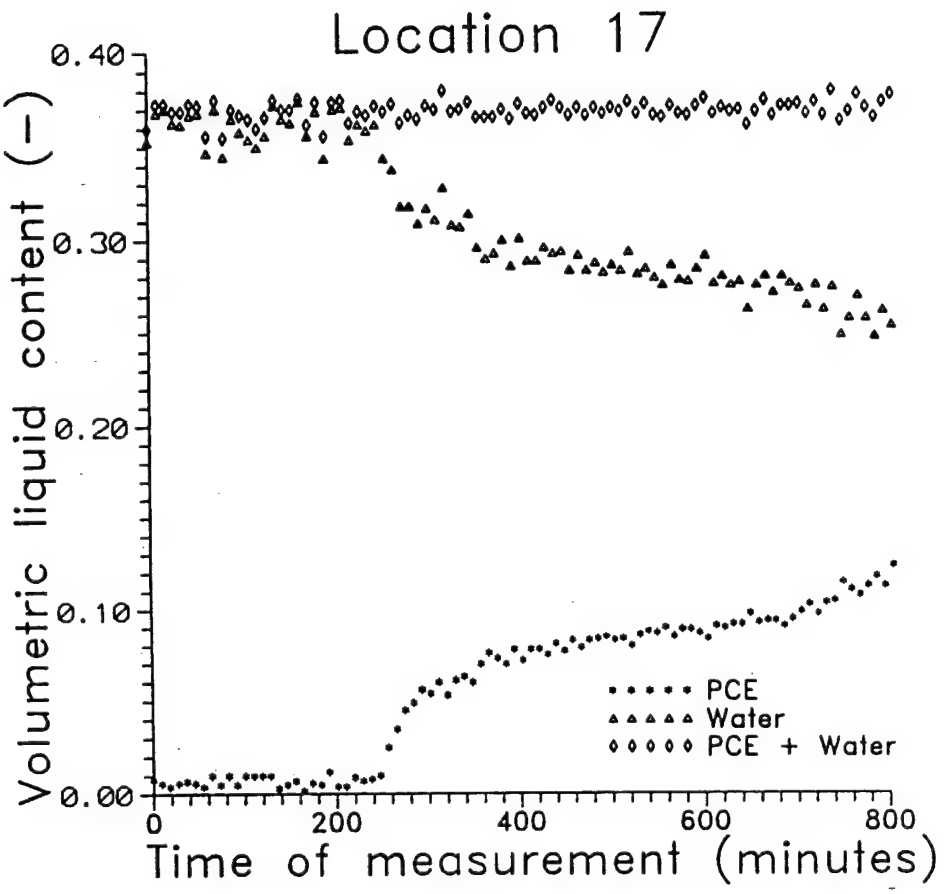

Figure 62. Displacement of Water by PCE at Location 17.

volumetric PCE and water content profiles as measured with the gamma system are shown in Figure 63. Again, very high PCE contents were observed just above the coarse/fine sand interface. The total amount of the PCE (557.14 mL) in the column during steady-state infiltration was measured by comparing the total inflow of PCE with the total outflow.

Figure 64 shows the initial water content distribution for the third experiment. The top of the capillary fringe is located 50 cm above the bottom of the sand column. The spill of 150 mL of PCE infiltrated into the vadose zone as soon as it was poured onto the surface. It was impossible to introduce the PCE quickly enough to form a layer of PCE on top of the sand without disturbing the surface. The initial infiltration was therefore a truly three-dimensional phenomenon. Air was observed visually to be displaced in the upward direction from the porous medium as indicated by rapid bubbling at the surface. The displacement of air by PCE had caused the air pressure to increase, which caused it to flow in the direction of least resistance. The in and outflow of water and PCE at the bottom of the column is shown in Figure 65. It shows that the outflow of water started immediately after the start of the PCE infiltration. The initial drainage of water was most likely due to the increased air pressure and was followed by the displacement of water by PCE. The infiltration process was too fast for the gamma system to monitor. While migrating downwards in the vadose zone, the PCE plume appeared to have a reasonably uniform infiltration front (Figure 66) relative to those observed in the saturated porous media, with a rather high PCE content just behind it. The PCE content declined with increasing distance from the front. Moving from the upper coarse layer into the fine layer did not seem to have a pronounced effect on the plume behavior. Some lateral spreading of the plume was observed (Figure 67), however, beneath the coarse/fine sand interface, which indicates that under the prevailing experimental conditions, capillary effects had relatively more impact on the flow of the intermediate wetting fluid (PCE) in the fine layer than in the coarse layer.

After encountering the top of the capillary fringe, the infiltration front started to disintegrate and distinct fingers started to form (Figure 68). Of the 150 mL of PCE added, eventually 25 mL drained from the bottom of the column. Some reversed flow of water into the column was measured as PCE was trapped in the buret (Figure 65). After about 6 days, static equilibrium had been reached, as indicated by the lack of liquid flow. Subsequently, volumetric PCE and water content profiles were obtained with the gamma system (Figure 69). The average residual PCE content in the fine layer was higher than in either of the coarse layers. The top of the capillary fringe at the end of the experiment was somewhat lower then at the start, which may have been caused by a reduction in surface tension of the water-air interface.

Figure 70 shows the inflow rate of PCE and the outflow rate of water during the constant head infiltration of PCE into a homogeneous, initially water saturated sand column (experiment #4). The infiltration rate increased with time, until the PCE had reached the bottom of the column. Similar to the second experiment, the PCE infiltration rate declined just before the first PCE was collected in the trap. After the PCE fingers had moved through the bottom boundary with high resistance to NAPL flow, and the first PCE exited the column, the infiltration rate increased very rapidly up to about 25 mL/min (not shown in Figure 70). The rapid increase of the infiltration rate indicates that the PCE fingers had formed a continuous path between the constant head source on top of the sand and the bottom of the column. These fingers could transmit large amounts of PCE without displacing water. The experiment was terminated soon after the first PCE exited the column due to the lack of storage capacity in the PCE trap.

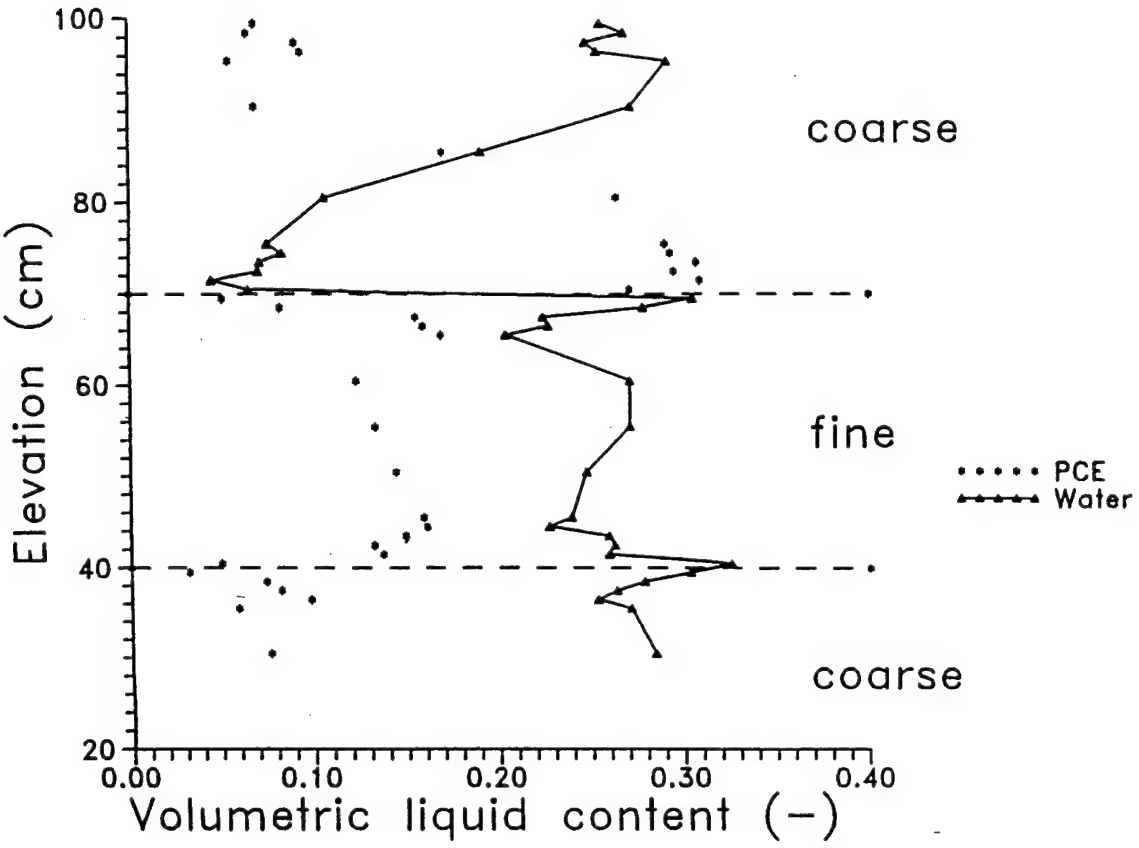

Figure 63. Profiles of Volumetric Water and PCE Content During Steady-State PCE Flow in an Initially Water-Saturated Stratified Porous Medium.

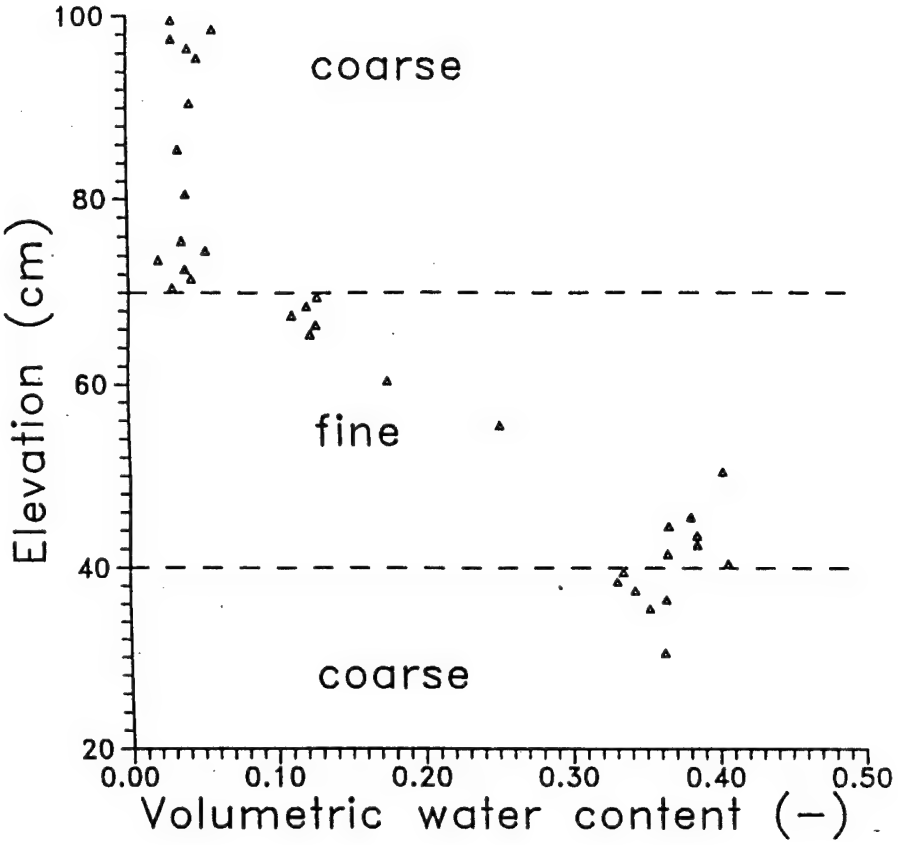

Figure 64. Initial Water Content Distribution for the Third Experiment.

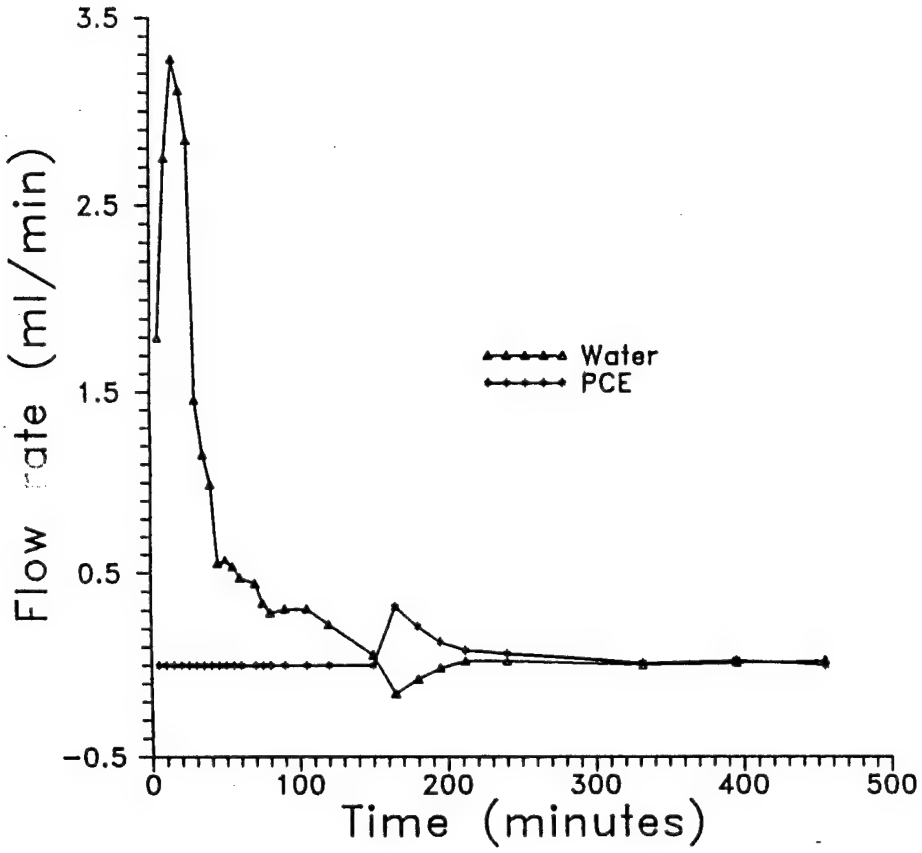

Figure 65. In- and Outflow of Water and PCE at the Bottom of the Column.

Figure 20. PCE Plume 3 Minutes After the Start of the Experiment

Figure 57 Lateral Spreading of the PCE Plume Beneath the Coarse Fine Sand Interface

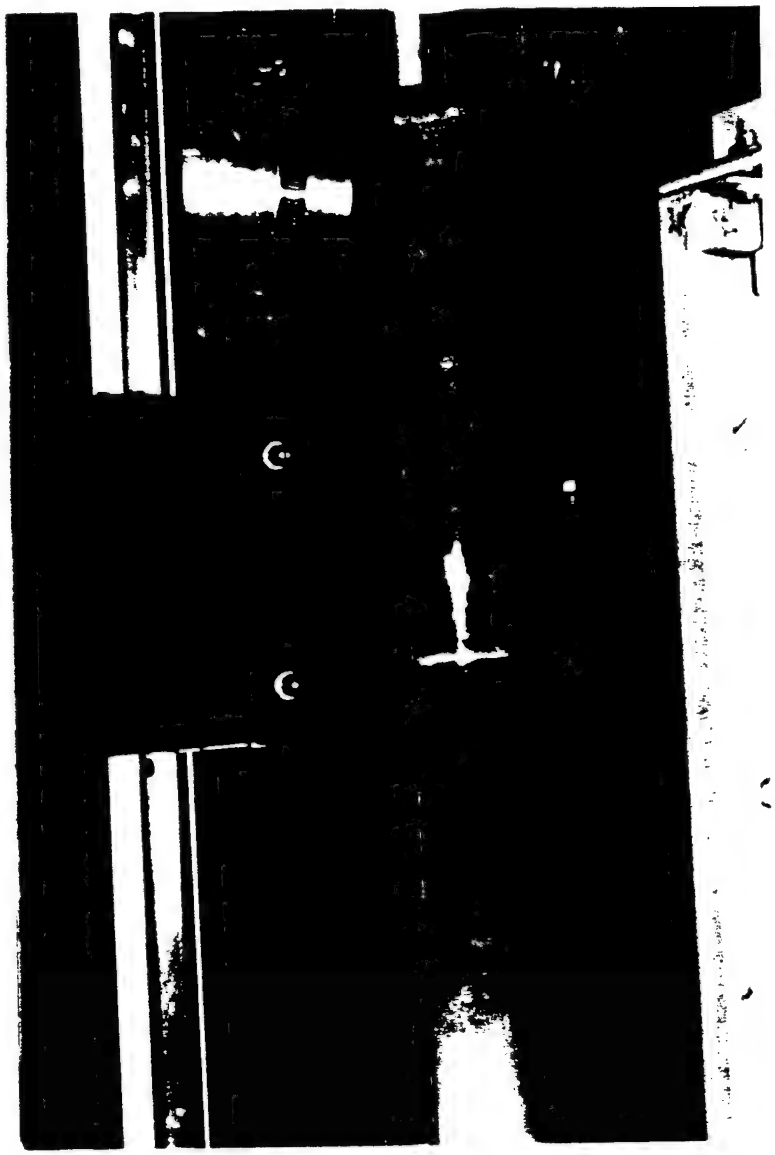

Figure 58 Disintegration of the PCE Infiltration Front at the Top of the Capillary Fringe about 15 Minutes After the Start of the Experiment

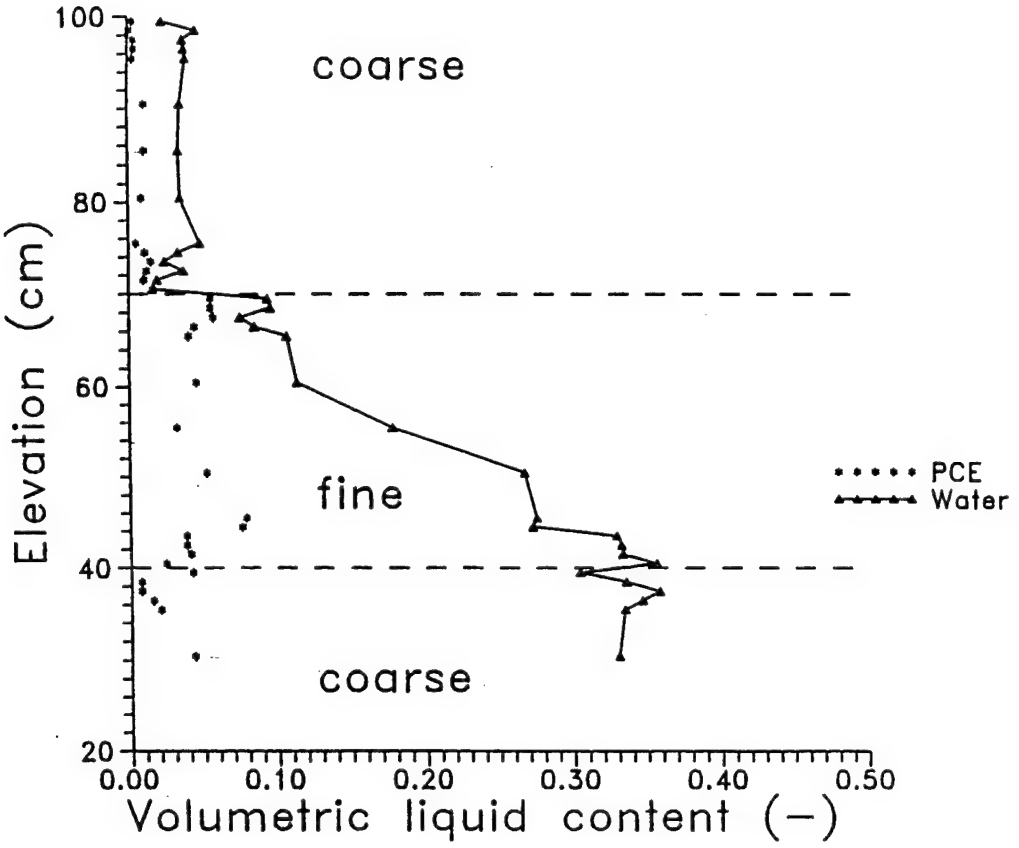

Figure 69. Profiles of Volumetric Water and PCE Content at Static Equilibrium During Experiment #3.

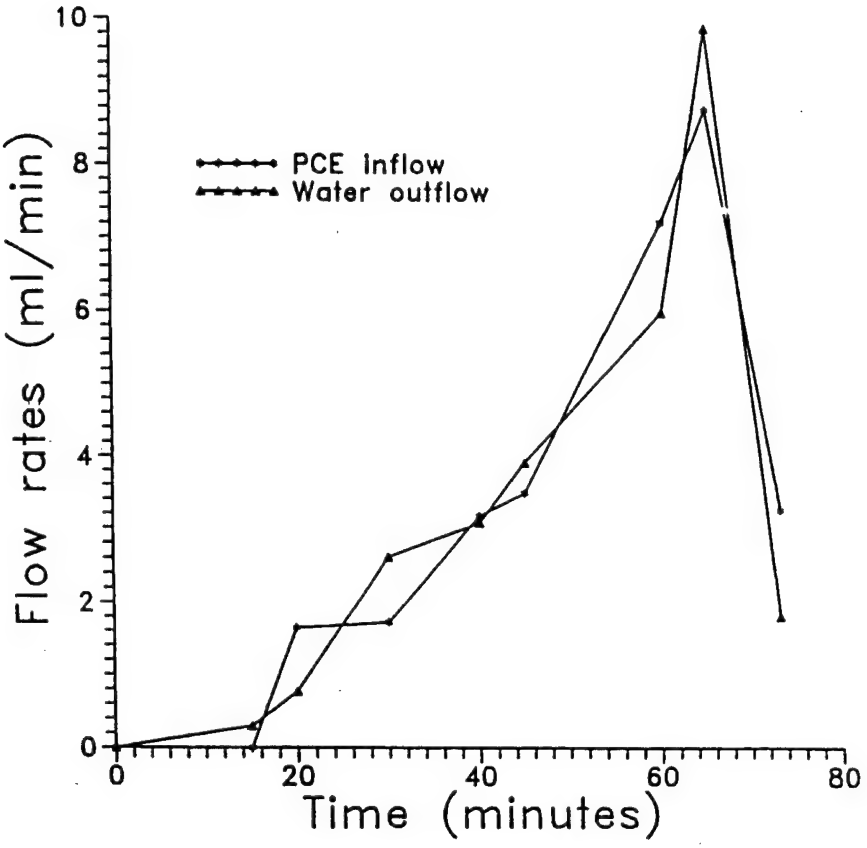

Figure 70. Inflow Rate of PCE and Outflow Rate of Water Versus Time During Experiment #4.

D. DISCUSSION

One should be cautious in interpreting the gamma system measurements. The measurements represent average volumetric liquid contents as encountered by the gamma radiation beam as it travels through the porous medium. Vertical infiltration of PCE is inherently unstable and fingers, which are likely to form, convey all the PCE within a small area. If a finger is located outside the range of the gamma radiation beam, it cannot be detected. Near the interface of the coarse sand overlying the fine sand, where accumulation of PCE occurred, the measurements should be much more representative. For this reason the gamma system was only used in the layered porous media. Overall, the smooth shape of most liquid profile data indicate that the gamma system readings were reasonable representations of the average fluid contents.

The existence of free-phase PCE at static equilibrium in Experiments 1 and 2 was solely due to the geometry of the columns. In a three-dimensional system the free phase would spread laterally until it reached residual saturation. The geometry of the column also limited the directions in which the water could flow. Consequently, pressure gradients in the water may, in some cases, have been higher than what they would have been under natural field situations.

E. CONCLUSIONS

Our experiments clearly indicate that in a field situation stratification in the saturated part of the subsurface is likely to increase the lateral dimensions of a PCE contaminated area. Stratification in the vadose zone, however, appears to be of minor importance to the overall flow behavior of PCE for the porous media used in the present experiments.

REFERENCES FOR SECTION VI

Dane, J. H., M. Oostrom, and B.C. Missildine, "An Improved Method for the Determination of Capillary Pressure-Saturation Curves Involving TCE, Water and Air." Journal of Contaminant Hydrology, 11: 69-81, 1992.

Güven, O., Dane, J.H., Hill, W.E., Hofstee, C., and Mamballikalathil, R., Subsurface Transport of Hydrocarbon Fuel Additives and a Dense Chlorinated Solvent, Interim Report, AL/EQ-TR-1994-0039, Armstrong Laboratory, Tyndall Air Force Base, Florida, January 1995.

Leverett, M.C., "Capillary Behavior in Porous Solids." Transaction of the American Institute of Mining Engineers, 142: 152-169, 1941.

SECTION VII
SURFACTANT ENHANCED REMOVAL OF ENTRAPPED PCE FROM ONE-DIMENSIONAL COLUMNS OF HETEROGENEOUS AND HOMOGENEOUS POROUS MEDIA

A. INTRODUCTION

This section describes a series of surfactant enhanced cleanup experiments performed with PCE-contaminated columns of heterogeneous and homogeneous porous media immediately following the experiments described in Section VI. The main purpose of these cleanup experiments was to obtain detailed basic data on the dissolution and removal of PCE from contaminated porous media. These experiments complement previous work done by others (e.g., Abdul et al., 1990; Miller et al.,1990; Imhoff et al., 1993; Pennell et al., 1993; Powers et al., 1994; Shiau et al., 1994; Geller and Hunt, 1993).

B. MATERIALS AND METHODS

Cleanup experiments were conducted immediately following the experiments described in Section VI -Transient Flow Experiments with Water, PCE and Air in Nominally 1-D, Homogeneous and Heterogeneous Porous Media. In those experiments different types of spills were released into homogeneous and heterogeneous media. Post experiment PCE saturations were high and implied that a continuous PCE phase existed. Therefore, all columns described in Section VI were flushed with water or a low concentration of surfactant solution (below the critical micelle concentration) to reduce the PCE saturations to near residual values prior to the cleanup experiments reported in this section. The amount of free PCE which left the column was measured during this pretreatment phase of the experiments. The PCE saturation values were also measured, using the dual-energy gamma radiation system (gamma system). The free PCE measurements were needed to determine a mass balance for each column. The final PCE saturation distribution at the end of pretreatment was needed so that the initial saturations for the surfactant flushing experiments would be known.

Four surfactant flushing experiments were performed using the four contaminated columns used previously in the spill experiments described in Section VI. The first three columns were heterogeneous, with the heterogeneity being three large-scale layers of a fine and a coarse sand. As described in Section VI (Figure 55), the layers consisted of a 30-cm layer of fine sand (Ottawa, F-75) between a 30-cm upper and a 40-cm lower layer of coarse sand (Ottawa, Flintshot 2.8), with a total height of 100 cm of sand in each column. The column inside diameter was 8 cm. The fourth column was packed in a homogeneous manner with the coarse sand (Flintshot 2.8). These columns, which correspond to the columns used in Experiments 1, 2, 3, and 4 of Section VI, are designated in this section as Columns 1, 2, 3 and 4, respectively. As described in Section VI, the media in Columns 1, 2, and 4 were nearly fully saturated, while the medium in Column 3 was unsaturated. The PCE spill for Column 1 occurred in a discontinuous manner (in increments of 75 mL), while the PCE spills for Columns 2 and 4 were continuous. The spill for Column 3 consisted of a single, quick release of 150 mL of PCE.

The surfactant solution used in the experiments was a mixture of deionized water and Tween 80 (a commercially produced biodegradable nonionic surfactant) with a surfactant concentration of 4% by volume. Thymol and mercuric chloride were added to the surfactant solutions to inhibit the growth of microbes. Tween 80 was used because it is nonionic, biodegradable and readily available. Nonionic surfactants tend to have the least amount of interaction with the solid surfaces and are usually characterized by a long

oxylethylenated chain (Rosen, 1978). This chain can increase the size of the micelles which can increase the amount of NAPL mass taken up by the micelle. This surfactant has proven to work well in sands (Pennell et al., 1993).

The experimental setup used in Section VI was modified to incorporate manometers at the top and bottom of the column to measure the water pressure and a sampling mechanism at the bottom to collect fluid samples. Measurements of the water pressures were taken over the duration of the experiment and hydraulic conductivities were calculated. In Columns 1, 2, and 4, the small vent on the top of each column, allowing constant atmospheric air pressure, was closed off so that a constant flow regime would be maintained. A Master-flex pump fitted with Viton tubing was attached to the top of the column. The pump was used to force the surfactant solution through the column in a downward manner at a constant rate (Q_{pump}=1.2 mL/min). In Column 3, the pump was attached to the bottom and the surfactant solution was applied from the top using a mariot bottle to produce a constant head of 5 cm above the top of the sand.

Before pumping the surfactant solutions through the columns, initial water and PCE contents were measured using the gamma system. After the pumping was started, water and PCE contents were measured using the gamma system, effluent samples were collected, and free PCE and pressure measurements were recorded every four to eight hours during the experiment. Near the end of each experiment, the sampling times were increased because fluctuations in the above measurements became smaller with time.

All effluent samples were immediately prepared for injection into a gas chromatograph. About 1 mL of effluent was injected into a clean and weighed glass vial. A dilute mixture of decane in isopropanol was injected into the vial containing the weighed sample. Enough decane/isopropanol mixture was added to reduce the head space to a minimum, so that PCE losses due to volatilization would be minimized. The decane/isopropanol mixture was used to homogenize the aqueous sample and the decane acted as an internal standard. All samples were injected into the GC by a Shimadzu autosampling device and a flame ionization detector (FID) was used to measure PCE concentrations.

C. RESULTS

In order to compare the results of the individual column experiments performed, breakthrough curves of PCE concentration are plotted in the form of relative concentration versus pore volumes for each experiment on the same plot in Figure 71. The definition of pore volumes (PV) used in this section is based on an average porosity value of 0.365, a column diameter of 8 cm and a length of 100 cm for all the columns. Hence, 1 PV corresponds to a volume of 1835 mL, or an elapsed time of 25.5 hours with the experimental flow rate of 1.2 mL/min. Relative concentration is defined as the actual concentration, C, measured with the GC divided by the equilibrium concentration, Ce. The equilibrium concentration was determined to be 25,100 mg/kg for a 4% solution Tween 80.

Figure 71 shows that Columns 1, 2, and 4 all have concentrations above the equilibrium concentration of 25,100 mg/kg or the relative concentration of 1.0. One possible explanation for the larger than 1.0 relative concentration values may be the formation of microemulsions in the columns. McAuliffe (1973), Schmidt et al. (1984), and Herzig et al. (1970), have all reported that emulsion formation in the presence of aqueous surfactants does occur. Most of this work was done by petroleum engineers for improving oil recovery. For oil recovery bulk transport of the oil is most important and the amount of oil stored in the aqueous/surfactant phase is relatively small. These factors resulted in research that concentrated on bulk flow rather than solubilized oil, so no concentration data was obtained. Therefore, no direct comparisons can be made between the experiments of this study and the petroleum industry studies. Under the conditions in the

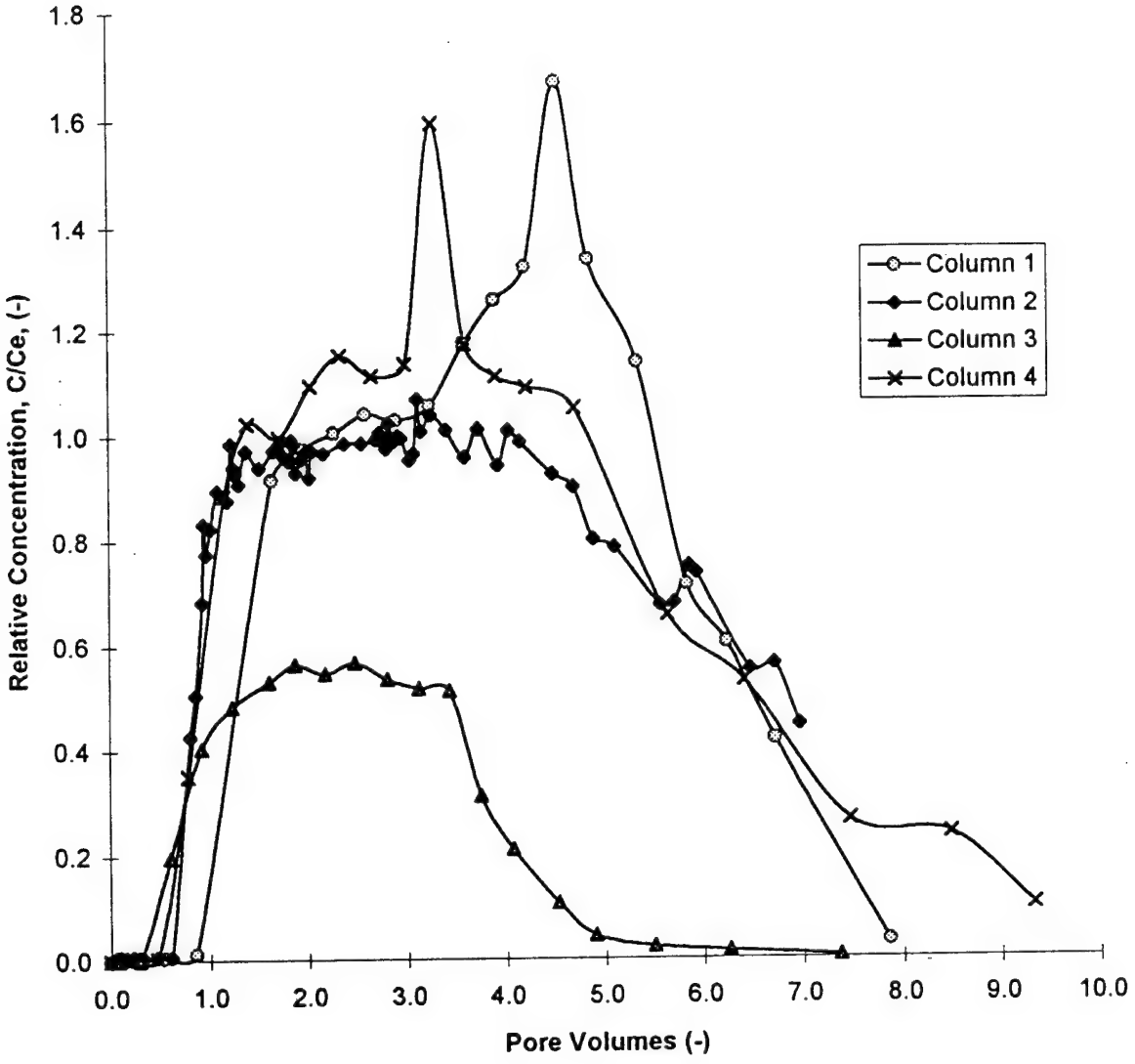

Figure 71. Relative Concentrations versus Pore Volumes for Columns 1, 2, 3 and 4 (Q_{pump}=1.2 mL/min and Ce=25,100 mg/kg).

columns emulsions may have formed and traveled through the column without coalescing with any of the attached ganglia. In fact, the aqueous-phase surfactant and PCE could have been under the necessary conditions for the formation of Winsor Type III microemulsions. Shiau et al. (1994) have shown that Type III emulsions do exist and have higher NAPL concentrations than what would occur by micelle solubilization alone. One of the defining physical characteristics of Type III microemulsions is the milky solutions they produce. This type of solution is due to the structure of Type III microemulsions, which is a combination of water-in-oil and oil-in-water emulsions with surfactant present at the interfaces in both cases. Indeed, solutions taken from the effluent of Columns 1 and 4 were milky in color.

The largest measured concentrations in Column 2, which occurred in the quasi-steady "plateau" portion of the breakthrough curve, were at or close to the equilibrium concentration over the duration of the experiment. Some concentrations were slightly higher than the equilibrium concentration, which implies that there might have been some emulsion formation or some error in the measurements. Columns 1 and 4 had measured concentrations up to 1.65 times the equilibrium concentration, which implies that some process other than micelle solubilization has occurred. It would be apparent, if the concentrations were close to the solubility limit, that the process occurring is micelle solubilization. Since the concentrations are on the order of 1.1 to 1.65 times the equilibrium concentration, some type of emulsion must be forming. Of the two types of emulsions suggested previously, the Winsor Type III microemulsion seems to be the most feasible explanation for the excessive measured concentrations.

Column 3, the unsaturated case, showed no evidence of Type III microemulsions. Here surfactant solutions were applied from the top and pumped from the bottom with the intention of maintaining an unsaturated zone in the upper levels of the column. The largest measured equilibrium concentrations for Column 3 were observed in the plateau portion of the breakthrough curve, which were approximately half of the equilibrium value of 25,100 mg/kg determined from batch tests. One reason for this behavior may be that mass transfer rates in the unsaturated zone are significantly lower than in the saturated case, where the concentrations approached the batch equilibrium value. This is due to the reduced interfacial area for mass transfer because of the presence of air. In this experiment the air contents were reduced when the surfactant solutions were applied to the top of the column. Air was seen bubbling out of the top of the porous medium as a direct result of the increased air pressure and density difference. The structure of the phases in an unsaturated sand is significantly different from that in the saturated case (Corey, 1994). Unsaturated sand with residual NAPL has a layer of continuous water adsorbed to the sand, followed by a NAPL layer and then an air pocket (Corey, 1994). Saturated sand has a layer of water enclosing a trapped NAPL blob. Another reason for the differences in the breakthrough curves of the different columns may be the different initial distributions of the PCE saturations in the columns. For example, as discussed in more detail below, gamma system measurements indicated that unsaturated zone NAPL saturations were initially lower than those in the saturated columns.

To illustrate the differences in saturation or volumetric PCE contents and mass transfer rates, changes in the volume of PCE in each column were calculated. The results are plotted in Figures 72 and 73 in the form of PCE volume in the column versus pore volumes. The values shown in Figure 72 were calculated from the breakthrough curves. The initial volume of PCE in the columns (corresponding to a pore volume of PV = 0) was measured by subtracting the amount of PCE that was spilled into the columns and the amount of PCE that was removed during the pretreatment phase. For comparison, the volume of PCE in the columns was also determined by integration of the volumetric PCE contents measured by the gamma system over the length of each column. The latter results are plotted in Figure 73. In the calculation of the PCE volumes based on the gamma system measurements, the volume of PCE between elevations 0 and 30 cm was estimated based on the average of the PCE contents observed between elevations 30 and 40 cm. This approach was used because

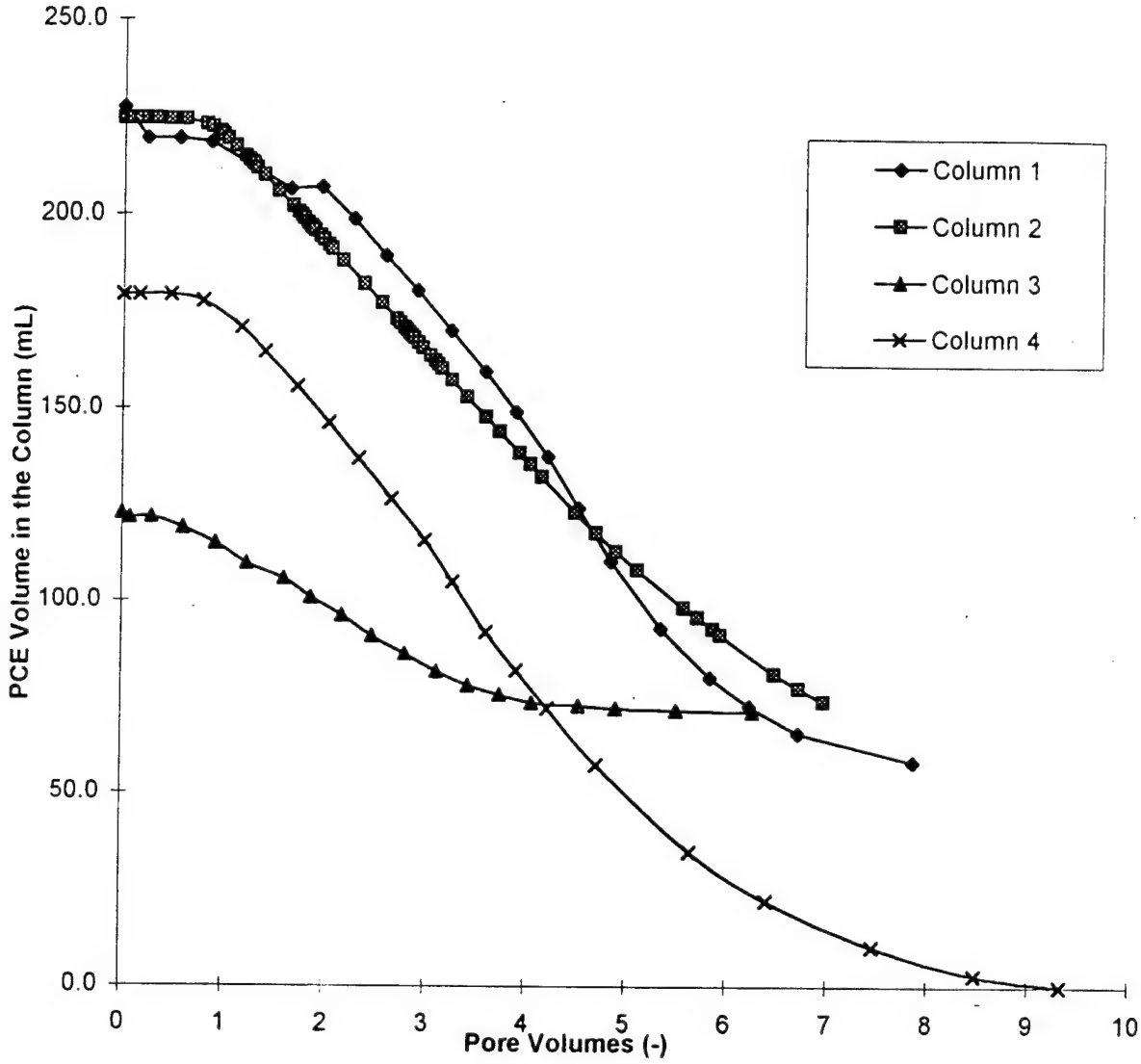

Figure 72. Calculated Volume of PCE in the Column (Based on the Effluent Concentration Breakthrough Data) as a Function of Pore Volumes for Each Experiment.

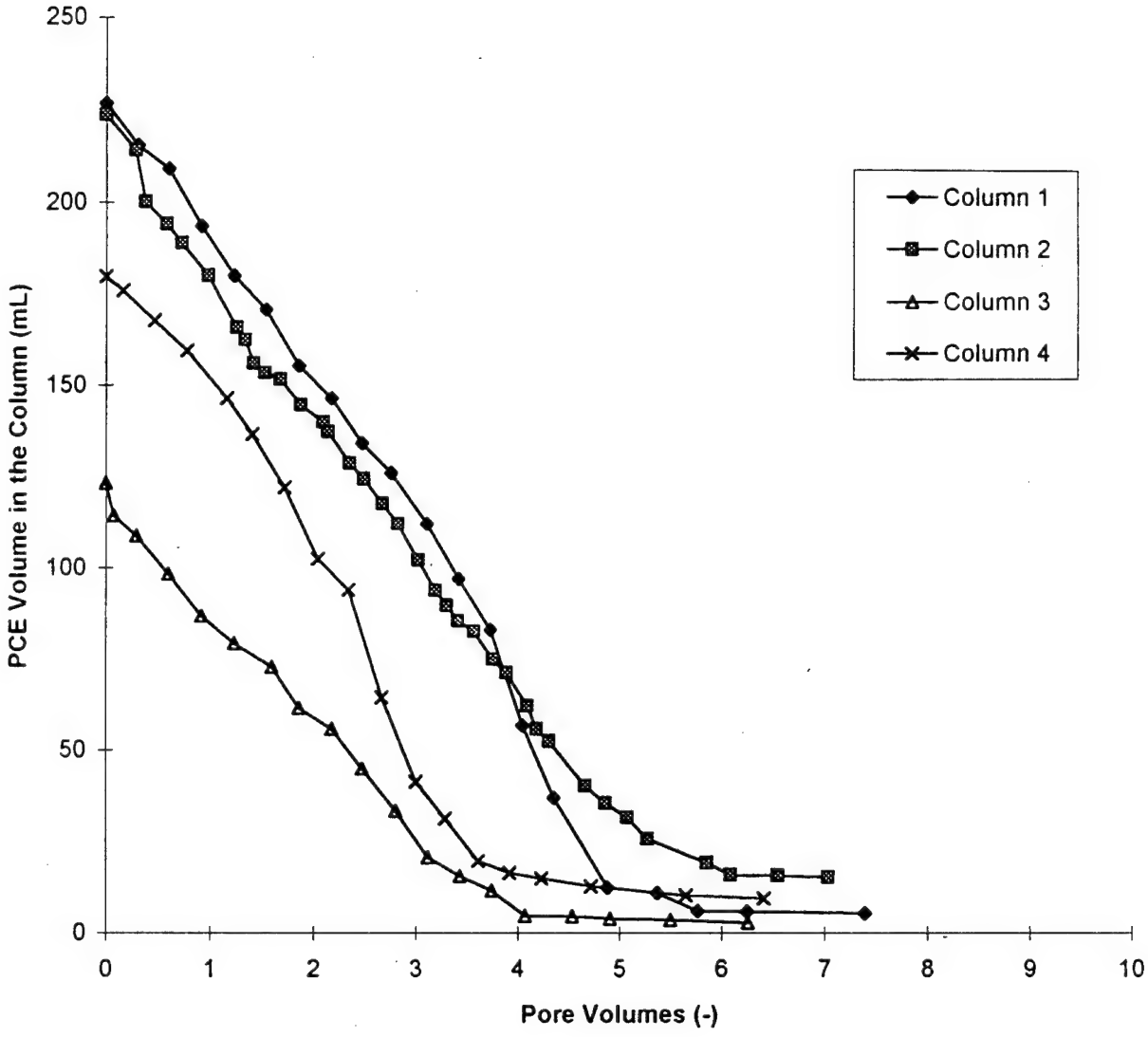

Figure 73. Volume of PCE in the Column (Obtained by Integration of the Volumetric PCE Contents Measured by the Gamma System) as a Function of Pore Volumes for Each Experiment.

no direct measurements of volumetric PCE contents were available for elevations 0 to 30 cm. Differences in the Figures 72 and 73 may be due to errors in both the chemical analysis and the gamma system measurements. It may be useful to note that the accuracy of the gamma system measurements is about ± 0.005 for volumetric PCE contents. Based on this, calculating the volume using the gamma system measurements may result in a maximum total error of 25 mL of PCE.

Figure 72 shows that the slope of the line for Column 3 is far less than the slopes for Columns 1, 2 and 4, implying that the mass transfer rates are smaller in the unsaturated case. However, in Figure 73, it is unclear as to whether or not Column 3 has a slope different from Columns 1, 2 and 4. This may be due to the experimental errors mentioned previously. The curve for Column 4, in Figure 73, had the most negative slope (for PV < 3). This suggests that the mass transfer rate in the homogeneous column was larger than in the other columns.

Spatial distributions of volumetric PCE contents as a function of elevation in the columns, at various times corresponding to several different pore volumes from 0 to 7.4, for Columns 1, 2, 3 and 4 are shown in Figures 74, 75, 76 and 77, respectively. Columns 3 and 4 are seen to have the lowest overall volumetric PCE contents, while columns 1 and 2 have higher overall volumetric PCE contents. The reasoning for these types of saturations in each of these columns has been discussed previously in Section VI. In general, the slowest reduction in volumetric PCE contents occurred in the fine layer (located between elevations 40 to 70 cm) while the quickest reduction occurred in the first coarse layer (located between elevations 70 to 100 cm). This suggests that there is some difference between the mass transfer in the two sands.

Figures 74, 75, 76, and 77 show that the PCE contents between elevations 99.5 to 40 cm decrease sharply with time for all the columns. For example, after 5 pore volumes there is a PCE content of 0.03 in the fine layer of Column 1, which corresponds to a reduction of 0.04 from 3 to 5 pore volumes (Figure 74). The fine layer still has detectable PCE at the second interface (elevation 40 cm) at the end of the experiment (7 PV). Column 2 has similar results except that in this case the initial volumetric PCE contents are lower at the second interface, therefore fewer pore volumes would be needed to reduce the saturations below detectable limits (Figure 75). After 4.9 pore volumes, the PCE contents were reduced from 0.06 to below 0.01 in the fine layer. This suggests that the mass transfer is related to the initial distribution of PCE in the porous media. For Column 3, the unsaturated case, Figure 76 shows that 2.8 pore volumes were needed to reduce the volumetric PCE contents from 0.08 to 0.025 at the second interface (located at elevation 40 cm). This implies that the rate of mass transfer is slower in the unsaturated zone as compared with the two saturated cases (Figures 74 and 75). The results for the homogeneous case (Column 4) appear to be similar to the results presented by Imhoff et al. (1993). Initially, the saturations of PCE are low and distributed relatively uniformly along the column with some perturbations. A dissolution region seems to move from the top of the column to the bottom as the pore volumes increase. After 4.7 pore volumes have passed , the volumetric PCE contents fall below the detectable limits of about 0.005.

It should be noted that the foregoing observations regarding the mass transfer rates and other aspects of the multiphase flow behavior are necessarily somewhat qualitative and preliminary. More quantitative and definitive conclusions can only be made based on more detailed analyses of the data and numerical simulations.

Hydraulic conductivity values were calculated from pressure measurements for each experiment except Column 3 (Figure 78), because the experimental setup for this column was not fitted with tensiometers. Figure 78 shows the hydraulic conductivities for Columns 1, 2 and 4 as a function of pore volumes. Over the duration of the experiments no significant changes in hydraulic conductivities were measured. This is

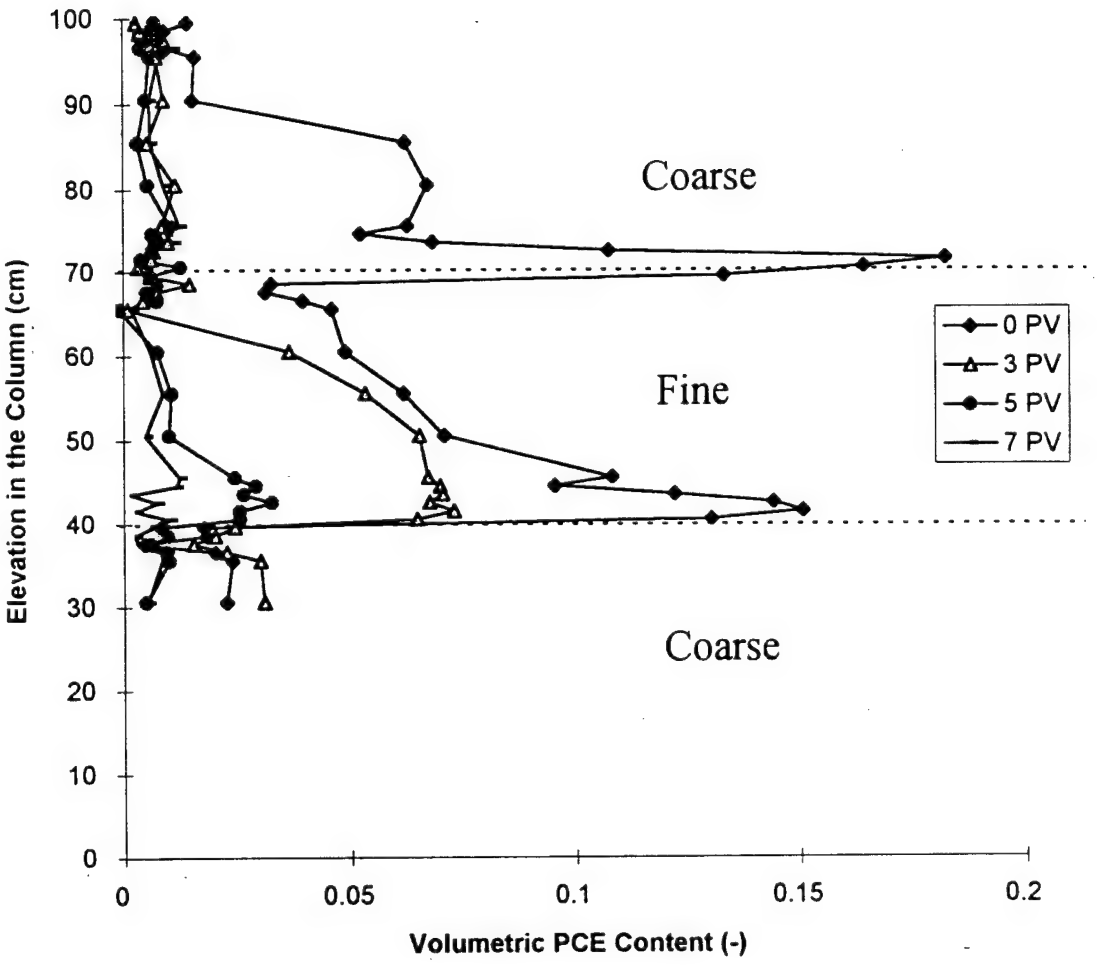

Figure 74. Distribution of Volumetric PCE Content as a Function of Elevation for Column 1 Based on Gamma System Measurements Taken at 0, 3, 5 and 7 Pore Volumes (PV).

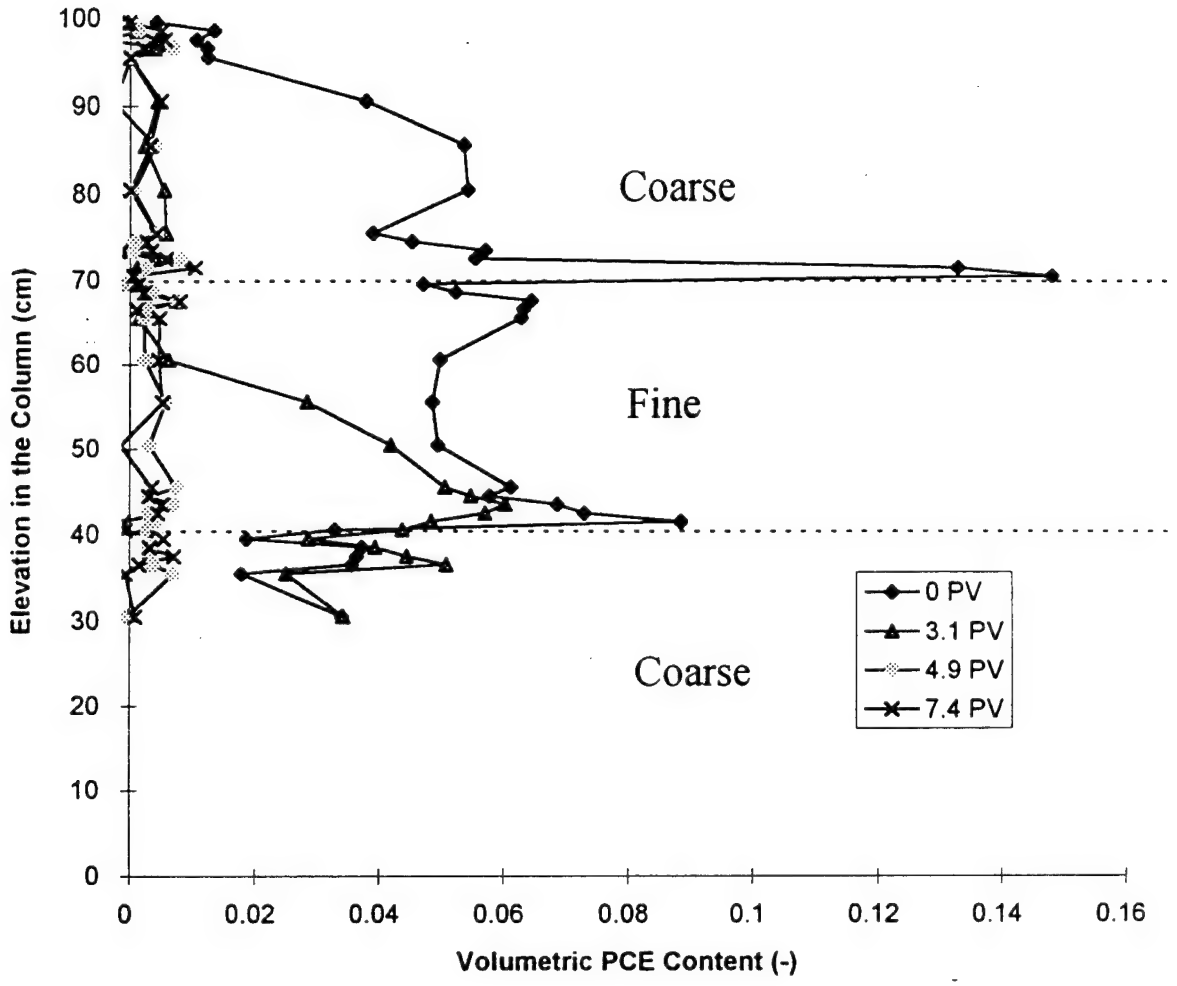

Figure 75. Distribution of Volumetric PCE Content as a Function of Elevation for Column 2 Based on Gamma System Measurements Taken at 0, 3.1, 4.9 and 7.4 Pore Volumes (PV).

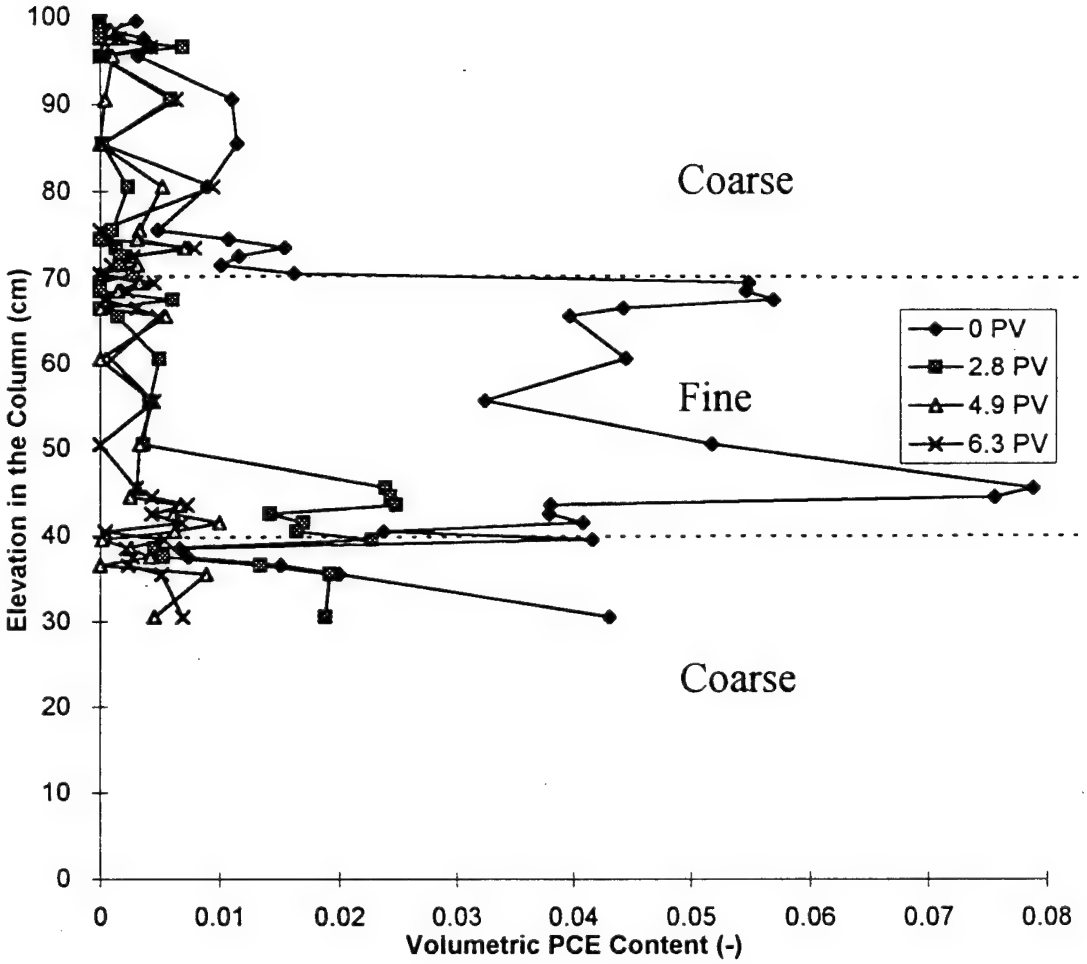

Figure 76. Distribution of Volumetric PCE Content as a Function of Elevation for Column 3 Based on Gamma System Measurements Taken at 0, 2.8, 4.9 and 6.3 Pore Volumes (PV).

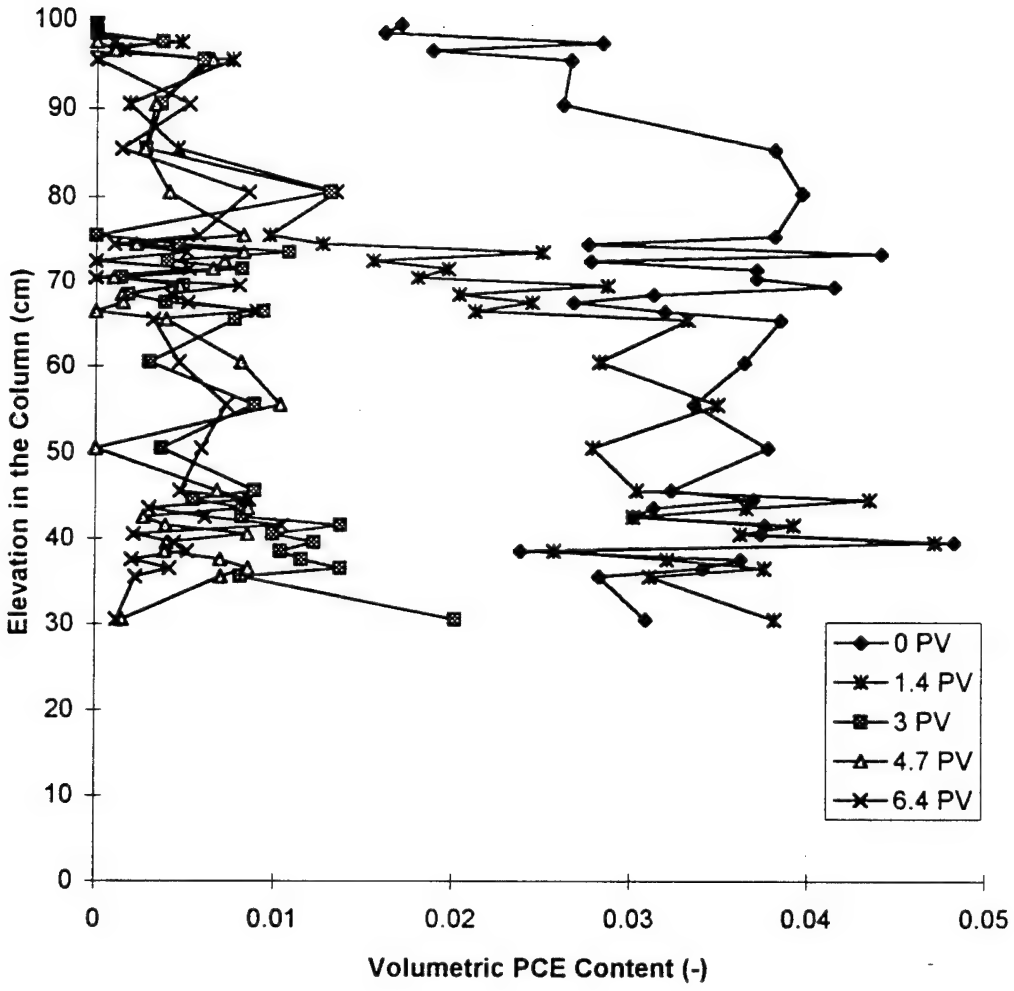

Figure 77. Distribution of Volumetric PCE Content as a Function of Elevation for Column 4 Based on Gamma System Measurements Taken at 0, 1.4, 3, 4.7 and 6.4 Pore Volumes (PV).

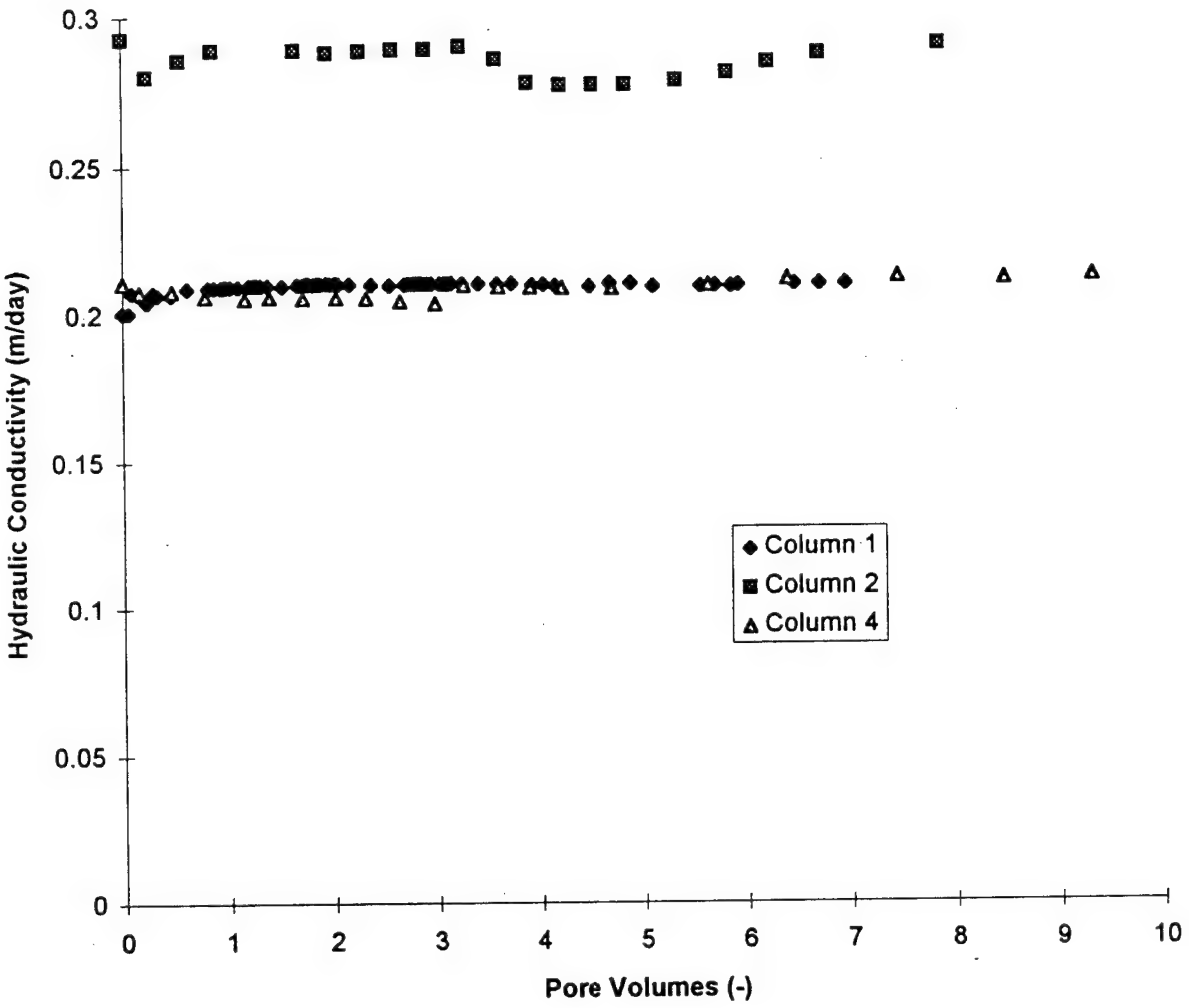

Figure 78. Hydraulic Conductivity Versus Pore Volumes for Columns 1, 2 and 4.

probably due to the fact that the pressure measurements were taken at the top and bottom of each column, therefore, the values presented are averages over the entire length of the column. To more closely study the effect of changes in hydraulic conductivity, tensiometers should be placed at intervals along the length of the column, so that the values are averaged over shorter distances.

The hydraulic conductivities can also be affected by the reduction in free PCE in each column. In Columns 1 and 2, 16 to 18 mL of free PCE was displaced from the columns during the course of the experiments (Figure 79). 16 to 18 mL of free PCE corresponds to a change in volumetric PCE content from 0.0032 to 0.0036 respectively. Comparing these values with an average porosity of 0.365 implies that there is insignificant change in the saturated water contents and therefore in hydraulic conductivities on average.

D. CONCLUSIONS

These experiments provide detailed data on the surfactant enhanced dissolution and removal of PCE from contaminated sands. Some of the breakthrough curves showed PCE concentrations larger than the equilibrium concentration, leading to the conclusion that microemulsions were formed and transported through the medium. The type of emulsion that exists in this situation is thought to be a Winsor Type III emulsion. Physical properties of the effluent, such as the milky white color, tend to suggest the Type III behavior as the most probable.

Qualitative conclusions can be made about the PCE mass transfer rates based on the observed changes in volumetric PCE contents as a function of time. These data suggest that, as expected, mass transfer is a function of the type of medium, as well as the liquid saturations. It was observed that mass transfer rates were less in the unsaturated case than in the saturated cases.

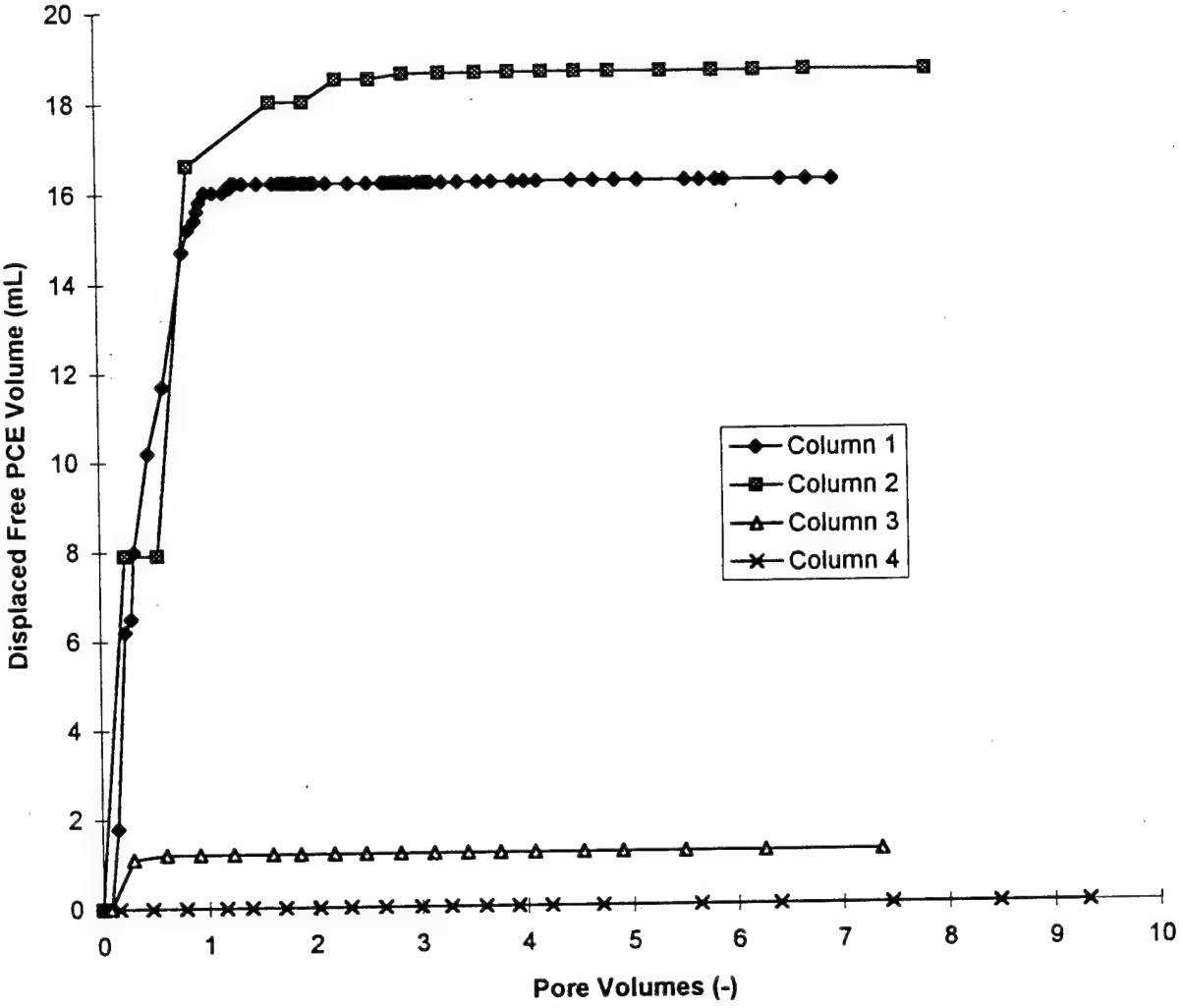

Figure 79. Cumulative Volume of Free PCE Displaced from Columns 1, 2, 3 and 4 as a Function of Pore Volumes.

REFERENCES FOR SECTION VII

Abdul, A.S, Gibson, T.L. and Rai, D.N., "Selection of Surfactants for the Removal of Petroleum Products from Shallow Sandy Aquifers." Ground Water, 28(6), 1990.

Corey, A. T., Mechanics of Immiscible Fluids in Porous Media, Water Resources Publications, Littleton, CO, 1994.

Geller, J.T. and Hunt, J.R., "Mass Transfer from Nonaqueous Phase Organic Liquids in Water Saturated Porous Media." Water Resources Research, 29(4), 833-845, 1993.

Herzig, J.P., LeClerc, D.M. and Le Goff, P., "Flow of Suspensions Through Porous Media-Application to Deep Filtration." Industrial and Engineering Chemistry, 62(5), 1970.

Imhoff, P.T., Jaffé, P.R. and Pinder, G.F., "An Experimental Study of Complete Dissolution of a Nonaqueous Phase Liquids in Saturated Porous Media." Water Resources Research, 30(2), 307-320, 1993.

McAuliffe, C.D., "Oil-in-Water Emulsions and Their Flow Properties in Porous Media." Journal of Petroleum Technology, June, 727-733, 1973.

Miller, C., Poirier-McNeill, M. M. and Mayer, A. S., "Dissolution of Trapped Nonaqueous Phase Liquids: Mass Transfer Characteristics." Water Resources Research, 26 (11), 2783-2796, 1990.

Pennell, K.D., Abriola, L.M. and Weber, W.J., "Surfactant Enhanced Solubilization of Residual Dodecane in Soil Columns." 1. Experimental Investigation. Environmental Science and Technology, 27. Washington, D.C.: American Chemical Society, 1993.

Powers, S.E., Abriola, L.M. and Weber, W.J., "An experimental Investigation of Nonaqueous Phase Liquid Dissolution in Saturated Subsurface Systems: Transient Mass Transfer Rates." Water Resources Research, 30(2), 321-332, 1994.

Rosen, M. J., Surfactants and Interfacial Phenomena, John Wiley & Sons, New York, 1978.

Schmidt, D.P., Soo, H. and Radke, C.J., "Linear Oil Displacement by the Emulsion Entrapment Process." Society of Petroleum Engineers Journal, Vol. 6, 351-360, 1984.

Shiau, Bor-Jier, Sabatini, D.A. and Harwell, J., "Solubilization and Microemulsification of Chlorinated Solvents Using Direct Food Additive (Edible) Surfactants." Ground Water, 32(4), 561-569, 1994.

SECTION VIII
TWO-DIMENSIONAL (2-D) EXPERIMENTS WITH TETRACHLOROETHYLENE (PCE) IN FLOW CONTAINER FC1

A. INTRODUCTION

A series of nominally 2-D spill and cleanup experiments conducted with PCE are described in this section. Details of the flow container used in these experiments are given in Section IV, and also described by Mamballikathil (1995). In these experiments spills were similuted by introducing PCE through a line source, and in some of the experiments cleanup of the spilled PCE from the porous medium by a surfactant solution was also studied. Several of these experiments were preliminary, exploratory flow visualization experiments which helped to understand the working of the flow container and to refine the procedures followed in performing the experiments. These preliminary experiments were also useful in designing the more detailed experiments conducted in another, larger, flow container using the dual-energy gamma radiation system (Section IX).

B. MATERIALS AND METHODS

The experiments were performed using the flow container FC1 and the experimental setup described previously in Section IV.

PCE (tetrachloroethylene 99%, Aldrich Chemical Company Inc., Milwaukee, WI) was dyed using Oil Red EBN dye (Aldrich Chemical Company). About 1 g/L of this dye was added to the PCE and stirred until it was completely dissolved. The solution was then filtered using a filter paper to remove any undissolved traces of the dye.

A fluorescein sodium salt, $C_{20}H_{10}Na_2O_5$ (Fisher Scientific Co., Chicago, IL), was used as an optical tracer. About 0.2 g/L of this salt was added to deionized water and stirred to produce a deep fluorescent coloring of the solution which can be easily distinguished in the visualization photographs.

The surfactant used in this study was polyoxyethylene (20) sorbitan monooleate (Tween 80, purchased from Aldrich Chemical Company, Milwaukee,WI). This nonionic surfactant was chosen because Pennell et al. (1994) had successfully used it in their experiments and hence, some correlation could be made in the results. A 4 percent (by volume) surfactant solution was used in the experiments. Thymol and mercuric chloride were added in a ratio of about 1 mL per 100 mL of the surfactant solution in order to inhibit microbial growth in the porous medium. 80 mL of surfactant was added to 1900 mL of deionized organic free water and 20 mL of the thymol and mercuric chloride solution to prepare a 4% solution. To this surfactant solution 0.2 g/L of fluorescein sodium salt was added as an optical tracer. This solution was prepared by using magnetic stirrers and adding the surfactant gradually while the solution was being stirred. The solution was stirred until the surfactant and fluorescein were completely dissolved.

The porous medium was saturated by gradually raising the water level to remove any entrapped air and to cause it to settle down. The water level was then lowered to the desired level and allowed to equilibrate. PCE, with Oil Red EBN dye, was then introduced into the porous medium through the source located at the surface. During the introduction of PCE and throughout the experiments photographs were taken at regular intervals to visualize the behavior of PCE in the porous medium. At the end of some of the experiments cleanup of the residual PCE from the porous medium by flushing with the surfactant solution was also studied. Visualization photographs were also taken during the cleanup process.

After the introduction of PCE it was allowed to redistribute. The water level was then gradually raised at about 2-3 cm every hour. An ambient horizontal flow of water was established through the porous medium by adjusting the water levels in the end chambers of the flow container. After the horizontal flow reached a steady state, injection and extraction (I/E) of fluorescein solution was started through the I/E ports provided at the back of the flow container. The I/E rates were equal and were set to about one-third of the horizontal flow rate. The horizontal flow rate was measured by measuring the outflow volume in a given period of time. A flow field as shown in Figure 80 was thus setup in the porous medium . Later, the surfactant solution was injected instead of the fluorescein solution. Samples were taken of the extracted solution in some of the experiments for chemical analysis. These samples were analyzed using a gas chromatograph (Shimadzu Model No. GC14A).

A summary of the experimental conditions are given in Tables 19 and 20. Table 19 shows the experimental conditions during the input of PCE, and Table 20 gives the experimental conditions during the injection and extraction of the fluorescein and surfactant solutions.

C. DESCRIPTION OF THE EXPERIMENTS

A description of each experiment and the results and observations are given below.

Experiment 1:

This experiment was a preliminary experiment performed to test the functioning of the flow container and to refine the experimental procedures. The flow container was packed with Flintshot 2.8 sand. The porous medium was first saturated by gradually raising the water level in the end chambers. Later, the water level was lowered and again raised to 20 cm above the bottom of the flow container. The top of the capillary fringe was at about 37.5 cm.

In this experiment, PCE with Oil Red EBN dye was first introduced in 4 mL volumes up to 20 mL. Subsequently another 100 mL was introduced in 4 mL volumes. Later, PCE was added in 8 batches of 100 mL each. In this way a total of 920 mL of PCE was input through the line source located at the surface of the porous medium. The source used in this experiment was a box source made of Teflon® with a slit at the bottom to simulate a line source. The input of PCE was manual and discontinuous.

After the introduction of PCE, the water level was raised to 40 cm and 38 cm in the inlet and outlet end chambers, respectively. An ambient horizontal flow was thus established through the porous medium. After reaching equilibrium, the I/E of fluorescein solution was started through the middle ports (Injection Port 2 and Extraction Port 4, Figures 29 and 30). The I/E flow rates were initially set at 100 mL/min and were later reduced to 60 mL/min to form a flow field sweeping a smaller area. The cleanup using surfactant solution was not done in this experiment.

During the introduction of PCE it was observed that small heterogeneities in packing of the porous medium caused PCE to flow along paths of least resistance. When the water level was raised before the redistribution of PCE was complete, it resulted in the displacement of a significant amount of the free phase PCE to the top of the porous medium. The flow field developed by the I/E of fluorescein solution is seen in Figure 81. The free phase PCE displaced by raising the water level is also seen in Figure 81 on top of the porous medium.

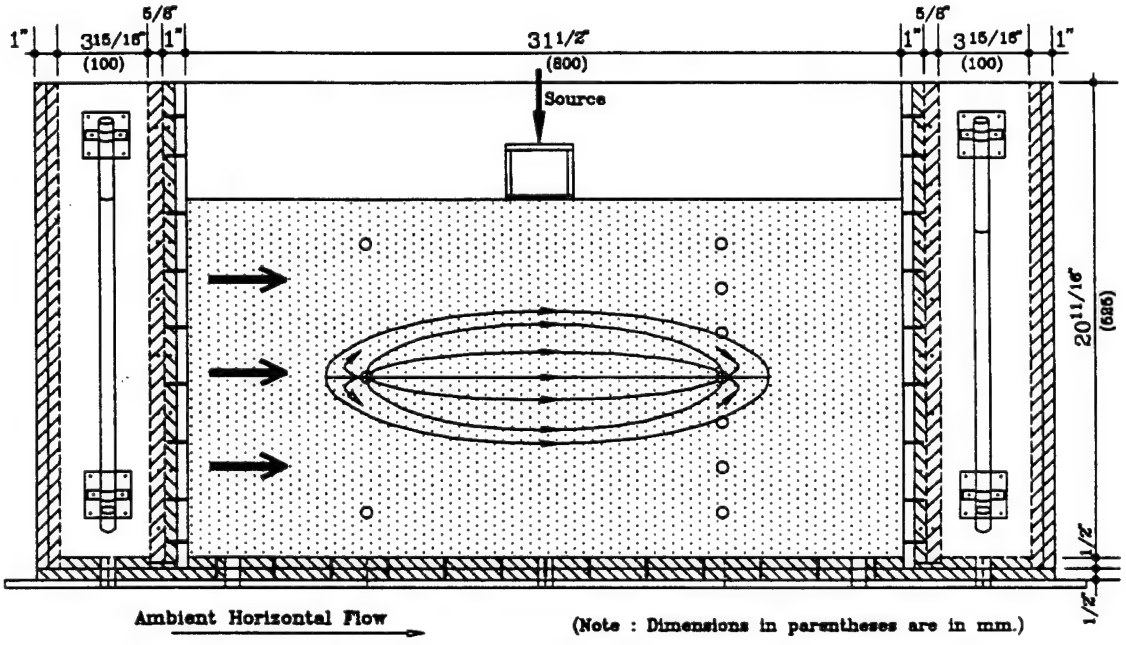

Figure 80. Sketch Showing a Typical Flow Field Established in the Porous Medium by Injection and Extraction of Liquids During Horizontal Flow of the Ambient Water.

TABLE 19. SUMMARY OF EXPERIMENTAL CONDITIONS DURING THE INPUT OF PCE.

Expt. #	Porous Medium	Total Amount of PCE Input (mL)	Water Level in End Chambers (cm)	Top of Capillary Fringe Level (cm)
1.	Homogeneous FS 2.8 sand	920	20.0	37.5
2.	Homogeneous FS 2.8 sand	900	10.0	27.5
3.	Homogeneous FS 2.8 sand	--	--	--
4.	Homogeneous FS 2.8 sand	--	--	--
5.	Homogeneous FS 4.0 sand	500	10.0	25.0
6.	Homogeneous FS 4.0 sand	500	10.0	25.0
7.	Heterogeneous* FS 4.0, FS 2.8 sand and Glass Beads (A120)	500	15.0	28.0
8.	Heterogeneous* Same as Exp. #7	500	24.0	36.5

* Figure 102 shows the distribution of different porous media lenses.

TABLE 20. SUMMARY OF EXPERIMENTAL CONDITIONS DURING INJECTION AND EXTRACTION.

Expt. #	Porous Medium	Water Level in End Chambers Inlet (cm)	Outlet (cm)	Horizontal Flow Rate (mL/min)	Rate of Inj./Ext. of Surfactant (mL/min)	Comments
1.	Homogeneous	40	38	n/a	100/60**	No Cleanup
2.	Homogeneous	40	39	10.7	50	No Cleanup
3.	Homogeneous	40	38	22.2	7	Cleanup
4.	Homogeneous	40	38	20.5	7	Experiment discontinued
5.†	Homogeneous	40	38	25.3	7	Cleanup
6.†	Homogeneous	40	38	35.6	13	Cleanup
7.†	Heterogeneous*	40	`38	27.6	13/26**	Cleanup
8.	Heterogeneous*	--	--	---	---	No Cleanup

* Figure 102 shows the distribution of different porous media lenses.
** Initial I/E rate/Later I/E rate.
† Samples taken for chemical analysis.

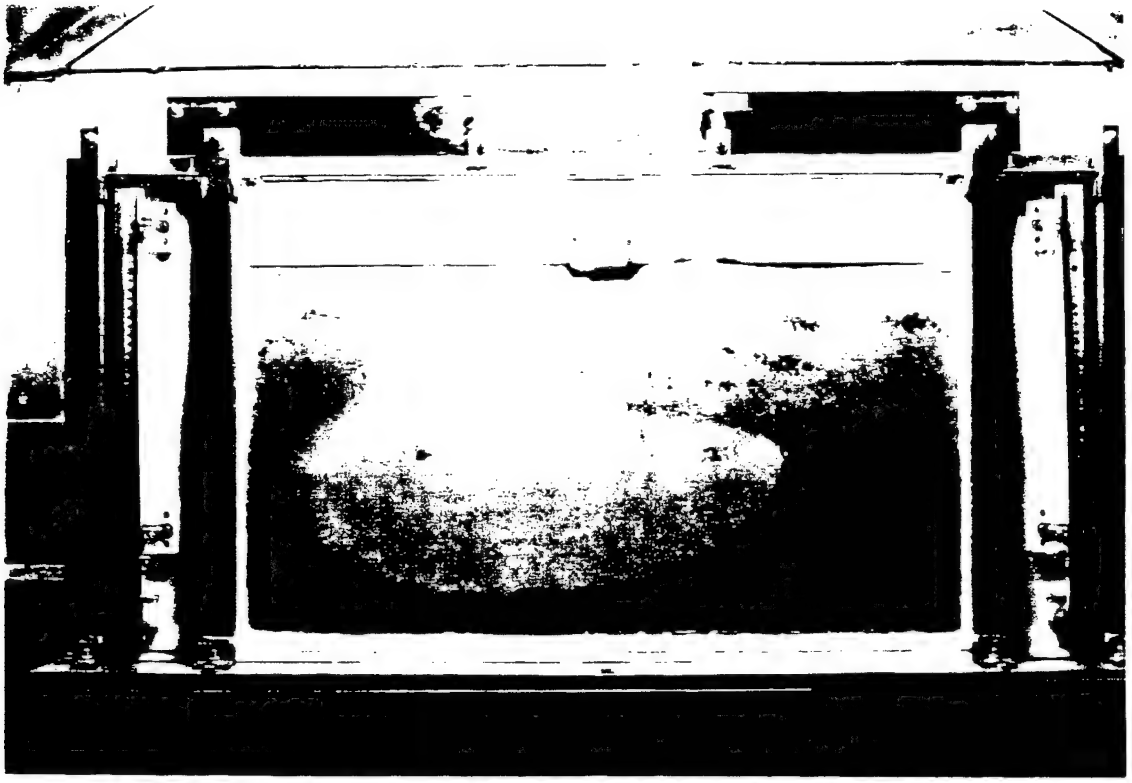

Figure 81 Experiment 1 Plume Developed by Injection and Extraction of Fluorescein Solution. Free Phase PCE Displaced by the Raising of the Water Level is Visible on Top of the Porous Medium

Experiment 2:

The porous medium used in this experiment was the same as that of Experiment 1. The fluorescein solution was not flushed out before the commencement of this experiment. The water level was maintained at 10 cm with the top of capillary fringe at 27.5 cm during the introduction of PCE. In this and the later experiments a new line source made of glass was used. PCE was pumped into the source, using a peristaltic pump, at 5 mL/min for 20 minutes and later at 10 mL/min. A total of 900 mL of PCE was input into the porous medium through the source. PCE was first allowed to redistribute and then the water level was raised slowly to 40 cm. A horizontal flow was established through the porous medium with the water levels in the inlet and outlet end chambers at 40 and 39 cm, respectively. About 59 hours after the introduction of PCE, I/E of fluorescein solution through the middle ports was started at 50 mL/min. Some of the spilled PCE was removed as a separate phase, along with the fluorescein solution. Later, instead of a fluorescein solution, clean deionized water was injected. Surfactant enhanced cleanup was not done in this experiment.

The spilled PCE developed sufficient pressure to displace water from the pores. It was also observed that PCE tends to spread out laterally over the capillary fringe (Figure 82), as was also noted by Schwille (1988) in model experiments . Fingers were formed which penetrated into the saturated zone. Figure 82 shows a photograph taken after the introduction of 600 mL of PCE. The regions of fluorescein seen in the photograph are remnants from Experiment 1. After the spilled PCE was allowed to redistribute, it was seen that most of it had migrated downwards to the bottom of the flow container. Figures 83 and 84 show the distribution of PCE 5.5 and 65 hours after the input of PCE, respectively. A horizontal ambient flow was maintained through the porous medium for about 60 hours before the start of I/E of fluorescein solution. The I/E of fluorescein solution and later clean water, did not result in any significant visible mobilization of the residual PCE (Figure 85).

Experiment 3:

This experiment was a continuation of Experiment 2. No more PCE was introduced during Experiment 3, but rather surfactant enhanced cleanup of the PCE was carried out. After the completion of Experiment 2 the ambient horizontal flow through the porous medium was continued for 12 hours to flush out the fluorescein solution from the porous medium. The horizontal flow was set up with the water levels in the inlet and outlet end chambers at 40 cm and 38 cm, respectively. The I/E was done through the middle ports (Injection Port 2 and Extraction Port 4, Figures 29 and 30). The I/E of fluorescein solution was started at 7 mL/min, which was about one-third of the ambient horizontal flow rate. This helped to establish an elliptical flow field in the porous medium (as shown in Figure 80). Figure 86 shows the initial distribution of PCE at the start of this experiment. The development of the flow field is seen in Figures 87, 88, and 89. The I/E of fluorescein solution was done for 11 hours; the I/E of 4% surfactant solution was then started at 7 mL/min. The surfactant solution used in this experiment was not dyed with fluorescein and was hence colorless. The I/E of the surfactant solution was continued for 48 hours until the elliptical flow field was cleared of residual PCE as observed at the front of the flow container. Horizontal flow rate measurements and photographs were taken at intervals. Figures 90, 91, and 92 show some stages during the cleanup. The PCE was removed by solubilization into the extracted solution.

Experiment 4:

This experiment was essentially a continuation of Experiment 3, except that the bottom I/E ports (Injection Port 3 and Extraction Port 7, Figures 29 and 30) were used instead of the middle ports. This

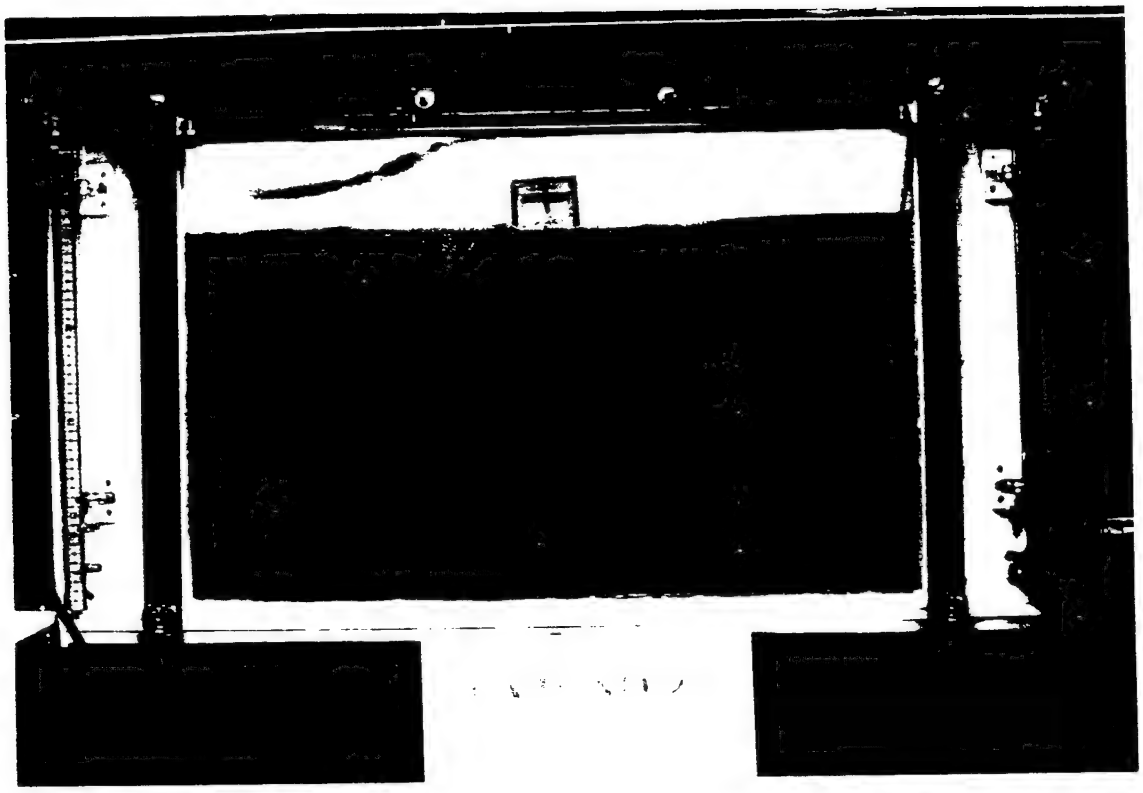

Figure 82. Experiment 2: Distribution of PCE in the Porous Medium After the Input of 600 mL

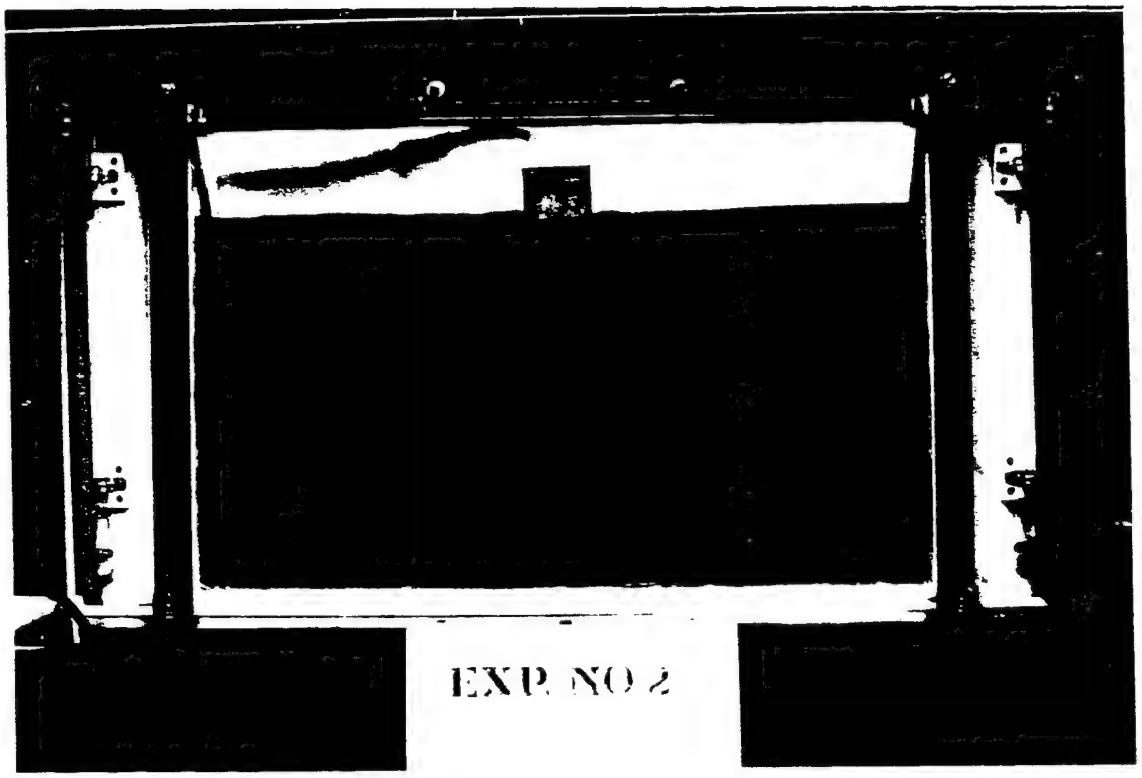

Figure 53 Experiment 2 Distribution of PCE in the Porous Medium 5.5 Hours After the Input of [illegible] mL

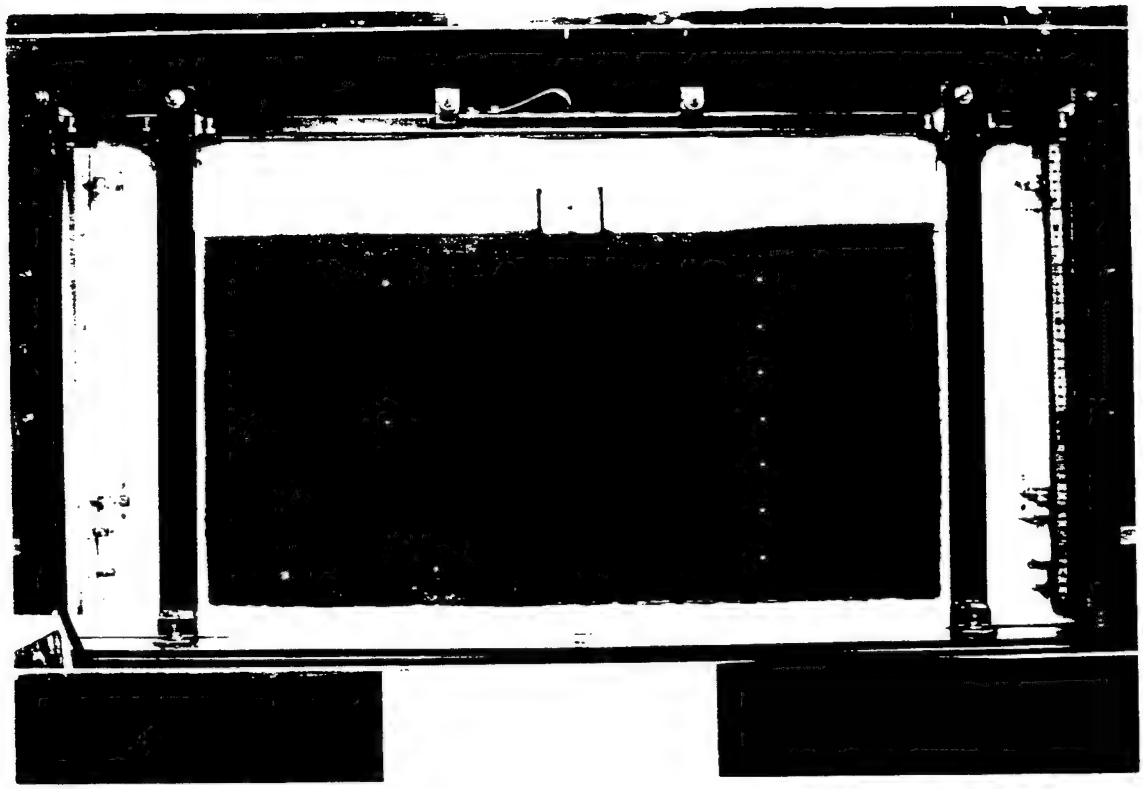

Figure [illegible] Experiment 2. Distribution of PCE in the Porous Medium 65 Hours After the Input of [illegible] mL.

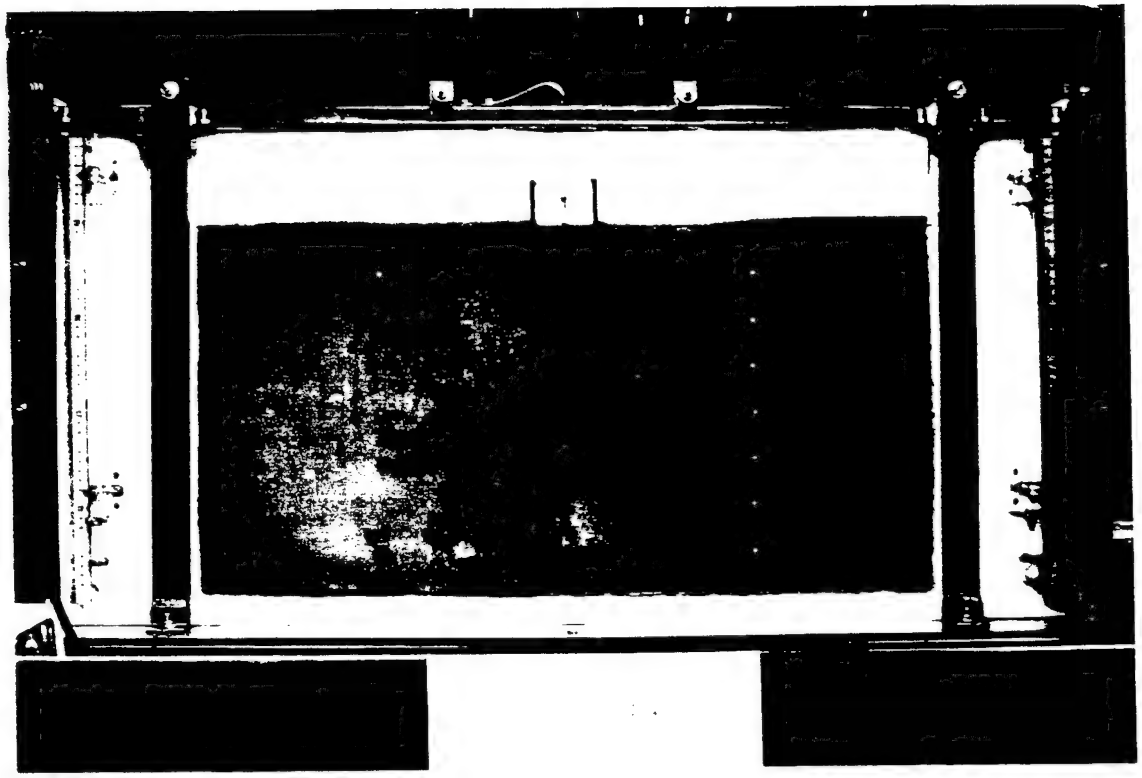

Figure 85 Experiment 2 Plume Developed by the Injection and Extraction of Fluorescein Solution at 50 mL min for 2 Hours

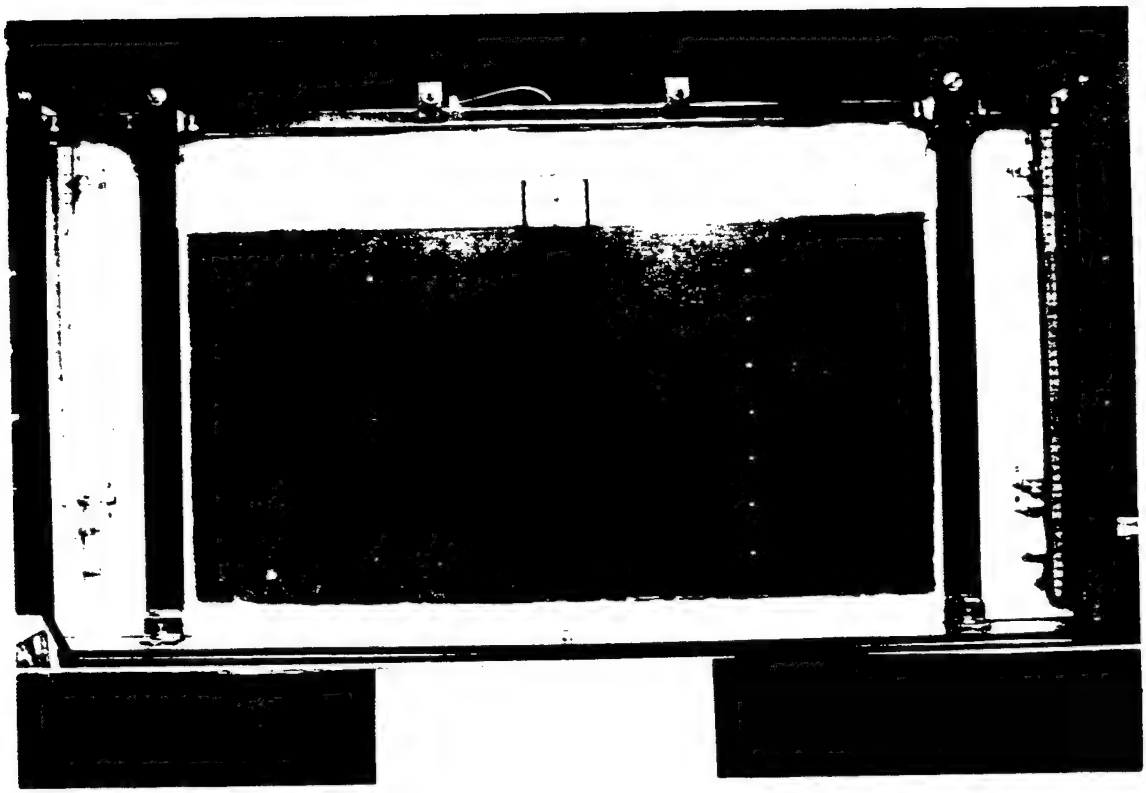

Figure 86 Experiment 3 Initial Distribution of PCE at the Start of the Experiment

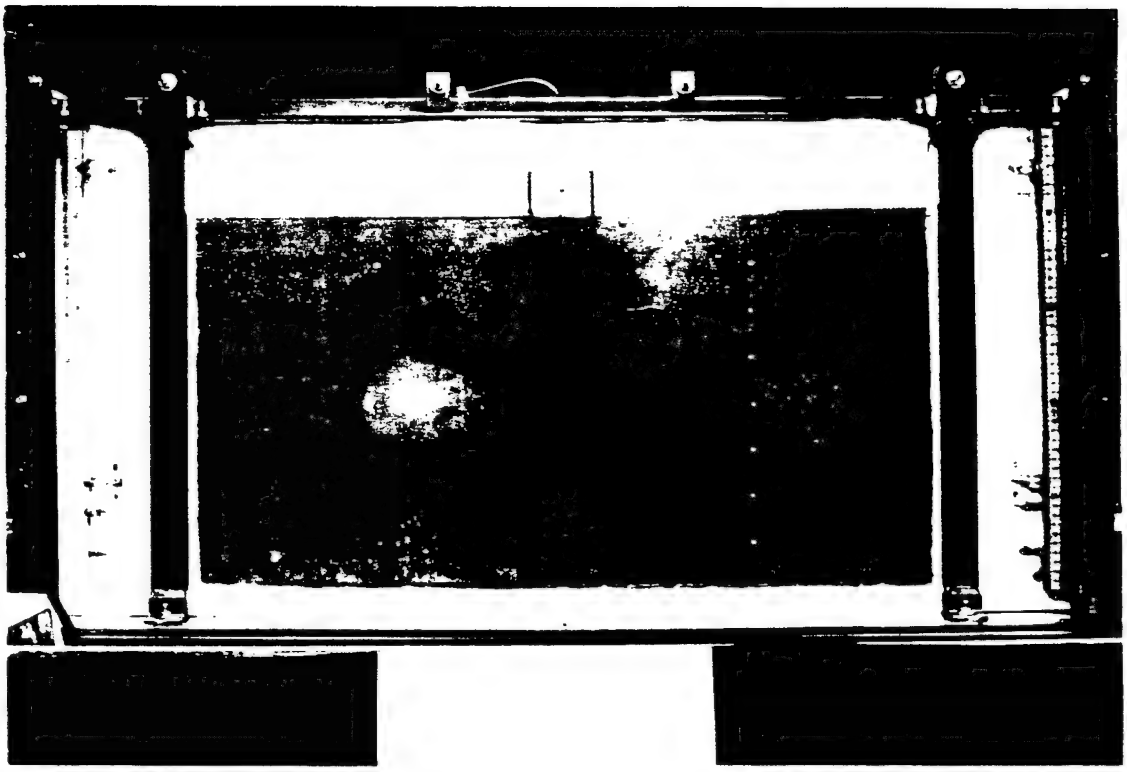

Figure 87. Experiment 3. Plume Developed by Injection and Extraction of Fluorescein Solution at 7 mL/min for 1 Hour

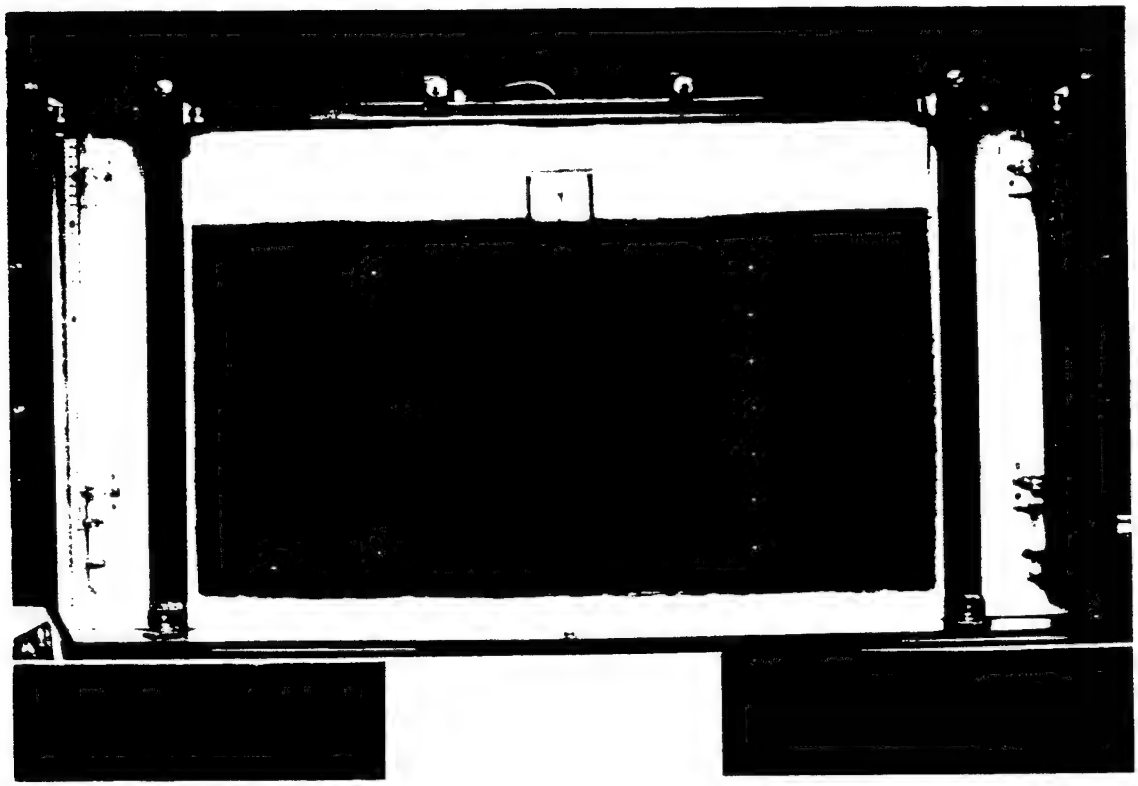

Figure 88 Experiment 3 Plume Developed by Injection and Extraction of Fluorescein Solution at 7 mL/min 2 Hours

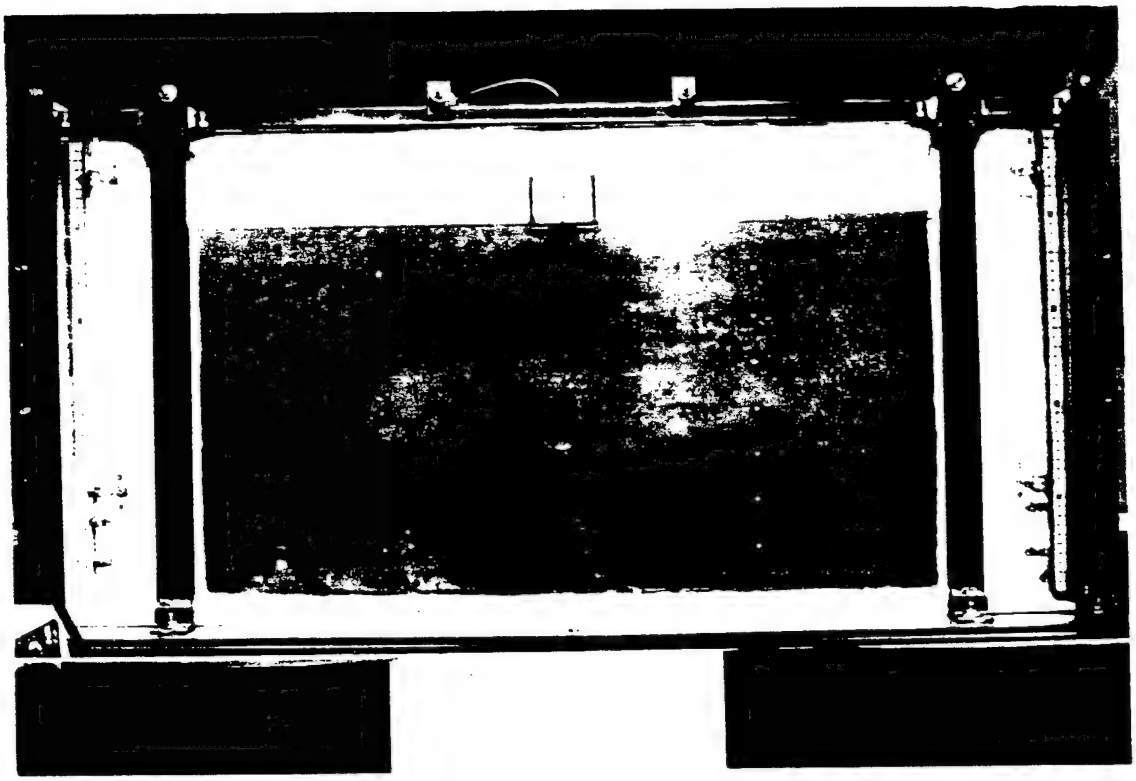

Figure 84. Experiment 3: Plume Developed by Injection and Extraction of Fluorescein Solution at ~ mL/min for ~ Hours

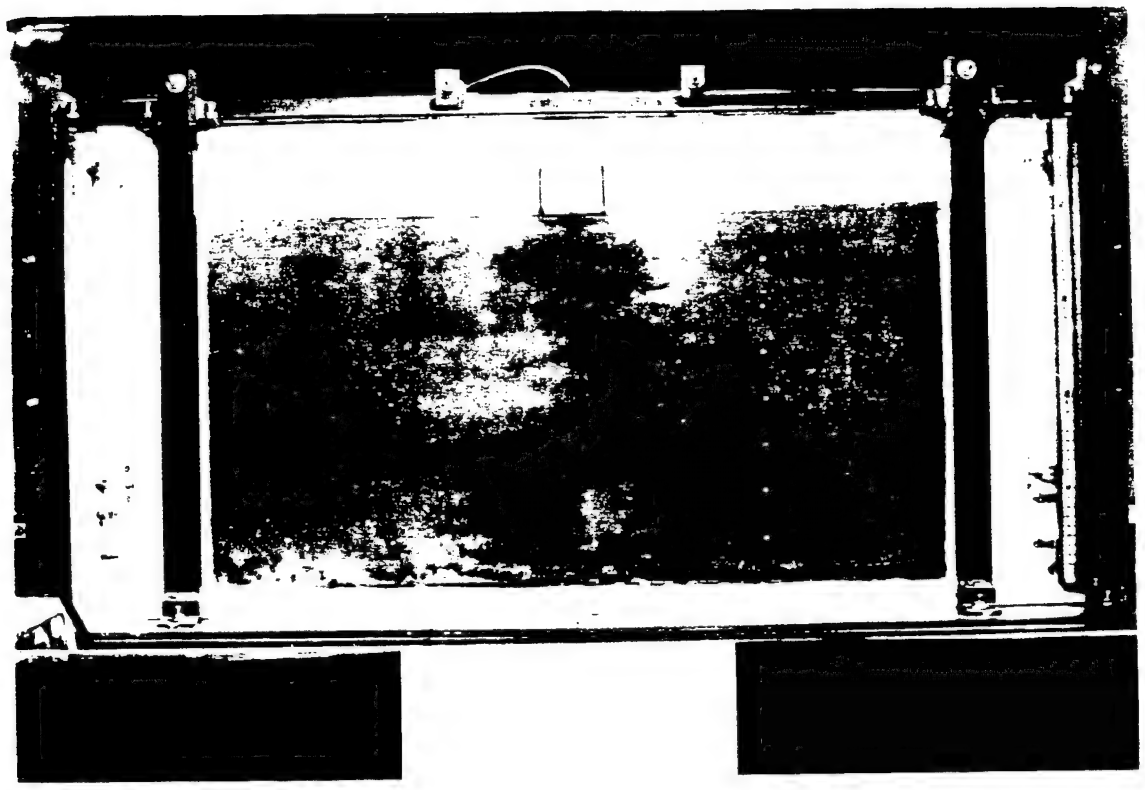

Figure 90 Experiment 3 Photograph Taken 12 Hours After the Start of Injection and Extraction of 4% Surfactant Solution

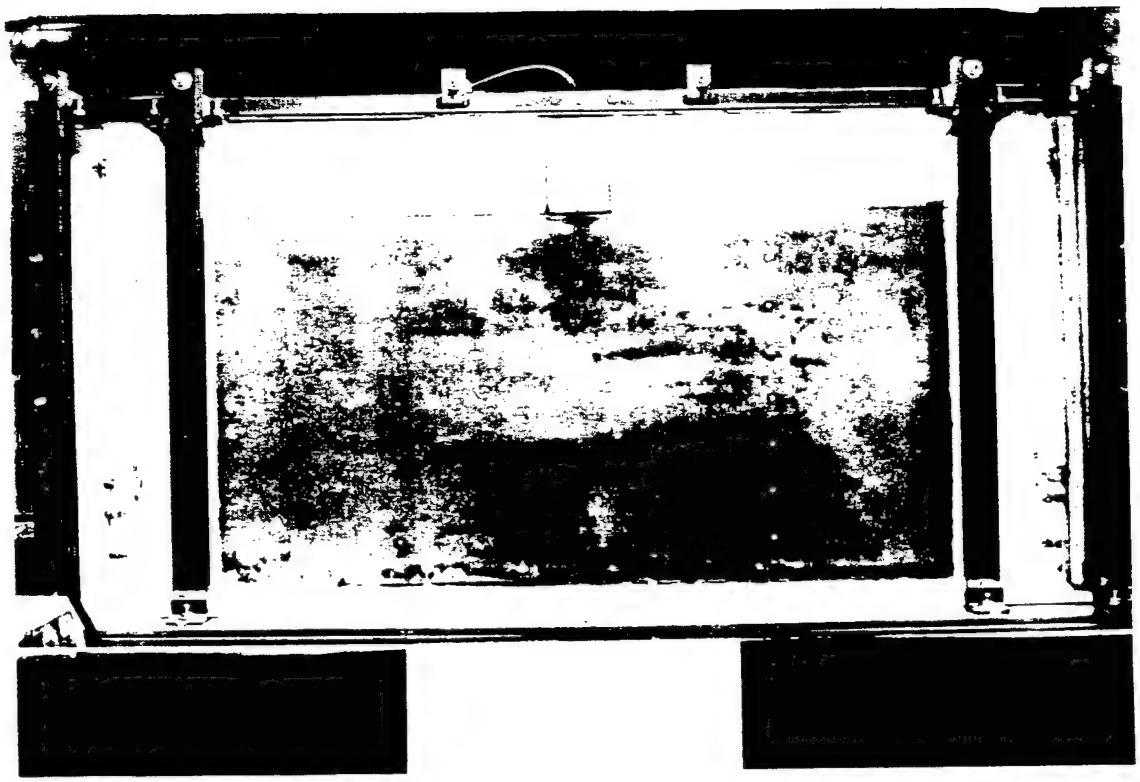

Figure 91 Experiment 3 Photograph Taken 24 Hours After the Start of Injection and Extraction of 4% Surfactant Solution

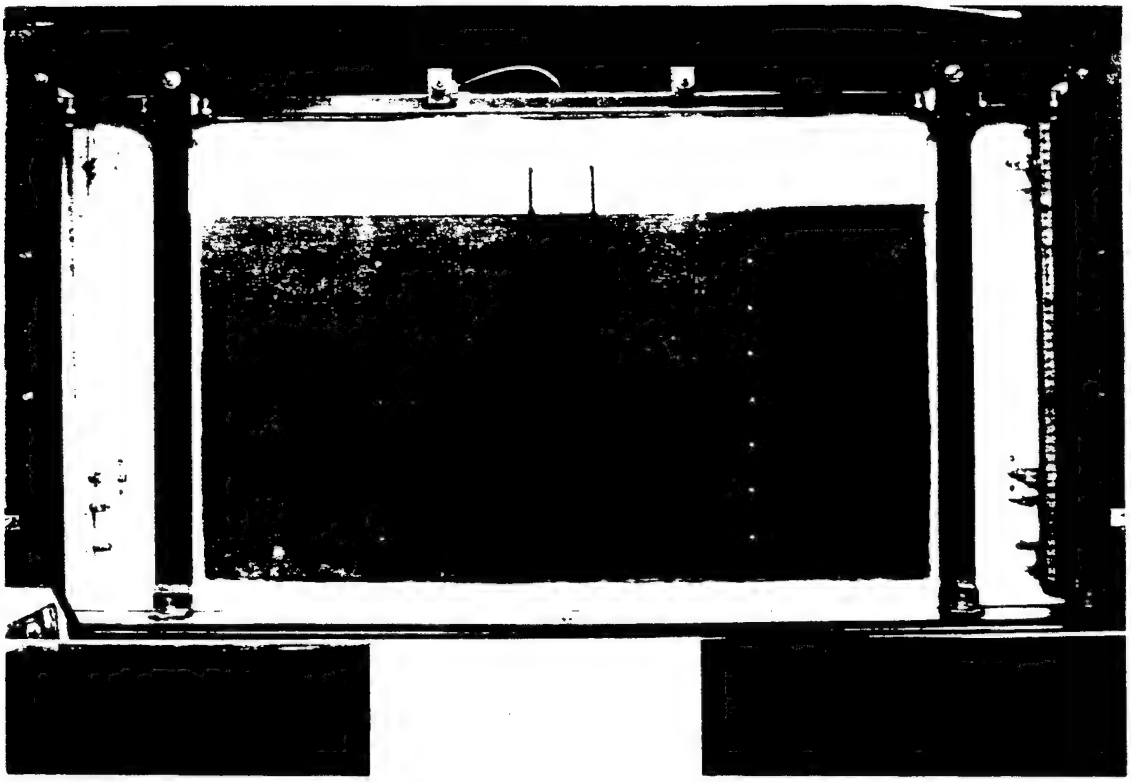

Figure 92 Experiment 3 Photograph Taken 48 Hours After the Start of Injection and Extraction of 4% Surfactant Solution at the Final Stage of the Cleanup

experiment was discontinued, however, because the surfactant solution pumped in at the rate of 7 mL/min was not visible at the front of the porous medium. This was probably due to the presence of some preferential flow paths along the back or middle of the porous medium, which caused the surfactant solution to flow through these paths. Alternatively, this could also have been due to some air entrapped in the injection port. The experiment was stopped after 48 hours.

Experiment 5:

The porous medium used for this experiment was Flintshot FS 4.0 sand. The porous medium was first saturated and then the water level was adjusted to a height of 10 cm with the top of the capillary fringe at 25 cm (Figure 93). PCE was introduced at 10 mL/min (Figure 94) until 500 mL was pumped in. The initial condition before the input of PCE is seen in Figure 93. The spilled PCE was seen to migrate downwards rapidly until the capillary fringe was encountered. Fingers began to penetrate into the saturated zone (Figure 94). PCE moved downward faster in the Flintshot FS 4.0 sand, which is coarser, than in the Flintshot FS 2.8 sand. Fingers were seen at different spots near the front (Figure 95). It was noticed that some of the fingers reached the bottom of the flow container within 40 minutes from the introduction of the PCE. Following the introduction of PCE, the water level was raised to 40 cm and 38 cm in the inlet and outlet end chambers, respectively, thus setting up a horizontal flow through the porous medium. The I/E of fluorescein solution at 7 mL/min through the middle ports was started after about 32 hours. Some of the spilled PCE was extracted as a separate phase along with the fluorescein solution. The I/E of fluorescein solution was stopped and the horizontal flow was continued for another 24 hours. The I/E of 4% surfactant solution containing fluorescein dye was then started at 7 mL/min. Figure 96 shows the residual PCE distribution just before the I/E of the 4% surfactant solution. Samples of the extracted solution were taken every hour for 48 hours.

The samples taken during the I/E of surfactant solution were chemically analyzed. The results are plotted in Figure 97. The peak effluent PCE concentration was 19,192 ppm (mg of PCE per kg of solution). As presented previously in Section VII, the maximum PCE solubility in a 4% solution of Tween 80 determined by batch experiments was 25,100 ppm. After 24 hours the effluent PCE concentration decreased to below its aqueous solubility limit which is about 240 ppm. Figure 98 shows the final PCE distribution after cleanup using the surfactant solution. This experiment showed again that surfactants could be used to clean up regions of PCE contamination in a sandy aquifer.

Experiment 6:

The medium used for this experiment was Flintshot FS 4.0 sand. The experimental conditions were the same as for Experiment 5. However, in this experiment the I/E rate used was 13 mL/min, which is about double that of the previous experiment. The I/E of surfactant solution was started about 12.5 hours after the input of the PCE. It was stopped after about 30 hours when no more PCE was visible in the region of the flow field on the front side of the porous medium. Based on the results of Experiment 5 it was decided to take more samples during the first 8 hours. Samples were taken at 20 min intervals for the first 8 hours and subsequently at 1-hour intervals.

Figure 99 shows the distribution of PCE before the start of I/E of the 4% surfactant solution. The effluent PCE concentration breakthrough data are shown in Figure 100. The maximum effluent PCE concentration in this experiment was 15,263 ppm compared with 19,192 ppm in experiment 5. The effluent PCE concentration was lower in this experiment probably due to the higher I/E rate which caused the surfactant to be in contact with the residual PCE for less time. This observation is consistent with the observation made by Pennell et al. (1994) that the effluent PCE concentration was higher after periods when

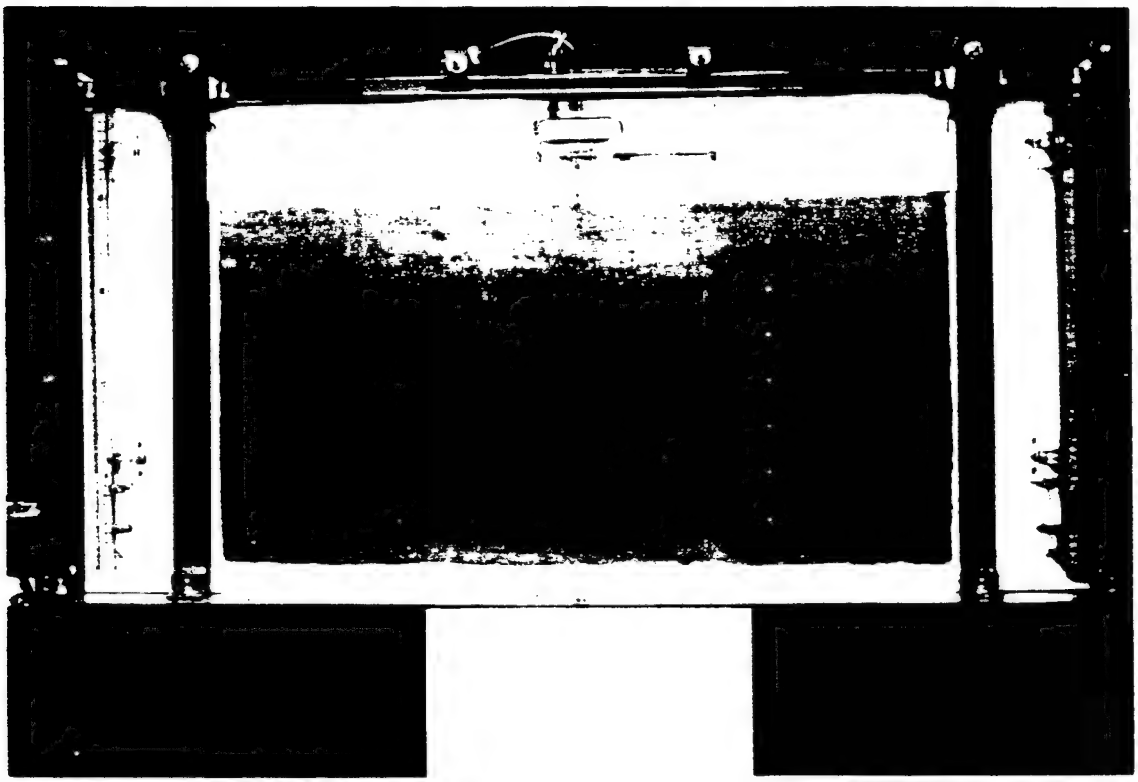

Figure 93 Experiment 5 Photograph Taken Before the Introduction of PCE

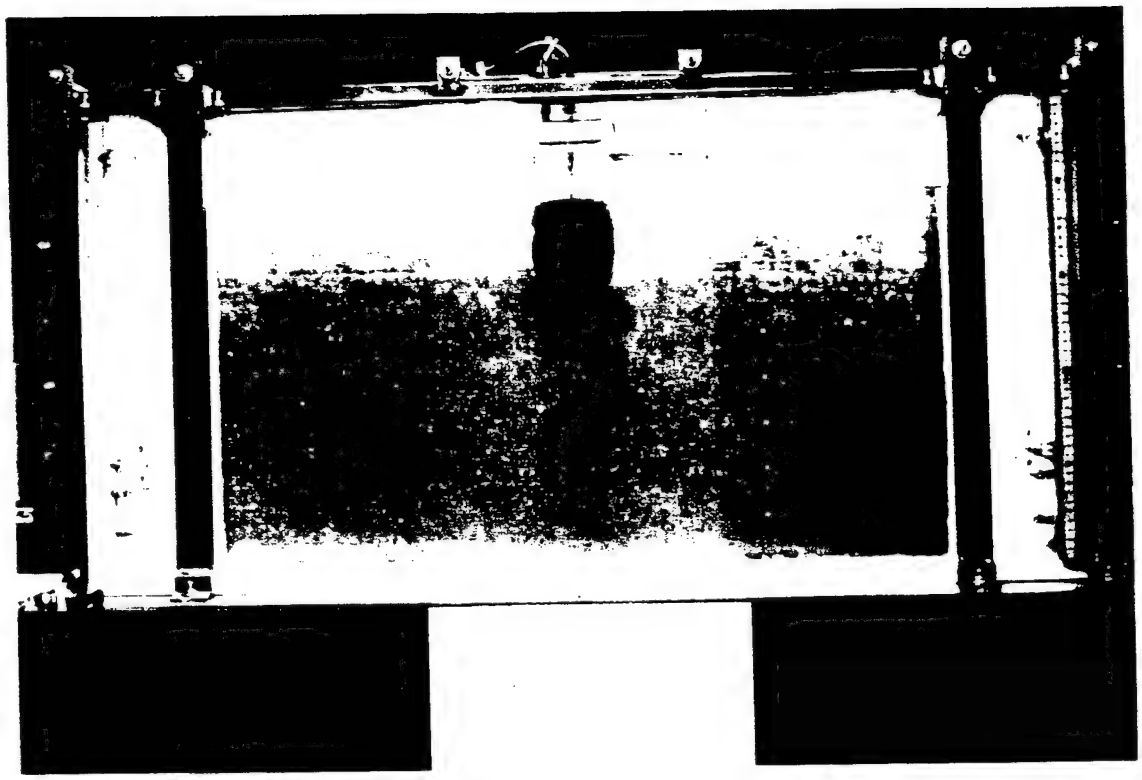

Figure 94 Experiment 5 Photograph Taken After the Input of 150 mL of PCE at 10 mL/min

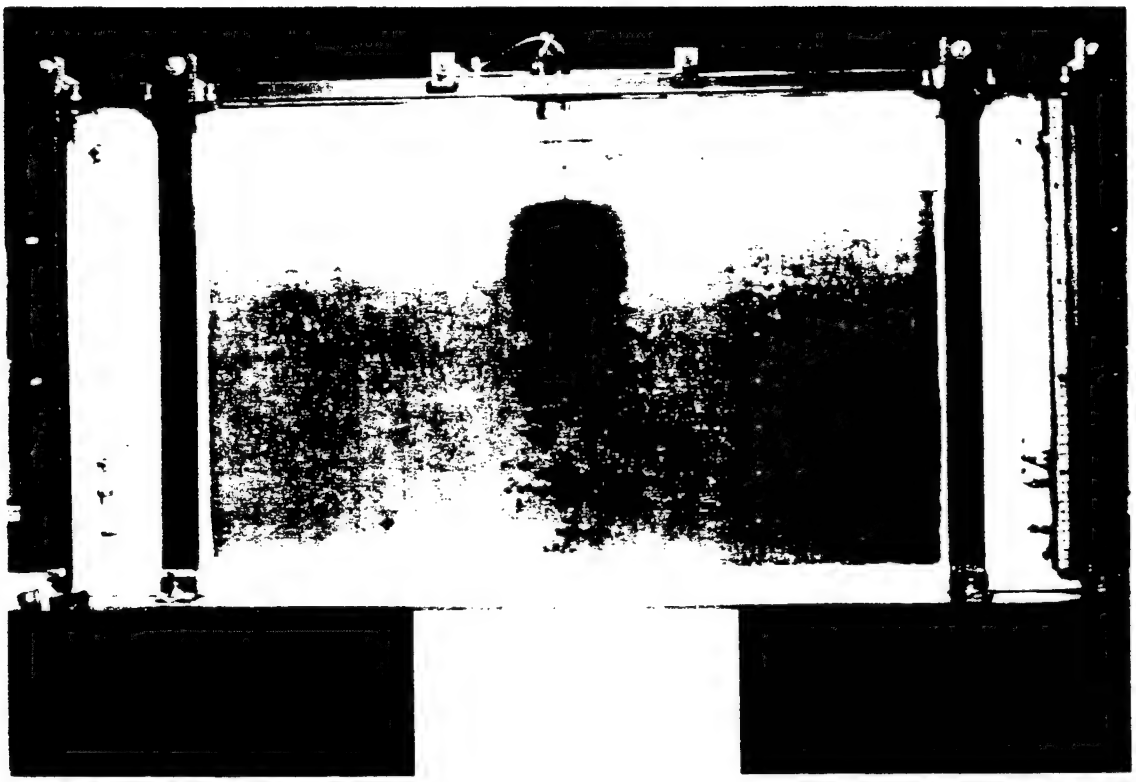

Figure 4.5 Experiment 5 Photograph Taken After the Input of 500 mL of PCE at 10 mL/min

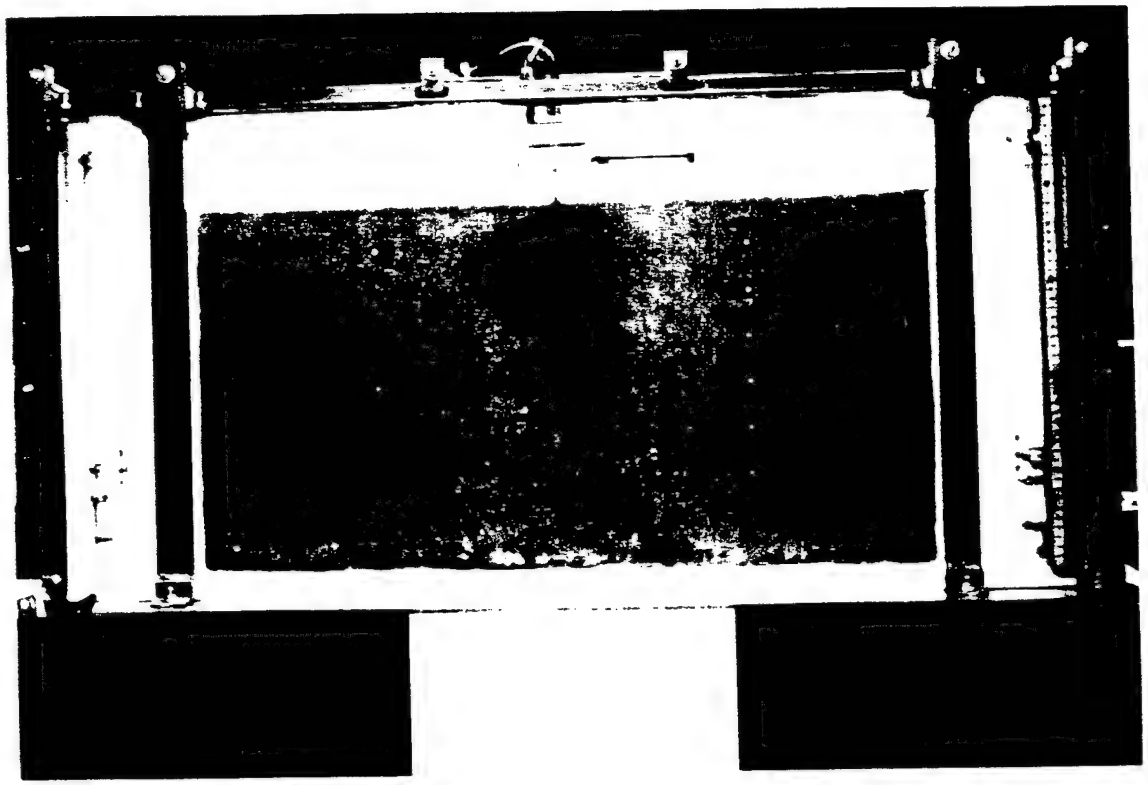

Figure [illegible] Experiment 5 Photograph of the PCE Distribution in the Porous Medium 56 Hours After Input

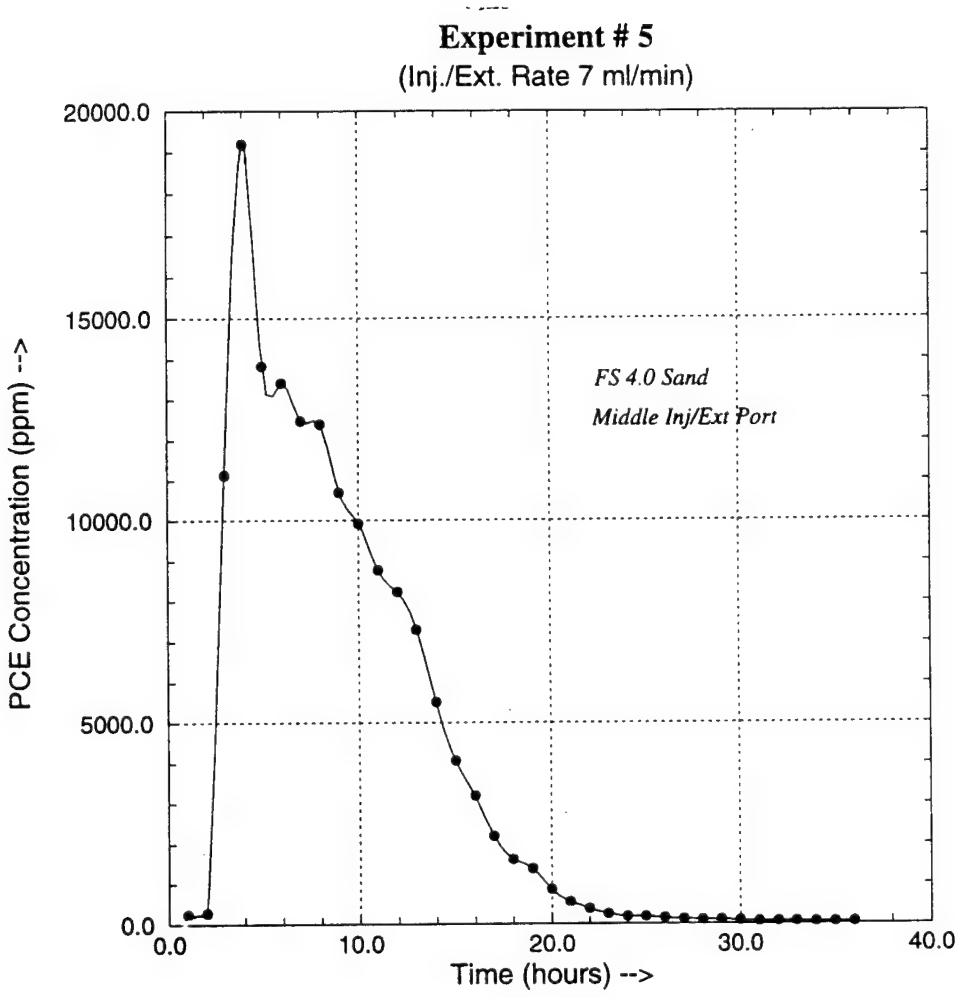

Figure 97. Experiment 5: Effluent PCE Concentration Variation With Time.

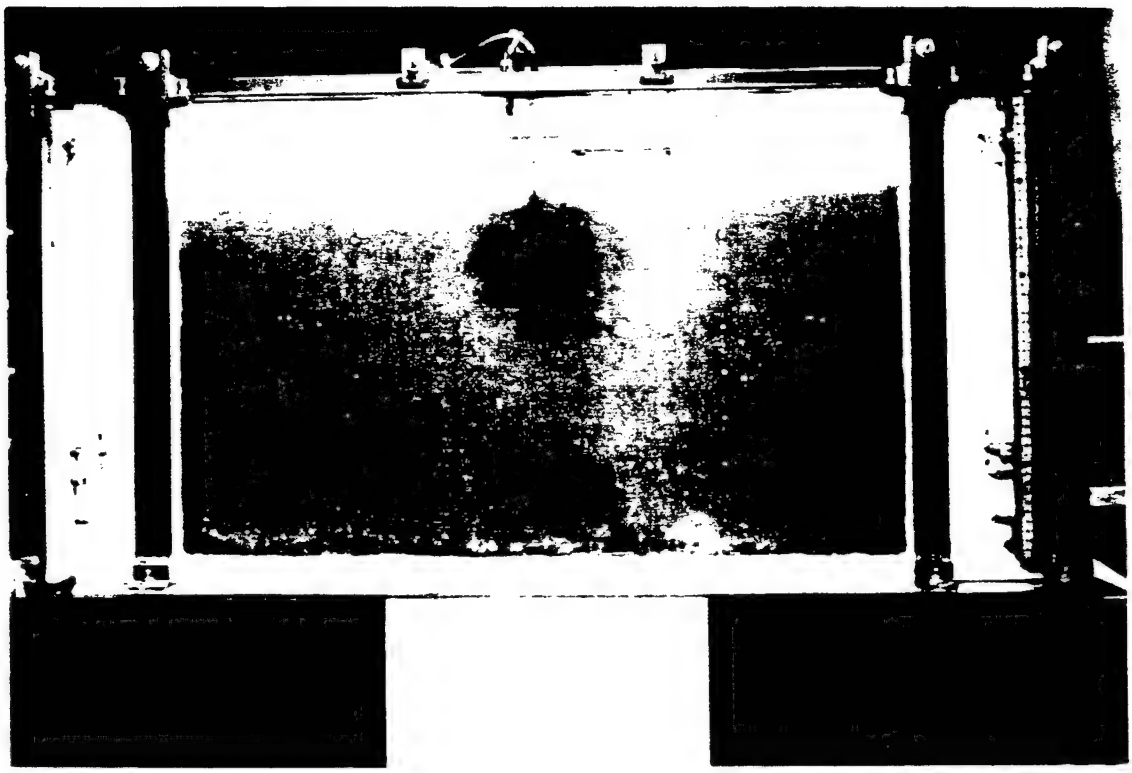

Figure 98 Experiment 5 Distribution of PCE in the Porous Medium After the Cleanup by Injection of 4% Surfactant Solution for 24 Hours

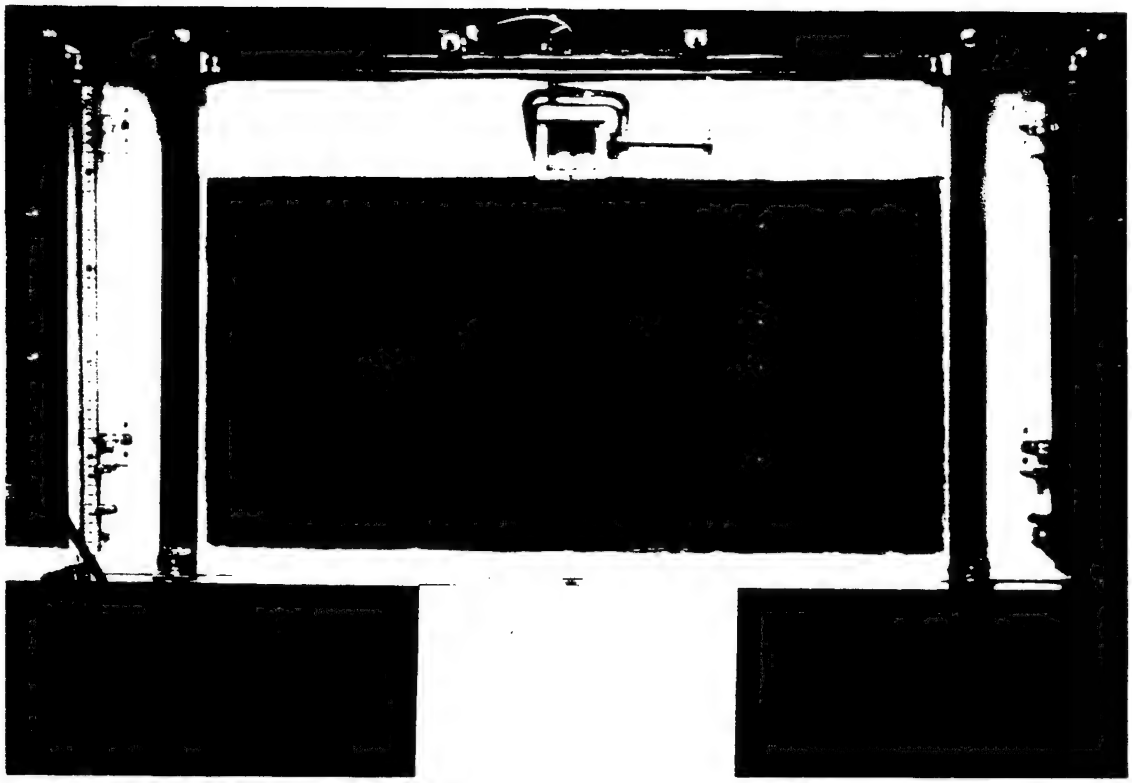

Figure 94 Experiment 5 Distribution of PCE Before the Injection and Extraction of 4% Surfactant Solution 17.5 Hours After Input of PCE

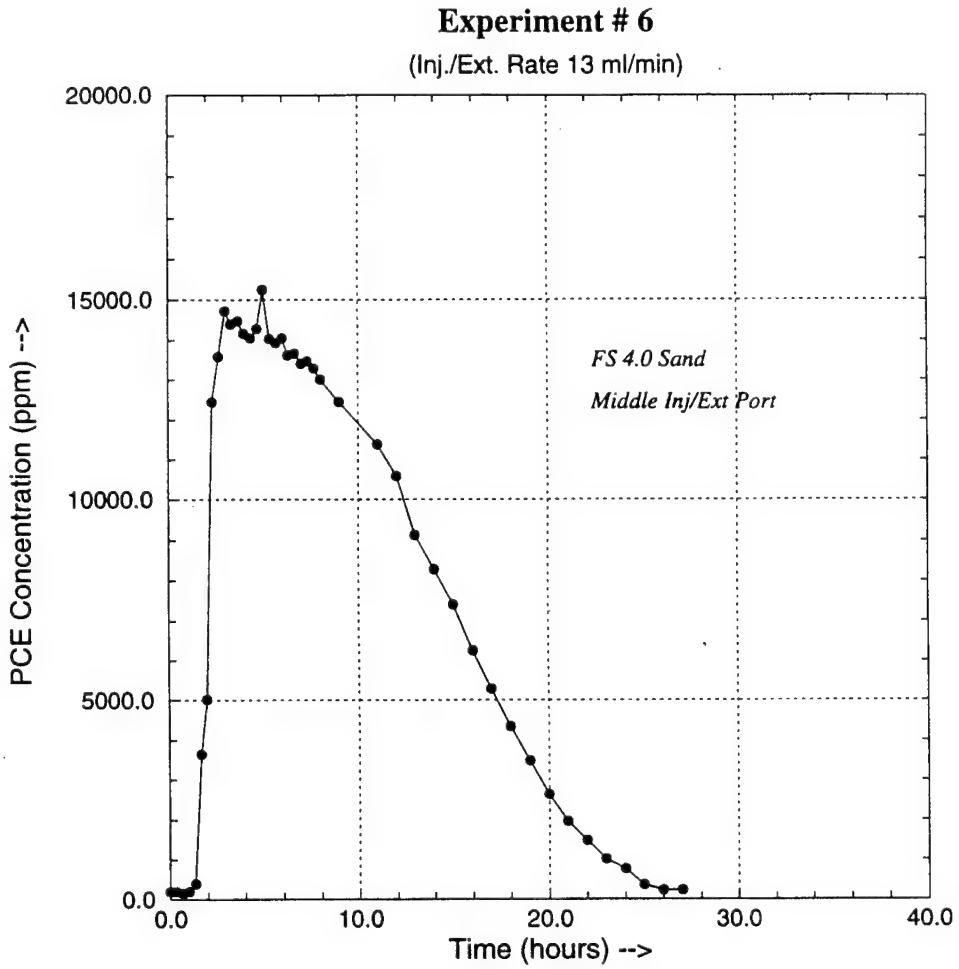

Figure 100. Experiment 6: Effluent PCE Concentration Variation With Time.

the pumping was stopped, indicating that the solubilization was rate limited. The peak effluent PCE concentration was reached earlier in this experiment, which again may have been due to the higher I/E rate, resulting in a shorter breakthrough time. The effluent PCE concentration remained at a higher level longer than for the previous experiment. This could have been due to the lower peak concentration and the larger area of the flow field swept by the surfactant solution.

The time taken for the effluent PCE concentration to decrease to about the aqueous solubility limit of 240 ppm was about 26 hours. Figure 101 shows the final PCE distribution in the porous medium at the end of the I/E of the surfactant solution for 30 hours.

Experiment 7:

This experiment was done with a heterogeneous medium. The different types of porous media lenses were distributed as shown in Figure 102. One of the problems faced during this experiment was the entrapment of air within the glass bead regions. This was circumvented by repeatedly raising and lowering the water level fairly quickly to force the air out of these regions. After saturation, the water level was lowered to 15 cm with the top of capillary fringe at 28 cm, about 5.5 cm below the lense consisting of Flintshot FS 2.8 sand. PCE was then pumped in at a rate of 10 mL/min for 50 min. Figures 103 and 104 show photographs of the PCE distribution at various stages of the PCE infiltration. Approximately 35 min after the start of the introduction of PCE some of it was noticed at the bottom of the porous medium, indicating the existence of some continuous fingers that had reached the bottom of the flow container. The water level was then raised to 40 cm and 38 cm in the inlet and outlet end chambers, respectively and the I/E of fluorescein solution was started at 13 mL/min through the middle ports. An elliptical flow field was thus established encompassing the two regions of the glass bead medium. The I/E of the fluorescein solution was then stopped and the fluorescein flushed out by the horizontal flow. After 42.25 hours, the I/E of 4% surfactant solution was started. Samples were taken every half-hour for the first 6 hours and every 1 hour for the next 29 hours. Later the I/E was done through the top ports (Injection Port 1 and Extraction Port 1, Figures 29 and 30). Samples were taken every half-hour for the first 6 hours, every 1 hour for the next 12 hours, and at 3 hour intervals for the remaining 6 hours of the experiment.

The effluent PCE concentration breakthrough data are presented in Figure 105. The I/E rate was initially 13 mL/min for 25 hours. Figure 106 shows the flow field developed by the I/E of surfactant solution at 13 mL/min for 3 hours. It was observed that the flow field became narrower with time (Figure 107). After about 12 hours of I/E of 4% surfactant, the surfactant was no longer visible on the front of the porous medium. This may have been due to the formation of flow channels which were cleared of the PCE residual. This result seems to confirm the prediction made by McKinney et al. (1992), using a 2-D simulation model, that under heterogeneous conditions channeling can occur which would cause the surfactant to take longer to remediate an aquifer (see, also, Brown et al., 1994). At about 12 hours (Figure 105), there is a drop in the effluent PCE concentration. After 25.5 hours the I/E rate of 13 mL/min was doubled to 26 mL/min. Figure 108 shows the flow field developed 3 hours after the I/E rate was doubled. The surfactant again became visible at the front of the medium. As seen in Figure 105, the effluent PCE concentration started to increase again which was probably due to the larger volume of the flow field swept by the surfactant. The effluent PCE concentration began to decrease again after another 3 hours. The I/E was continued for 10 hours after doubling the I/E rate and was then stopped because the surfactant solution was exhausted.

t, the I/E of surfactant was started through the top I/E ports at 13 mL/min. The flow field
enco ssed the lense of FS 2.8 sand. It was again observed that the flow filed became narrower with time.
It toc out 20 hours for the effluent PCE concentration to reach a concentration below the aqueous

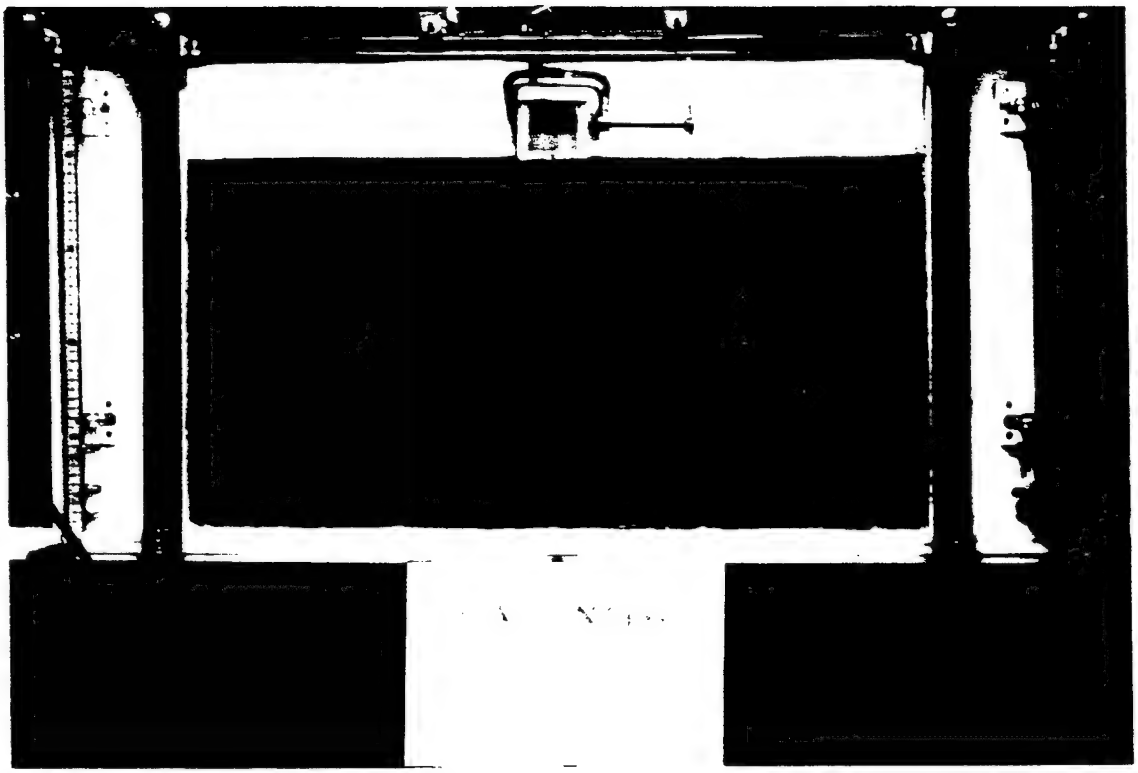

Figure 101 Experiment 6 Distribution of PCE at the End of the Cleanup Using Surfactant for 30 Hours

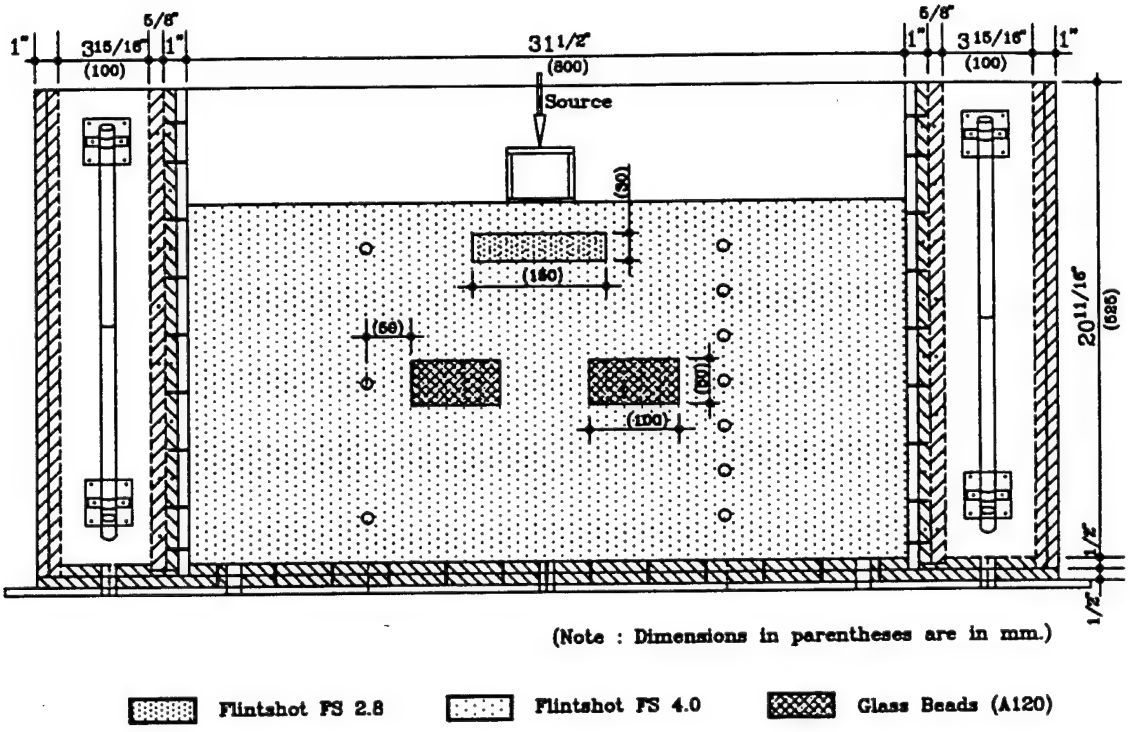

Figure 102. Elevation View of the Flow Container Showing the Distribution of the Different Media for the Heterogeneous Medium Experiments.

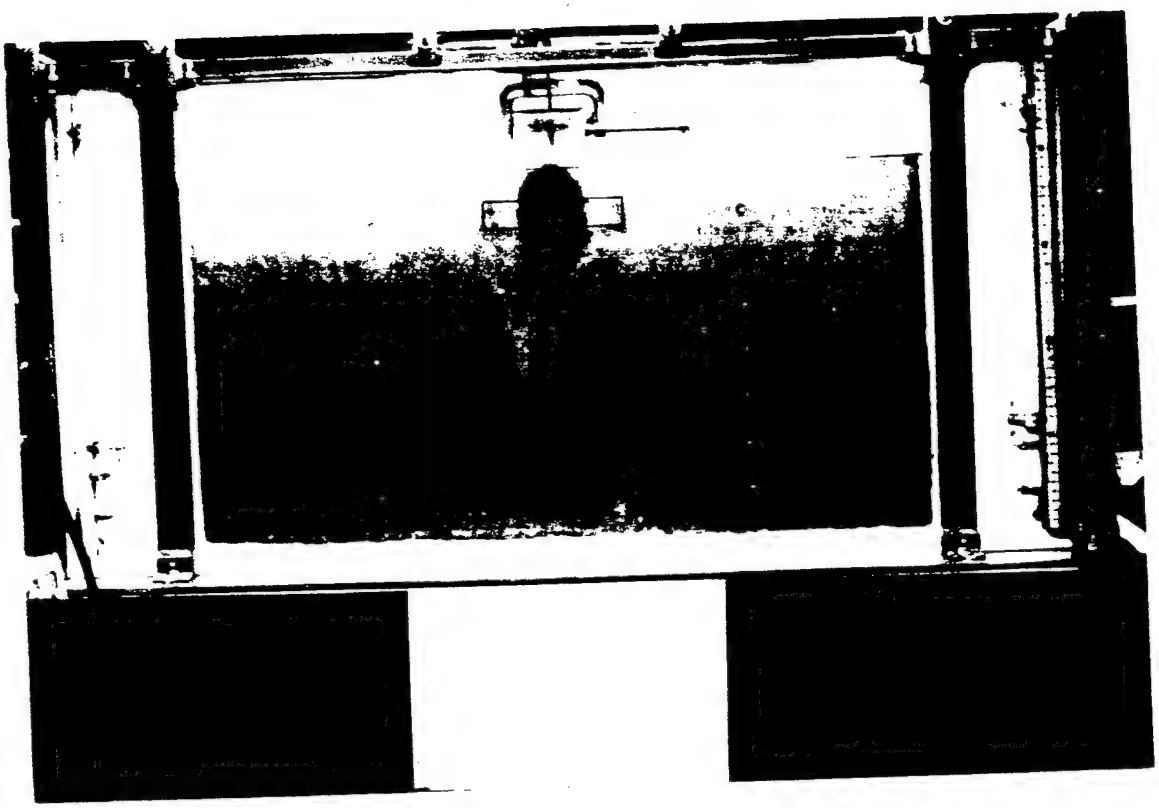

Figure 1c3 Experiment 7 Distribution of PCE After the Input of 100 mL at 10 mL min

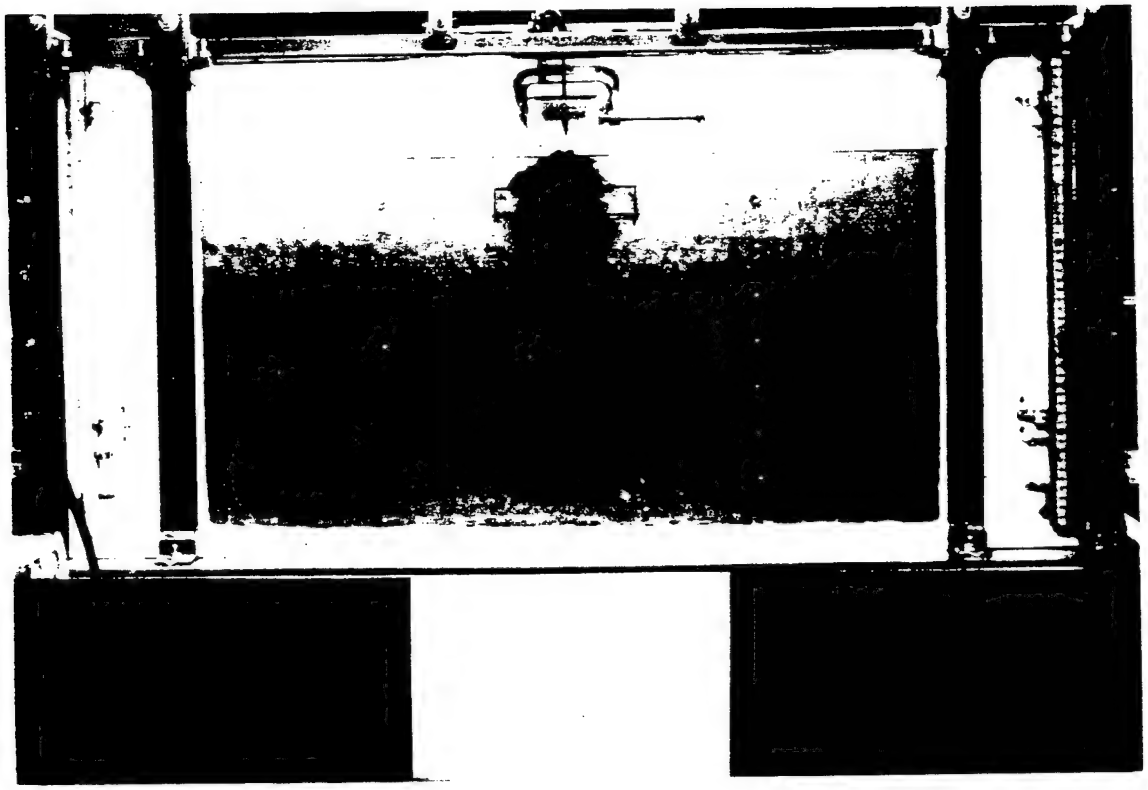

Figure 104 Experiment 7 Distribution of PCE After the Input of 350 mL at 10 mL/min

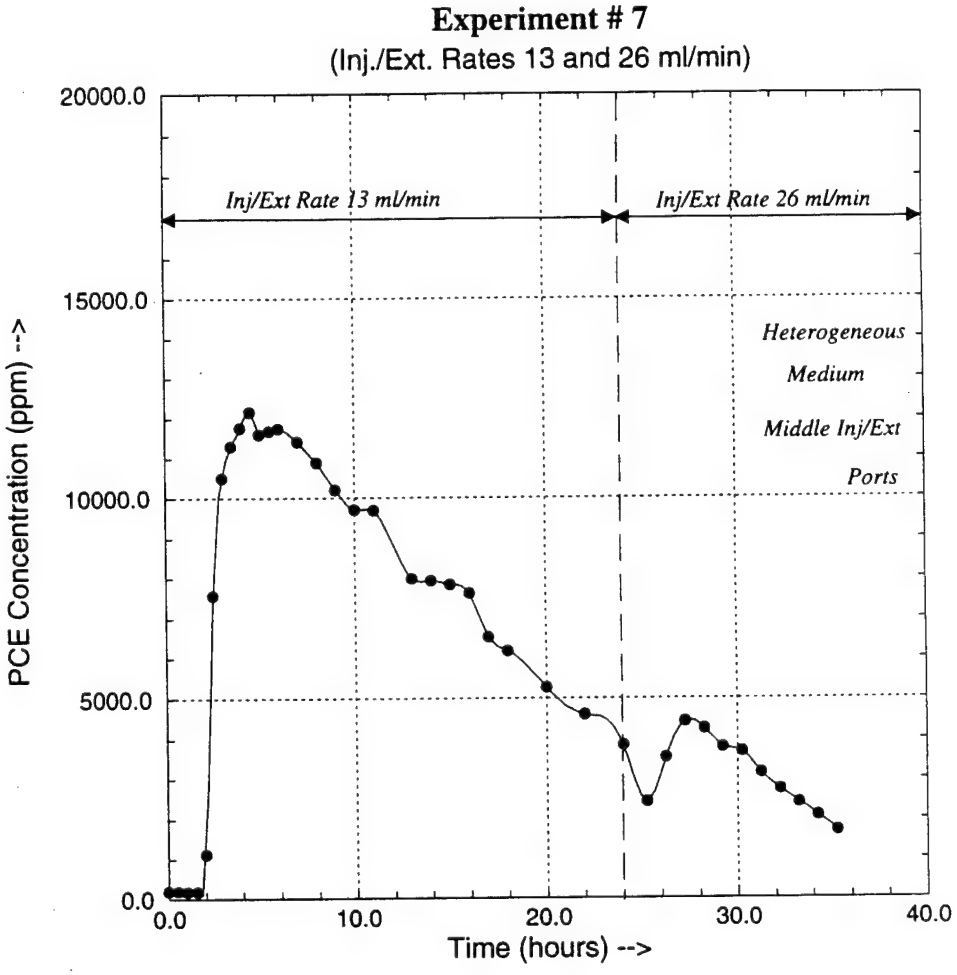

Figure 105. Experiment 7: Effluent PCE Concentration Variation With Time (Injection and Extraction Through the Middle Ports).

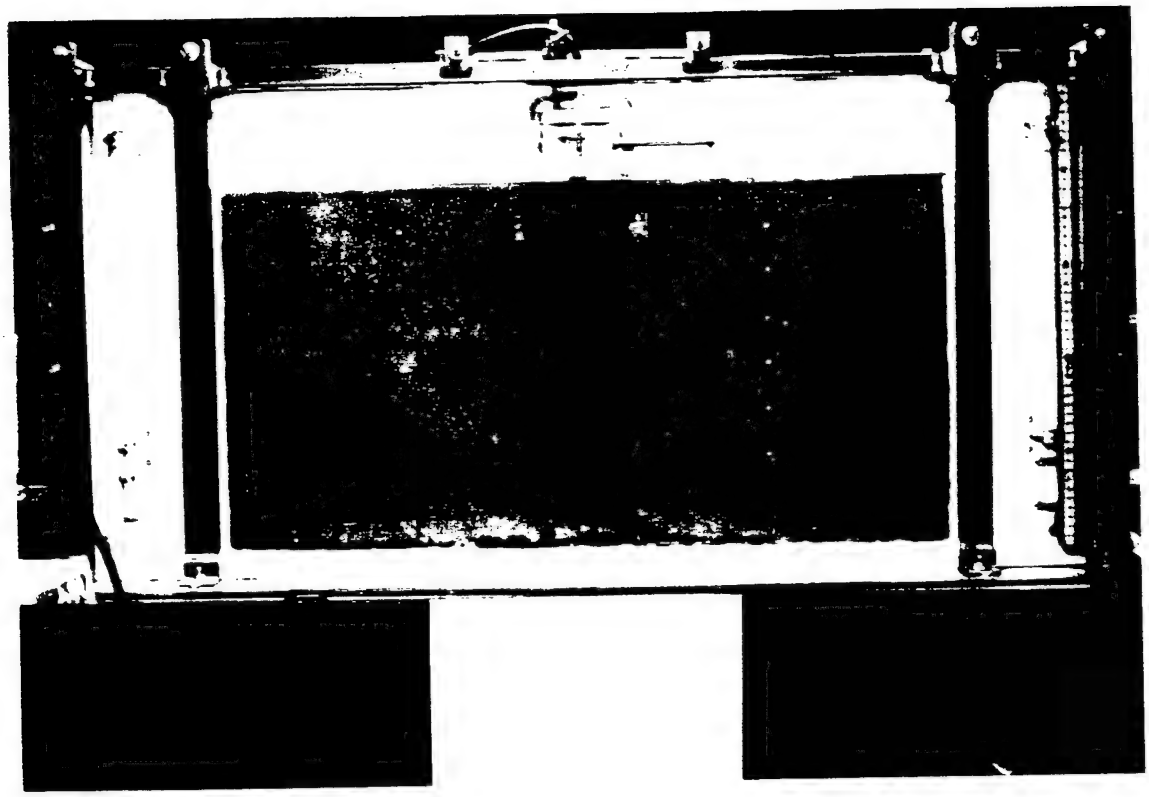

Figure [illegible] Experiment 7 Flow Field Developed by Injection and Extraction of Surfactant Solution at 13 mL/min for 3 Hours

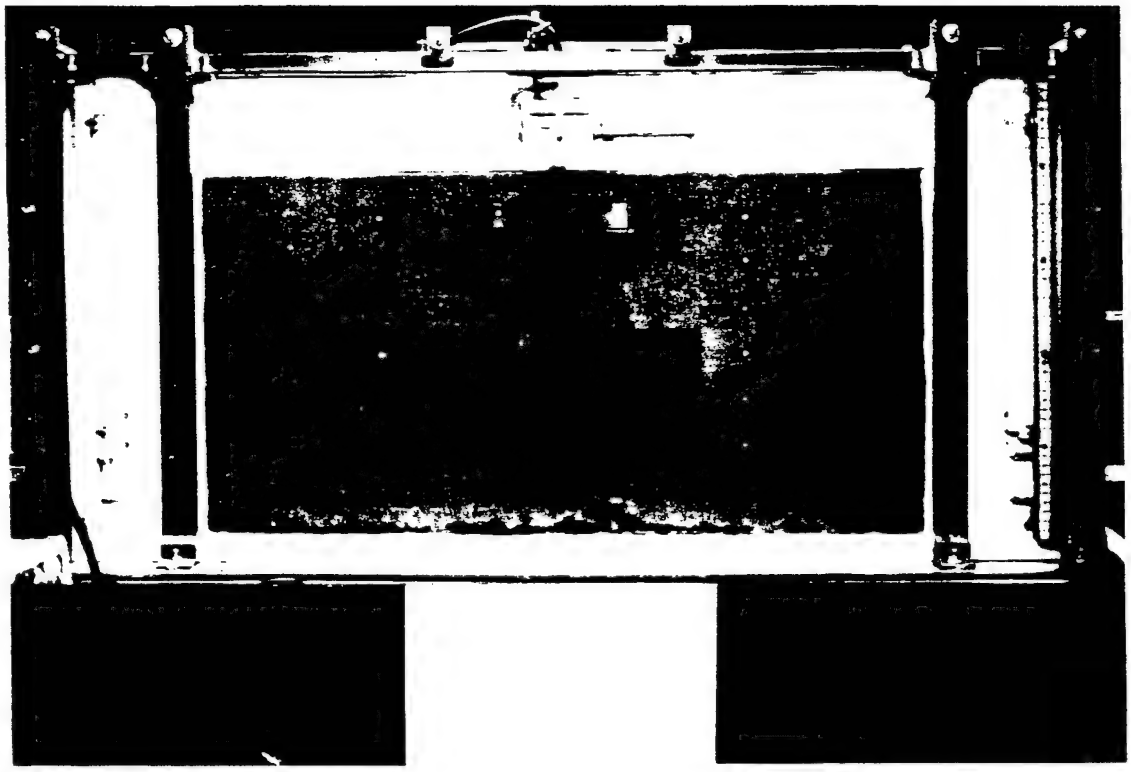

Figure [illegible] Experiment [illegible] Flow Field Developed by Injection and Extraction of Surfactant Solution at 13 mL min for [illegible] Hours

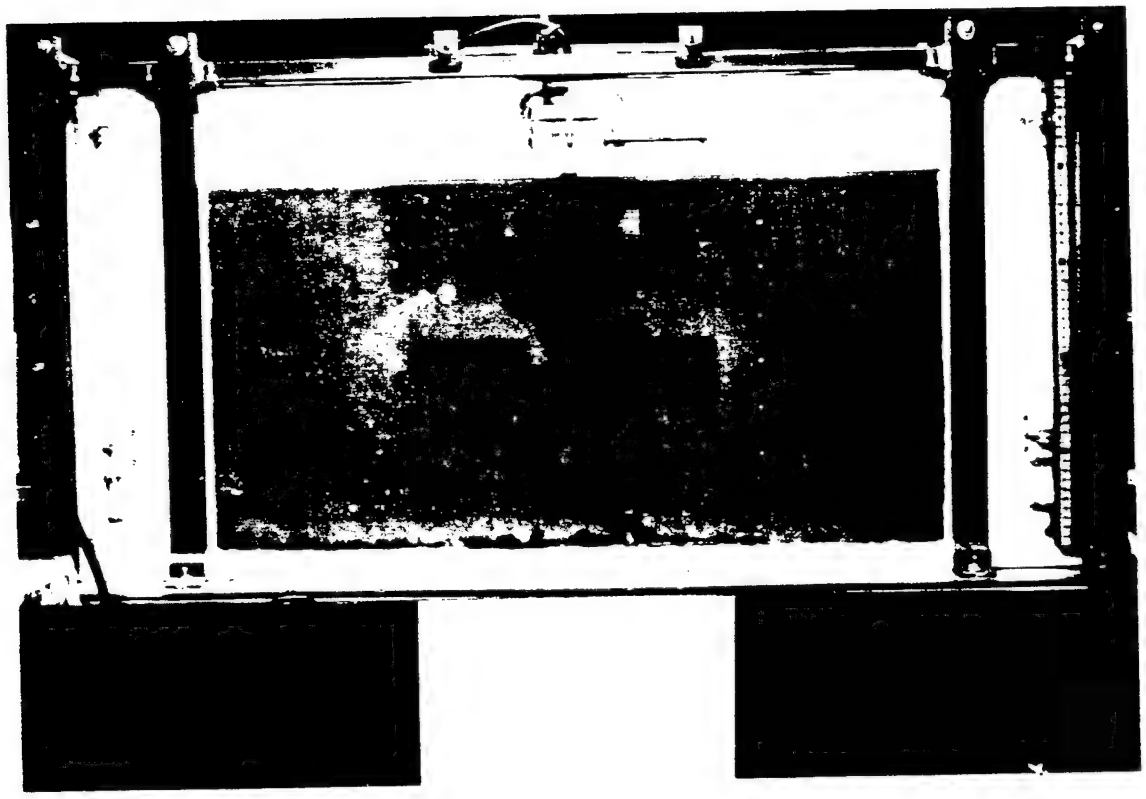

Figure 108 Experiment 7 Flow Field Formed 3 Hours After Increasing the Injection and Extraction Rate of Surfactant Solution to 26 mL/min

solubility limit of PCE. Figure 109 shows the effluent PCE concentration variation observed with time. Figure 110 shows the final stage of the cleanup just before the I/E of surfactant was stopped.

From this experiment it appears that the regions of heterogeneous distribution of porous media could pose a more difficult problem for remediation. It may be more difficult to remediate the higher permeability zones located within a less permeable region, because the PCE could accumulate in the higher permeability zones, and also due to the formation of the preferential flow paths within it.

Experiment 8:

For this experiment the contaminated heterogeneous medium of Experiment 7 was used. The water level was adjusted to 24 cm with the top of the capillary fringe at 36.5 cm. As in Experiment 7, 500 mL of PCE was pumped in at a rate of 10 mL/min. The Flintshot FS 2.8 sand layer was saturated with water in this experiment. As the PCE was introduced it was observed that this lower permeability region of saturated finer sand did not retard the PCE movement much. As seen in Figure 111, the PCE did spread more in this experiment than in experiment 7 (Figure 103). This was probably because the PCE first had to develop sufficient pressure before it could displace the water present in the pores of the Flintshot FS 2.8 sand. Figure 112 shows the PCE distribution after the input of 350 mL. From Figures 112 and 104 it is seen that the distribution of the PCE was not very different for the two experiments. The cleanup, using the surfactant solution, was therefore not performed in this experiment.

D. CONCLUSIONS

The migration of DNAPLs in the subsurface and their surfactant enhanced remediation was studied. It is widely accepted that present knowledge about the behavior of NAPLs in the subsurface and their cleanup is inadequate.

Some of the important observations made during the introduction of PCE are as follows. The heterogeneities caused the PCE to flow along paths of least resistance. The PCE migrated rapidly downwards through the aquifer until it encountered the capillary fringe, where it spread laterally and fingers developed which penetrated the saturated zone. The PCE moved downwards quickly, but through a narrower region in the Flintshot FS 4.0 sand than through the Flintshot FS 2.8 sand, which has a lower permeability. The fingers formed reached the bottom of the flow container and spread out laterally. Thus, if PCE is spilled in sufficient quantity it can be expected to migrate downwards rapidly through the unsaturated zone in the aquifer and then continue as fingers through the saturated zone until an impermeable layer or low permeability layer is reached where it will spread laterally.

The following observations were made during the cleanup of the residual PCE using the 4% surfactant solution. Flushing with the surfactant solution increased the removal of the PCE residual from the porous medium significantly. The surfactant solution was deflected by the presence of the PCE blobs and ganglia in the pores. Later, as these pores were cleared of the PCE residual, the flow field became narrower. The concentration of PCE in the effluent reached a higher concentration peak for the lower injection and extraction rates than for the higher ones, indicating that the solubilization may have been rate limited. When the injection and extraction rates were increased (Experiment 7), the effluent PCE concentration also increased, which could be due to the larger volume of the medium swept by the surfactant solution. The flow region near the injection port was cleaned up first by the surfactant and, gradually as the experiment progressed, the region near the extraction port was cleared of the PCE residual. The cleanup of the PCE residual from the heterogeneous medium took longer. One of the reasons for this could be the accumulation

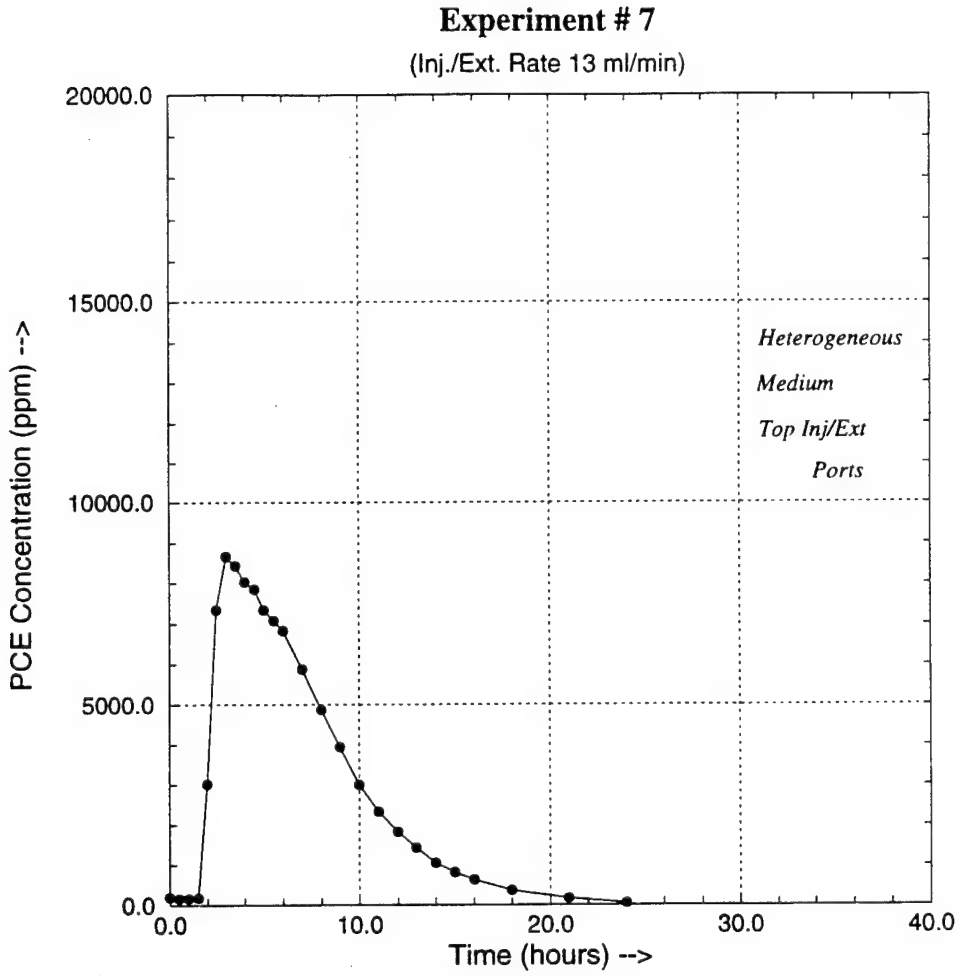

Figure 109. Experiment 7: Effluent PCE Concentration Variation With Time (Injection and Extraction Through the Top Ports).

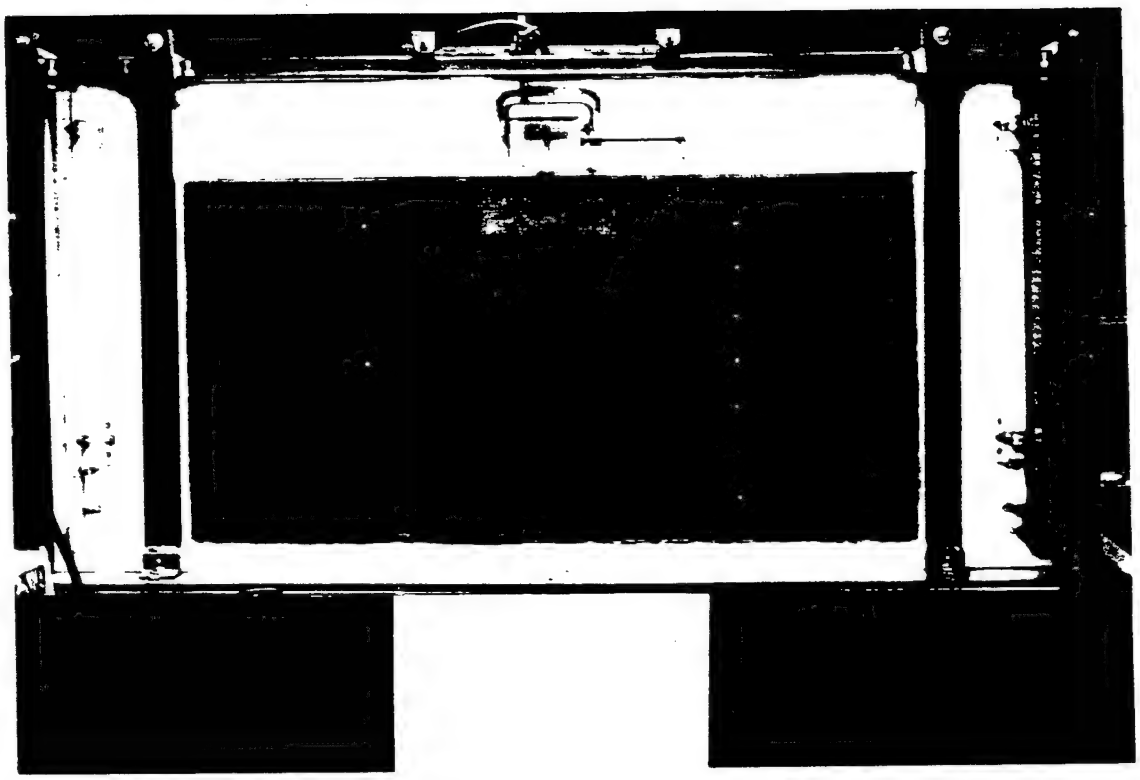

Figure 110 Experiment 7 Distribution of PCE at the End of the Cleanup Using Surfactant for 24 Hours

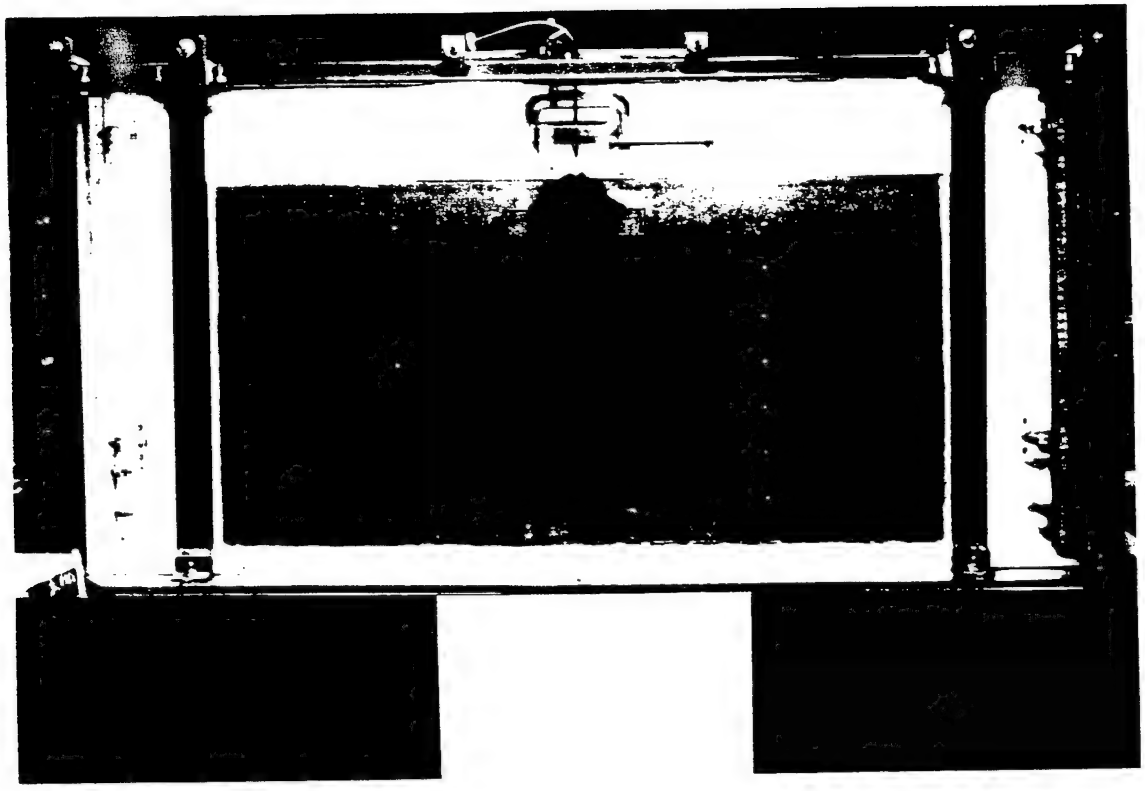

Figure 111 Experiment 8 Distribution of PCE After the Input of 100 mL at 10 mL min

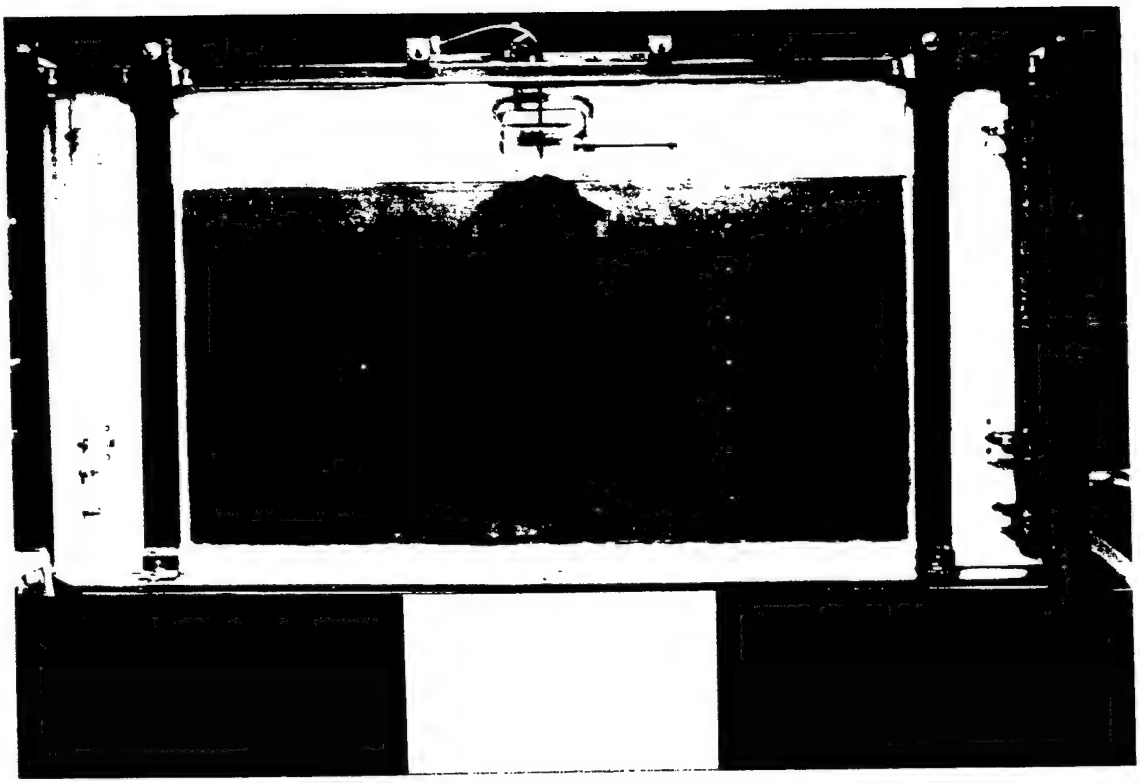

Figure 112 Experiment 8 Distribution of PCE After the Input of 350 mL at 10 mL/min.

of larger amounts of PCE residual in the higher permeability region. The other reason may be the formation of flow channels through the higher permeability regions thus reducing the contact between the surfactant and the PCE residual. The difference in the permeabilities of the regions may play a significant role in terms of the time required for cleanup. A higher injection and extraction rate may have to be applied in order to increase the rate of removal of the PCE residual as the remediation progresses.

Based on the results and observations made during the course of this study it can be concluded that surfactant enhanced remediation is a promising method for cleanup of PCE contaminated aquifers. However, several factors need to be considered, such as the quantity, distribution and type of the NAPL, the ambient horizontal groundwater flow, the location and the rate of injection and extraction of the surfactant, the aquifer characteristics like heterogeneities, organic matter, pH, and the properties of the surfactant.

REFERENCES FOR SECTION VIII

Brown, C.L., G.A. Pope, L.M. Abriola, and K. Sepehnoori, "Simulation of Surfactant-Enhanced Aquifer Remediation." Water Resources Research, 30, 2959-2977, 1994.

Mamballikalathil, R., "A Laboratory Study of the Subsurface Transport of Tetrachloroethylene and its Surfactant Enhanced Cleanup." M.S. Thesis, Dept. of Civil Engineering, Auburn University, 1995.

McKinney, D.C., C.L. Brown, M. Jin, G.A. Pope, K. Sepehnoori, and L.M. Abriola, "Simulation of the Performance of Surfactant Enhanced Remediation of DNAPL Contaminated Aquifers." Subsurface Restoration Conference, National Center for Groundwater Research, Houston, TX, 247-249, 1992.

Pennell, K.D., M. Jin, L.M. Abriola, and G.A. Pope, "Surfactant Enhanced Remediation of Soil Columns Contaminated by Residual Tetrachloroethylene." Journal of Contaminant Hydrology, 16, 35-53, 1994.

Schwille, F., Dense Chlorinated Solvents in Porous and Fractured Media Model Experiments. Lewis Publishers, Chelsea, MI, 1988.

SECTION IX
PCE SPILLS IN A TWO-DIMENSIONAL, HETEROGENEOUS POROUS MEDIUM

A. INTRODUCTION

A major limitation in our current ability to predict DNAPL migration in natural aquifers is a lack of understanding the effect of porous medium heterogeneities. The major objective of the research reported in this section is therefore to study multiphase fluid flow behavior by means of physical simulations of PCE spills into a two-dimensional, heterogeneous porous medium. This section forms a logical continuation of the earlier reported PCE spills into one-dimensional, stratified sand columns (Section VI).

First a description will be given of the design and construction of the two-dimensional flow container. Second, a series of physical simulations of PCE spills into a partially water saturated, stratified, two-dimensional porous medium will be described. Third, the results of the physical simulations in the two-dimensional flow container will be discussed and compared with the physical simulations in the one-dimensional columns (Section VI).

B. EXPERIMENTAL SETUP AND METHODS

1. Construction of the Two-dimensional Flow Container.

Following the design of Oostrom et al. (1992a, 1992b), the flow container consisted of three parts (Figure 113): a porous medium chamber consisting of two vertical, parallel, 1/4-inch glass plates resting on a Teflon® base, and two constant head end chambers made of Teflon®. The inside width of the flow container was 5 cm, which coincides with the optimum path length for dual-energy gamma radiation measurements (Oostrom and Dane, 1990). The length and height of the container were 2 meter and 1 meter, respectively. Because of the use of PCE (a solvent), all materials used in the construction of the flow container consisted of either glass, stainless steel, or Teflon®. All connections were sealed with a silicon sealant (Dixie Bearings, Atlanta, Georgia) and held together with stainless steel screws. The flow container was supported externally by vertical steel bars in exactly the same manner as described by Oostrom et al. (1992a, 1992b). Stainless steel fittings (Birmingham Valve and Fitting Inc., Pelham, Alabama) connected the bottom of the flow container to seven glass PCE traps to collect and measure the outflow volumes of PCE. The water levels in the end chambers were regulated by constant head reservoirs connected to the end chambers. To avoid vapor losses from the flow container it was covered with glass plates containing small ventilation holes to maintain atmospheric pressure in the gas phase.

2. Experimental Setup.

The flow container was packed with three grades of Ottawa sand (Figure 113), consisting of a coarse (FS2.8), a fine (F75), and a very fine sand (F55). The coarse sand, approximately 100 cm high, occupied most of the container but had a 30-cm thick layer of the fine sand embedded in it. The very fine sand at the bottom served as funnels to guide the PCE, emanating from a source on top of the sand, into the traps. It should be noted that the sequence and thickness of the coarse and fine sand layers was similar to those of the one-dimensional columns (Section VI). The procedure to pack the flow container was the same as described in Section IV.

Upon flushing the porous medium with CO_2, it was saturated with deionized water by gradually raising the water levels in the end chambers. Once water was ponded on the surface of the porous medium,

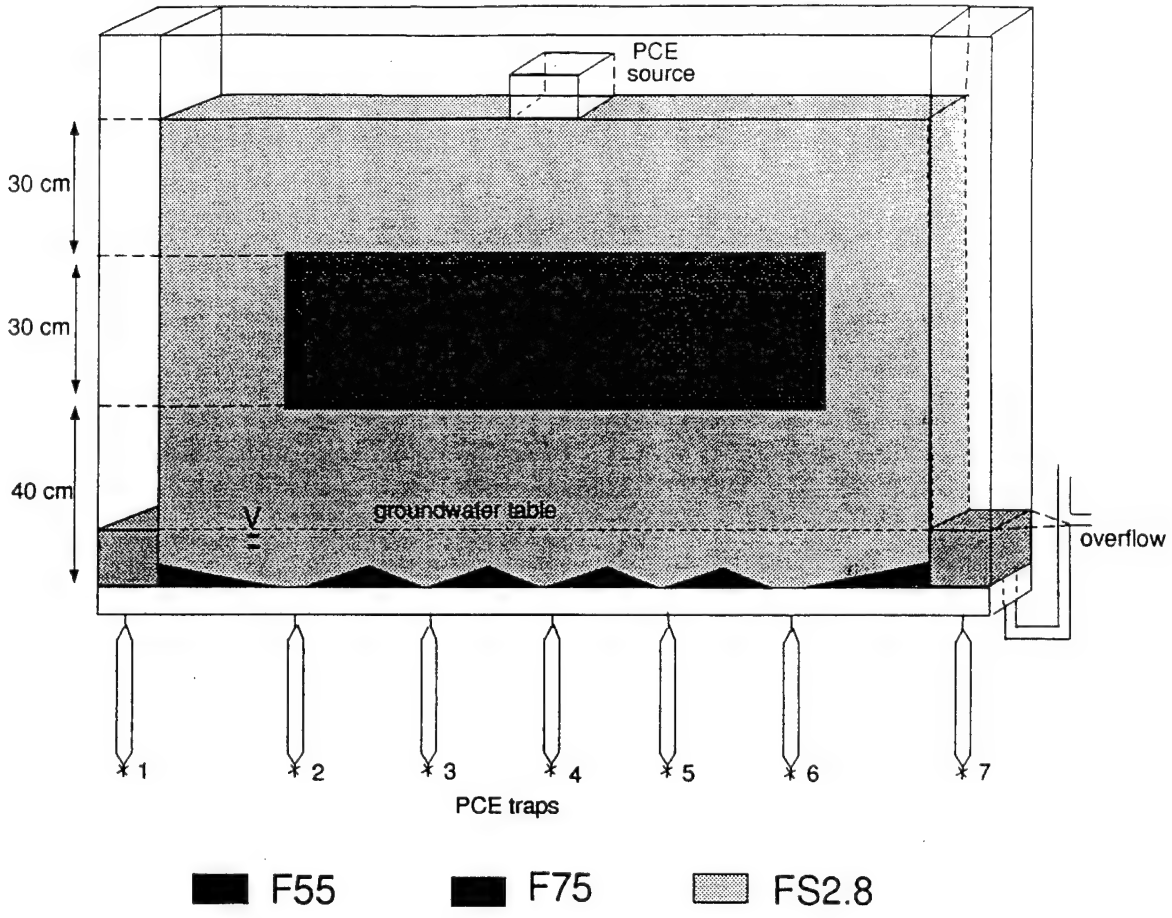

Figure 113. Schematic of the Experimental Setup.

horizontal flow was established and several pore volumes were flushed through to remove dissolved CO_2. When the horizontal flow was stopped, the water levels in the end chambers were gradually reduced until the groundwater table was at 11 cm from the bottom of the flow container. Once static equilibrium had been reached, the dual-energy gamma radiation system was used to determine the bulk density and the volumetric water content at 23 locations along each of 59 vertical transects (Figure 114). Porosity values, calculated from bulk density values, are shown in Figure 115, while the volumetric water content values for the water at static equilibrium with the water table are shown in Figure 116. The packing (porosity values) seemed to be less uniform than for the one-dimensional columns. Visual inspection of the flow container revealed, indeed, some layering as indicated by the irregular height of the capillary fringe and the slight differences in color between layers due to differences in volumetric water content. It is also obvious that the unsaturated volumetric water content values in the fine layer were much greater than the approximate value of 0.15 for the surrounding coarse sand.

To simulate the spills, PCE was introduced through the 2.7 by 4.3 cm open ended bottom of a rectangular stainless steel box located on top of the porous medium. The long side of the box ran perpendicular to the glass plates. The PCE was supplied from a reservoir to the box with a peristaltic pump (Masterflex L/S Digital Console). The flow of PCE (Aldrich Chemical Company), dyed with Oil Red (Aldrich Chemical Company) to improve its visibility, was monitored by visual inspection, photography, and video recordings. During the first simulated spill, PCE was applied for 10 minutes at a rate of 65 mL/min. The outflow of water (overflow connected to one of the end chambers) and PCE from the flow container were measured as a function of time. Air flow into and from the porous medium was determined from changes in total liquid content. Once the outflow of PCE and air had become negligible, static equilibrium was assumed and the dual-energy gamma radiation system was used to simultaneously determine the volumetric water and PCE contents at all 1357 measurement locations. Two additional spills, with the same application rate as during the first spill, were subsequently simulated for durations of 15 and 10 minutes, respectively. All measurements as during and after the first spill were repeated.

C. RESULTS

During the first spill, PCE infiltrated instantly into the porous medium without accumulating on top of the sand. The PCE plume migrated downwards through the coarse layer with a uniform infiltration front, similarly as in the previously described one-dimensional experiment with the partially saturated sand (Section VI). After 2.7 minutes the front reached the coarse/fine sand interface and, without delay, the PCE plume infiltrated into the fine layer, initially without any significant spreading above the interface (Figure 117). However, some minor spreading was observed below the interface (Figure 118). This was attributed to the relatively high gradients in capillary pressure across the PCE-air interfaces in the unsaturated fine sand. After some time, the PCE also started to accumulate and spread above the coarse/fine sand interface (Figure 119). Apparently, enough PCE had infiltrated into the fine layer to reduce the capillary pressure gradients, leaving gravity the main driving force for PCE flow. At the same time, the supply rate of PCE from the coarse sand layer had exceeded the hydraulic conductivity for PCE in the fine sand layer. Another contributing factor in the spreading and accumulation above the coarse/fine sand interface was the encounter of water saturated layers by the PCE plume, thus further hindering its downward movement.

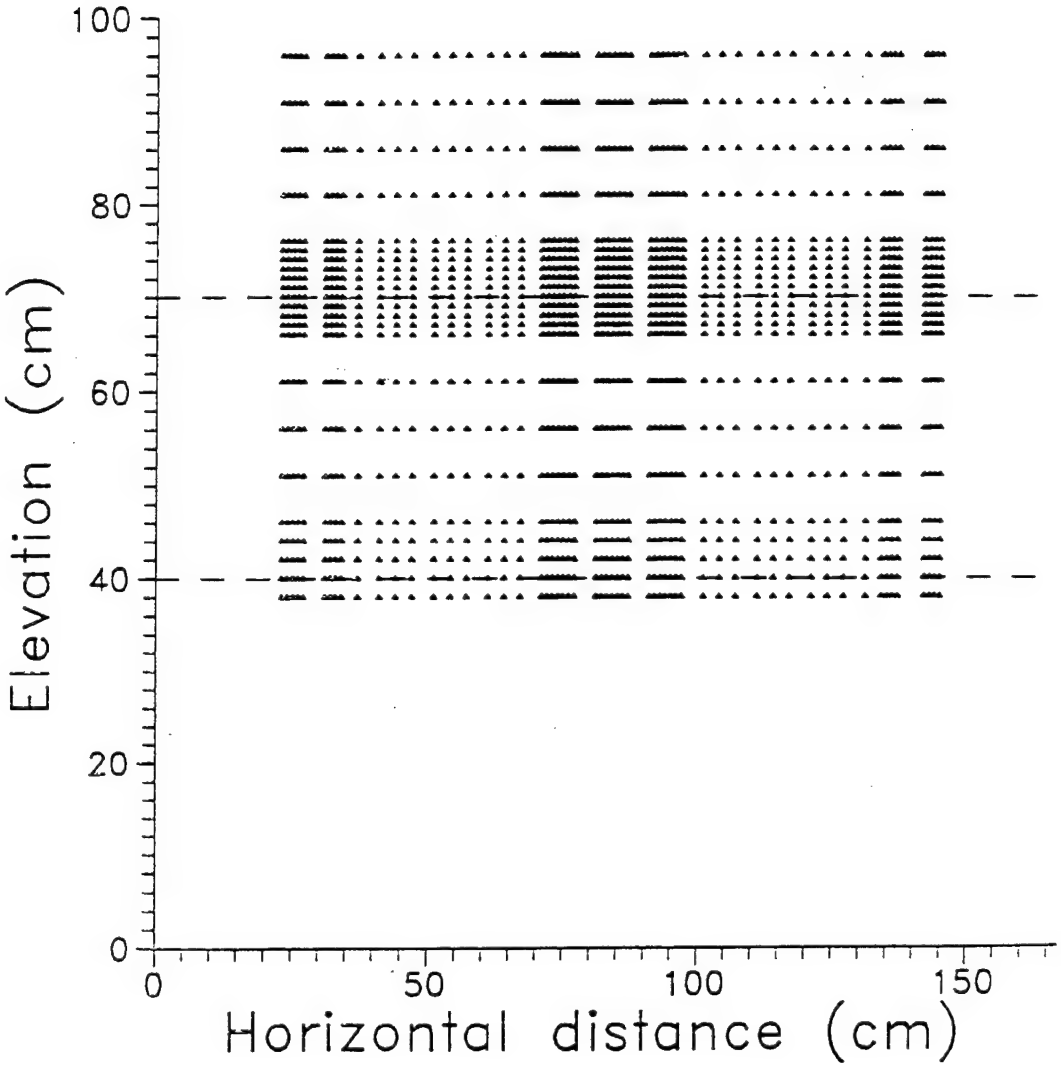

Figure 114. Measurement Locations Along 59 Vertical Transects.

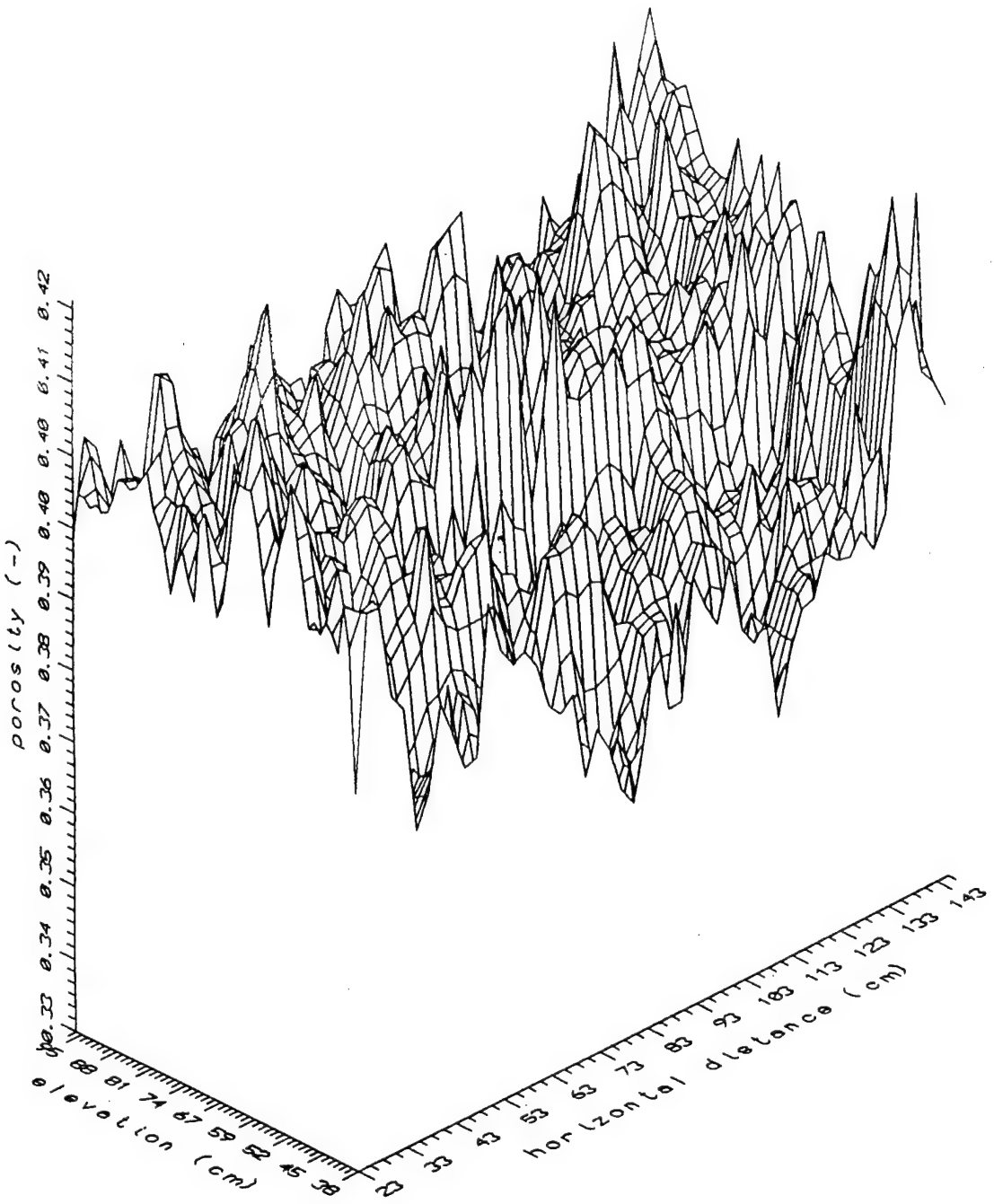

Figure 115. Measured Values for the Porosity.

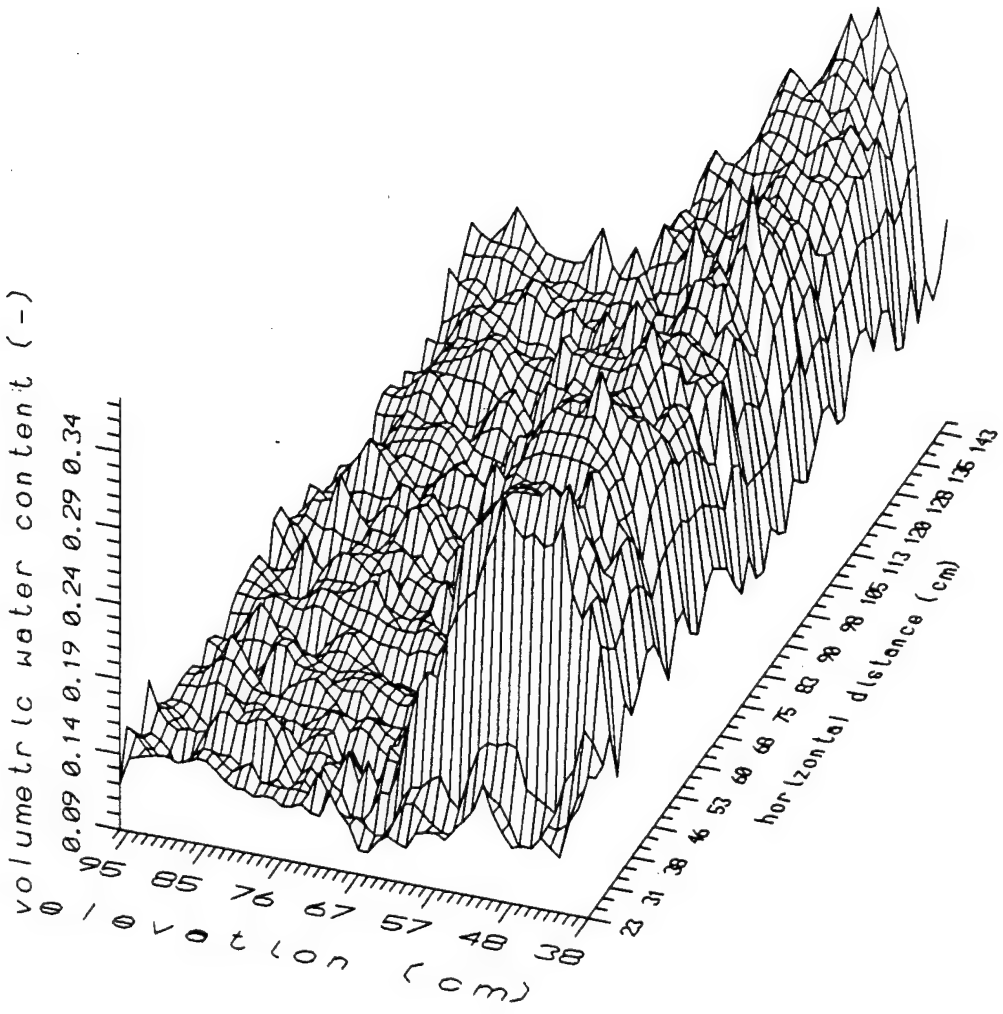

Figure 116. Measured Values for the Volumetric Water Content.

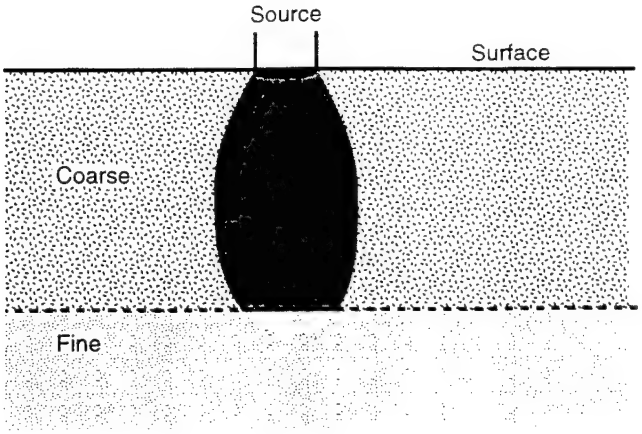

Figure 117. PCE Plume Readily Infiltrates the Fine Layer Without Spreading.

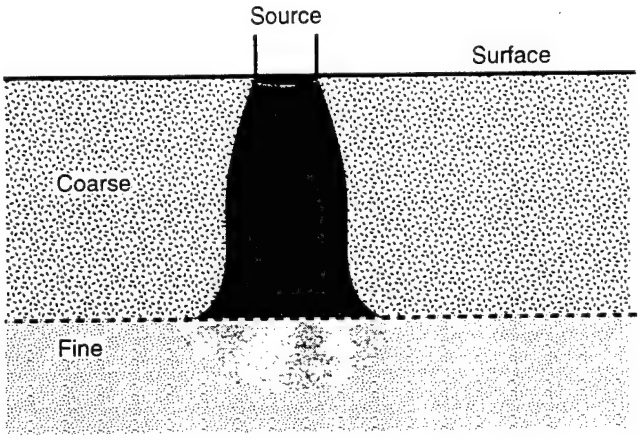

Figure 118. Spreading in the Fine Layer due to Capillary Effects.

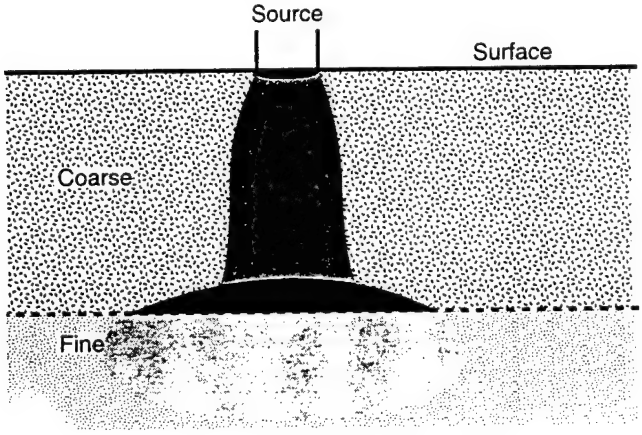

Figure 119 ..ateral Spreading in both the Coarse and the Fine Layer.

In- (positive) and outflow (negative) rates of water, PCE, and air into and from the flow container are presented in Figure 120 for the first 60 minutes upon initiating the first spill. During the first few minutes PCE displaced air only, indicating that within the unsaturated zone water acted as an immobile phase, as was assumed by Kueper and Frind (1988) and observed by Reible and Illangasekare (1989). After 6.7 minutes, water started to discharge from the container. This coincided with the plume reaching the saturated zone in the fine sand layer. Air was now flowing back into the container as the PCE displaced the water, which in turn was being discharged from the flow container. The highest outflow rate of water was measured a few minutes after the PCE spill was terminated. The first PCE discharged from the flow container was collected 6.5 hours after the start of the spill in Trap #5 (Figure 113). A total of 66 mL of PCE was collected , all in Trap # 5, during the week following the spill, while the cumulative water outflow was 975 mL. The latter is substantial greater than the 650 ml of PCE spilled into the container or the 584 mL of PCE that remained in the flow container upon reaching near static equilibrium conditions.

The in-(positive) and outflow (negative) rates of water, PCE, and air into and from the flow container during the second (Figure 121) and third spill (data not shown) were very much the same as during the first spill. This would seem to indicate that the initial outflow of water, following a spill, was solely due to the displacement by PCE rather than a intermediate reduction of the interfacial tension at the water-air interface near PCE contaminated areas. The very fine sand funnels at the bottom of the flow container seemed to function as expected during the first spill. However, during the subsequent spills, PCE failed to drain into some of the traps, although it was clearly visible in the porous medium above the traps. No explanation of this observed phenomenon is available at present.

As in the first experiment, the total outflow of water after each of the subsequent spills exceeded the cumulative infiltration of PCE. Although Figures 120 and 121 only display the outflow rates during the first 60 minutes after the start of the first and second spill, respectively, measurements were continued for a week. During this time period, both water and PCE continued to discharge from the porous medium, although at the end of the week the discharge rate of both liquids had approached zero, thus indicating a condition of near static equilibrium. The continuant, but continuously reducing, outflow rate of water and occasional outflow of PCE were attributed to a decrease in surface tension between water and air, especially near the capillary fringe. This reduction in surface tension not only allowed some of the water to drain from the flow container, but apparently also allowed mobilization of some of the previously trapped PCE.

Similar to the one-dimensional column experiments, the PCE fingers, which developed after the PCE plume had entered the water saturated zone, were found to be extremely sensitive to heterogeneities in the porous medium. Slight heterogeneities in the saturated part of the coarse sand (near the bottom of the flow container) caused extensive spreading of PCE. It appeared that PCE fingers originating during the second and third spill, tended to follow similar pathways as during the first spill. This explains the increased degree of spreading in the saturated zone after each additional spill. After the first spill, the total horizontal length of the PCE contaminated area was 1.2 meters. After the second spill this length had increased to 1.6 meters and after the third spill PCE started to flow into the end chambers of the flow container.

The volumetric PCE and water content values during the near static equilibrium condition after the first spill are shown in Figure 122 and 123, respectively. Figure 122 shows a significant accumulation of PCE in the unsaturated part of the fine sand layer just above the water saturated part. This agrees with the observations described in Section VI. However, since the pressure head of the water in the saturated zone of the fine sand layer was -29 cm or less, the capillary pressure across the water-PCE interface was expected to easily exceed the entry pressure whenever a continuous PCE phase is present, allowing for the penetration of PCE into the saturated zone of the fine layer. The rather high PCE saturations seem to support the concept of

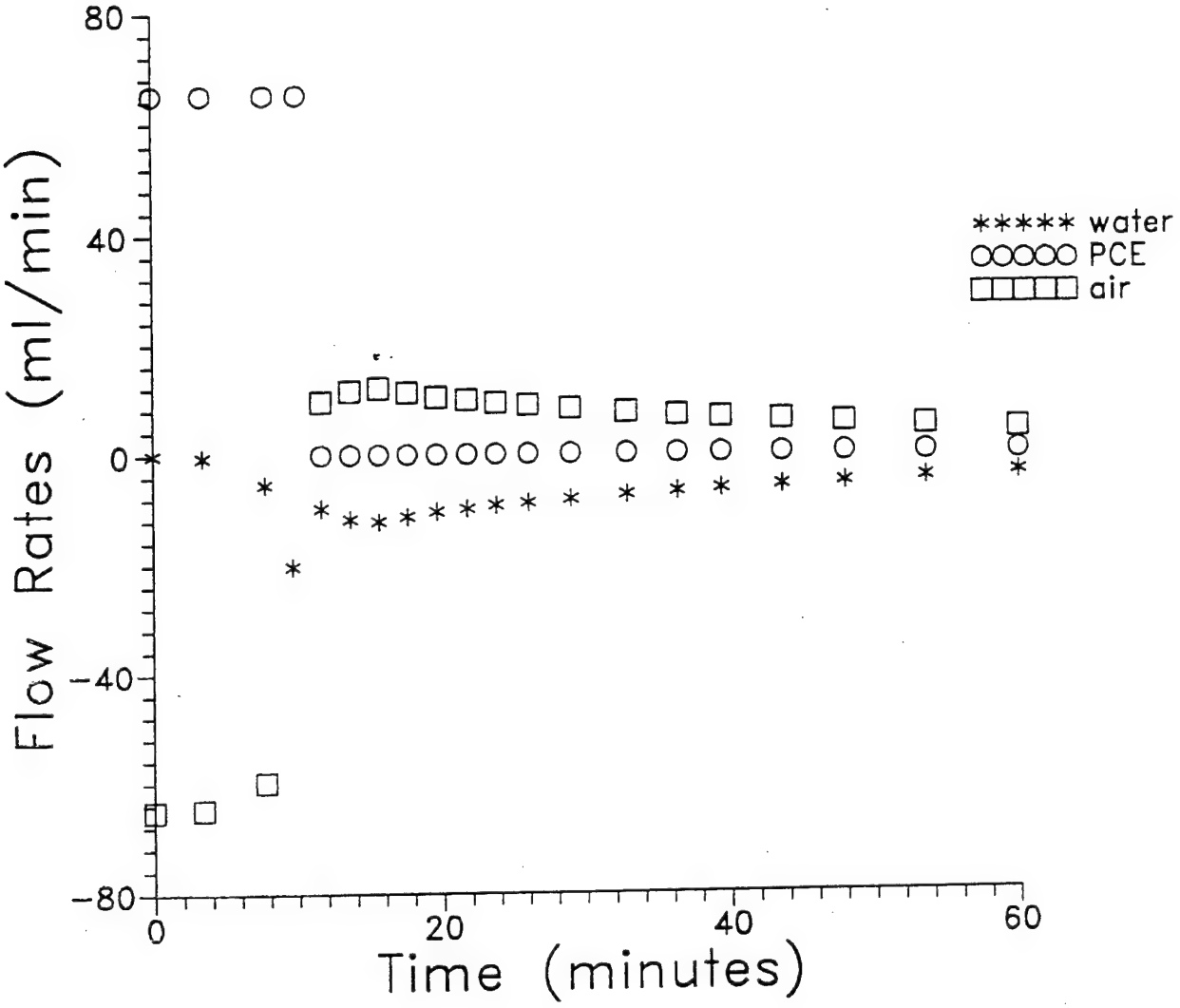

Figure 120. In- and Outflow Rates of Water, PCE, and Air During the First 60 Minutes After the First Spill.

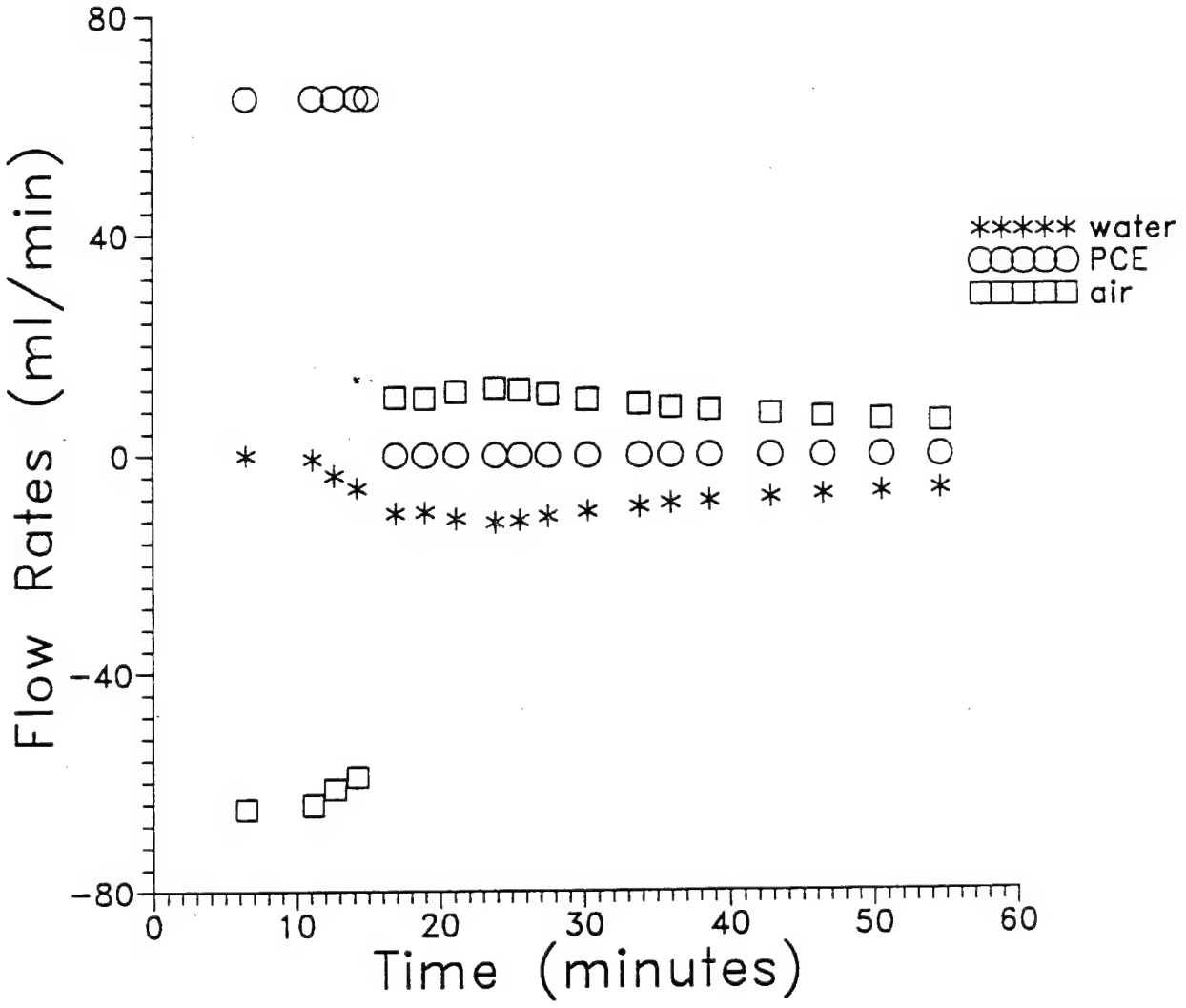

Figure 121. In- and Outflow Rates of Water, PCE, and Air During the First 60 Minutes After the Second Spill.

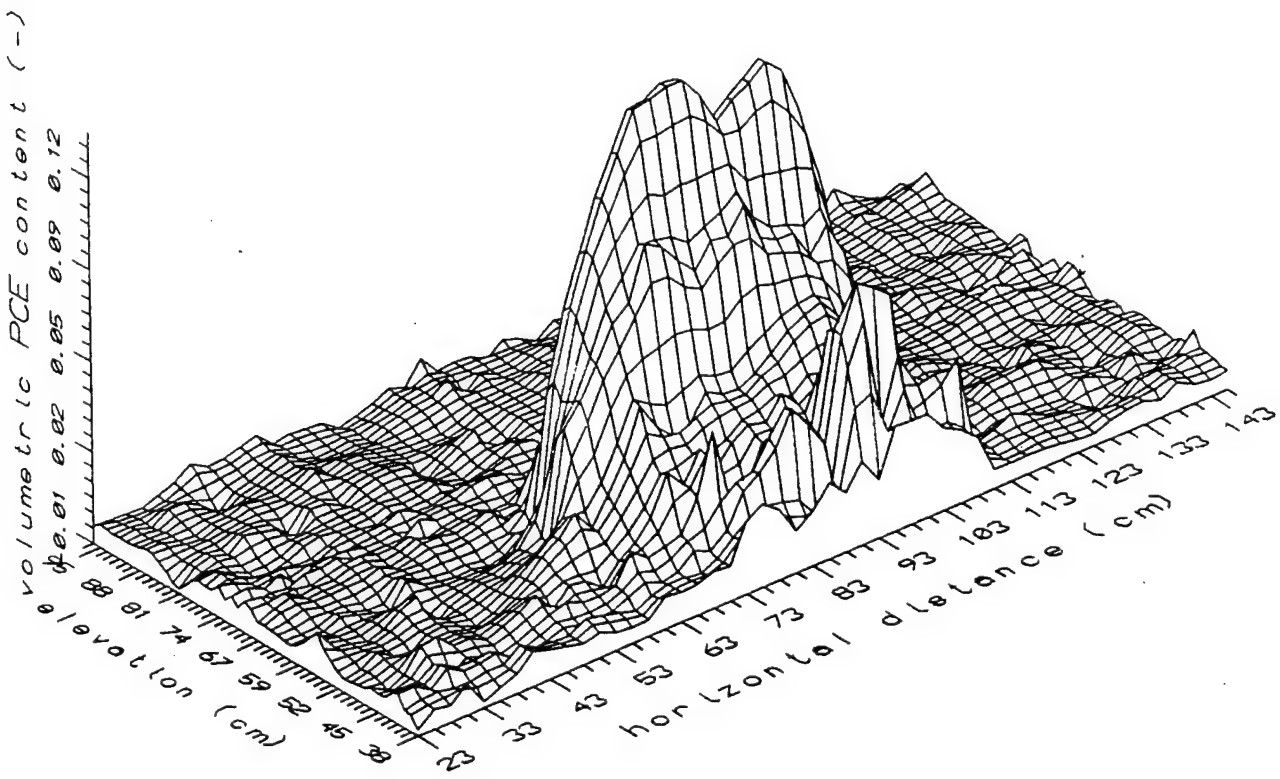

Figure 122. Volumetric PCE Content Values After Static Equilibrium Was Assumed (Spill 1).

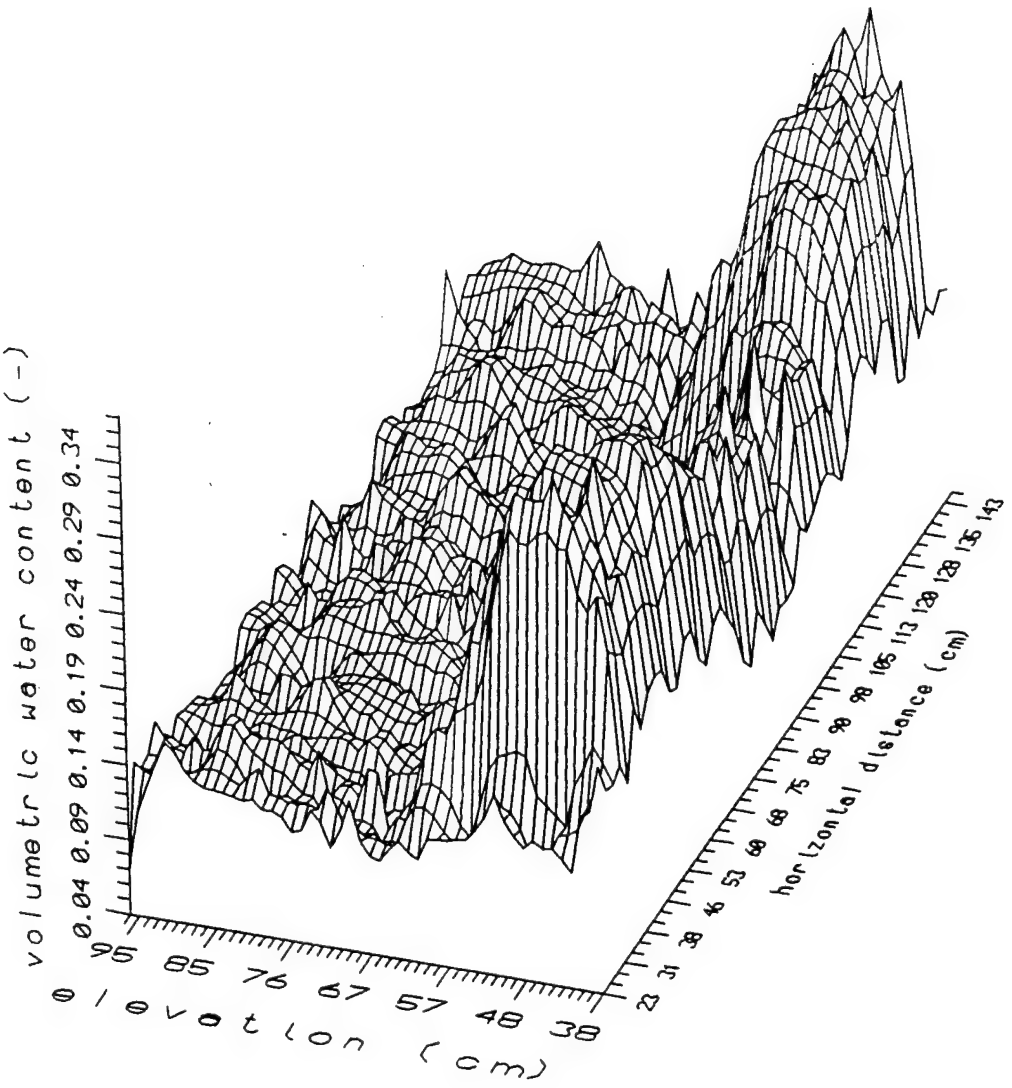

Figure 123. Volumetric Water Content Values After Static Equilibrium Was Assumed (Spill 1).

"minimum" volumetric PCE content, which is a combination of PCE entrapped by water and present in discontinuous lenses on top of the water-air interface (Section V). The decrease of the volumetric PCE content with height within the fine sand layer indicates that the "minimum" PCE content decreases with decreasing volumetric water content. The residual PCE saturations in the initially rather dry part of the coarse sand below and above the fine layer were very low. A three-dimensional graph of the volumetric PCE content after the third spill is shown in Figure 124. The PCE contaminated area was wider than after the first spill (Figure 124). The volumetric PCE contents within the area, however, did not seem to have changed.

D. SUMMARY AND DISCUSSION

The results indicate that PCE migrates through the vadose zone without displacing water. As a consequence it should be possible to model PCE movement in the unsaturated zone as two-phase (PCE and air) flow by considering water as an immobile phase. If we further assume that the resistance to air flow is negligible, the flow of PCE in the unsaturated zone can simply be described by the Richards equation, which to date has been widely applied to model water flow in unsaturated porous media. Similar conclusions were drawn by Reible and Illangasekare (1989). Since the stagnant water appears to be immobile, PCE can be considered as a secondary wetting fluid, which would make its migration patterns resemble those of water in initially dry soils. The latter have been studied extensively in the soil science literature (Gardner, 1979). Furthermore, the resemblance of water flow in dry porous media and that of PCE in unsaturated porous media should allow us to apply the stability theory of water infiltration into dry soils (Raats, 1973; Philip, 1975) to predict the conditions under which migrating PCE plumes tend to break up in fingers.

The rather high PCE saturations above the saturated part of the fine sand layer seem to confirm the concept of "minimum" volumetric PCE content as presented in Section V.

Although the PCE phase itself does not seem to displace water in the unsaturated region, it is important to consider the drainage of water caused by a reduction in interfacial tension due to dissolved PCE. Drainage due to changes in interfacial tension is much slower than that directly due to displacement of water by PCE in saturated regions. The displacement of water by air may even mobilize some of the trapped PCE, especially just below the top of the capillary fringe.

Behavior of PCE in the unsaturated regions of the stratified two-dimensional experiments agree with some of the findings of the corresponding one-dimensional experiments (Section VI). Especially the behavior in the vadose zone was similar in both the one- and two-dimensional systems. Overall, the two-dimensional experiments corroborate the findings in Section IV in that heterogeneity in the saturated zone had a far more pronounced effect on lateral spreading than stratification in the unsaturated zone. Furthermore, individual fingers originating from the initially coherent contaminant plume were observed to follow their own preferential pathways while traveling through the saturated parts of the porous medium. Since natural aquifers almost inherently show some degree of stratification, it can be expected that the lateral dimensions of a PCE contaminated site will be far greater than the vertical dimensions. This result will be further investigated by physically simulating PCE spills in a fully saturated two-dimensional porous medium.

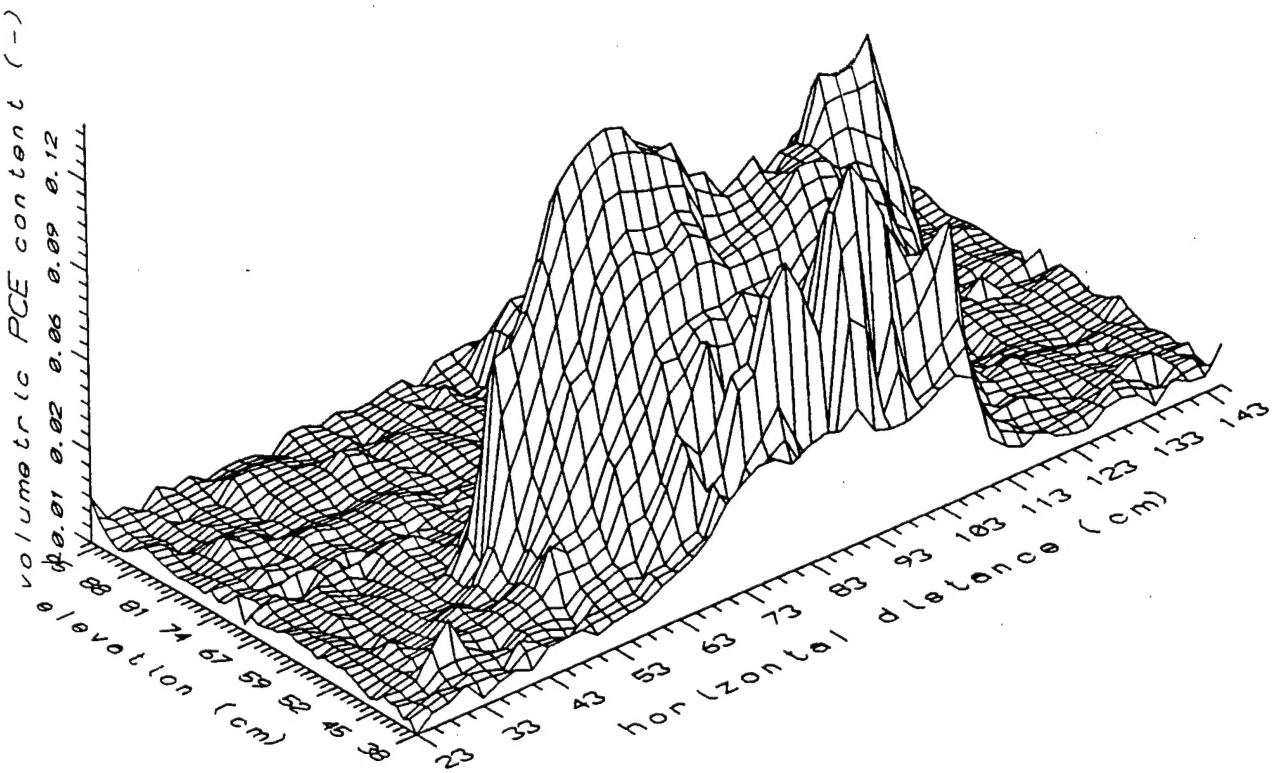

Figure 124. Values for the Volumetric PCE Content After Static Equilibrium Was Assumed (Spill 3).

REFERENCES FOR SECTION IX

Gardner, W. H., How Water Moves in the Soil, American Society of Agronomy, Madison, WI, 6 pp, 1979.

Kueper, B.H. and E.O. Frind, "An Overview of Immiscible Fingering in Porous Media." Journal of Contaminant Hydrology, 2: 95-110, 1988.

Oostrom, M., J.S. Hayworth, J.H. Dane, and O. Güven, "Behavior of Dense Aqueous Phase Leachate Plumes in Homogeneous Porous Media." Water Resources Research, 28(8): 2123-2134, 1992a.

Oostrom, M., J.H. Dane, J.S. Hayworth, and O. Güven, "Experimental Investigation of Dense Solute Plumes in a Unconfined Aquifer Model." Water Resources Research, 28(9): 2315-2326, 1992b.

Oostrom, M. and J.H. Dane. Calibration and Automation of a Dual-Energy Gamma System for Applications in Soil Science. Agronomy and Soils Department Series No. 145. Alabama Agricultural Experiment Station. Auburn University, AL, 1990.

Philip, J.R., "Stability Analysis of Infiltration." Soil Science Society of America Journal, 39(6): 1042-1049, 1975.

Raats, P.A.C.," Unstable Wetting Fronts in Uniform and Nonuniform Soils." Soil Science Society of America Journal, 37(5): 681-685, 1973.

Reible, D.D. and Illangasekare, T.H., "Subsurface Processes of Nonaqueous Phase Contaminants." In: Allen, D.T., Cohen, Y., and I.R. Kaplan (eds.), Intermedia Pollutant Transport: Modeling and Field Measurements, Plenum Press: 237-254, 1989.

SECTION X
CONCLUSIONS

Specific conclusions of this research related to each major task of the project have been presented in the corresponding sections of the report. The experiments with quadricyclane, presented in Sections II, III and IV, have provided new, detailed information on the subsurface behavior of this compound, while the experiments with PCE, presented in Sections V, VI, VII, VIII and IX, have resulted in unique data sets providing detailed quantitative information on the behavior of this chemical.